Structure-activity studies on inhibitors of the tankyrases

Kumpan, Katerina

Award date:
2014

Awarding institution:
University of Bath

Structure-Activity Studies on Inhibitors of the Tankyrases

submitted by

Katerina Kumpan

for the degree of Doctor of Philosophy

of the University of Bath

2014

The research work in this thesis has been carried out in the Department of Pharmacy and Pharmacology, under the supervision of Prof. Michael D. Threadgill, Dr. Andrew S. Thompson and Dr. Matthew D. Lloyd.

……..…….

……..……

Abstract

Tankyrases-1 and -2 (TNKS-1 and -2) are members of the poly(ADP-ribose)-polymerase (PARP) enzyme superfamily, which modify and regulate target proteins by addition of multiple (ADP-ribose) units from the substrate NAD^+. TNKS-1 and -2 have many cellular roles, including regulation of elongation of telomeres, activation of nuclear mitotic apparatus protein (NuMA) in mitosis and regulation of the *Wnt* signalling pathway. This makes the tankyrases attractive new targets for design and development of new anti-cancer drugs.

2-(4-Trifluoromethylphenyl)-7,8-dihydro-3*H*-thiopyranopyrimidin-4-one (XAV939) was one of the few active inhibitors of tankyrases reported until 2013. The aim of this project was to explore the structure-activity relationships towards enhancing potency and selectivity by replacing the saturated sulfur-containing ring with saturated and unsaturated nitrogen heterocycles and by varying the aromatic side-chain.

Firstly, ascorbate-modified Sonogashira couplings of bromocyanopyridines and a variety of 4-substituted arylethynes, followed by acidic cyclisation and conversion of the lactone into the lactam, gave differently substituted arylnaphthyridinones. The alternative route used transition-metal-free reaction of bromopyridinecarboxylic acids with symmetrical β-diketones. 7-Phenyl-1,6-naphthyridin-5-one and 7-(4-methylphenyl)-1,6-naphthyridin-5-one were converted to the N^1-oxides. Alkylation at 1-N gave 7-aryl-1-methyl-5-oxo-5,6-dihydro-1,6-naphthyridin-1-ium iodides and subsequent reduction gave saturated target 7-aryl-1-methyl-1,2,3,4-tetrahydro-1,6-naphthyridin-5-ones.

Other target compounds included pyridopyrimidinones, which were prepared from the corresponding bromopyridinecarboxylic acids by a copper-catalysed reaction with 4-substituted benzamidines. Target tetrahydropyridopyrimidinones, however, were obtained from condensation of 1-benzyl-4-oxopiperidine-3-carboxylic esters with substituted benzamidines.

All compounds were evaluated *in vitro* for inhibition of the catalytic activity of TNKS-2. The best compounds were investigated further, including *in vitro* TNKS-1 and PARP-1 inhibition and anti-proliferative studies on HT29 and FEK4 cell lines. Notably, 1-methyl-7-(4-trifluoromethylphenyl)-1,2,3,4-tetrahydro-1,6-naphthyridin-5-

one and 1-methyl-7-(4-methoxyphenyl)-1,2,3,4-tetrahydro-1,6-naphthyridin-5-one showed 50% inhibition of TNKS-2 at 1.5 nM and 1.1 nM, respectively, showing also high selectivity (IC_{50} against PARP-1: 4.8 μM and 3.4 μM, respectively). This high potency and selectivity point to potential for development towards therapeutic use in cancer. A patent covering these discoveries has been filed.

We thank the University of Bath for part-funding of this project through a fee-waiver scholarship.

Acknowledgements

First of all, I am immensely grateful to my supervisors, Prof. Mike Threadgill, Dr. Andy Thompson and Dr. Matthew Lloyd for their essential support, guidance and encouragement throughout my PhD. I especially wish to thank Mike for his infinite patience, insight and enthusiasm during the hopeless hard times.

It was a great privilege (and a great fun) for me to work with Dr. Amit Nathubhai, Dr. Elvis Twum, Dr. Helen Paine and Miss Rihaf Al-Faraj all these years. They taught me so many things and made my work so pleasant, that I cannot express my gratitude to them. I also want to thank the Shandong University summer student, Miss Chenlu Zhang, for taking an invaluable part in the project.

I would like to show my deepest appreciation to my colleagues from the Department of Pharmacy and Pharmacology: Dr. Elizabeth O'Donovan, Dr. Joanna Swarbrick, Dr. Emma Casey, Dr. Patricia Marcé-Villa, Dr. Stefan Hader, Dr. Wolfgang Dohle, Dr. Ricardo Resende, Mr. Maxims Jevglevskis, Dr. Benjamin Young, Dr. Alexander Ciupa, Mr. Terrence Kantner, Mr. Kunal Tewari, Dr. Mehrnoosh Ostovar, Dr. Christopher Roche, Dr. Ruggero Dondi, Dr. Gerta Kami-Cobeci, Mrs Natalie Griffits, Mrs Guat Lee Ling, Dr. Tina Radka and Dr. Olivier Reelfs for their help, advice and pleasure to work with.

I am thankful to Dr. Tim Woodman for his inestimable help with NMR and to Dr. Anneke Lubben and Mr. Christian Rehbein for their guidance into an art of mass spectrometry. I would like to make a special acknowledgement to Dr. Pauline Wood, whose help with the biological part of the project was absolutely invaluable.

I cannot thank Dr. Marco Mottinelli enough for virtually everything.

I am immensely grateful to all my dear friends. Especially I want to thank Ksenia, Nik, Tony, Ann and Mila – for being true friends regardless of the distance, for supporting me in some tough moments and for lots of fun. Special thanks to Dr. Dmitry Momotenko for patiently settling my countless doubts.

I am indebted to everyone who deepened my interest in science: Dr. A. B. Sheremetev, Dr. G. M. Rodionova, Dr. N. E. Sedyakina, Dr. M. A. Fokina, Dr. O. I. Tuntsova, Dr. N. A. Palysaeva, Mrs. N. A. Aleksandrova and Miss V. A. Rtischeva.

Lastly, I would like to thank my dearest family: Mum, Dad, Polina, Anton, Artem, Arina and Arseny for an endless encourage and support. I would also like to thank my grandparents, whom I did not know, but who had established the scientific tradition in our family.

Contents

List of Figures, Schemes and Tables

Figures

Schemes

Tables

Abbreviations

3-AB	3-Aminobenzamide
5-AIQ	5-Aminoisoquinolin-1-one
Ac	Acetyl / Acetate
ADP	Adenosine diphosphate
ADPr	Adenosine diphosphate ribose
ANK	Ankyrin
ARTD	ADP-ribosyltransferase diphtheria toxin
b-NAD^+	Biotinylated nicotinamide adenine dinucleotide
bp	Base pair
br	Broad (NMR)
BER	Base Excision Repair
BRCT	BRCA1 C-terminal domain
COX	Cyclooxygenase
d	Doublet
DBD	DNA binding domain
DCM	Dichloromethane
DLBCL	Diffuse large B-cell lymphoma
DME	1,2-Dimethoxyethane
DMEM	Dulbecco's modified Eagle's medium
DMF	*N,N*-Dimethylformamide
DMSO	Dimethylsulfoxide
DMSO-d_6	Deuterated dimethylsulfoxide
DNA	Deoxyribonucleic acid
EDTA	Ethylenediaminetetraacetic acid
ELISA	Enzyme-linked immunosorbent assay
ESI	Electrospray ionisation
Et	Ethyl
FBS	Foetal bovine serum
Gly	Glycine
HMBC	Heteronuclear multiple bond correlation / coherence
HSQC	Heteronuclear single quantum

	correlation / coherence
HPS	His-Pro-Ser domain
HRP	Streptavidin / horse-radish peroxidase
IC_{50}	Inhibitory concentration 50%
IHRP	Inter-alpha-trypsin inhibitor family heavy-chain-related protein
Ile	Isoleucine
IR	Infrared
KDa	KiloDalton
LHMDS	Lithium hexamethyldisilazide
Leu	Leucine
Lys	Lysine
m	Multiplet
m-CPBA	3-Chloroperoxybenzoic acid
mg	Milligrams
min	Minutes
mL	Millilitres
mmol	Millimoles
mp	Melting point
M	Mesomeric (effect)
MEM	Modified Eagle's medium
MS	Mass spectroscopy
MVP BD	Major vault protein binding domain
NAD^+	Nicotinamide adenine dinucleotide
NADH	Nicotinamide adenine dinucleotide (reduced form)
NADPH	Nicotinamide adenine dinucleotide phosphate (reduced form)
NMR	Nuclear magnetic resonance
NTD	N-terminal domain
Nu	Nucleophile
NuMA	Nuclear mitotic apparatus protein
OD	Optical density
ppm	Parts per million

PARP	Poly(ADP-ribose)polymerase
PARPi	Poly(ADP-ribose)polymerase inhibitor
PARsylation	Poly(ADP-ribose)sylation
PBS	Phosphate buffered saline
PBS-T	Phosphate buffered saline Tween® 20
PG	Prostaglandin
Phe	Phenylalanine
PPA	Polyphosphoric acid
Q	Quartet (NMR)
quin	Quintet (NMR)
RNA	Ribonucleic acid
s	Singlet (NMR)
SAM	Sterile alpha motif
SAR	Structure activity relationship
sat	Saturated
SD	Standard deviation
Ser	Serine
SSBR	Single Strand Break Repair
TBAF	Tetrabutylammonium fluoride
TEP1	Telomerase-associated protein
TFAA	Trifluoroacetic anhydride
THF	Tetrahydrofuran
Thr	Threonine
TMS	Trimethylsilyl
TMSE	Trimethylsilylethyne
TNKS	Tankyrase
TNKSi	Tankyrase inhibitor
TLC	Thin-layer chromatography
t	Triplet (NMR)
TRF1	Telomeric-repeat binding factor-1
TRF2	Telomeric-repeat binding factor-2
Tyr	Tyrosine
u-NAD^+	Unlabelled nicotinamide adenine dinucleotide

vPARP	Vault poly(ADP-ribose) polymerase

Chapter 1. Introduction

1.1 Cancer – a major global problem.

Cancer is one of the major mortality causes worldwide (Figure 1). The World Health Organisation claims cancer to be the major cause of death worldwide, bringing on 13% of deaths.[1] According to Eurostat, an average of 166.9 deaths per 100,000 inhabitants were caused by cancer across Europe in 2010.[2] In the U.S.A., cancer was the second leading cause of lethality, as stated by the National Center for Health Statistics, resulting in 574,743 deaths in 2010.[3] According to International Agency for Research on Cancer GLOBOCAN database, 12.7 million of new cancer cases were diagnosed worldwide in 2008; 7.6 million of those were lethal.[4]

These numbers show the undoubted importance of cancer research, especially in the field of antineoplastic therapy. Existing anti-cancer drugs are, in the vast majority, highly-toxic and not efficient enough. The high toxicity of anti-cancer therapy leads to some extremely severe adverse effects, including anaemia, neutropenia, multi-organ

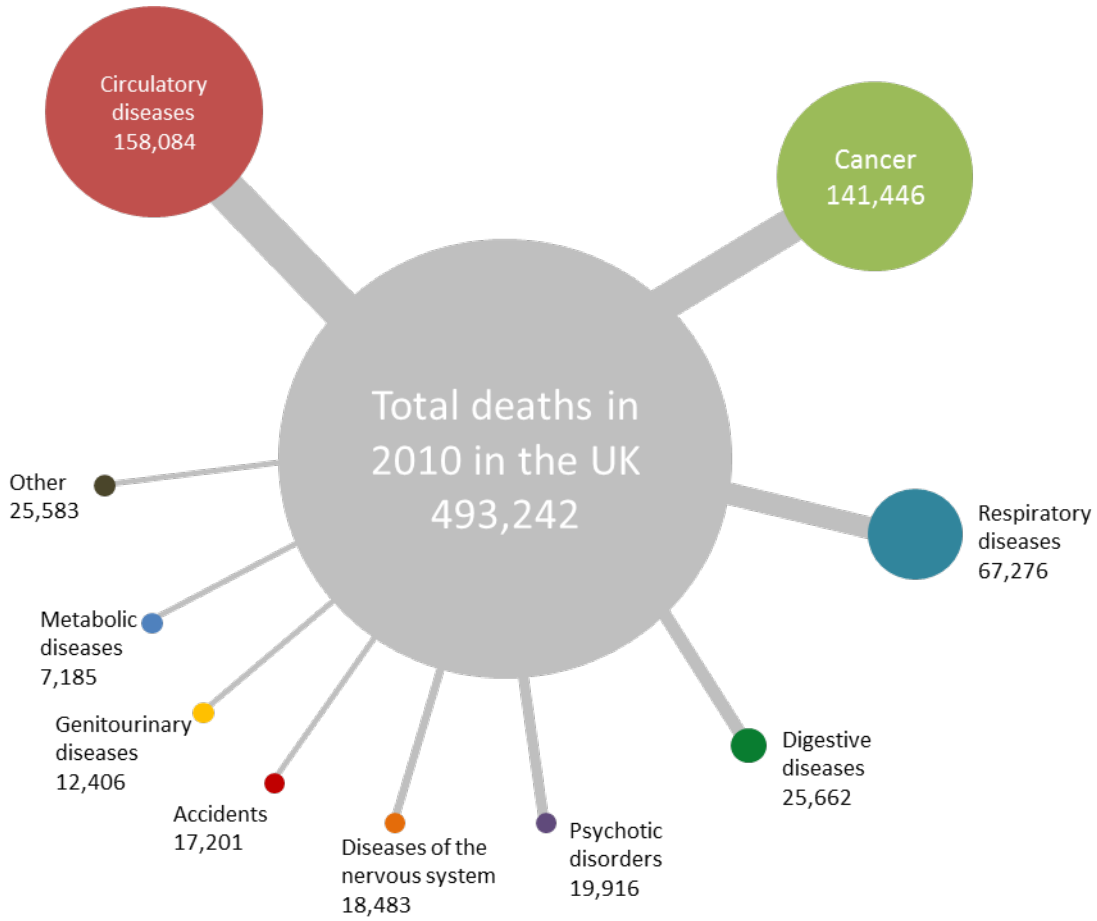

Figure 1. The primary cause of death recorded in death certificates in the UK in 2010 (Source: ONS Mortality statistics).[5]

failure, neuropathies, infertility, sickness and fatigue (Table 1). These adverse reactions are caused by low selectivity of existing drugs towards cancer cells. Thus, there is a clear demand for more efficient, highly selective and less toxic anti-cancer agents.

Table 1. The most common chemotherapeutic agents, grouped by their mode of action, and corresponding characteristic adverse effects.

Chemotherapeutic agent	Major adverse effects
Alkylating agents	
Examples: Cyclophosphamide, busulfan, temozolomide	Long-term damage to the bone marrow, acute leukaemia
Platinum derivatives	
Examples: Cisplatin, carboplatin, oxaliplatin	Long-term damage to the bone marrow
Antimetabolites	
Examples: 5-fluorouracil, cytarabine, methotrexate	Myelosupression, immunosuppression
Antitumour antibiotics	
Examples: Doxorubicin, bleomycin	Cardiotoxicity, anaphilactoid reaction
Topoisomerase I and II inhibitors	
Examples: Topotecan, irinotecan, etoposide	Acute myelogenous leukaemia
Mitotic inhibitors	
Examples: Paclitaxel, vinblastine, estramustine	Peripheral nerve damage

1.2. Poly(ADP)polymerases family.

Poly(ADP)ribose polymerases (PARPs) and effects of their inhibitors (PARPi) have been widely studied during recent years. Increasing scientific interest in this superfamily of enzymes can be explained by their polyfunctionality. Their activity as a cellular response to DNA damage,[6] together with their roles in replication of telomeres and in signalling, makes them interesting targets. It has been shown that they play pivotal roles in inflammation,[7,8] ischaemia-reperfusion injury,[7] tumourigenesis,[9,10] angiogenesis[9] and metastasis.[11] Hence, PARPi may have excellent clinical potential in the treatment of cancer and metastases, stroke, myocardial infarction,[10] shock (*e.g.* haemorrhagic shock),[12] colitis, diabetes mellitus and its complications,[10] certain retinopathies,[9] pulmonary fibrosis,[12] *etc*. Especially interesting is the ability of PARPi to sensitise cancer cells to the DNA-damaging activity of some anti-cancer agents, such as topoisomerase I poisons, temozolomide and platinum drugs.[13-17] Moreover, there is a large therapeutic window between inhibitory activity towards PARPs and toxicity.[13,18,19] Table 2 summarises some known effects of the PARP inhibitor 3-aminobenzamide (3-AB) in animals.

PARPs belong to a large family of enzymes that use NAD^+ as a substrate to transfer ADP-ribose units to proteins (see section **1.3.3** and Scheme 1, pp 9-10).[20,21] There are at least eighteen PARPs coded in the human genome and the functions of some of them are still unknown.[22,23] The only homologous site in these enzymes is the *C*-terminal catalytic domain but, outside this part, they may vary a lot (Figure 2). However, this domain shows high homology between different species (*e.g.* human, rat, mouse).[24] This may point to similar functions of the enzymes and, hence, similar potential for inhibition.[25,26] The most-studied enzymes in this group are PARP-1, PARP-2, PARP-3, vault-PARP (vPARP, PARP-4) and the tankyrases (PARP-5a and -5b).

Table 2. Effects of 3-AB in animal models of various diseases.[7]

Organ	Disease model	Main results
Brain	Stroke	Reduction in necrosis of the neurons, improvement in neurological status.
	Traumatic brain injury	Improved neurological status.
	Meningitis	Improved survival, improved neurological status, reduced inflammatory mediator production.
Heart	Myocardial infarction	Reduced myocardial necrosis, reduced infarct size, improved myocardial contractility, reduced inflammatory mediator production, reduced neutrophil infiltration.
	Transplantation	Improved myocardial contractility, reduced inflammatory mediator production, extension of transplant survival, synergy with cyclosporine treatment.
Lung	Ovalbumin-induced asthma	Reduced inflammatory mediator production, improved pulmonary function.
Endocrine pancreas	Diabetes	Protection against necrosis of islets and reduction in the degree of hyperglycaemia.
GI tract	Colitis	Improved survival, protection against gut shortening, reduced neutrophil infiltration, lipid peroxidation and nitrosative damage, attenuation of inflammatory markers.
Joint	Arthritis	Reduced severity and incidence of arthritis.
Skeletal muscle	Reperfusion injury	Reduction in reperfusion injury necrosis markers.
Kidney	Reperfusion injury	Accelerated recovery of normal renal function.
Liver	Acetaminophen toxicity	Reduced hepatic necrosis, protection against hepatic leukostasis.
Eye	Optic nerve transection	Inhibition of secondary retinal ganglion cell death.
Ear	Acoustic trauma	Improvement of cochlear function.
Various	Haemorrhagic, endotoxic and septic shock	Protection against haemodynamic decompensation, improved survival, protection against gut hyperpermeability and myocardial, vascular, hepatic and renal failure, reduced inflammatory mediator production.

The first PARP enzyme to be discovered, PARP-1, a 116-KDa protein, resides mostly in the nucleus (Figure 2). Four out of six main domains of PARP-1 have been identified with a particular function:

1) *Domain A*, containing three zinc-fingers, two of which interact with DNA;
2) *Domain B* is responsible for nuclear residence of the enzyme;
3) *Domain D*, an auto-modification motif;
4) *Domain F*, being the smallest moiety, contains the catalytic site of PARP-1.[23]

Following damage to DNA, the enzyme modulates DNA-repair events. It binds to a damaged DNA with two zinc-fingers, which induces auto-poly(ADP-ribosyl)ation of PARP-1. PARP-1 also poly(ADP-ribosyl)ates other target proteins, including histones, topoisomerases, DNA polymerases and ligases. (PAR)sylated and, therefore, negatively charged histones open the chromatin and recruit the base excision repair complex.[27] The auto-modification releases the enzyme from the DNA.[24,27,28]

PARP-2, a 62 KDa protein, is structurally and functionally the most similar to PARP-1. However, they have different DNA-binding sites, suggesting different substrate-specific properties for these two enzymes.[29-31] It was claimed that PARP-2 prefers to modify histone H2B, whereas PARP-1 interacts with histone H1. PARP-2 is encoded by a different gene and its functional specificity may be explained by a different *N*-terminus.[29] Also PARP-2 interacts with PARP-1 and works together with it in the Single Strand Break Repair (SSBR) and Base Excision Repair (BER) pathways.[23]

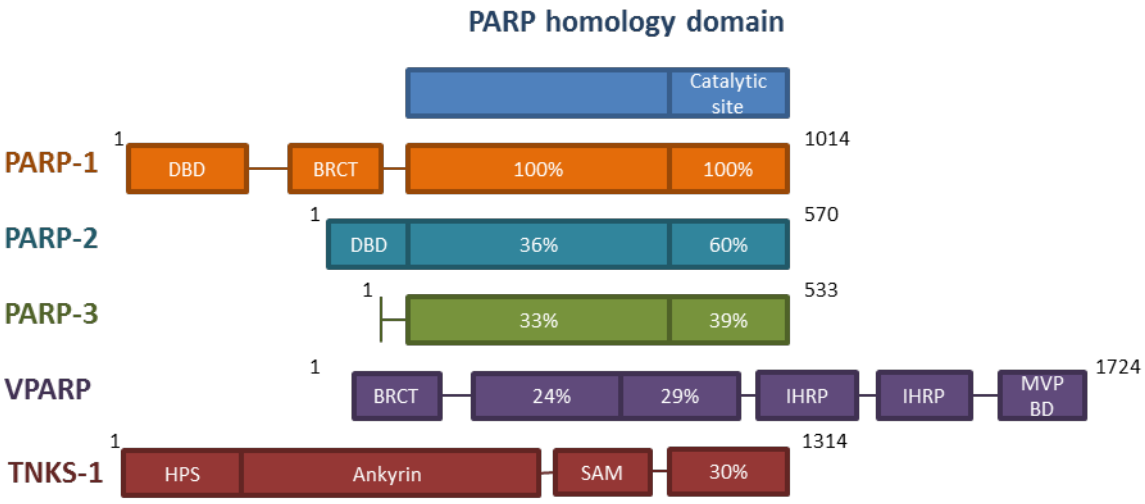

Figure 2. Schematic structures of the five members of the PARP family. Percentage shows resemblance to the structure of PARP-1. Abbreviations: ANK, Ankyrin domain; DBD, DNA binding domain; BRCT, BRCA1 C-terminal domain; IHRP, inter-alpha-trypsin inhibitor family heavy-chain-related protein; MVP BD, major vault protein binding domain; HPS, His-Pro-Ser domain; SAM, sterile alpha motif.

PARP-3, a much smaller protein, has not yet been widely studied. It was noticed to be a key component of the centrosome, located at the daughter centriole throughout the cell cycle.[23,32] This enzyme can be inhibited by common pan-(PARP) inhibitor 3-amino-benzamide (3AB).[32] It was also found that PARP-3 interacts with PARP-1 in the centrosome, suggesting a link between DNA repair system and mitosis.[23,33]

Vault-PARP (vPARP) is a component of a special cytoplasmatic organelle, called the vault complex. The vault complex consists of three proteins, major vault protein (MVP), telomerase-associated protein (TEP1), vault poly(ADP)polymerase (vPARP) and an untranslated vault RNA (vRNA). vPARP catalyses poly-(ADP-ribosyl)ation of MVP[23] and auto-poly(ADP-ribosyl)ation and thereby regulates the conformations of vaults, such as opening and closing the barrels to allow cargo molecules to pass in and out.[34]

The knowledge of the other PARP enzymes is rather limited. TiPARP (PARP-7) was identified in 2001.[35] The exact function of this member of the PARP family remains unclear. However, it is speculated that PARP-7 is involved in the function of T-cells and somehow contributes to carcinogenesis. Its PARP function was proven by its ability to catalyse (PAR)sylation of histones *in vitro* in the absence of PARP-1. PARP-7, together with PARP-8 and PARP-13, has one zinc finger, when PARP-12 has three zinc fingers. All of them differ from the zinc finger found in PARP-1.[23] Other PARPs, PARP-10 and PARP-15, have a special moiety for binding to RNAs. PARP-10 was claimed to be a potent inhibitor of transformation of immortalised fibroblasts but it is not a general growth-inhibitory protein.[36] PARP-9 has recently been found in patients with different types of diffuse large B-cell lymphomas (DLBCLs).[23] It contains a duplicated A1pp domain, so-called macro domain, which also was found in PARP-14 and PARP-15.[23]

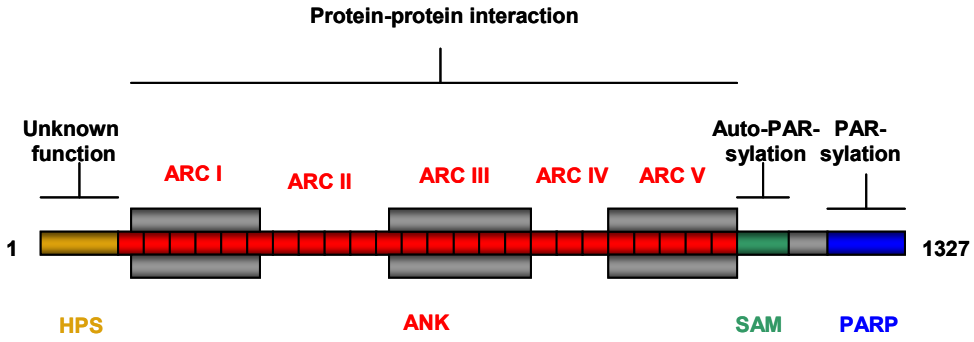

Figure 3. Domain structure of tankyrase-1: HPS (yellow), ANK (red), SAM (green), PARP (blue).

1.3 Tankyrases.

1.3.1 Structure and properties of tankyrase-1.

Tankyrase-1 (TRF1-interacting Ankyrin-related ADP-ribose polymerase 1; PARP-5a; ARTD-5) was first identified in 1998[37,38] through its interaction with TRF-1, one of the proteins in the telosomal complex. Smith *et al.* performed a yeast two-hybrid screen with human TRF1 as a bait. This screen revealed an open reading frame of 1327 amino acids, proposing a protein of *ca.* 140 KDa.[38] Tankyrase-1 is present in the nucleus as well as in the cytoplasm.[39] It is a 142 KDa protein, which consists of four major domains (Figure 3):[39,40]

- *HPS domain* at the *N*-terminus, rich in histidine, proline and serine residues. Its function is unknown. However, it was observed that this domain conceals a MAP kinase consensus motif.[23] If phosphorylated upon insulin stimulation, it enhances the activity of tankyrase-1.[23]

- *Ankyrin (ANK) domain (residues 208-945)*, which is composed of 24 ANK repeats. Ankyrin is present in a number of proteins (SMART database contained 19,276 ankyrin repeats sequences in 3,608 proteins identified).[41] This 33-residue motif was discovered in 1987[42] and was named after the cytoskeletal protein Ankyrin, which contained 24 replications of this repeat.[43] It was shown that this motif is present in prokaryotes, as well as in eukaryotes, and also in some viruses. Usually, Ankyrin repeats are involved in protein-protein interactions and no enzymatic function has been detected for them.[41] In tankyrases, this domain is a platform for protein-protein interactions. The *ANK*-domain is divided into five *ANK*-repeat clusters (ARCs) and all of them can serve as an individual protein-binding site, *e.g.* ARC V

is needed for recognition of TRF-1. This suggests that tankyrase-1 may interact with several substrates simultaneously.[40,41,44]

- *Sterile alpha motif (SAM) domain (residues 1028-1087)*, which is represented by five small helical bundles. *SAM* domains are rather common structures: they were found in more than one thousand proteins, according to the SMART database. Typically they mediate homo- and heterotypic protein-protein interactions.[45-47] *SAM* domain is essential for the auto-poly(ADP-ribosyl)ation of tankyrase-1. Because of the ability of tankyrase to form high-molecular-mass complexes, mediated by *SAM* domain, it was speculated that this enzyme may act as a scaffolding molecule, regulating formation of a protein pattern.[47]

- *PARP domain (residues 1104-1313)*, located at the *C*-terminus of the protein. It shares 30% of identity with PARP-1 catalytic domain. The secondary structures of the active site in PARP-1 are conserved in tankyrase-1 and are represented by nine β-strands, surrounded by four α-helices and loops. The α2 helix is relatively longer than the one in PARP-1. These secondary structures form a cavity known as the NAD^+-binding fold.[37,38] The function of this domain is to catalyse poly(ADP-ribosyl)ation of acceptor proteins using NAD^+ as a substrate. This provides negative charges to the acceptor proteins and disrupts their normal functions. The PARP catalytic domain contains two distinct binding sites, referred to as the donor and the acceptor sites. In the initiation reaction, when ADP-ribose is first added to a target protein, NAD^+ occupies the donor site. During this reaction, the target protein must occupy the acceptor site to position itself for the reaction. In the elongation reaction, the donor site is occupied by NAD^+ and the acceptor site is occupied by the growing poly(ADP-ribose) chain.[37] In the donor site was also found an adenosine-binding (AD) subsite, which is quite different from this type of subsite in PARP-1. This suggests another opportunity for rational design of selective tankyrase inhibitors.

- *Short zinc-binding motif (residues 1224-1247)*, unique to tankyrase-1 and tankyrase-2 (discussed below). The zinc ion is coordinated by three cysteines (Cys^{1234}, Cys^{1242}, Cys^{1245}) and one histidine (His^{1237}). This metal atom is located 33 Å away from the catalytic Glu^{1291} and *ca*. 20 Å away from the donor NAD^+-binding site. However, it is connected with the donor site through a G-loop. Considering these facts, the zinc atom appears to be catalytically unimportant. It is

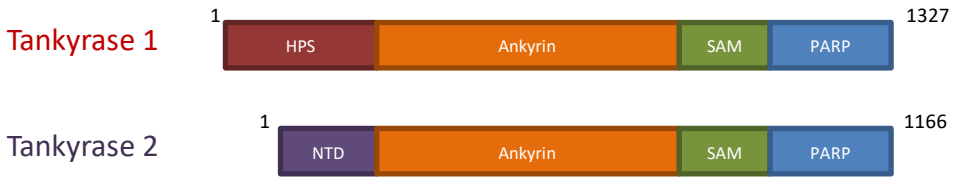

Figure 4. A comparison of domain structures of human tankyrase-1 and tankyrase-2. Abbreviations: NTD, N-terminal domain; PARP, poly(ADP-ribosyl)ation catalytic site.

involved in forming protein-protein interactions, having a purely structural role in maintaining the protein fold. The electrostatic potential of the tankyrase-1 zinc-binding motif is positive, indicating that it could interact with a negatively charged partner, such as DNA.[37]

1.3.2 Structure and properties of tankyrase-2.

Tankyrase-2 (PARP-5b; ARTD-6) was discovered in 2001.[48,49] It was shown that this isoform is encoded by a different gene in human chromosome 10, a 66-kilobase-pair gene *TNKS2*, containing twenty-eight exons, which expresses a 6.7 kilobase mRNA and a 1166-amino-acid protein. Structurally, tankyrase-2 shares more than 80% identity with tankyrase-1, lacking only the HPS motif (Figure 4).[40] The isoforms are 89% identical in the catalytic site. The variable residues are allocated away from the active site, as is common for the enzymes catalysing the same reaction on the same substrate.[48] The isoforms also share multiple cellular localisations: nucleus, Golgi vesicles, centrioles. Tankyrase-2, like tankyrase-1, interacts with TRF1 in yeast. However, tankyrase-2 shows a special property when overexpressed: it induces human cell death due to the loss of mitochondrial membrane potential, featuring some signs of necrosis. This process can be inhibited by the pan-PARP inhibitor 3AB.[23,48] This significant difference between the properties of the two isoforms points to a serious dissimilarity in their regulation or functions. Moreover, tankyrase-2 may be a more easily activated isoform.[48] To sum up, tankyrase-1 and tankyrase-2 have both differences and similarities, which might be interesting for their selective inhibition.

1.3.3 Mechanism of action of the tankyrases and involvement in the different physiological processes.

Tankyrases, like other members of the PARP family of enzymes, use NAD^+ as a substrate for poly(ADP-ribosyl)ation.[20,21] The PARP-enzyme binds substrate NAD^+. The positively charged nicotinamide acts as a leaving group, expelled by the lone pair from the ribose oxygen (Scheme 1, A). This generates an intermediate electrophilic oxonium ion which is attacked by a nucleophilic carboxylate of an acceptor protein (initiation reaction) or a ribose secondary alcohol (elongation reaction) (Scheme 1, B). As a result, an ADP-ribosylated protein is produced. Further ADP-ribose units are added through reaction of secondary alcohols of the ribose units of the growing chain (Scheme 1, C).[20] Tankyrases are overexpressed in cancer cells and show a minute presence in normal somatic cells. Different substrates for tankyrases, with which they interact through the Ankyrin domain, are summarised in Table 3.

Recently, it was shown that *Herpes simplex* virus (HSV) requires PARsylation by tankyrase-1 for efficient replication.[50] In the early stage of the infection, HSV induces phosphorylation of tankyrase-1 and the modified enzyme colocalises with the viral protein ICP0 in the HSV nuclear compartment. Interestingly, tankyrase-2 remains intact during the infection but, in the absence of tankyrase-1, can take its place in the process. It was shown that HSV could not replicate efficiently in the absence of tankyrases. Inhibition of tankyrase-1/2 with 3-AB led to significant decrease of viral titres.[50]

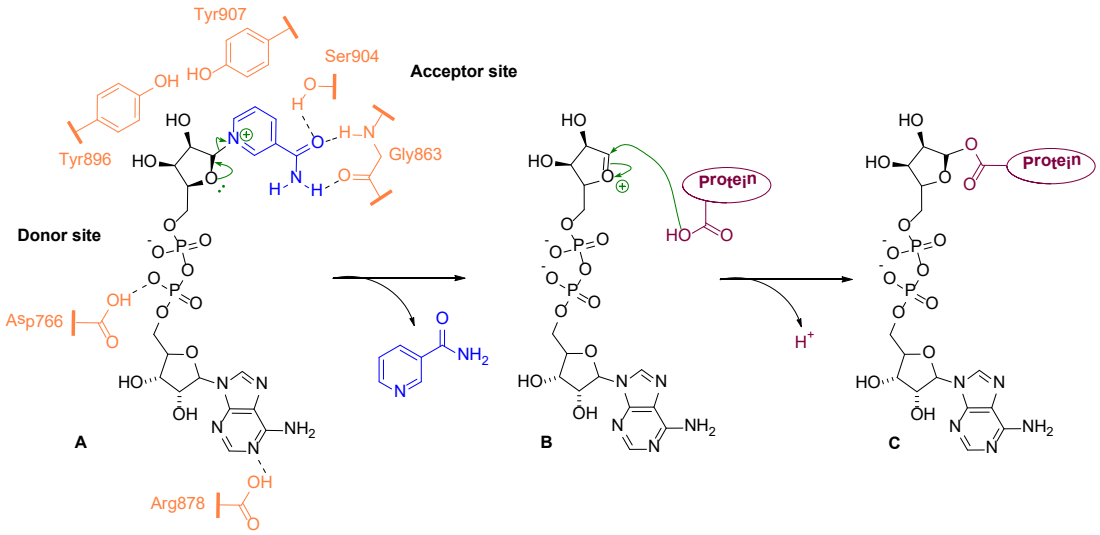

Scheme 1. Chemical mechanism of poly(ADP-ribosyl)ation.

Table 3. The major acceptors of tankyrase-mediated PARsylation and the processes in which they are involved.

Partner protein	Process
TRF1	DNA replication[38]
NuMA	Mitosis[22]
Axin1/2 / BLZF1 / CASC3	*Wnt* signalling pathway[60]
Miki	Mitosis[55]
PI31	Proteasome regulation[56]
3BP2	Cherubism[51,52]
Grb14	GLUT vesicles trafficking[49,53,54,61]
IRAP	GLUT4 migration[49,53,54,61]
TAB182	Not known[62]
Mcl-1	Apoptosis[57]
ICP0	*Herpes simplex* virus infection[50]
EBNA1	Epstein-Barr virus DNA replication[59]
FBP17	Cytoskeletal regulation[63]

In 2011, it was proven that tankyrase-2-mediated destruction of an adaptor protein is a key factor in the development of cherubism. Cherubism is an autosomal-dominant syndrome, marked by severe bone inflammation, which results in symmetrical deformation of facial bones, loss of teeth and distortion of the orbital socket. It is caused by the mutations in the gene encoding the adaptor protein 3BP2. However, the exact mechanism of 3BP2 causing the bony lesions remains fairly unclear. It was noticed that 3BP2 stability is regulated *via* the poly(ADP-ribosyl)ation activity of the tankyrases.[51,52]

One of the first discoveries on the field of tankyrase activity was the fact that tankyrases interact with GLUT4 vesicles, especially with insulin-responsive amino-peptidase (IRAP). This binding involves ankyrin repeats in tankyrase-1/2 and a certain sequence

of amino-acids (^{96}RQSPDG^{101}) in the IRAP. When stimulated by insulin, tankyrase-1/2 undergoes phosphorylation by mitogen-activated protein kinase (MAPK), which enhances its PARsylation activity. GLUT4 trafficking depends on the presence of IRAP; therefore tankyrases regulate it through their PARP activity.[53,54]

An essential initial event in mitosis is, as it seems, the PARsylation of a special protein Miki, carried out by tankyrase-1. Modified Miki then translocates to mitotic centrosomes, which leads to the next mitotic phase, prometaphase. Thus, inhibition of tankyrase-1 results in damaged or altered chromosomes.[55]

Tankyrases appear to be involved in the regulation of the proteasome complex. The proteasome is a special ubiquitin-based protein-degradation system, which plays an essential role in cellular homeostasis. The 26S proteasome is a large protease complex, which consists of a catalytic 20S subunit and a 19S regulatory particle. The assembly of this proteasome is tightly regulated by a number of different proteins. One of these proteins, PI31, is PARsylated by tankyrases. This posttranslational modification of PI31 dramatically reduces the affinity of this protein for binding to the 26S proteasome. This stimulates the assembly of the proteasome and overactivates it. Interestingly, inhibition of the tankyrases blocks overactivation of the proteasome, but not its basal activity.[56]

Another tankyrase binding partner, Mcl-1 (myeloid cell leukemia 1 protein) does not accept PARsylation mediated by tankyrase-1. Moreover, it inhibits PARsylation of other tankyrase partners *in vitro*, as well as auto-PARsylation of tankyrase-1.[57,58]

Tankyrases were found to be encoded in and replicated by the origin plasmid of Epstein-Barr virus (EBV).[59] It was speculated that their function in EBV was similar to the one in humans. It was involved in protection of telomeres and was associated with viral protein EBVA1, an analogue of human TRF1 (see below). The main function of this complex is believed to be protection of the viral genome from host-mediated destruction.[59]

In general, tankyrases are involved in normal cellular metabolism much less than in tumourigenesis and growth. This provides an interesting opportunity for rational anti-cancer drug design.

The three major partners of tankyrases, TRF1, NuMA and Axin1/2, involved in carcinogenesis, are reviewed below.

1.3.4 Telomeres, telomerase and the tankyrases.

Tankyrase-1 was initially identified as a component of the telomeric complex. Telomeres are special protective structures at the ends of linear chromosomes (Figure 5).[64] This complex represents a combination of 5 to 15 Kb (up to 30 Kb in some cells) of TTAGGG repeats and proteins. The ends of the telomeres carry single strands of 130 to 210 bases of TTAGGG repeats, called G-strand overhangs. It appeared that the disruption of these structures resulted in dysfunction of the telomeres.[65]

Figure 5. Schematic representation of chromosomes with (left) and without (right) telomeres.

G-rich telomeric strands can form four-stranded conformations called G-quadruplexes and higher order structures called T-loops (Figure 6). These structures may protect the single-stranded termini from being converted back into a double strand.[66] The proteins in the telomeric complex also are involved in its stability. Several telomere-binding proteins have been identified so far. Six of them form a so-called shelterin complex, which can be found in the T-loop: TRF1 and TRF2 (Telomeric Repeat-binding Factors), TIN2 (TRF-Interacting Nuclear protein), POT1 (Protection Of Telomeres), RAP1

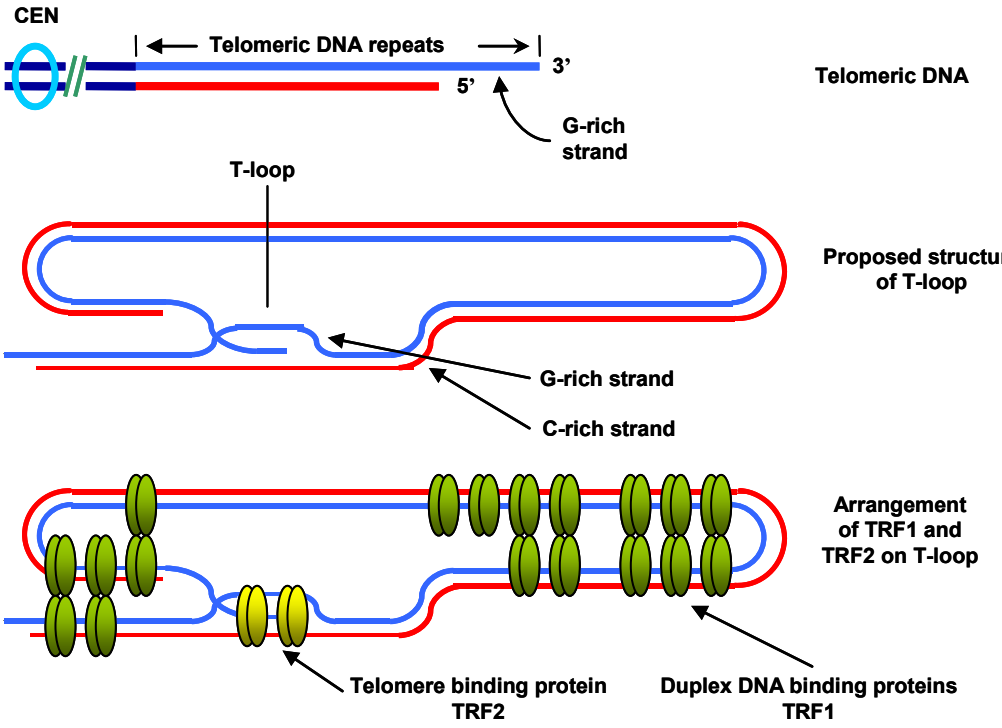

Figure 6. Structure of the T-loop. The T-loop occurs in telomeric DNA and consists of a complex of DNA-binding proteins, which maintain telomere in a well-packed state. Abbreviations: CEN, centromere.

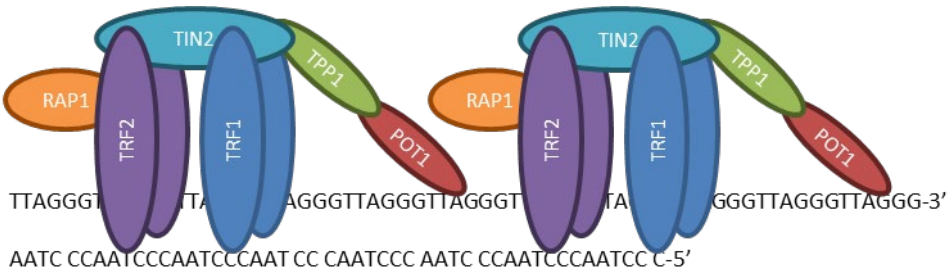

Figure 7. Structure of the telomere with the shelterin complex.

(Repressor/Activator Protein) and TPP1 (TIN2 and POT1 interacting Protein) (Figures 6, 7).[66-69] Their telomeric roles are summarised in the Table 4.

Telomeres, as protective structures at the ends of linear chromosomes, have two functions. Firstly, since replication of DNA during the S-phase of the cell cycle cannot copy right to the end of the chromosome (the so-called "end-replication problem"), they provide a length of non-coding DNA which shortens at each cell division by 50 to 200 bp.[64] This is used by the body to "count" the number of cell divisions. After around eighty divisions, telomeres reach the length of 5 to 7 Kb (known as Hayflick limit) and the cell switches into apoptosis.[64,66] Secondly, they prevent the ends of the chromosomes being recognised by the repair machinery as a "double-strand break", thus avoiding inappropriate fusion of chromosomes.[64]

Table 4. Functions of the shelterin complex proteins.

Function	**Proteins**
Recombination[65,67]	TRF1, TRF2, TIN2, TPP1, RAP1
G-strand protection[71,72]	POT1
Length regulation[65,67]	TRF1, TRF2, TIN2, TPP1, RAP1
Inhibition of DNA damage response[65,67,73,]	TRF1, TRF2, POT1, RAP1
Telomere replication[74,75]	TRF1
Telomerase recruitment[76,77]	TPP1

In development of organisms, in stem cells and in cancer, enhanced cell-division accelerates shortening of the telomeres. Consequently, these cells often have shorter telomeres, compared to cells in normal tissues; however, they are not short enough to activate apoptosis. These actively dividing cells have an enzyme, telomerase, to regrow

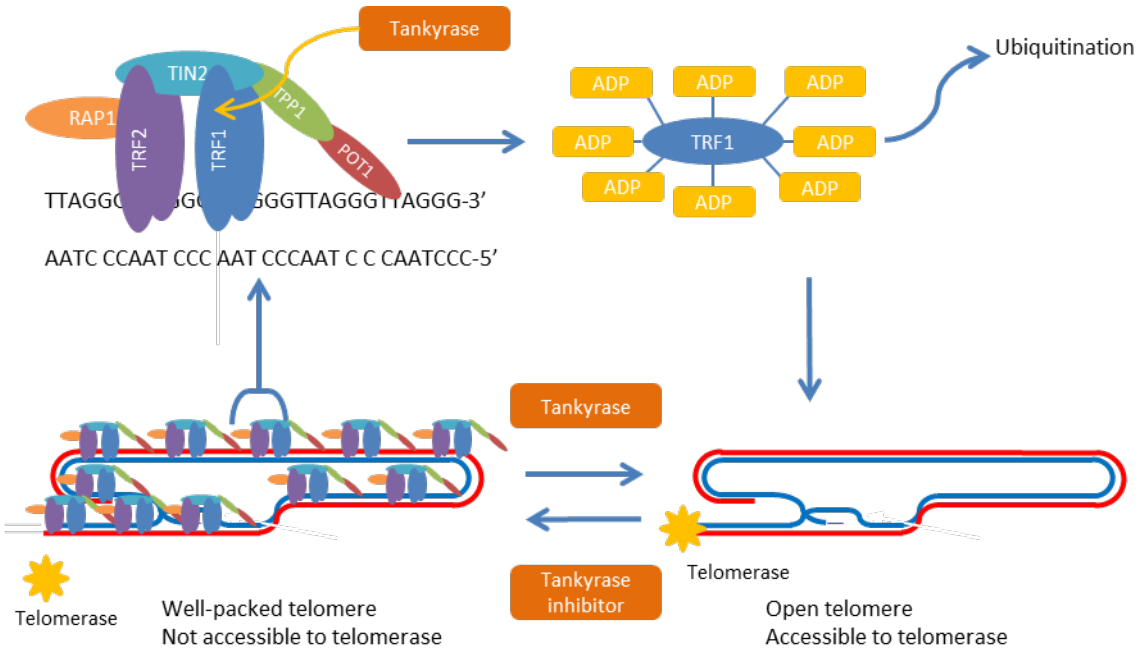

Figure 8. Mechanism of action of tankyrase in telomeres.

the telomere between divisions. This enzyme belongs to a reverse transcriptase family. Telomerase is a ribonuclear complex consisting of two major components: telomerase RNA (TR) and a telomerase-reverse transcriptase protein (TERT) – the catalytic subunit. Telomerase elongates the 3'-end of the G-rich strand of a telomere by adding TTAGGG repeats.[64] Cancer cells bypass the telomere-shortening crisis by activating telomerase. Telomerase activity has been detected in *ca.* 85% of human cancers.[66,70] However, cells have a natural mechanism for regulating the activity of telomerase. It can elongate telomeres only if they are free from the shelterin complex. The TRF1 protein of this complex binds to the telomere and blocks access of telomerase to the target DNA.[64] Cancer cells must have elaborated a mechanism to dissociate TRF1 from telomeres.

Cancer and other actively proliferating cells deactivate the TRF1 protein by poly(ADP-ribosyl)ation (see Scheme 1). Tankyrase-1 or -2 binds to TRF1 with the ARC V in its ankyrin domain and poly(ADP-ribosyl)ates TRF1.[62] The latter loses its ability to bind to DNA because of a dramatic change of its charge.[38,39] Tankyrases also induce proteasome-mediated degradation of TRF1. It was shown that poly(ADP-ribosyl)ated TRF1 is ubiquitinated *in vivo* and *in vitro*.[78,79] This step is crucial, because, if TRF1 is not destroyed by the ubiquitinating machinery, it can reassociate with telomeres even in presence of tankyrases.[78,79] Next, the telosomal complex opens and telomerase gains access to telomeres (Figure 8). When tankyrases are inhibited, TRF1 remains

unchanged and remains bound to DNA. This leads to shortening of telomeres and, consequently, to death of the cancer cell.

1.3.5 The tankyrases in mitosis.

It was shown that tankyrase-1 has some important roles not only in telomeres, where it was initially discovered, but also at spindle poles.[80,81]

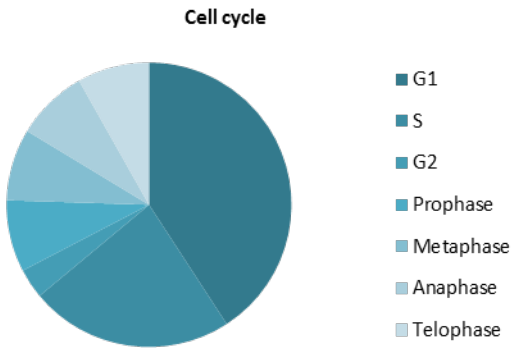

Figure 9. The life cycle of a cell dividing with mitosis.

Mitosis is an asexual cell division process. In this process, the cell initially doubles its DNA, separates the chromosomes and forms two identical nuclei; this is followed by the separation of the cytoplasms. A simplified cell cycle, which includes mitosis, is described below (Figure 9):

1) *Interphase*
    a) *G1* – cell grows.
    b) *S* – the cell duplicates its DNA and centrosome.
    c) *G2* – cell grows.
2) *Mitosis*
    a) *Prophase* - chromatin condenses in the chromosomes; the nucleoli disappear.
    b) *Prometaphase* – nuclear membrane breaks down;
    c) *Metaphase* – chromosomes line up along the imaginary metaphase plane.
    d) *Anaphase* – chromosomes break down at centromeres, which form sister chromatids. Sister chromatids move to the opposite poles of the cells.
    e) *Telophase* – nuclear membrane and nucleoli reappear.
    f) *Cytokinesis* – the cell splits into two (division of the cytoplasm).

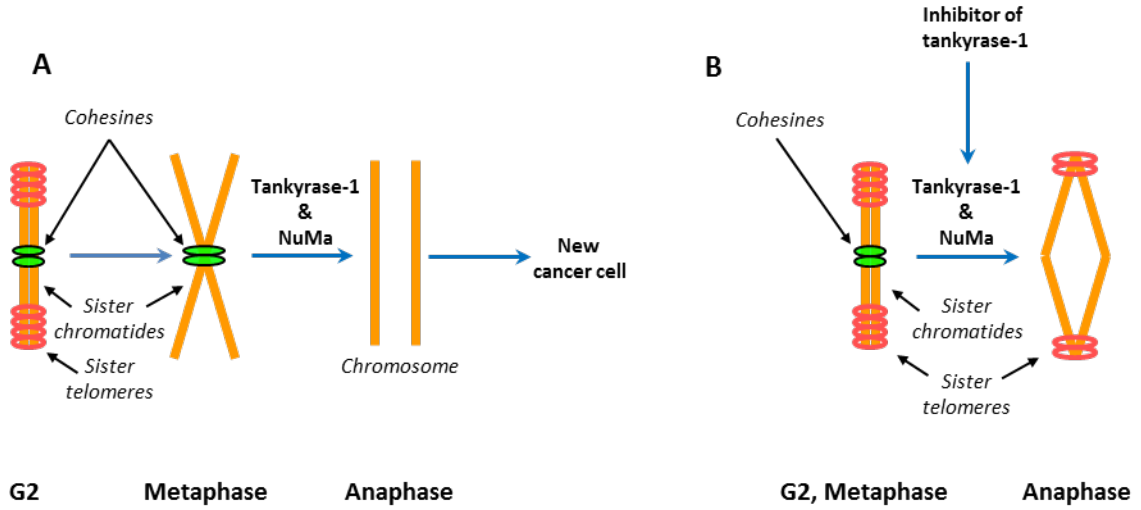

Figure 10. Role of tankyrases in the mitotic process. **A**, when tankyrase is active, it favoures cell proliferation; **B**, tankyrase, deactivated by an inhibitor, cannot take part in cell division, leading to mitosis arrest.

NuMA (Nuclear Mitotic Apparatus protein) is a large coiled-coil protein, found in both proliferating and differentiated cells. It has a globular head and tail domains, separated by a 1500-amino acid α-helical domain. This protein has key roles in the mitosis, post-mitotic reassembly of the nucleus and some interphase processes. When the nuclear envelope opens before mitosis, NuMA moves to the cytoplasm, binds to the microtubules and concentrates with them at the pericentrosomal region.[82] From prophase to anaphase, tankyrase-1 binds to NuMA, PARsylates it and moves with it towards the spindle poles.[80,81] The spindle includes mostly DNA and some proteins, but also other macromolecules, including RNA and lipids. It was shown that tankyrase-2 also has the ability to bind to NuMA and to co-localise with it, but apparently the endogenous level of tankyrase-2 is not enough to PARsylate NuMA.[22] In the absence of tankyrase-1 activity, NuMA still localises to spindle poles but the sister telomeres fail to separate and cells arrest in anaphase (Figure 10).[22] Therefore, tankyrase-1 catalytic activity is crucial for the dividing cells.[83]

1.3.6 The tankyrases in *Wnt* signalling.

Another target for the tankyrases is β-catenin, a component of the *Wnt*-signalling system. Normally, the cytoplasmatic level of β-catenin remains quite low. It was found that, in many tumours, particularly in colorectal cancers, β-catenin is abundant both in the cytoplasm and the nucleus.[84-86] Constantly activated *Wnt* signalling leads to an excessive stem cell proliferation, which is one of the factors of tumourigenesis.[84,85]

Wnt signalling is an evolutionarily conserved signalling cascade with essential roles during development and in maintenance of adult stem cells. A simplified canonical (which interacts with β-catenin only) *Wnt* pathway is represented in Figure 11. This signalling is regulated through the controlled degradation of β-catenin in the cytoplasm. In the absence of *Wnt* (Figure 11.A), β-catenin is constantly degraded by a special "destruction complex". This complex consists of several proteins: APC (*adenomatous polyposis coli* gene product), CK1 (casein kinase 1), GSK3 (glycogen synthase kinase 3) and the scaffolding protein axin. Axin uses different domains to interact with all members of the destruction complex. CK1 and GSK3 phosphorylate Ser^{45}, Thr^{41}, Ser^{37} and Ser^{33} at the *N*-terminus of β-catenin, which allows the latter to be recognised by β-Trcp, an E3 ubiquitin ligase subunit. Thus, phosphorylated β-catenin undergoes proteosomal degradation. This process prevents β-catenin from penetrating the nucleus and reaching the *Wnt* target genes.

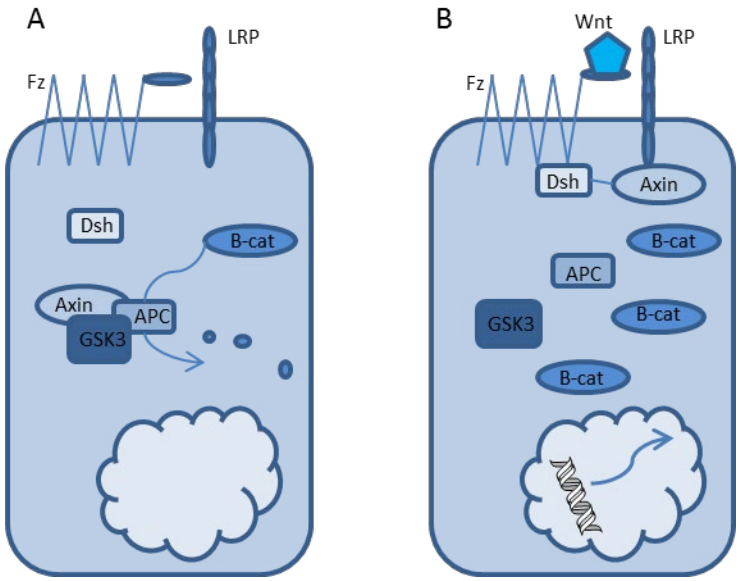

Figure 11. A canonical *Wnt* pathway; **A**, without *Wnt*; **B**, in presence of *Wnt*.

On the cell surface, there is a special complex of Frizzled (Fz) receptor and low-density lipoprotein receptor-related protein (LRP). The Fz receptor is a seven-transmembrane-domain protein with a long *N*-terminal extension (Cys-rich domain). *Wnt* binds directly to the Cys-rich domain of Fz. The receptor complex transduces the signal to a system of cytoplasmatic proteins (Figure 11.B). This leads to the inhibition of the destruction complex. Therefore, β-catenin is not phosphorylated by GSK3 and CK1 and cannot be recognised by the proteasome. Non-destroyed β–catenin reaches the nucleus and activates expression of target genes.[84-87]

The concentration of axin is a rate-limiting factor that regulates the efficiency of the destruction complex.[88] Overexpression of axin induces degradation of β-catenin in cell lines (Figure 12.A). Therefore, stabilisation of axin would provide a mechanism by which to stimulate degradation of β-catenin in the presence of *Wnt*.

It was found that both tankyrase isoforms destabilise axin by poly(ADP)ribosylating it

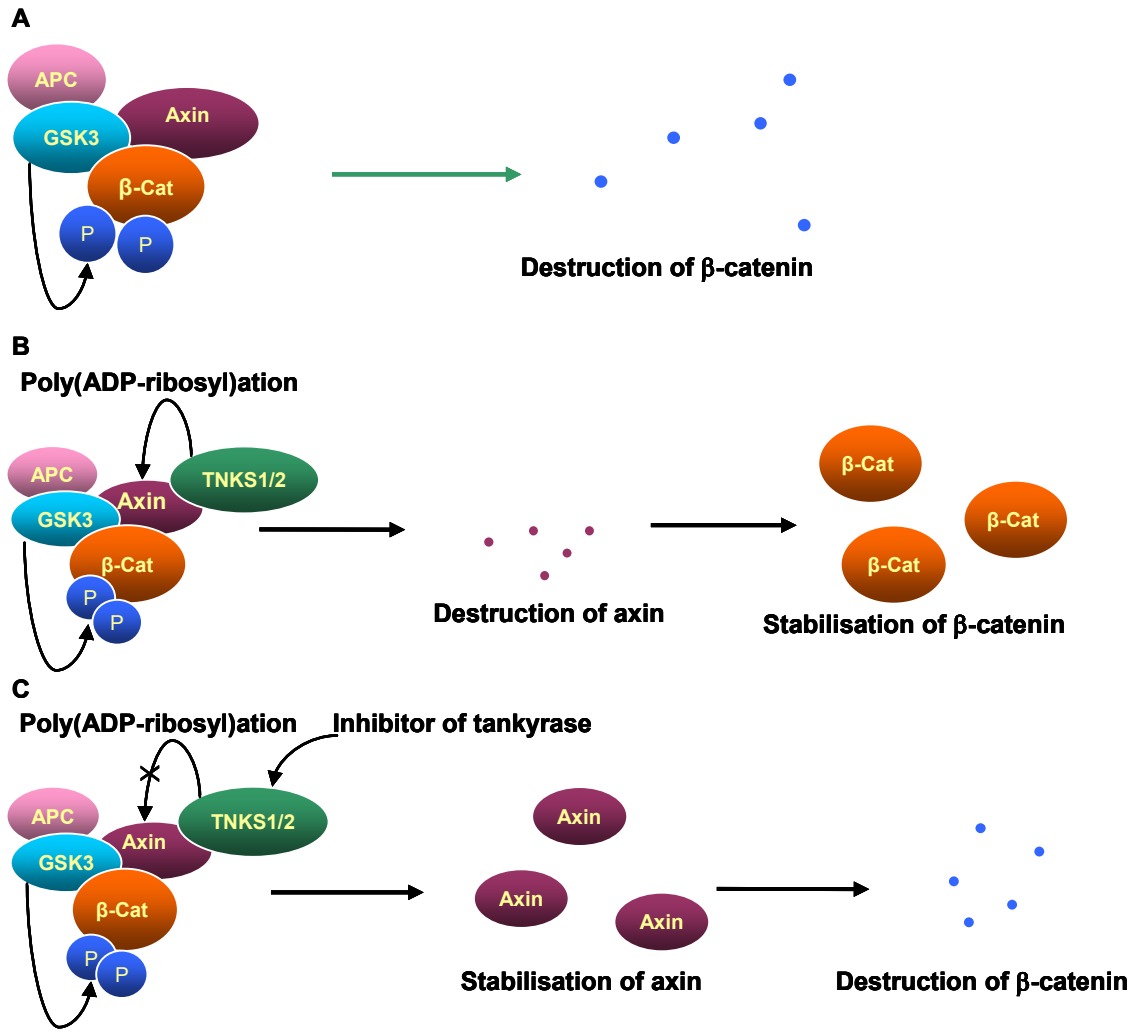

Figure 12. A. Action of axin in the *Wnt* signalling system. **B.** Tankyrase poly(ADP-ribosyl)ates axin, leading to its destruction and stabilisation of β-catenin. **C.** Effect of tankyrase inhibitor.

(Figure 12.B).[89,90] Axin contains two tankyrase-binding domains, which simultaneously bind to ARC II and III of the tankyrases Addition of several ADP-ribose units, induced by the tankyrases, modifies axin, which leads to its ubiquitinylation and degradation.[91] Hence, inhibition of tankyrase would lead to β-catenin degradation, induced by stabilised axin[87] (Figure 12.C). Indeed, it was found that stabilisation of axin by blocking tankyrase results in inhibition of the whole *Wnt* pathway.[60]

1.4 PARP inhibitors.

Some groups of known inhibitors of PARPs, as well as inhibitors of major tankyrase-recruiting targets, are reviewed below.

1.4.1 Structure-activity relationship.

The inhibition of PARPs, especially of PARP-1, has been widely studied since the 1990s. It has two potential therapeutic benefits. Firstly, PARP-1 and PARP-2 inhibitors may act as chemopotentiators. Many anti-cancer agents cause damage to DNA as a rapid mechanism to destroy cancer cells. The PARP-1-induced DNA repair machinery is one of the key drivers of resistance to cytotoxic drugs. Therefore, inhibition of PARP-1 would lead to a disruption of this mechanism and, combined with DNA-damaging agents or radiotherapy, to cell death. Secondly, PARP-1 inhibitors may be used as a stand-alone therapy in those tumours, whose cells lack in other types of DNA repair systems.[92-94] Breast cancer associated genes *BRCA1* and *BRCA2* play a pivotal role in the repair of double strand breaks (DBS) through a process called homologous recombination (HR). The inhibition of PARP-1 leads to the increase of single strand breaks (SSB) and, *via* replication fork collapse, to DBS. If the cell is HR-deficient, the increase of DSB would lead to genomic instability, resulting in the cell death. This phenomenon is known as synthetic lethality: the loss of one gene function results in cell liability, but the loss of both is lethal.[96] Therefore, PARP-1 inhibitors could be used in *BRCA1/2*-deficient cells.[92,97,98] The first crystal structures of a PARP protein (the catalytic fragment of chicken PARP-1), with and without a nicotinamide-mimicking inhibitor, 3-aminobenzamide **2** (Figure 13), were described by Ruf *et al*. in 1996.[99] It was shown that the inhibitor forms one hydrogen bond between the amide N-H and the carbonyl of Gly^{863} and two from the amide C=O to the OH of Ser^{904} and to the N-H of Gly^{863} of the protein.

This was similar to the way in which the nicotinamide part of NAD^+ was binding to the enzyme. Hence, most inhibitors of PARPs contain a benzamide pharmacophore, mimicking the nicotinamide moiety of NAD^+ and binding to the donor site of the enzyme. It was proved by the co-crystal structures that the amide group of such inhibitors interacts with Ser^{904} and Gly^{863}, while the aromatic ring forms π-π interactions with Tyr^{907} and Tyr^{896} (see Scheme 1).[10] These hydrogen bonds require the carboxamide group of the inhibitor to be in the *anti*-conformation **1a** rather than in the *syn*-conformation **1b** (here *anti* refers to the conformation about the Ar-carbonyl bond). However, there is an equilibrium between these two conformations (Figure 13). A PARP-1 pharmacophore is presented in Figure 14.

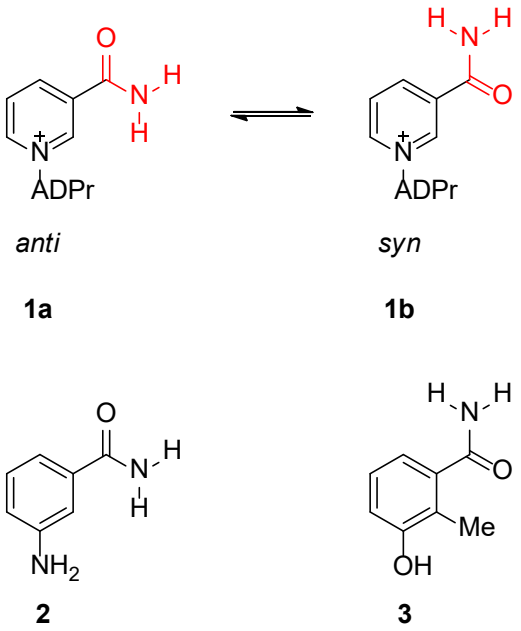

Figure 13. Top: *anti* and *syn* conformations of the nicotinamide amide in NAD^+, the substrate for PARPs. **Bottom:** examples of early inhibitors of PARP-1. Compound **2** (3-aminobenzamide, 3-AB, IC_{50} = 33 mM)[95] can readily adopt the required *anti*-conformation, whereas the *ortho*-methyl group in **3** (IC_{50} = 590 mM)[95] precludes this arrangement.

The conformational flexibility of the carboxamide was a possible reason for the low potency of some early inhibitors of PARP-1, such as 3-substituted benzamides **2** and **3** (Figure 13). Therefore, constraining the free rotation and leaving only the biologically active *anti*-conformation of the carboxamide group should increase the potency of inhibition of PARPs. This could be achieved either by intramolecular hydrogen bonding or by containing the amide in a lactam ring.[95] All existing inhibitors of PARP-1 catalytic activity can be classified into hydrogen-bonded carboxamides, bicyclic lactams, tri- and tetracyclic lactams and structures lacking the lactam.

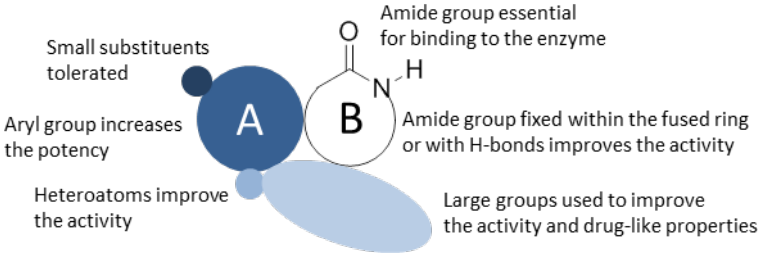

Figure 14. PARP-1/2 pharmacophore.

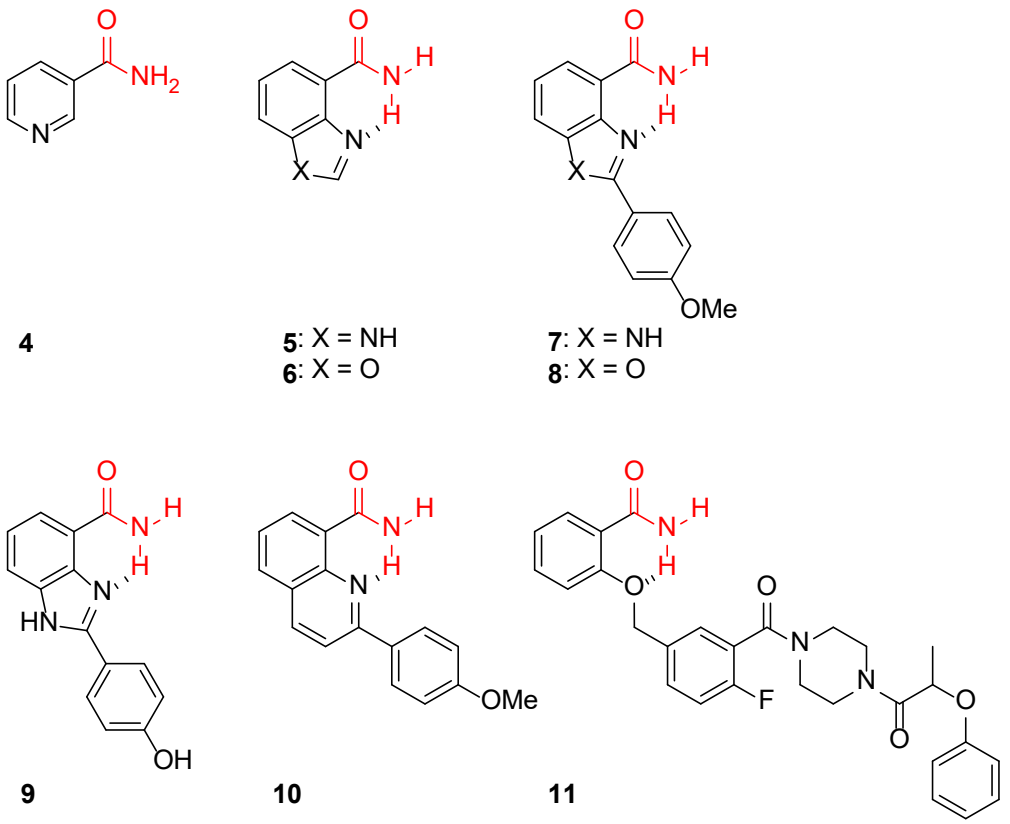

Figure 15. Structures of carboxamide inhibitors of PARP-1 activity: A starting point – nicotinamide **4** (IC_{50} = 210 μM)[92]; Intramolecularly hydrogen-bonded amides **5** (K_i = 95 nM),[92] **6**, **7** (IC_{50} = 60 nM),[95] **8** (IC_{50} = 1.1 μM),[95] **9** (K_i = 6 nM),[95] **10** (IC_{50} = 1.1 μM),[100] **11** (IC_{50} = 5 nM). [101]

1.4.2 Carboxamide PARP inhibitors.

The programme of design of inhibitors of PARP-1 started in the 1980s from two simple structures, 3-aminobenzamide (**2**, Figure 13) and nicotinamide (**4**, Figure 15).[92] Considering the facts mentioned above, active carboxamides possess an amide group stabilised in the *anti*-conformation with hydrogen bonds. This group includes benzimidazole-4-carboxamides, benzoxazole-4-carboxamides and quinoline-8-carboxamides (**5 - 10**, Figure 15).[95,100]

A special group of compounds, featuring both hydrogen bonding and a bicyclic core, was designed by the Griffin group at the University of Newcastle. In this scaffold (**5 - 9**, Figure 15) there is either a benzoxazole-4-carboxamide or a benzimidazole-4-carboxamide.

The heterocyclic nitrogen atom acts as an intramolecular hydrogen bond acceptor to the hydrogen atom of the NH group in benzoxazole. This leads the amide to adopt an *anti*-conformation, favouring outstanding inhibition of PARP-1.[92,102]

Another scaffold, 2-benzyloxybenzamides (**11**, Figure 15), which used intramolecular hydrogen bonding, was developed by KuDOS / AstraZeneca.[92,101] A *pseudo*cycle, which fixed the amide in the desired conformation, was formed by a hydrogen bond between the benzyloxy group and the primary amide.

1.4.3 Bicyclic PARP inhibitors.

Bicyclic inhibitors have been proved to be more potent than monocyclic carboxamides.[10] The skeletons of these compounds include isoquinolin-1-ones **12**, dihydroisoquinolin-1-ones **13**, quinazolin-4-ones **14** and phthalazin-1-ones **15**.[95,103] Addition of substituents at position-5 (position-8 for quinazolin-4-ones) and position-3 (position-2 for quinazolin-4-ones) improves the potency (Figure 16).

Very promising compounds were designed, synthesised and evaluated in the Threadgill group at the University of Bath. Quinolin-8-carboxamide **19** and, especially, 2-substituted quinolin-8-carboxamides **20-23** proved to be a potent scaffold for the inhibition of PARP-1. The IC_{50} values obtained for these compounds showed better inhibition of PARP-1, when compared to the standard inhibitor 5-AIQ (5-aminoisoquinolin **48a**, Figure 21, discussed below).[100]

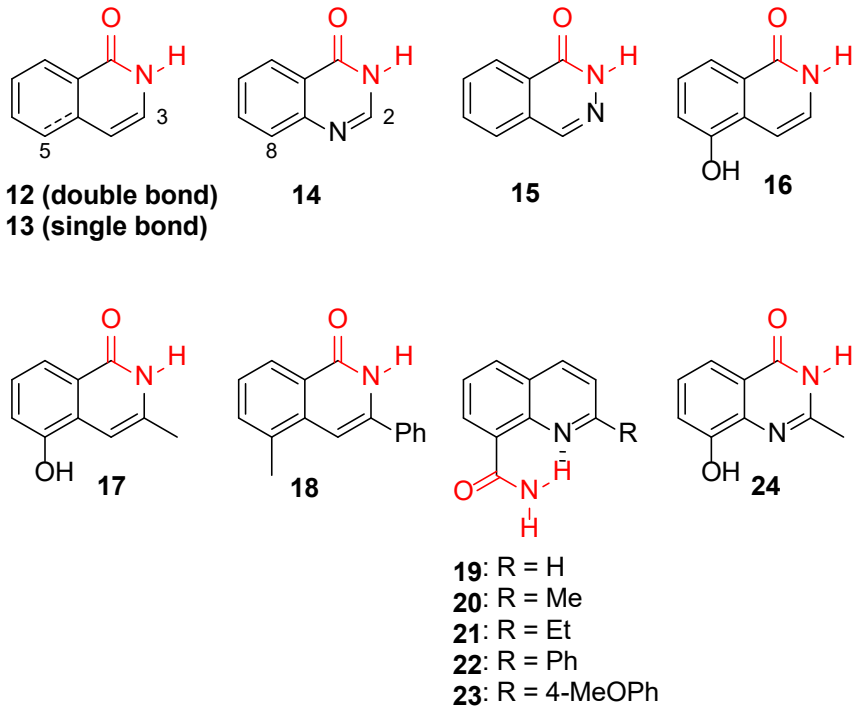

Figure 16. Structures of bicyclic inhibitors of PARP-1 activity: core structures of bicyclic lactams **12** (IC_{50} = 7 μM),[95] **13**, **14** (IC_{50} = 9.5 μM),[95] **15** (IC_{50} = 12 μM)[95], **19-23** and substituted bicyclic lactams **16** (IC_{50} = 0.39 μM),[95] **17** (IC_{50} = 0.4 μM),[95] **18** (IC_{50} = 0.87 μM)[95] and **24** (IC_{50} = 0.44 μM).[92]

Compound **24** was a result of the optimisation of the core structure **14**. Despite potent inhibition of PARP-1 activity *in vitro*, this compound did not achieve the clinical trials stage, presumably, because of a lack of solubility.[92]

An interesting optimisation was performed on the drug candidate **25** (Olaparib, Figure 19, KuDOS / AstraZeneca). An addition of the second ring instead of hydrogen-bond-formed *pseudo*ring did not influence on the activity. In contrary, it resulted in increased solubility and improved oral bioavailability.[92,97] This structure is discussed further as a member of clinical trials.

1.4.4 Tri- and tetracyclic PARP-1 inhibitors.

Tri- and tetra-cyclic lactams are represented by a wide range of fused isoquinolinones and phthalazinones (**26**-**28**, Figure 17). On one hand, introduction of the extra rings increases the potency of inhibition of PARP-1 but, on the other hand, such planar structures are poorly water-soluble. This is overcome by introduction of an acidic or basic substituent to the core structure (shown in green, Figure 17).

An interesting structure was presented by Agouron/Pfizer, a [5,6,7]-tricyclic indole lactam **29**.[92,104] The optimisation of this compound has led to the development of a clinical candidate, which is discussed further below.

Another drug candidate, which structure has not been disclosed yet, was developed by

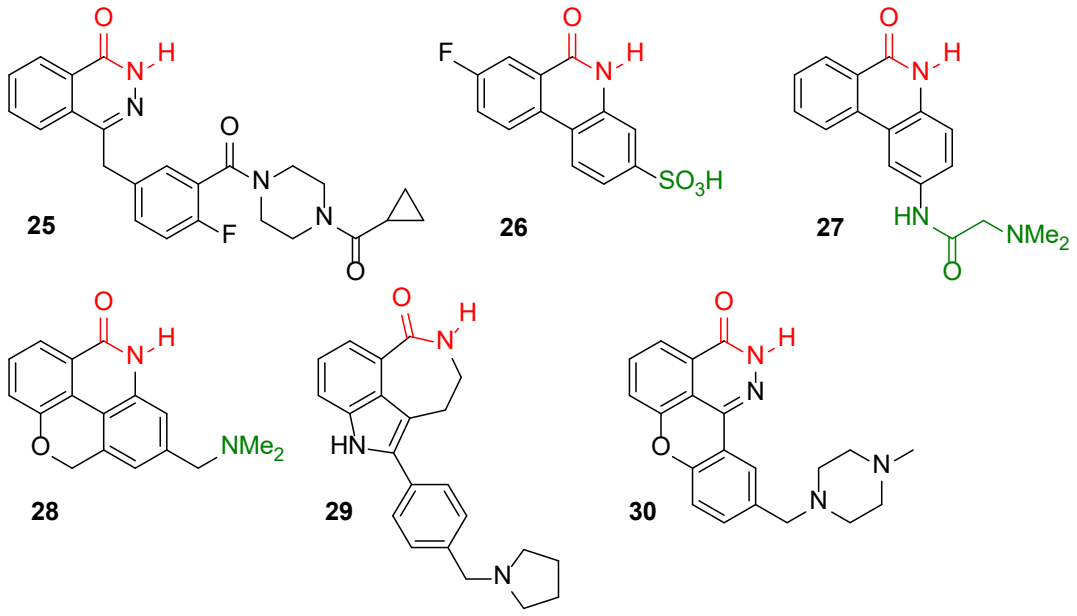

Figure 17. Structures of tri- and tetra-cyclic lactam inhibitors of PARP-1: **26** (IC_{50} = 10 nM),[95] **27** (IC_{50} = 20 nM),[95] **28** (IC_{50} = 17 nM),[95] **29** (K_i = 5.6 nM),[92] **30** (IC_{50} = 31 nM).[92]

Guilford / MGI Pharma. Presumably, it is similar to another lead compound, **30** (Figure 17), which was a result of the optimisation of core structure **28**.[92,105] It exhibited promising chemopotentiating activity together with temozolomide against brain cancer and together with cisplatin against murine leukaemia.

1.4.5 PARP-1 inhibitors without the lactam moiety.

There are a few examples of PARP-1 inhibitors, which lack the lactam moiety (Figure 18). Nevertheless, their structures contain either an aldehyde, as in **31**, or a ketone, as in **32**, carbonyl groups that form hydrogen bonds with Gly^{863} and Ser^{904} in the same way as the carbonyls of carboxamide and lactams do. Moreover, phenyl groups form a van der Waals interaction with Gln^{763}.[95] Other examples include compounds **33** (despite having an amide group) and **34**, which interact with the zinc-binding site of PARP-1 instead of the catalytic domain. It was determined that these compounds interact with Arg^{34} and therefore disrupt the interaction of PARP-1 with DNA.

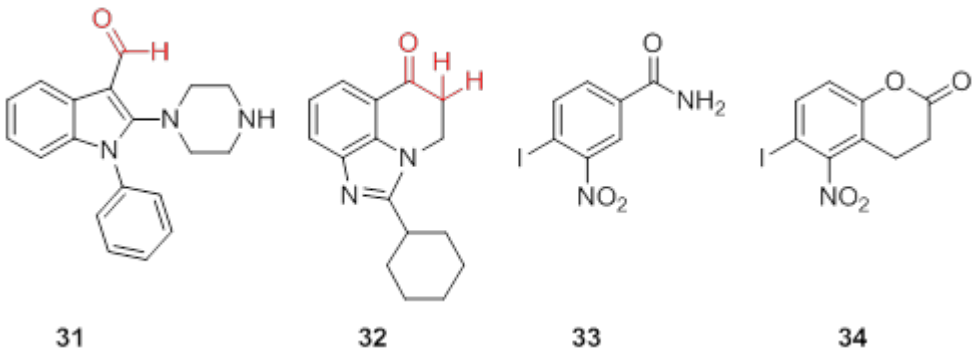

31 32 33 34

Figure 18. Structures of PARP-1 inhibitors lacking the lactam moiety: **31** (IC_{50} = 3.5 μM),[95] **32**,[95] **33, 34** (IC_{50} is estimated to be 50 – 200 μM).[92]

1.4.6 PARP inhibitors in the clinic.

At present, several inhibitors of PARPs are undergoing clinical trials and a number of these are summarised in Table 5.

Veliparib (ABT-888) (**35**, Figure 19), an orally bioavailable PARP-1 and PARP-2 inhibitor (K_i (PARP-1) = 5.0 nM,[106] K_i (PARP-2) = 5.0 nM;[106] EC_{50} = 2.0 nM),[106] is involved in thirty-two ongoing clinical trials in ovarian, breast, colorectal, prostate and liver cancers, together with neurological malignancies and leukaemias.[107]

Table 5. Current data for PARP-1/2 inhibitors in clinical trials.

Company	Compound	Phase I	Phase II	Phase III	Therapeutic indications
BiPar/Sanofi	BSI-201 (**33**)	+	+	+	Triple negative breast cancer
KuDOS/Astra-Zeneca	Olaparib (**25**)	+	+	+	Metastatic breast cancer, advanced ovarian cancer
Abbott	Veliparib (**35**)	+	+		Metastatic breast cancer, metastatic melanoma, brain cancer
University of Newcastle/Pfi-zer	Rucaparib (**36**)	+	+		Metastatic breast cancer, advanced ovarian cancer
Inotek	INO-1001 (not disclosed)	+	+		Malignant melanoma
Cephalon	CEP-9722 (**38**)	+			Advanced solid tumours
Merck	MK-4827 (**42**)	+			Advanced solid tumours

Olaparib (AZD-2281) (**25**, see Figure 17, IC_{50} = 5 nM[108]), an orally active small-molecule inhibitor, was recently employed in Phase II clinical trials. The design of the studies was as follows: a group of fifty-four patients was divided into two cohorts;

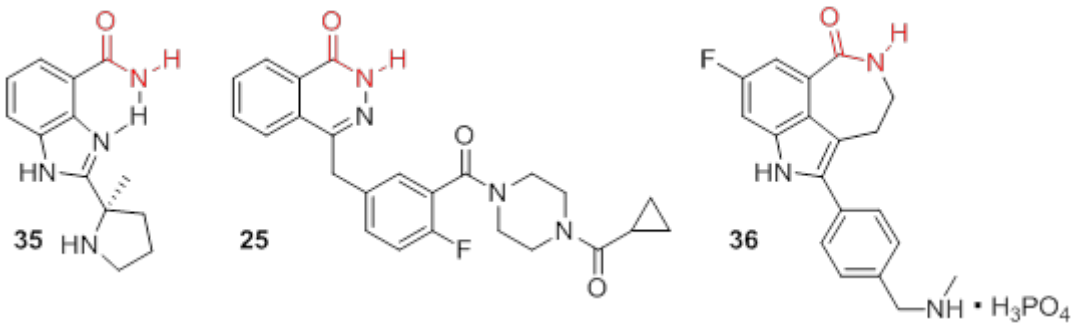

Figure 19. Veliparib (**35**) ($K_{(i)}$ (PARP-1) = 5.0 nM,[106] $K_{(i)}$ (PARP-2) = 5.0 nM;[106] EC_{50} = 2.0 nM[105]), olaparib (**25**) (IC_{50} = 5 nM[101]) and rucaparib (**36**) (K_i = 1.4 nM),[92] three PARP-1/2-inhibitors involved in clinical trials.

twenty-seven patients received 400 mg of olaparib twice daily for 28 days and another twenty-seven patients received 100 mg of olaparib twice daily. The overall response rate was 41% for 400 mg, and 22% for 100 mg. It is should be noticed that adverse effects were relatively mild; the most common were nausea, fatigue, vomiting and constipation.[109]

Rucaparib (AG014699) (**36**, Figure 19), an orally available small-molecule inhibitor, was developed by the University of Newcastle in collaboration with Agouron / Pfizer from the core structure **29** (see Figure 17). Its exceptional activity against PARP-1, combined with good drug-like properties, helped to rapidly transfer it into clinical trials. This drug displayed no toxicity alone or in combination with temozolomide and

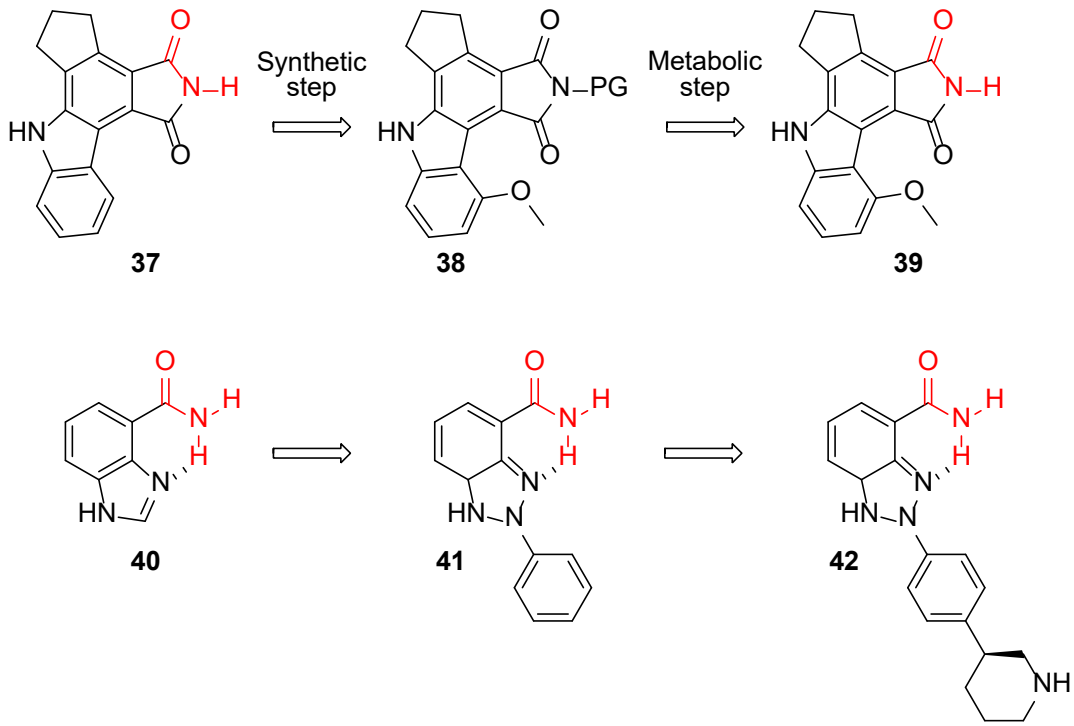

Figure 20. A strategy of synthesis of PARP-1/2 inhibitors, introduced into clinical trials: CEP-9722 (**38**) (PG = CH_2NR_2), a prodrug for **39** (PARP-1 K_i = 20 nM; PARP-2 K_i = 6 nM); MK-4827 (**42**) (IC_{50} = 3.8 nM; EC_{50} = 4 nM).[92]

currently it is in a phase II trial against breast and ovarian cancer.[92,98]

Cephalon used a pyrrocarbazole lactam core to develop their PARP-1 inhibitors. The core by itself (**37**, Figure 20) was already very potent (IC_{50} = 36 nM, K_i = 5 nM).[92] It was proposed that the molecule can form hydrogen bonds not only between its lactam moiety and Ser^{904} and Gly^{863} but also between the indole NH and Glu^{988}. Optimisation led to the compound **38** (Figure 20), with much improved cellular potency and aqueous solubility. This compound was a prodrug for the molecule **39**, which suffered from a lack of solubility. Compound **39** did not show any myelosuppressive effect alone nor in

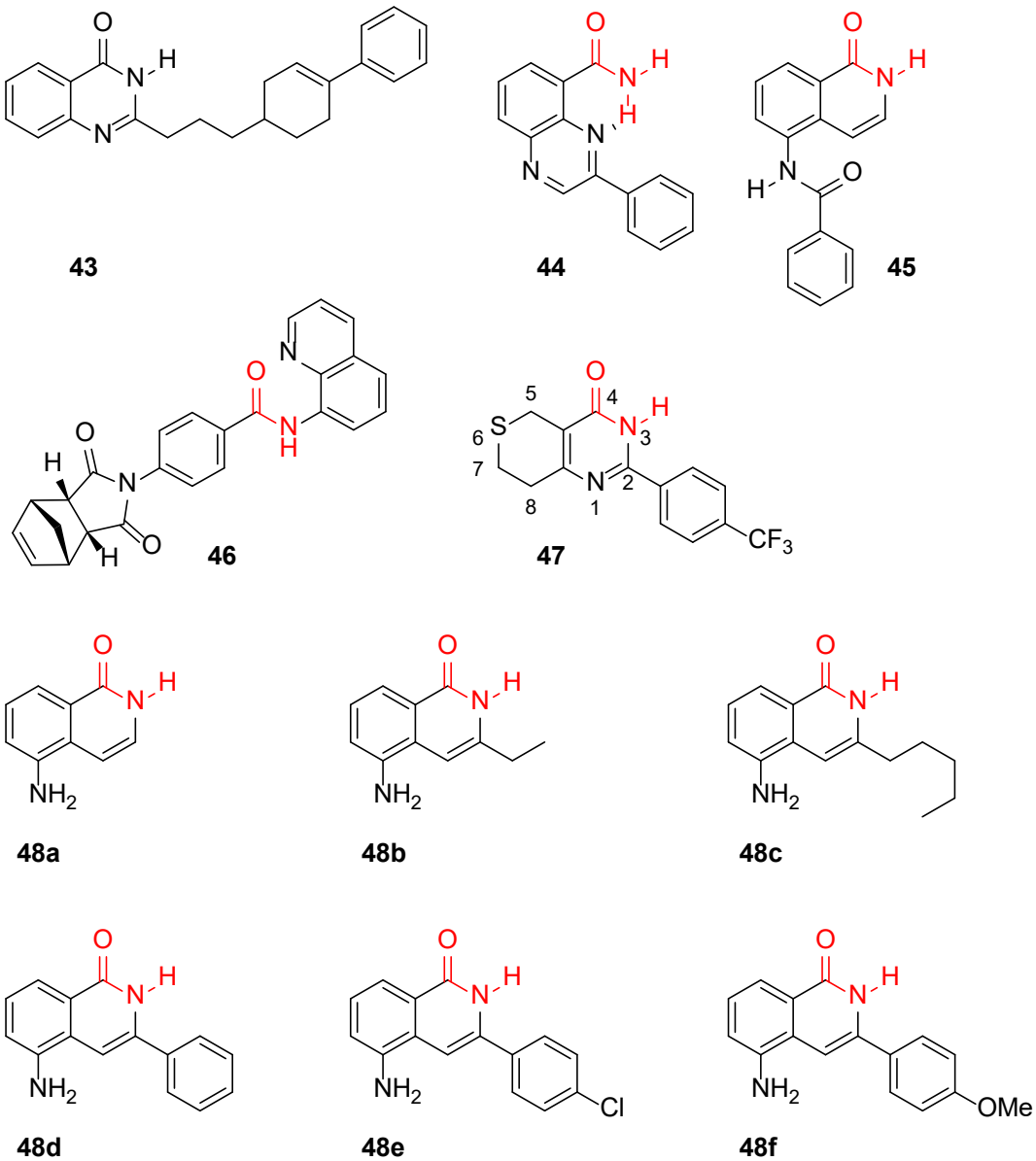

Figure 21. Structures of selective PARP-1 inhibitor **43** (IC_{50} (PARP-1) = 21 nM,[25] IC_{50} (PARP-2) = 608 nM),[25] selective PARP-2 inhibitors **44** (IC_{50} (PARP-2) = 14 nM,[25] IC_{50} (PARP-1) = 131 nM),[25] **45** (IC_{50} (PARP-2) = 1.5 μM,[110] IC_{50} (PARP-1) = 13 μM),[110] tankyrase inhibitors **46** (IC_{50} (tankyrase-1) = 131 nM;[111] IC_{50} (tankyrase-2) = 56 nM),[111] **47** (IC_{50} (tankyrase-1) = 11 nM;[111] IC_{50} (tankyrase-2) = 4 nM)[111] and cytotoxic 3-aryl-5-AIQs **48a-f**.

combination with temozolomide or camptothecin in a human bone marrow cell assay. In May 2009, compound **38** was introduced into phase I of clinical trials.

Merck's drug candidate **42**, a derivative of triazolopyridinecarboxamide **41** (IC_{50} = 24 nM),[92] belongs to indazolecarboxamide core structure **40** (Figure 20). In the light of improved aqueous solubility and a good pharmacokinetic profile, the drug was transferred into phase I clinical trials in 2008.

1.4.7 Selective inhibitors of PARPs.

Very few compounds show selectivity between the various members of the PARP superfamily. Some quinazolin-4-one derivatives **43** are relatively selective for PARP-1 over PARP-2, while quinoxaline derivatives, such as **44**, display selectivity for PARP-2, as does the isoquinoline-1-one **45** (Figure 21).[25,110,111] In the context of modulation of the *Wnt* / β-catenin pathway, some small molecules **46** and **47** were used to inhibit the tankyrase isoforms (see Figure 21).[111] It has been shown that both compounds inhibit tankyrase-1 and -2, as well as PARP-1 and PARP-2, but **47** (XAV939) has less affinity for PARP-1 (K_d (PARP-1) = 1.2 μM;[60] K_d (TNKS-1) = 99 nM,[60] K_d (TNKS-2) = 0.093 μM). [60] Unpublished data from the Threadgill group have shown that, of the library of PARP-1 inhibitors, one subset (the 3-aryl-5-AIQs **48d-f**) were unexpectedly cytotoxic.* Cytotoxicity is not a direct consequence of inhibition of PARP-1, so this observation indicated an additional target for these compounds. Very preliminary data from our collaborator also showed that these compounds inhibited tankyrase-1 activity, with structure-activity relationship paralleling their cytotoxicity (Figure 22).† The lactam is

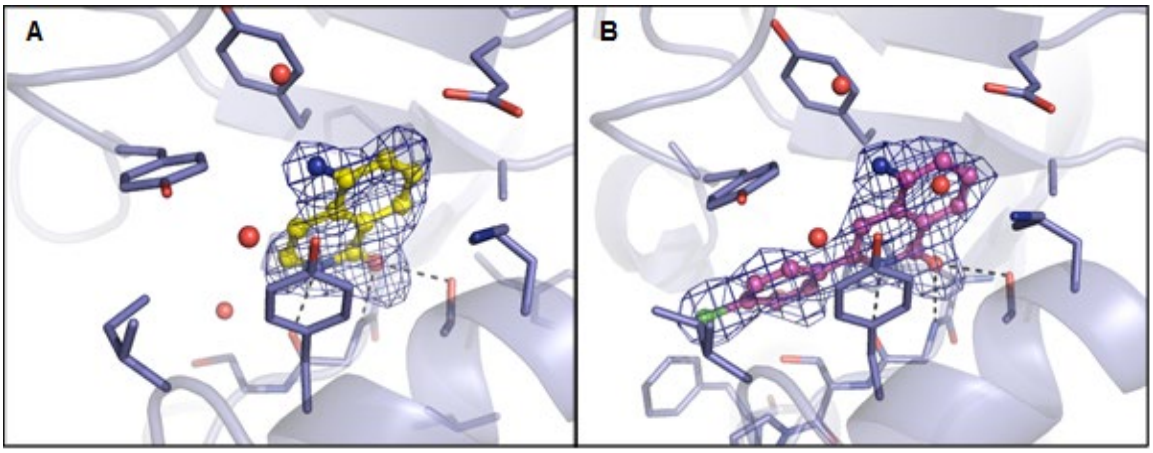

Figure 22. Crystal structures of the catalytic NAD^+-binding domain of tankyrase-2 with 5-AIQ **48a** (A) and 5-amino-3-(4-chlorophenyl)isoquinolin-1-one **48e** (B) bound. We thank Dr. Lari Lehtiö for these unpublished structures and images.

* P. J. Wood, unpublished results.
† L. Lehtiö (University of Oulu, Finland), unpublished results.

Table 6. Preliminary data for cytotoxicity and inhibition of tankyrase-1 by 3-substituted-5-AIQs.

Compound	Tankyrase-1 IC_{50} (μM)	HT29[a] IC_{50} (μM)	MDA-MB-231[b] IC_{50} (μM)	LNCaP[c] IC_{50} (μM)	MOLT4[d] IC_{50} (μM)	FEK4[e] IC_{50} (μM)
3-Ph-5-AIQ **48d**	0.1	2	8	16		52
3-(4-ClPh)-5-AIQ **48e**	*ca.* 0.1	18	11	10		4
3-(4-MeO-Ph)-5-AIQ **48f**	*ca.* 0.5	85	14	34	12	28
5-AIQ **48a**	>10	>200	170	>200	188	>200
3-Et-5-AIQ **48b**	*ca.* 10	>200	101	>200		>200
3-Pentyl-5-AIQ **48c**	*ca.* 0.5	34	23	23		49

[a] Human colon adenocarcinoma cells.

[b] Human breast invasive ductal carcinoma cells.

[c] Human androgen-sensitive prostate adenocarcinoma cells.

[d] Human leukaemic T-lymphoblasts.

[e] Human fibroblasts.

hydrogen-bonded to Ser^{1068} and Gly^{1032} of tankyrase-1. There is a large hydrophobic pocket (with Tyr^{1050}, Tyr^{1060} and Tyr^{1071} in the surface) to the lower left of the isoquinolinone in these structures, in which an aromatic 3-substituent can make π-stacking and hydrophobic interactions. Thus, 3-alkyl-5-AIQ **48a-c** (see Figure 21) were not cytotoxic, whilst 3-phenyl-5-AIQ **48d**, 3-(4-chlorophenyl)-5-AIQ **48e** and 3-(4-methoxyphenyl)-5-AIQ **48f** showed significant cytotoxicity in MTS assays against HT29 (endothelial cells from human colorectal adenocarcinoma), MDA-MB-231 (epithelial cells from human breast adenocarcinoma), LNCaP (epithelium cells from human hormone-dependent prostate adenocarcinoma) and MOLT4 (T-lymphoblasts from human acute T-lymphoblastic leukaemia) cell lines. These compounds have also been tested against the FEK4 immortalised "normal" human fibroblast cell line, showing less cytotoxicity (Table 6). These data suggest that 3-aryl-5-AIQs are a

valuable lead in the design of more potent and selective inhibitors of the tankyrases, which might be cytotoxic.

1.5 Telomerase inhibitors.

Telomeres, telomerase and the role of the tankyrases in these structures were described in detail in section 1.2.4. Telomerase has been an attractive target since the 1980s. Some of the small molecule inhibitors, *e.g.* Imetelstat (GRN163L) is undergoing clinical development.[112,113] However, extensive development of small-molecule inhibitors of human telomerase activity showed several disadvantages of this strategy. The structural basics of inhibition of telomerase remain unclear, partly because of the high complexity of the structure of telomerase and partly because some compounds act by binding to the G-quadruplex, not the telomerase. Telomerase consists of several catalytic proteins, RNA and dyskerin proteins, which makes mechanistic studies rather difficult. The association of telomerase with several shelterin proteins does not make the problem easier. As a result, not many small-molecule direct inhibitors of telomerase are known to date. Some of them are presented in Figure 23. The spiroketal moiety of β-rubromycin **49**, which belongs to a class of quinone antibiotics, appeared to be beneficial for the telomerase inhibition, since α-rubromycin, which lacks the spiroketal

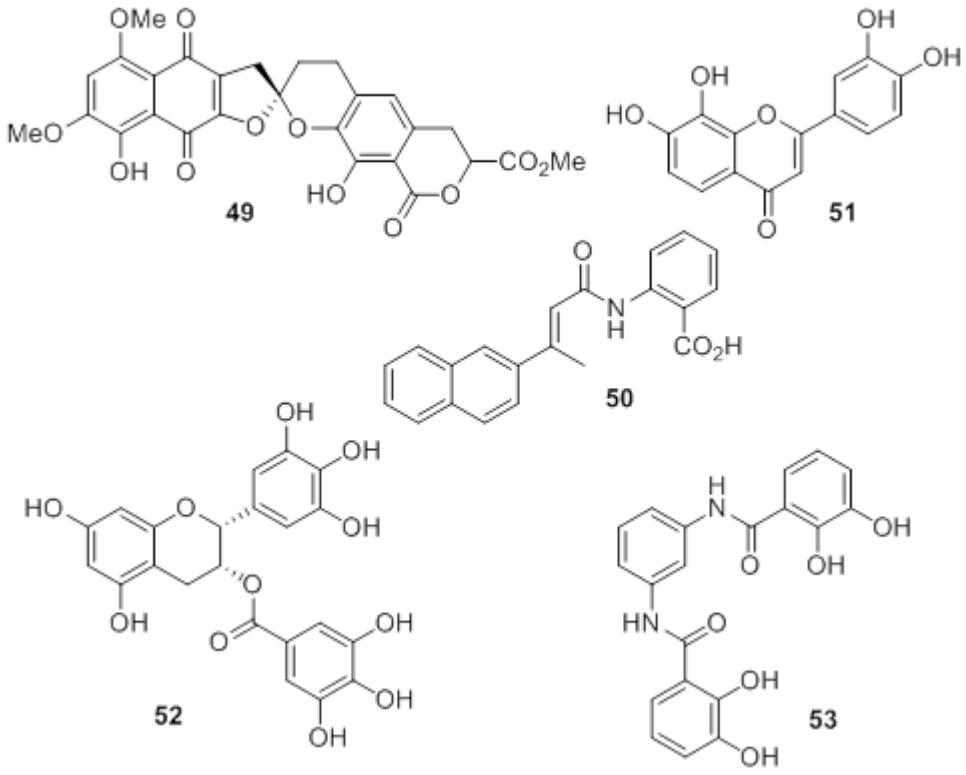

Figure 23. Structures of telomerase inhibitors: β-rubromycin, **49** (IC_{50} = 3.0 μM);[114] BIBR-1532, **50** (IC_{50} = 0.093 – 20.0 μM);[115] 7,8,3',4'-tetrahydroxyflavone, **51** (IC_{50} = 0.2-1.4 μM);[116] epigallocatechin gallate, **52** (IC_{50} = 1.0 μM);[117] MST-312, **53** (IC_{50} = 0.67 μM).[118]

system, did not inhibit telomerase.[114] Compound **49** was also found to be cytotoxic, inhibiting the proliferation of cancer cells; however, it is yet to be determined if this cytotoxicity is related to the inhibition of telomerase. Compound **50**, when introduced into a study of mechanism of action, was revealed to be a selective inhibitor of telomerase, both natural and recombinant. It was showed to be a non-competitive inhibitor, causing the dissociation of telomerase from DNA.[115] 7,8,3',4'-Tetrahydroxyflavone **51** became a lead compound in the investigation of flavones as inhibitors of telomerase, exhibiting micromolar range inhibitory activity.[116] A major tea catechin component, epigallocatechin gallate **52**, was shown to be a strong telomerase inhibitor, exhibiting mild cytotoxicity against leukemia and colon cancer cells.[117] At the same time, compound **53** was proposed as a more effective alternative to **52**, requiring the effective dose of 1–2 μM for the telomere shortening, which was 15- to 20-fold lower than that of epigallocatechin gallate **52**.[118]

There are some concerns about telomerase inhibition as an anti-cancer strategy. Firstly, there is a lag phase between the time when telomerase is inhibited and the time when telomeres are short enough to switch on the apoptotic mechanism.[70] Secondly, since telomerase activity is detected in normal haematopoietic, stem and germline cells, there is a possibility of severe side-effects, related to the damage to this tissues, induced by inhibition of telomerase activity.[70,119] Thirdly, some cancer cells have mechanisms to maintain their telomeres without activation of telomerase, which leads to increased cell survival.[70,120] Finally, telomerase inhibition may lead to increased genomic instability in surviving cells, thus leading to more aggressive tumours.[70,121]

Therefore, telomerase inhibitors *per se* might not be sufficiently effective and safe. However, in combination with some other agents, particularly, tankyrase inhibitors, inhibition of telomerase activity may be useful. Inhibition of the tankyrases should provide shortening of the lag phase in telomerase activity inhibition and apoptosis; it will also provide more specific anti-cancer activity and should reduce cellular viability.[70]

1.6 NuMA and mitosis inhibitors.

NuMA, its function in mitosis and their linkage to the tankyrases were described in section 1.3.5. There is no information in the literature found about inhibition of NuMA itself. However, anti-mitotic approaches in cancer therapy have been developed extensively. Anti-mitotic activity was found in some natural products, such as paclitaxel and vinblastine. Paclitaxel **54** (Figure 24) is a drug that targets tubulin in the cytoskeleton. It stabilises the microtubule polymer and protects it from disassembly. Therefore, chromosomes are unable to achieve a metaphase spindle configuration, which blocks progression of mitosis.[122] Vinblastine **55** (Figure 24) is one of the microtubule-disruptive drugs. These agents have been reported to act by two mechanisms. At very low concentrations, they suppress microtubule dynamics, while at higher concentrations they reduce microtubule polymer mass. Both of these lead to the cell arrest in mitosis.[123] Taking into account the clinical success of these two drugs, NuMA disruption becomes an attractive target for anti-tumour drug development.

Unfortunately, the major disadvantage of such a therapy is its potential toxicity. These agents may affect also proliferating normal cells. Moreover, one of the major adverse effects of paclitaxel and vinblastine is peripheral nerve damage. However, it is not known if inhibition of poly(ADP-ribosyl)ation of NuMA by tankyrases will cause similar adverse reactions.

1.7 *Wnt* pathway inhibitors.

The crucial roles of the *Wnt* signalling pathway in cancer development were discussed in section 1.3.6. For example, its activation has considered being the key event in colon cancer formation, transforming the intestinal endothelial cells into immortal adenomas and forcing their malignisation. *In vitro* suppression of *Wnt* activity blocks the tumour growth and forces cancer cells to differentiate into normal endothelial cells.[124,125] There

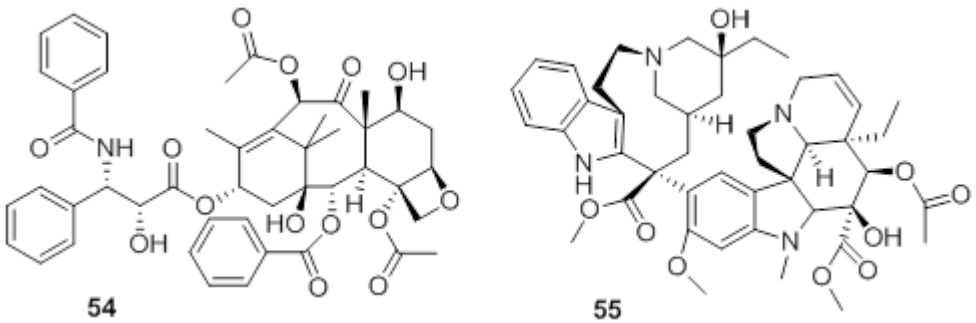

Figure 24. Structures of anti-mitotic drugs paclitaxel **54** and vinblastine **55**.

is no wonder that *Wnt* has become an attractive target for anti-neoplastic therapy.

Currently there is a number of screening and rational drug design programmes in place to identify potent *Wnt* pathway inhibitors. However, some *Wnt*-orientated drugs have been already developed. These include non-steroidal anti-inflammatory drugs (NSAIDs) and vitamin derivatives.

1.7.1 NSAIDs.

Numerous studies have shown the benefits of regular use of aspirin and other NSAIDs in reducing and preventing human cancers.[126,127] NSAIDs inhibit the activity of cyclooxygenase (COX), which was shown to play an important role in various human cancers. In colorectal cancer, both COX1 and COX2 are considered to force the formation of polyps. Increased COX activity stimulates the production of prostaglandins (PG), which leads to tumour growth and metastasis.[128] In colon cancers, COX and *Wnt* cooperate: increased COX activity elevates PG levels, which then stimulate *Wnt* signalling by disrupting the capacity of cells to destroy β-catenin.[129]

Therefore, inhibition of COX activity drives towards normal degradation of β-catenin. However, not all human tumours show elevated levels of COX but NSAIDs are still efficient in these tumours. This suggests that there is not only one mechanism of action for this group of drugs.

Aspirin (acetylsalicylic acid, **56**, Figure 25), when used in concentrations equivalent to

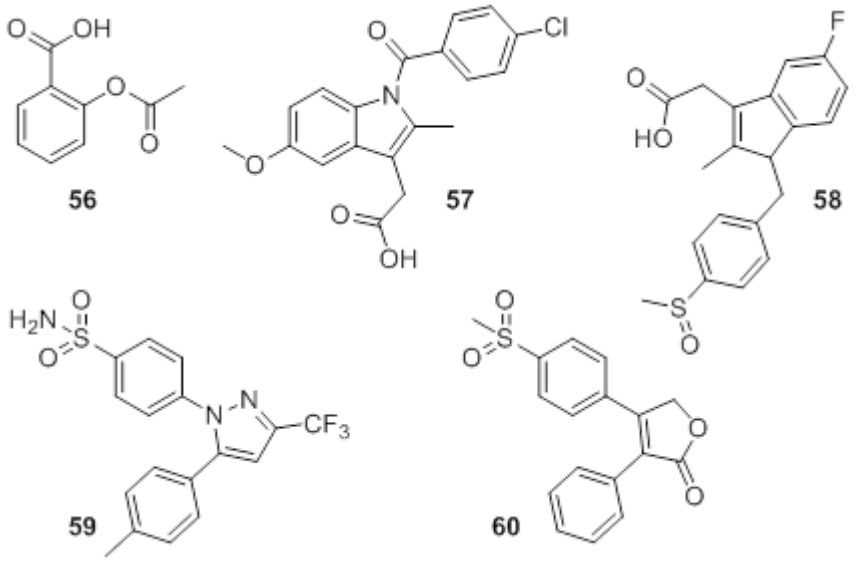

Figure 25. Structures of selected NSAIDs: acetylsalicylic acid (aspirin), **56**; 2-{1-[(4-chloro-phenyl)carbonyl]-5-methoxy-2-methyl-1*H*-indol-3-yl}acetic acid (indomethacin), **57**; {(1*Z*)-5-fluoro-2-methyl-1-[4-(methylsulfinyl)benzylidene]-1*H*-indene-3-yl}acetic acid (sulindac), **58**; 4-[5-(4-methyl-phenyl)-3-(trifluoromethyl)pyrazol-1-yl]benzenesulfonamide (celecoxib), **59**; 4-(4-methylsulfonyl-phenyl)-3-phenyl-5*H*-furan-2-one **(**rofecoxib), **60**.

the cardioprotective dose, was shown to inhibit cancer cell growth by both COX-dependent and COX-independent pathways.[124] *In vitro* studies suggest that aspirin triggers conversion of β-catenin into a phosphorylated form, which is not capable of activating target genes.[130] Similarly, indomethacin (**57**, Figure 25) reduced tumour growth in a rat colorectal cancer model, although the concentration was higher than one which can be used in humans.[131] Moreover, the precise mechanism of action of indomethacin remains unclear.

Sulindac (Exisulind, **58**, Figure 25) was extremely effective for the treatment of colorectal tumours in rats. It selectively induced apoptosis in cancer cells by targeting cyclic GMP phosphodiesterase (cGMP PDE). The inhibition of this enzyme led to the elevation of cellular cGMP levels and, subsequently, to apoptosis. Despite the promising clinical results, sulindac was not approved for chemoprevention by the FDA. It was revealed that sulindac caused major adverse effects, such as abdominal pain and liver-related problems, which would not allow the use of this drug in a long-term treatment.[124]

The classic side effects of NSAIDs, like gastrointestinal bleeding and kidney problems, have prompted the development of safer NSAID derivatives. Selective COX2 inhibitors celecoxib (Celebrex, **59**, Figure 25) and refecoxib (Vioxx, **60**, Figure 25) and nitric oxide-releasing NSAIDs were shown to be safer and more effective solutions.[124] Currently, celecoxib is the only drug approved by the FDA to be used as a chemoprotector. NO-releasing aspirin (NO-ASA) is several thousand-fold more effective than is aspirin in inhibiting growth of colon cancer cells and is significantly less toxic.[132]

1.7.2 Vitamin derivatives.

Vitamin A derivatives, retinoids, have essential functions in embryonic development, reproduction, vision and immune response. Recent studies show that retinoids and their synthetic analogues may act as therapeutics in cancer treatment and prevention. Their anti-tumour effect might be linked to their capacity to restore cell adhesion by stabilising components of the adherence junctions and to supress the *Wnt* pathway. The retinoid-activated receptors are able to interact with β-catenin, thus reducing cellular β-catenin levels. This leads to the inhibition of tumour growth. However, some studies revealed growth of increased intestinal tumours when treated with retinoids. With no

doubt, more studies are necessary to make clearer the effects of vitamin A on the development of cancer.[124]

Vitamin D derivatives, apart from playing a pivotal role in the maintenance of healthy muscles and bones, are of great importance in cancer prevention. Some studies pointed that the stimulation of vitamin D synthesis in the skin exposed to sunlight had a protective effect against various types of cancer.[133] Synthetic derivatives of vitamin D were capable of halting the growth of cancer cells *in vitro*. This is expected to happen due to blocking cell proliferation.[134] Also, similarly to vitamin A receptors, vitamin D receptors bind β-catenin and decrease its cellular levels.[135] Recent development of non-hypercalcaemic vitamin D derivatives should reduce severe side effects, associated with long-term vitamin D treatment. However, an expression of vitamin D receptors has been seen in late-stage colon cancer. This can be a serious problem in the development of vitamin D derivatives as anti-cancer drugs.[124]

1.7.3 Antibody-based therapeutics.

The *Wnt* signalling possesses a variety of characteristic proteins, which are overexpressed in cancer cells, thus creating an opportunity to develop antibodies (AB) against them. These therapeutics may act through the inhibition of the *Wnt* signalling or through the immune response. As a proof of concept, it was shown that the treatment of head and neck human cancer cell lines, overexpressing Wnt1, with Wnt1 monoclonal antibody disrupted the *Wnt* signalling, blocked proliferation and induced apoptosis.[136] Apart from head and neck tumours, Wnt1 is overexpressed in non-small-cell lung cancer. Treatment of such a tumour in mice with Wnt1 antibody blocked the cell growth.[137] Other cancers, *e.g.* gastric, colon, melanoma, mesothelioma and non-small-cell lung carcinoma overexpress Wnt2. The treatment of non-small-cell lung carcinoma, mesothelioma and melanoma with Wnt2 monoclonal antibody induced apoptosis *in vitro*.[124]

1.7.4 Small-molecule inhibitors.

Several screening programmes have revealed a number of small molecules, which have an ability to inhibit *Wnt* signalling through various pathways. Some structures of these molecules and their mode of action are shown in Figure 26 and summarised in Table 7. It was discovered that a common feature in many types of cancer was the presence of Tcf-β-catenin complexes in the cancer cell nuclei. The inhibition of these complexes *in*

vitro inhibited tumour growth, providing an interesting target for the development of small-molecule inhibitors.[125] The crystal structures of Tcf-β-catenin complexes revealed key interaction "hot-spots" that could be targeted by small molecules.[138,139] However, the main difficulty of this approach is that β-catenin is a multi-functional protein that interacts with several targets.

Table 7. Small-molecule inhibitors of *Wnt* signalling.

Name	Screening method	IC_{50} (μM)	Interaction target
ZTM000990 (**61**)[140]	ELISA-based HTS* of 7000 natural products	0.64	β-catenin-Tcf§
PKF118-310 (**62**)[140]	ELISA-based HTS of 7000 natural products	0.8	β-catenin-Tcf
PKF118-744 (**63**)[140]	ELISA-based HTS of 7000 natural products	2.4	β-catenin-Tcf
PKF115-584 (**64**)[140]	ELISA-based HTS of 7000 natural products	3.2	β-catenin-Tcf
PKF222-815 (**65**)[140]	ELISA-based HTS of 7000 natural products	4.1	β-catenin-Tcf
CGP049090 (**66**)[140]	ELISA-based HTS of 7000 natural products	8.7	β-catenin-Tcf
PNU-74654 (**67**)[141]	*In silico* screen of 18000 synthetic compounds	ND&	β-catenin-Tcf
ICG-001 (**68**)[142]	Cell-based HTS of 5000 synthetic compounds	3.0	CBP†-β-catenin
NSC668036 (**69**)[143]	*In silico* screen of 250000 drug-like compounds	ND	Dsh‡-Fzd+

*HTS, high-throughput screening.

§Tcf, T-cell factor (β-catenin target).

&ND, not determined.

†CBP, cAMP-responsive element binding protein (CREB) binding protein.

‡Dsh, Dishevelled receptor.

+Fzd, Frizzled receptor.

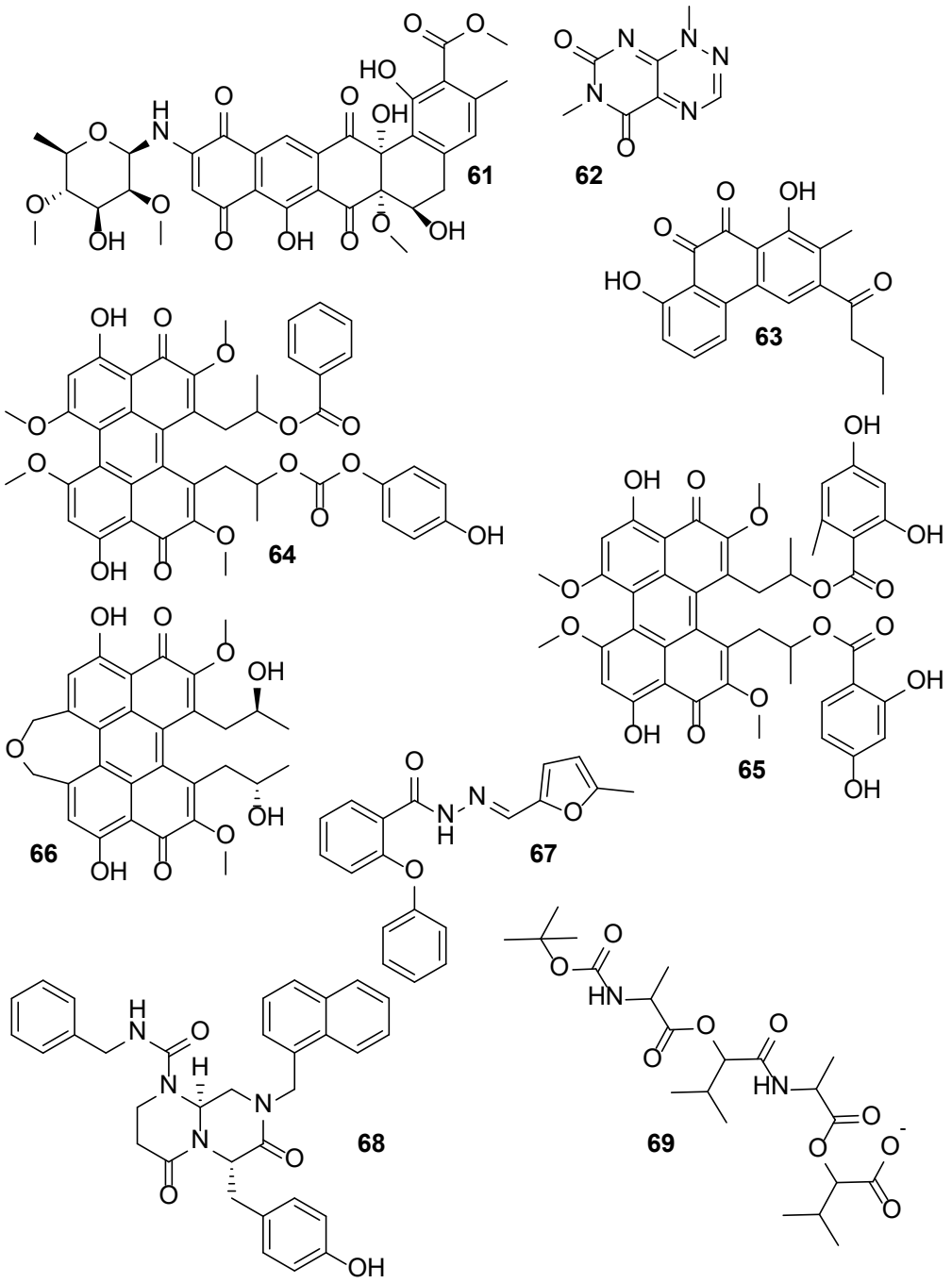

Figure 26. Structures of some small-molecule inhibitors of *Wnt* pathway.

Therefore, it is crucial that the small molecule should inhibit the Tcf-β-catenin interaction only and no other interactions of β-catenin, otherwise it would lead to major side effects. Interestingly, high throughput screening of several libraries of compounds did not reveal any synthetic inhibitors of these interactions. However, a number of natural products were found to be disruptors of Tcf-β-catenin complex *in vitro*. These compounds might serve as a port of departure for further investigation (see Figure 26, Table 7).

Another generation of small-molecule inhibitors of *Wnt* signalling appeared when it was discovered that tankyrase poly(ADP)riboylates axin and therefore stabilises β-catenin (discussed in section 1.3.6). Tankyrase inhibitors in *Wnt* will be discussed below.

1.8 Tankyrase-1/2 inhibitors.

Since its discovery in 1998, tankyrase-1 and -2 became a highly interesting target for drug design and discovery. Tankyrases are involved not only in many tumourigenesis pathways but also in the development of some other diseases. As anti-cancer drugs, tankyrase inhibitors may act through inhibition of the *Wnt* pathway and subsequent reversion of cancer cells into normal cells, or they can be utilised to shorten telomeres and induce apoptosis, as well as block the separation of sister chromatids and stop the mitosis. Through the ability of tankyrases to destabilise *Wnt* signalling, its inhibitors may also be therapeutics for newborn brain injury, multiple sclerosis and cystic fibrosis.[144,145] Recent discoveries of the involvement of tankyrases in the development of cherubism,[51,52] herpes[50] and insulin-mediated glucose uptake[53,54] make the design of tankyrase inhibitors even more urgent. Interestingly, the tankyrase inhibitors may interact not only with classical PARP nicotinamide pocket, but also with an allosteric adenosine-binding pocket. Therefore, the tankyrase inhibitors may be divided into two groups: (i) compounds which act through the nicotinamide-binding site, *e.g.* XAV939 (**47**, see Figure 21) and (ii) compounds which act through the adenosine-binding site, *e.g.* IWR1 (**46**, see Figure 21). Recent results on the development of tankyrase inhibitors are summarised in this section.

1.8.1 Tankyrase-1/2 inhibitors which interact with the nicotinamide-binding site.

Tankyrases might be inhibited by non-specific pan-PARP inhibitors, *e.g.* 3-AB (**2**, Figure 13), through the catalytic site of the enzyme. These molecules mimic nicotinamide interactions with Ser^{1068} and Gly^{1032} of the enzymes (as shown in Scheme 1), causing a restraint of the tankyrases activity.

A selective PARP-1/2 inhibitor olaparib (**25**, see Figure 19), possessing a lactam moiety, also weakly inhibits tankyrases (TNKS-1 IC_{50} 1.5 μM). It was shown that **25** forms hydrogen bonds with Ser^{1068} and Gly^{1032}, similarly to nicotinamide **1**, 3-AB **2** and XAV939 **47** (discussed below). The pyrimidine ring forms π–π interactions with Tyr^{1071} and the fluorophenyl group π–π stacks with Tyr^{1050}. The carbonyl groups form

hydrogen bonds with the backbone amide groups of Tyr[1060] and Asp[1045]. Cyclopropyl moiety interacts hydrophobically with the helix 1035-1042. However, when olaparib binds to tankyrase, it causes major conformational alterations in the D-loop residues (*e.g.* Asp[1045], His[1048], Ala[1049], Tyr[1050]). Fluorine, being within van der Waals distance from carbonyls on Ala[1049] and His[1048], may be one of the reasons of this movement of the D-loop.[146] This indicates that PARP-1/2 and tankyrases have significant differences in the catalytic binding site. Therefore, it is very possible to design selective tankyrase inhibitors with no activity towards other PARPs.

Few examples of selective inhibitors of the tankyrases appear in the literature. Perhaps the first selective tankyrase-1/2 inhibitor described was XAV939 (**47**, see Figure 21).[60] Found with high-throughput screening (HTS), this molecule was shown to inhibit both tankyrase isoforms and to disrupt the *Wnt* signalling by stabilising axin. Moreover, XAV939 was cytotoxic against APC-null DLD1 colon cancer cells under severely serum-deprived conditions.[147] This molecule interacts with the active site of tankyrase-1 through hydrogen bonding of the pyrimidine NH and carbonyl with Ser[1068] and Gly[1032] and through π–π stacking between the phenyl ring and Tyr[1071] (Figure 27). Tankyrase-2 and XAV939 also have numerous non-polar interactions: the phenyl ring π-π stacks with Tyr[1050] and Tyr[1071]; the trifluoromethyl group interacts hydrophobically with Pro[1034], Phe[1035] and Ile[1075].[146] Moreover, Karlberg *et al.* claimed that "the sulfur atom in the thiopyrano ring [of XAV939] is within hydrogen bonding distance of the Phe[1061] backbone".[148] However, it is practically impossible that sulfide sulfur atom would form a hydrogen-bond interaction since it is a soft nucleophile. These interactions partly determine the outstanding potency and selectivity of XAV939 **47** (TNKS-1 IC_{50} = 0.011 μM; TNKS-2 IC_{50} = 0.004 μM; PARP1 IC_{50} = 2.194 μM; PARP2 IC_{50} = 0.114 μM).[60] Regarding the studies *in vivo*, there is no evidence of notable toxicity of XAV939, which is a positive sign for further development of inhibitors of tankyrase. Structure-activity relationship studies revealed that the position corresponding to the

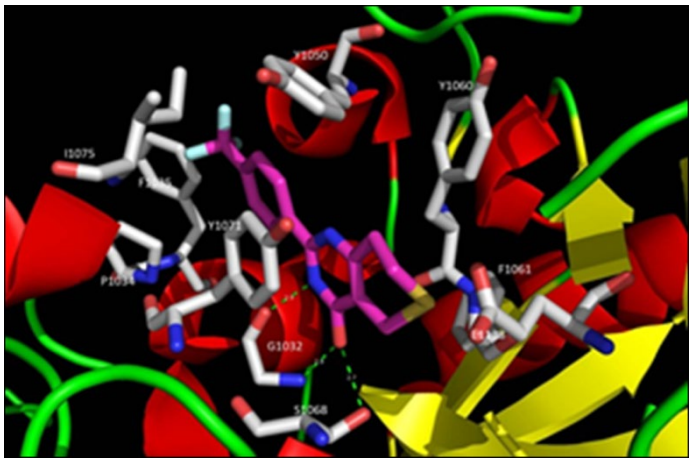

Figure 27. Crystal structure of human tankyrase-1 with XAV939 **47** bound. Re-rendered from pdb file (see ref. 148).

sulfur in the thiopyran ring does not tolerate any bulky substituents. However, substitution of the trifluoromethyl group could lead to additional interactions with the amino-acid residues. It was also found that some polar substituents at positions 7 and 8 (see Figure 21) of the thiopyran ring could establish some interactions with several amino acids, *e.g.* Glu^{1138}.[148] These considerations provide an interesting opportunity for further optimisation of the inhibitors carrying a lactam moiety.

Table 8. Calorimetric properties of XAV939 **47** binding to the tankyrases and PARP-1.[148]

Enzyme	K_d, nM	N	ΔH, Kcal mol^{-1}	ΔS, cal mol^{-1}
TNKS-1	14 ± 8	0.92 ± 0.01	-2.4 ± 0.4	28 ± 3
TNKS-2	8 ± 3	1.09 ± 0.08	-3.7 ± 0.4	25 ± 1
PARP1	620 ± 130	1.35 ± 0.09	-9.3 ± 0.1	2.6 ± 0.5

1.8.2 Tankyrase inhibitors, which interact with the adenosine binding site.

Other compounds, discovered by cell-based high throughput screening (HTS) in 2009, were endo-IWR1 and endo-IWR2 (**46a**,**b**, Figure 28).[149,151] These structures stabilised axin and inhibited *Wnt* signalling and proliferation in DLD1 colon cancer cells.[147] Remarkably, these compounds do not bind to the NAD^+-site of the enzymes. This suggests that these compounds are probably non-competitive tankyrase inhibitors. They induce a major movement of the D-loop, subsequently closing the nicotinamide-binding site and preventing nicotinamide from interacting with it. The two carbonyls at the norbornyl moiety form hydrogen bond interactions with the amides of Tyr^{1050}, Tyr^{1060} and Asp^{1045}. Tyr^{1070}, together with Ile^{1075}, also forms non-polar interactions with the norbornyl part of **46**. The quinoline part has some non-polar interactions with hydrophobic residues of amino-acids at the helix 1035-1042.[146] After the disclosure of these structures, a structure-activity relationship study was performed. However, any modifications of **46** led to compromised activity (Figure 29). Substitution of the quinolone with benzyl, pyridyl and other smaller aromatic rings dramatically decreased the activity (EC_{50} > 20 μM). This is might be due to the increased steric bulk of the quinolone ring, which is large enough to alter the D-loop. Nonetheless, the introduction of 4-halophenyl ring resulted in slightly better activity (EC_{50} = 1 μM), possibly, because of the interaction with Lys^{1042}. Any alterations of the phenyl ring, linking the norbornyl and amide parts, resulted in moderate-to-complete loss of activity. This is likely to be

due to the length of this region, which allows the norbornyl moiety to fit exactly in the pocket. An addition of one extra atom between the amide and the norbornyl group abolishes the activity completely.[146,149]

JW55 (**70**, Figure 28) was found by the HTS of a library of 37000 small molecules (ChemBioNet). It was firstly identified as an inhibitor of the *Wnt* pathway, selectively inhibiting tankyrases and leaving PARP-1 unaffected. This compound was found to be cytotoxic against SW480 colon cancer cells. Molecular docking of **70** into the adenosine-binding site of tankyrase-2 revealed strong similarities of binding site and position of the molecule with those of IWR1.[152]

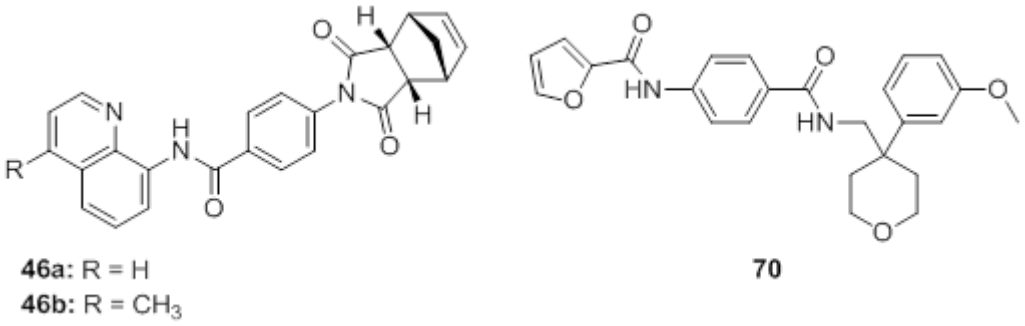

Figure 28. Structures of tankyrase inhibitors IWR1 **46a** (TNKS-1 IC_{50} = 0.131 μM; TNKS-2 IC_{50} = 0.056 μM; PARP-1 IC_{50} >18.75 μM), IWR2 **46b**, JW55 **70** (TNKS-1 IC_{50} = 1.9 μM).[60,150]

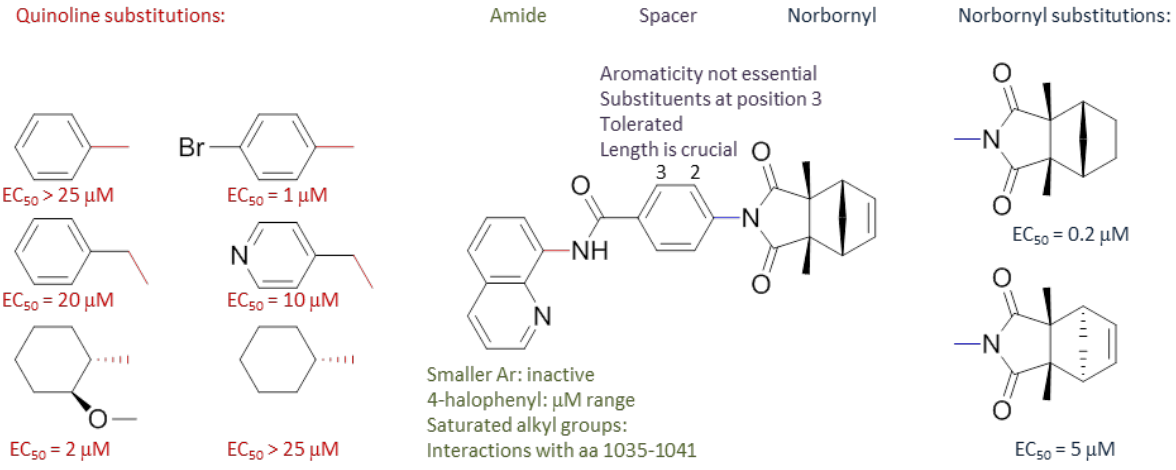

Figure 29. SAR studies on IWR1/2 **46**. Quinoline substituents added on the *p*-position.

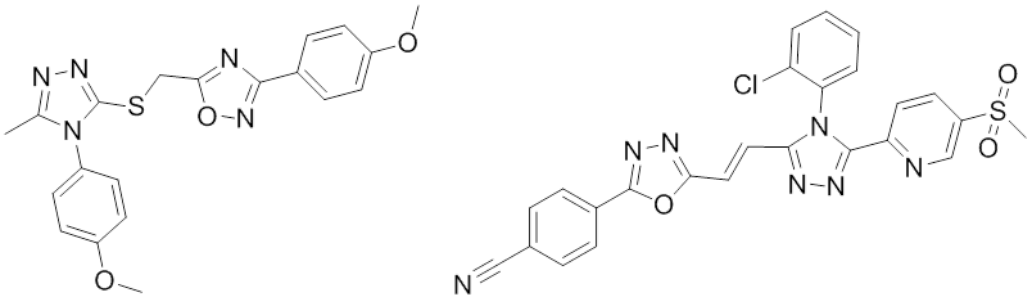

71 72

Figure 30. Structures of triazole-based tankyrase inhibitors: **71** (TNKS-2 IC_{50} = 0.033 μM; PARP-1 IC_{50} > 19 μM; PARP2 IC_{50} > 19 μM);[153] **72** (TNKS-1 IC_{50} = 0.046 μM; TNKS-2 IC_{50} = 0.025 μM).[154]

3-(4-Methoxyphenyl)-5-((4-(4-methoxyphenyl)-5-methyl-4*H*-1,2,4-triazol-3-yl)thio)-1,2,4-oxadiazole **71** (Figure 30) was found to be a nanomolar-range inhibitor of tankyrases (TNKS-2 IC_{50} = 0.033 μM; PARP-1 IC_{50} >19 μM; PARP-2 IC_{50} > 19 μM). Its distinguished activity might be explained with numerous non-covalent interactions with the adenosine-binding site of the enzyme. Structural studies revealed some key interactions, including two hydrogen bonds between (i) a triazole nitrogen atom and the amide of Tyr^{1213} and (ii) between an oxadiazole nitrogen atom and the amide of Asp^{1198}. Various van der Waals interactions were observed between the molecule and side chains of Phe^{1188}, Ala^{1191} and Ile^{1192}, together with stacking interactions with His^{1201}. The methoxyphenyl moiety also made van der Waals interactions with Ser^{1186}, Pro^{1187}, Phe^{1188} and Ile^{1228} of a hydrophobic pocket. Another part of the molecule, which formed van de Waals interactions with Phe^{1188}, was the sulfur atom. Notably, this amino-acid residue is unique for tankyrases and not present in other PARPs, suggesting a reason for the extreme selectivity of **71** towards tankyrases.[153]

Another triazole derivative to be found extremely active against tankyrases was 4-{5-[(*E*)-2-{4-(2-chlorophenyl)-5-[5-(methylsulfonyl)pyridine-2-yl]-4*H*-1,2,4-triazol-3-yl}ethenyl]-1,3,4-oxadiazol-2-yl}benzonitrile (**72**, Figure 30) (TNKS-1 IC_{50} = 0.046 μM; TNKS-2 IC_{50} = 0.025 μM). The structural basis for such remarkable activity is similar to the previous example, triazole **71**. Two hydrogen bonds are formed by the nitrogen atoms of triazole and oxadiazole with backbone amides of Tyr^{1060} and Asp^{1045}, respectively. Apart from those, there are three π–π stacking interactions. The first one involves the nitrile-substituted

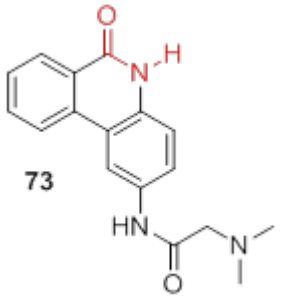

73

Figure 31. Structure of PJ34 (**73**) (TNKS-1 IC_{50} = 1.0 μM).[155]

aromatic ring and His[1048]. Another one is speculated to be established between the chlorinated benzene ring and Phe[1035]. Lastly, the pyridyl ring π–π stacks with side chains of Tyr[1060] and Tyr[1071].[154]

Recently, it was discovered that a well-known PARP inhibitor PJ34 (**73**, Figure 31) exhibited micromolar activity against tankyrases (TNKS-1 IC_{50} = 1.0 μM). Remarkably, it was shown that two molecules of the inhibitor are involved in the interaction with the enzyme: one molecule bound to the nicotinamide-binding site, while the other coordinated to the adenosine-binding site. In the nicotinamide-binding site, there were three hydrogen bonds: (i) between the phenanthridinone oxygen atom and the side-chain hydroxyl of Ser[1221], (ii) the backbone amide of Gly[1185] and (iii) between the phenanthridinone nitrogen atom and the carbonyl oxygen of Gly[1185]. π–π Stackings have been observed between phenanthridinone and Tyr[1224], together with some van der Waals interactions with Tyr[1213]. In the adenosine binding site, the second molecule of **73** formed hydrogen bonds between the phenanthridinone oxygen atom and the backbone amide of Asp[1198], as well as between the phenanthridinone NH group and the carbonyl oxygen of Gly[1196].[155]

1.8.3 Natural products – inhibitors of the tankyrases.

Interestingly, several natural products have been discovered, which have an ability to inhibit the tankyrases. Firstly, flavone, which occurs in the leaves of many primroses, (**74**, Figure 32) was identified as a modestly potent and selective tankyrase inhibitor (TNKS-1 EC_{50} = 10 μM; PARP1 EC_{50} = 100 μM) using a HTS method.[156] Later, Narwal *et al.* performed a screening of inhibitory activity of five hundred flavonoids from nine different classes: flavones, chalcones, flavanones, dihydroflavonols, flavonols, flavans, anthocyanins, isoflavonoids, and neoflavonoids.[157] This screening showed that only flavones inhibited the catalytic activity of the tankyrases. Recent studies performed by the Lehtiö group at University of Oulu shed the light on the structural evidence of the inhibitory activity of flavones.[158,159]

The co-crystallisation of flavone **74** with tankyrase-2 revealed that it binds to the nicotinamide binding site of the enzyme despite lacking a lactam moiety, typical for nicotinamide-binding PARP inhibitors. The oxygen atom from the benzopyran ring forms hydrogen bonds with the amide of Gly[1032] and hydroxyl of Ser[1068]. The phenyl ring makes a π-π

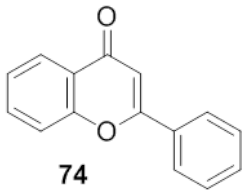

Figure 32. Structure of flavone, **74** (TNKS-1 IC_{50} = 10 μM; PARP1 IC_{50} = 100 μM).[156]

stacking interaction with side chain of Tyr^{1071}. Interestingly, it was shown that the carbon at position-3 of **74** might form hydrogen bonds interactions with the carbonyl of Gly^{1032}, since the distance between C-3 and the carbonyl oxygen was between 2.96 and 3.15 Å in the crystal structures.[158]

Another naturally occurring inhibitor of tankyrase activities is GDP-mannose-4,6-dehydratase (GMD). It is required for the first step of fucose synthesis in the cytoplasm. It was revealed that this enzyme is one of the major partners of tankyrase-1, possessing a tankyrase-binding motif, RGSGDG. GMD did not accept PARsylation and, moreover, inhibited the PARsylation activity of tankyrase-1 as well as its autoPARsylation. Surprisingly, GMD seems to have no effect on PARP-1. Some human colon cancers lack GMD, suggesting that the deficit of GMD could lead to liberation of tankyrase-1.[58]

1.9 Work in the Threadgill Group at Bath.

The research group of the Threadgill laboratories at the University of Bath achieved significant results in the field of inhibition of PARP-1, PARP-2 and especially the tankyrases. Several papers have been published, and a patent has been filed.[100,110, 160-166] A series of potent and selective tankyrase inhibitors, the 2-arylquinazolin-4-ones (compounds **75-86**, Figure 33), was synthesised.[166] A methyl substituent at position-8 dramatically improved the effectiveness and a variety of substituents are tolerated at the *para*-position of the 2-phenyl ring. Structural evidence of this remarkable activity was revealed by molecular modelling. The 2-aryl groups lay in a large hydrophobic pocket with a *para*-substituent at the end of the aromatic ring. The methyl group at position-8 fits snugly into another small hydrophobic nook. The compounds are highly selective towards tankyrases, showing no inhibition of PARP-1 or IMPDH2, an NAD^+-requiring oxidoreductase, up to the 10 μM limit of solubility (Table 9). Further SAR studies were undertaken, considering the effect of the methyl group at position-8 (compounds **87**-**98**, Figure 34). A series of 5-methyl-3-arylisoquinolin-1-ones was made to investigate the effect of the nitrogen atom at position 1 in 2-arylquinazolin-4-ones. No significant impact on the activity against tankyrases was observed (Table 10).

Table 10. IC_{50} values for inhibition of enzyme activity by test compounds **87-90, 93-98.**

Compound number	TNKS-1 IC_{50} (μM)	TNKS-2 IC_{50} (μM)	PARP-1 IC_{50} (μM)
87	0.021	0.001	1-10
88	0.043	0.009	0.55
89	0.276	0.032	>10
90	N/A	0.009	>10
93	N/A	0.029	0.111
94	N/A	0.019	0.720
95	N/A	0.004	>10
96	N/A	0.005	>10
97	N/A	0.056	1
98	N/A	0.244	0.86

Table 9. IC_{50} values for inhibition of enzyme activity by test 2-arylquinazolin-4-ones.

Compound number	TNKS-1 IC_{50} (μM)	TNKS-2 IC_{50} (μM)	PARP-1 IC_{50} (μM)	IMPDH2 IC_{50} (μM)
75	0.042	0.041	0.8	>10
76	0.035	0.007	0.7	>10
77	0.048	0.01	>5	>10
78	0.032	0.03	0.9	>10
79	0.037	0.012	0.9	>10
80	0.036	0.033	>5	>10
81	0.032	0.006	>5	>10
82	0.044	0.04	>5	>10
84	0.035	0.003	0.5	>10
85	0.052	0.005	1.2	>10
86	0.073	0.044	>5	>10

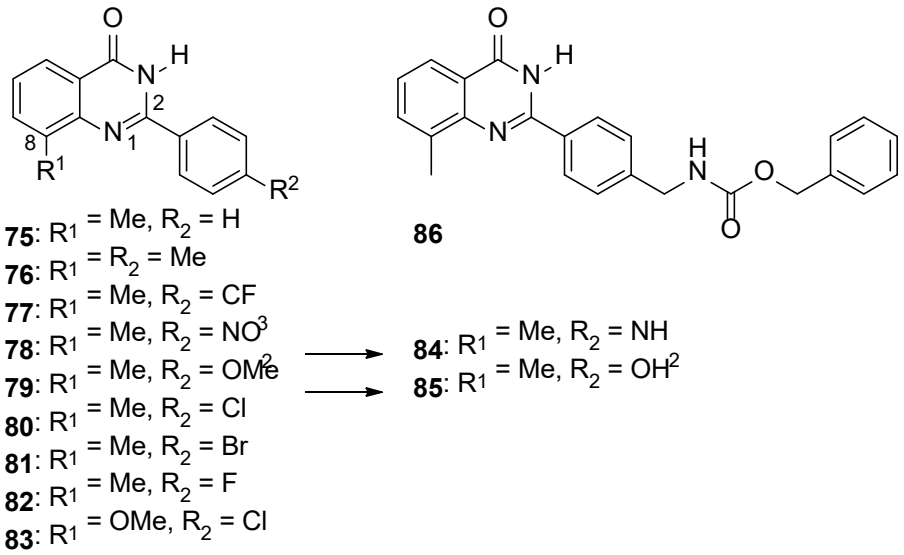

Figure 33. 2-Arylquinazolin-4-ones **75-85** synthesised in the Threadgill laboratories.

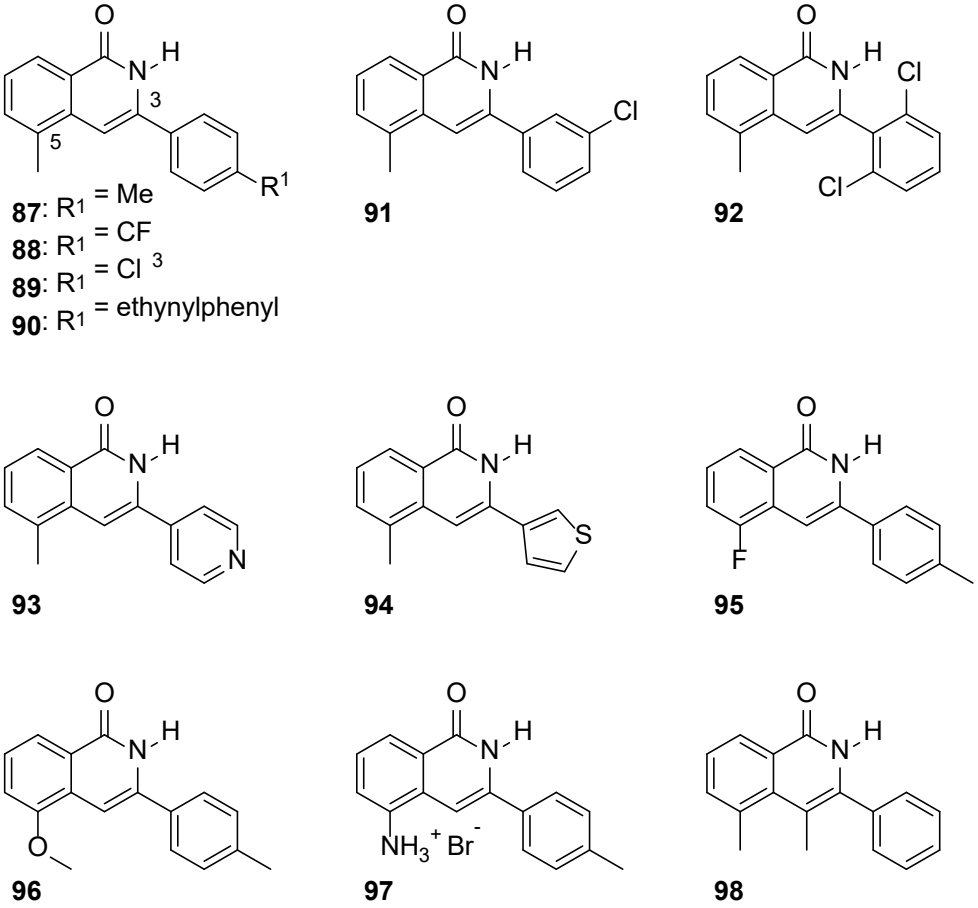

Figure 34. 5-methyl-3-arylisoquinolin-1-ones **87-92**; 5-methyl-3-pyridylisoquinolin-1-one **93**; 5-methyl-3-thiophen-3-ylisoquinolin-1-one **94**; 5-fluoro-3-(4-methylphenyl)isoquinolin-1-one **95**; 5-methoxy-3-(4-methyl)phenylisoquinolin-1-one **96**; 1-oxo-3-(4-methylphenyl)-isoquinolin-5-aminium bromide **97**; 4,5-dimethyl-3-phenylisoquinolin-1-one **98**.

The aryl group in this library of structures was *ortho*-, *meta*- and *para*-substituted, revealing *para*-substitution as the best option. The phenyl group was also replaced with pyridine and thiophene heterocycles. The alteration of position-5 with a fluorine or

methoxy group, however, showed a slight decrease of activity. More significantly compromised activity was found if position-5 was occupied by an amino-group.

1.10 Conclusions.

The frightening statistics of cancer spread world-wide shows the absolute importance of the development of new anti-oncological therapy. High toxicity and weak activity are the two major disadvantages of existing anti-cancer drugs. Recently discovered new members of poly(ADP)polymerases superfamily, tankyrases, are an attractive target for anti-neoplastic therapy for several reasons. Tankyrases are over-expressed in cancer cells compared to normal cells, which may provide high selectivity of tankyrase-based anti-cancer agents. These enzymes are involved in three major tumourigenesis pathways: (i) they maintain the telomere length through the regulation of telosomal complex and telomerase; (ii) they provide sister telomere division in mitosis through interacting with NuMA protein and (iii) most importantly, they keep high levels of β-catenin, triggering cancerous *Wnt* signalling. Taken together, these reasons made tankyrases a very important drug target.

Existing knowledge on PARP inhibitors and crystal structures of the enzymes allowed the performance of rational drug design. Accomplished SAR studies also provided some information towards the drug development.

1.11 Aims and Objectives.

As discussed before, the development of novel anti-cancer agents is of crucial importance nowadays.[1-5] Tankyrases became a promising target in cancer research since their triple-acting role in cancer was discovered.[22,38,60] Moreover, their involvement in non-cancerous processes, *e.g.* cherubism[51,52] and brain injury,[144,145] provides new prospects for the design of tankyrase inhibitors. Thus far, few studies have been conducted on selective inhibitors of the tankyrases. It is known, however, that several compounds (XAV939 **47**,[60] 3-aryl-5-AIQs **48d-f** (Figure 21)[162]) display good inhibition activity against tankyrase-1/2. There were obtained some crystal structures of tankyrase-2 with different inhibitors bound.[167] It can be seen that the lactam structure is essential for hydrogen-bonding to Ser^{1068} and Gly^{1032}. It was also shown that a (4-substituted) aryl ring at position-3 (isoquinolin-1-one numbering) is needed for binding to Tyr^{1050}, Tyr^{1060} and Tyr^{1071}, which are part of the surface of a hydrophobic pocket.[146] The

pharmacophore of tankyrase inhibitors (Figure 35) illustrates the knowledge of the SAR to date.

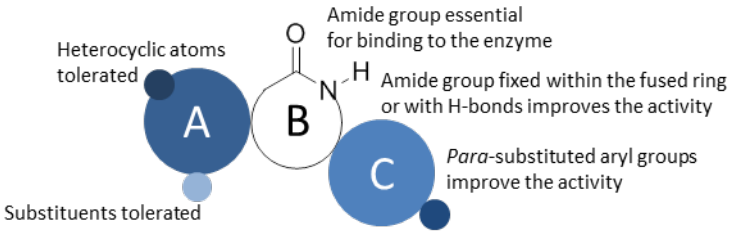

Figure 35. Pharmacophore for tankyrase-1/2 inhibitors.

The aim of this project was to synthesise and evaluate biochemically a range of efficient and selective tankyrase-1/2 inhibitors. For this purpose, it was decided to modify known structures, such as 5-AIQ **48a**, replacing isosterically the amino-substituted phenyl group with a pyridine. The 3-aryl substituents are included, as these appear to be required for binding to the tankyrases. To study the influence of the nitrogen atom on the inhibitory activity it was proposed to make a series of 3-aryl-2,6-naphthyridin-1-ones **100** and 3-aryl-2,7-naphthyridin-1-ones **101**. The naphthyridinones **99-101** were then suggested to be N^1-oxidised or N^1-alkylated and reduced with the aim of study the effect of substituted nitrogen, charged species and reduced ring. Also, for further investigation of the effect of the heterocyclic nitrogen atom, a variety of pyridopyrimidinones **109-111** was planned to be synthesised and evaluated. Moreover, it was proposed to examine SAR by replacing heterocyclic sulfur in the well-known tankyrase-1/2 inhibitor XAV939 **47** with the NH (tetrahydropyridopyrimidinones **113**, Figure 36). It was also planned to synthesise XAV939 **47** to make sufficient material available cheaply for further biological evaluation.

From a druggability point of view, designed compounds meet all "druglikeness"

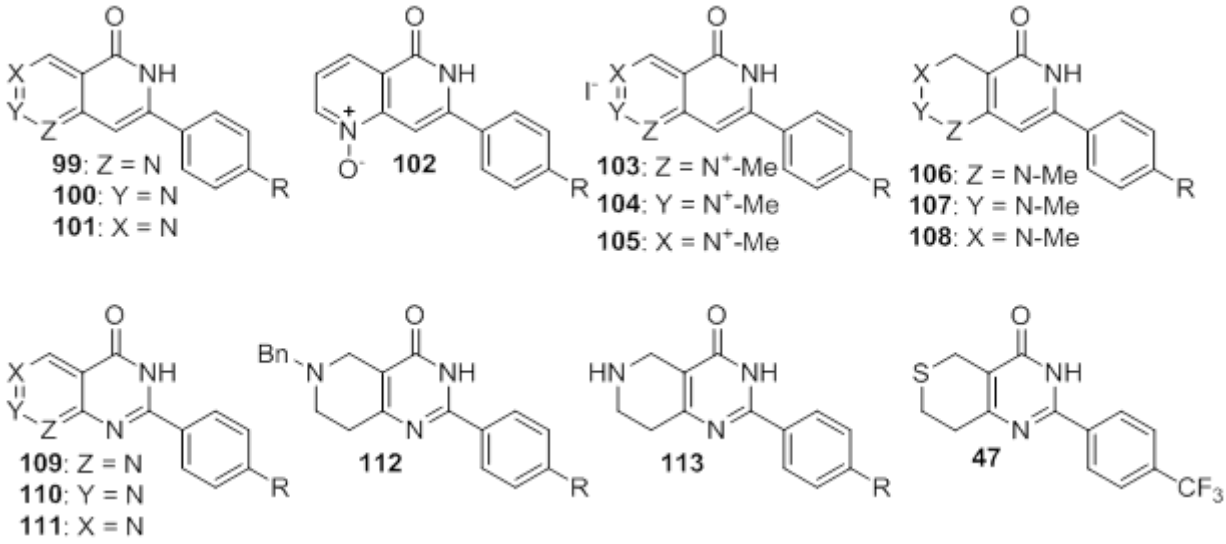

Figure 36. Structures of target tankyrase inhibitors **99-113** and the known tankyrase inhibitor XAV939 **47**.

requirements (Table 11). This means that they are likely to have good enteral and parenteral bioavailability in humans.

Table 11. "Druglikeness" properties of designed compounds **99-113.**

Criterion	**Reference value**[168-170]	**Calculated values for designed tankyrase-1/2 inhibitors** 99-113[a]
Molecular mass, Da	180 – 500[168,169]	222 - 317
Number of hydrogen-bond donors	≤ 5[168]	1 - 2
Number of hydrogen-bond acceptors	≤ 10[168]	1 - 3
Partition coefficient log P	-0.4 - +5.6[168,169]	0.08 - 4.97[b]
Molar refractivity, $cm^3\ mol^{-1}$	40 – 130[169]	63.03 – 95[c]
Number of atoms	20 – 70[169]	26 - 44
Polar surface area, $Å^2$	≤ 140[169,170]	32.34 - 76.20[d]
Number of rotatable bonds	≤ 10[170]	1 - 4

[a] Values given as a range from a minimum to a maximum number.

[b, c, d] Values calculated in ChemBioDraw Ultra 12.0.

In order to evaluate biochemically the synthesised compounds they were planned to be introduced into preliminary in-house developed three-point ranging studies against catalytic activity of tankyrase-2. Further biological evaluation was proposed to be carried out for the active compounds, including IC_{50} determination against tankyrase-2 and tankyrase-1. To investigate the selectivity of the target compounds it was decided to test them against PARP-1 and IMPDH2, another NAD^+-requiring enzymes. The cytotoxic effect of the most potent compounds was proposed to be evaluated through the MTS anti-proliferative assay on HT29 human colon adenocarcinoma cell line and FEK4 human fibroblasts cell line. To envisage the structural basis of the inhibition, it was suggested to make the crystal structures of the compounds bound to the nicotinamide-binding site. This was possible through a collaboration with Dr. Lari Lehtiö (University of Oulu, Finland).

Chapter 2. Chemical synthesis

2.1 Overview of the designed synthesis.

A summary of the planned synthesis of the target compounds is represented in Scheme 2. In order to make target naphthyridinones **99-101** and their derivatives, two strategies were employed: (i) a Sonogashira coupling, followed by electrophilic cyclisation and (ii) an Ullmann-type condensation reaction, Hurtley coupling, followed by conversion of the lactone to a lactam. For further structure-activity relationship (SAR) studies, some derivatives of **99-101** were planned to be synthesised (**102-108**, Scheme 2). Another Ullmann-type condensation was proposed to make pyridopyrimidinones **109-111** from the corresponding benzamidines and bromopyridinecarboxylic acids **126-128**. Tetrahydropyridopyrimidinones **113** were planned to be obtained *via* sodium methoxide-mediated condensation of methyl 1-benzyl-4-oxopiperidine-3-carboxylate **129** and a variety of benzamidines with subsequent deprotection of the benzyl group. The partly saturated ring of the compounds **113** was expected to form different conformations, which would be interesting to investigate. Known tankyrase-1/2 inhibitor XAV939 **47**,[60] which was essential for the biological evaluation as a positive control, was proposed to be made according to the patented procedure, *via* Dieckmann condensation of an ester of 4-oxotetrahydrothiopyran-3-carboxylate and transition-metal-free cyclisation of the latter with the corresponding benzamidine.

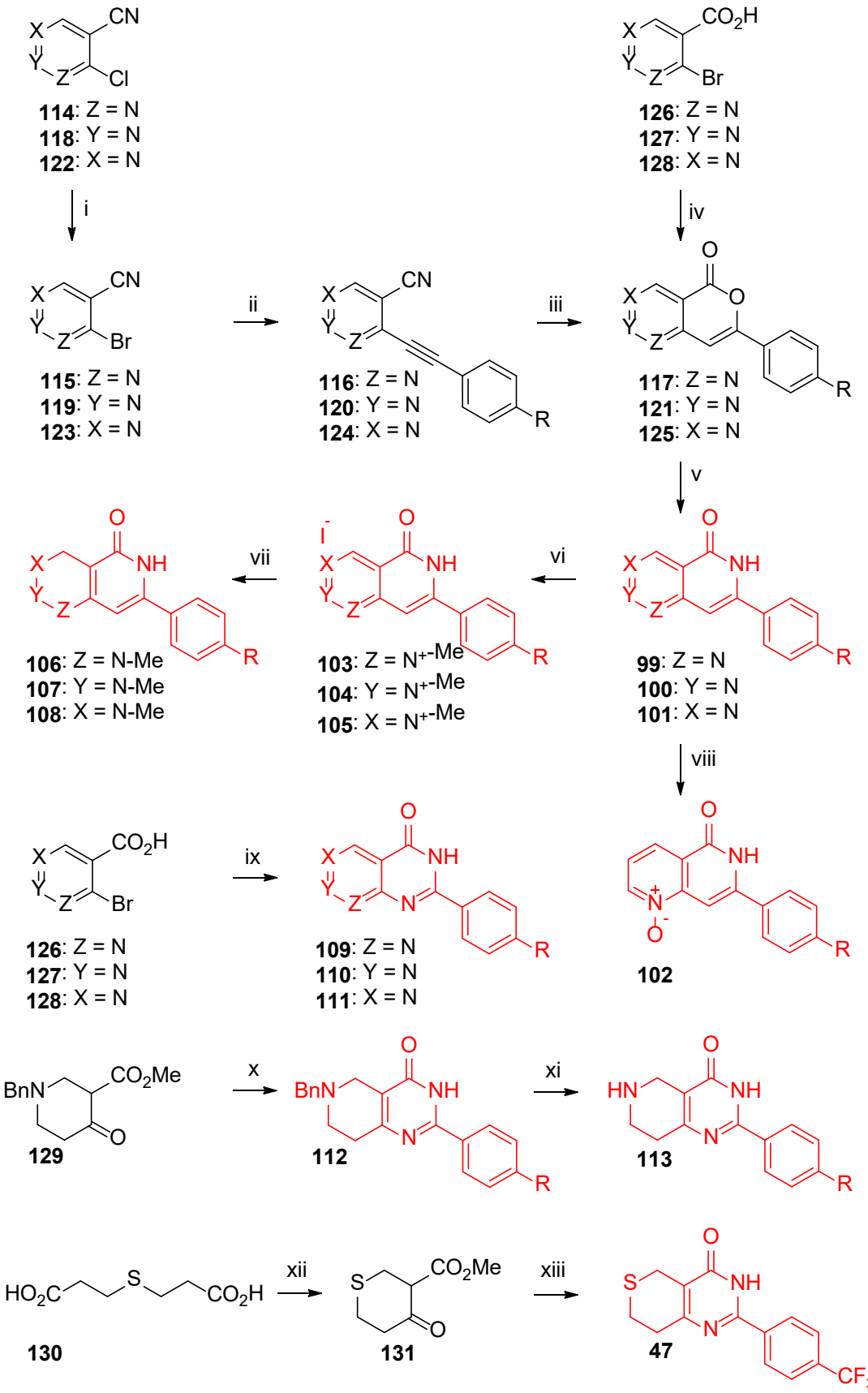

Scheme 2. Proposed synthesis of target compounds (shown in red). i, AcOH/water, then Bu_4NBr, P_2O_5; ii, Sonogashira coupling; iii, electrophilic cyclisation; iv, Hurtley coupling; v, NH_3, pressure, Δ; vi, N-alkylation; vii, reduction; viii, N-oxidation; ix, Ullmann-type condensation; x, $ArC(=NH)NH_2$, NaOMe; xi, removal of Bn group; xii, esterification, then Dieckmann condensation; xiii, $4\text{-}F_3CPhC(=NH)NH_2$, NaOMe.

2.2 Synthesis of 7-aryl-1,6-naphthyridin-5-ones and their derivatives *via* Sonogashira coupling.

Approaching the target 7-aryl-1,6-naphthyridin-5-ones **99**, three possible routes were investigated (Scheme 3). The first route (Scheme 3, Route A, blue) started with hydration of the nitrile in starting 2-chloro-3-cyanopyridine **114** to a primary amide. An arylethynyl moiety was then planned to be introduced at the 2-position of **132**. To approach this, a two-step pathway was proposed. The amide **132** would be introduced into a Sonogashira coupling with trimethylsilylethyne, in which the trimethylsilyl group would protect the ethyne from coupling at one end and also make the reagent a liquid, rather than an inconvenient gas. The trimethylsilyl group in **133** would then be removed to give a deprotected terminal ethyne **134**. A second Sonogashira coupling of **134** was planned with 4-substituted iodobenzenes to give 2-arylethynylpyridine-3-carboxamides **135**. These coupled compounds could be cyclised into 7-aryl-1,6-naphthyridin-5-ones **99** with various electrophilic agents.

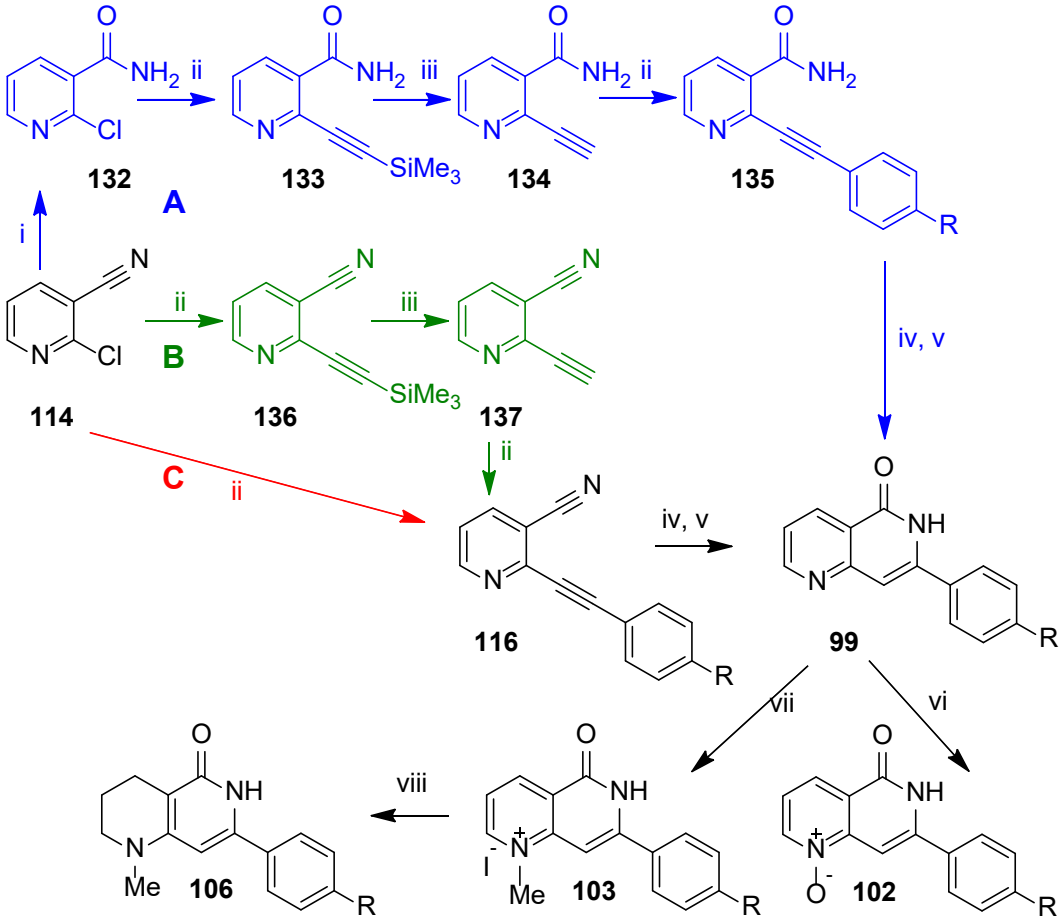

Scheme 3. Proposed routes of synthesis of 7-aryl-1,6-naphthyridin-5-ones and their *N*-derivatives. i, Radziszewski reaction; ii, Sonogashira coupling; iii, TMS group removal; iv, electrophilic cyclisation; v, NH_3, pressure, Δ; vi, *N*-oxidation; vii, *N*-alkylation; viii, reduction.

Several groups have reported the possibility of electrophilic cyclisation of 2-arylethynylarenes mediated by mercury(II). For example, 2-arylethynylbenzoate esters, when treated with mercury(II) under acidic conditions, resulted in 3-arylisocoumarins after appropriate work-up.[171,172] Similarly, methyl 3-nitro-2-(2-phenylethynyl)benzoate was cyclised into 5-nitro-3-phenylisocoumarin with mercury(II) sulfate in sulfuric acid and acetone.[173] More importantly, 3-cyano-2-(phenylethynyl)pyridine, when treated with 9 M aqueous sulfuric acid, gave a mixture of 1,6-naphthyridinone and the corresponding pyranopyridinone.[174] Therefore, 2-arylethynylpyridine-3-carboxamides **135** were expected to undergo cyclisation, mediated by an electrophilic agent. It should also be possible to oxidise or alkylate compounds **99** to N^1-oxides **102** and to N^1-alkyl analogues **103** and **106**.

The second route (Scheme 3, Route B, green) also applied two Sonogashira coupling reactions, however the nitrile **114** was not hydrated at the start. This was planned to avoid difficulties with palladium-catalysed coupling in the presence of the bulky and co-ordinating primary carboxamide. Cyclisation of coupled compound **116** was proposed to be carried out with an electrophilic agent, *e.g.* 9 M aq. sulfuric acid.[174]

The third route (Scheme 3, Route C, red) also involved a Sonogashira coupling reaction. In contrast to the routes discussed above, 2-chloro-3-cyanopyridine **114** was proposed to be the aryl halide component, while substituted arylethynes acted as the terminal alkynes. The resulting 2-arylethynyl-3-cyanopyridines **116** should then be hydrated / cyclised with sulfuric acid[174] and converted into N^1-oxides and N^1-alkyl analogues, similarly to other routes.

The first reaction in route A required hydration of a nitrile to a carboxamide. This reaction type could be achieved with acid or base at elevated temperature or by treatment with hydroperoxide ion under mild conditions. Hydroperoxide anion, generated from hydrogen peroxide and hydroxide ion in an alcoholic solvent or in water, is a powerful

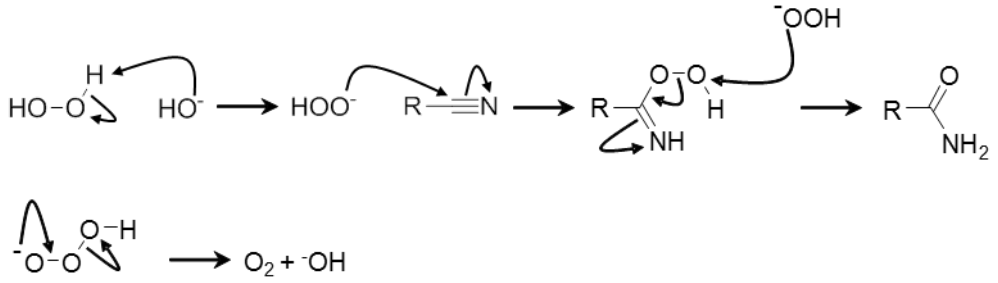

Scheme 4. Mechanism of the Radziszewski reaction.

nucleophile and attacks the δ^+-carbon of the nitrile (Scheme 4). This is known as the Radziszewski reaction[175] and it has previously been employed in our group to hydrate 8-cyanoquinolines to quinoline-8-carboxamides and 3-substituted benzonitriles to the corresponding benzamides.[100,176] The Ritter reaction, which is a more common and better-known way to generate an amide from a nitrile, is inappropriate, as it results in secondary amides.[177] The primary amide cannot be generated during this reaction, as it involves the acid-induced formation of a carbenium anion, with which the nitrile is reacting. Other advantages of the Radziszewski reaction included mild temperature conditions and the possibility to avoid the formation of a carboxylic acid through over-reaction. The Radziszewski reaction on **114** gave 2-chloropyridine-3-carboxamide **132** in 50% yield (Scheme 5).

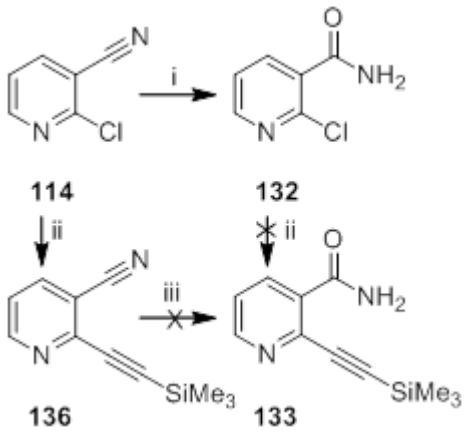

Scheme 5. Synthesis of 7-aryl-1,6-naphthyridin-5-ones. First attempt. *Reagents & conditions:* i, H_2O_2, KOH, EtOH, 60-70 °C, 50%; ii, $Me_3SiC{\equiv}CH$, $Pd(PPh_3)_2Cl_2$, CuI, Pr^i_2NH, THF, 40 °C, 62%; iii, H_2O_2, KOH, EtOH, 60-70 °C.

Sonogashira couplings of **132** were then investigated. Generally, the Sonogashira coupling is a palladium-catalysed coupling between a haloarene or haloalkene and a terminal alkyne.[178] In this case, **132** is the haloarene component. Trimethylsilylethyne (TMSE) was used as the alkyne as a conveniently masked liquid synthetic equivalent of ethyne, a gas. However, this reaction did not proceed and only starting material **132** was recovered. This could be explained either by the steric bulk of the amide group, since bulky haloarene substrates are not very reactive in Sonogashira couplings,[179] or by inappropriate coordination of the palladium with the carboxamide. Investigating an alternative route to intermediate **133**, Sonogashira coupling of 2-chloro-3-cyanopyridine **114** with TMSE gave 62% of the trimethylsilylethynylpyridine **136**. However, the Radziszsewski hydration failed in this case, giving only an inseparable mixture of compounds (Scheme 4).

For routes B and C, we sought to improve the Sonogashira coupling conditions in several directions. The reactivity of the (*pseudo*)haloarene component in palladium-catalysed couplings decreases in the order OTf = I > Br > Cl.[180] Chlorine generally reacts only if it is activated by being *ortho* to an electron-withdrawing group or a heterocyclic nitrogen atom. Catalysis in the Sonogashira coupling is performed by

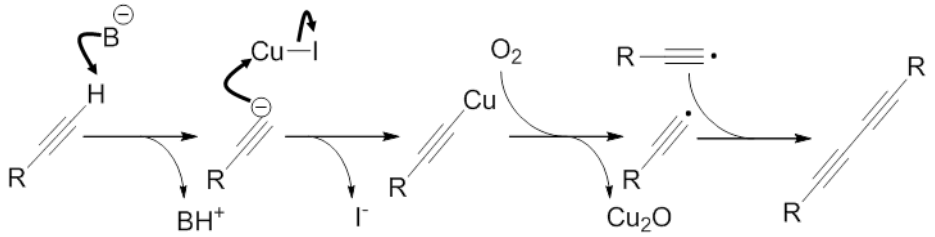

Scheme 6. The Glaser coupling. Competing formation of 1,4-diarylbutadiyenes by oxidative homo-coupling of arylethynes.

palladium (commonly bis(triphenylphosphine)palladium(II) dichloride or tetrakis(triphenylphosphine)palladium(0)) and copper(I). A base is also essential for this type of coupling. Different amines are widely used but inorganic salts, such as potassium carbonate, could be used as alternatives.[181,182] Anaerobic conditions are important for this coupling, since, in the presence of oxygen, a competing oxidative Glaser coupling takes place (Scheme 6). The Glaser coupling involves the synthesis of symmetrical butadiynes *via* oxidative coupling of terminal alkynes.[183] This coupling is promoted by copper(I) salts and molecular oxygen, so degassing is essential to minimise this side-reaction. The mechanism of the Sonogashira coupling is represented in the Scheme 7. As for the majority of palladium-catalysed carbon-carbon cross-couplings, it comprises four steps:

- *Oxidative addition*, during which a molecule of haloarene is added to the 14-electron species of a palladium catalyst. Palladium(0) becomes oxidised to palladium(II).

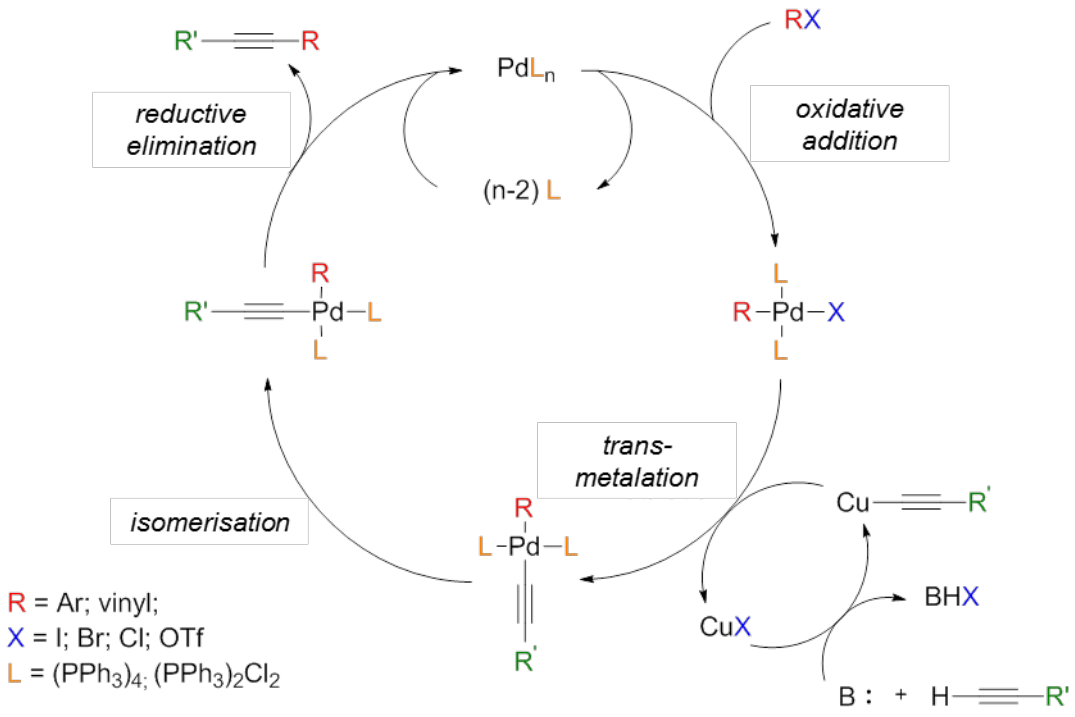

Scheme 7. The mechanism of the Sonogashira coupling.

- An alkynyl-copper species is generated from the copper co-catalyst (usually copper(I) iodide), the base and the terminal alkyne. This alkynyl-copper is then involved in a *transmetalation* stage, which forms copper(I) halide and the alkynyl-palladium intermediate.

- The alkynyl-palladium intermediate then undergoes an *isomerisation*. Initially, the complex formed in the *transmetalation* step is *trans*-orientated on the square-planar palladium. However, in order to favour the concerted reductive elimination of the palladium, this complex should be *cis*-orientated.

- During the last step, *reductive elimination*, ligand-bound palladium is liberated to form a new σ-bond-coupled product and the regenerated 14-electron palladium catalyst, ready for another cycle.

Firstly, Sonogashira couplings were investigated using 2-chloro-3-cyanopyridine **114** as the haloarene component. Commercially available phenylethyne was used as the terminal alkyne. The co-coupled product **116a** was obtained in 52% yield using $Pd(PPh_3)_2Cl_2$ as catalyst and in the excellent yield of 98% using $Pd(PPh_3)_4$. However, bromoarenes are usually much more reactive in palladium-catalysed couplings than are chloroarenes.[180] In principle, the iodo-analogue would be even more reactive but it is known that iodopyridines are photolabile.[184] To exploit any increased reactivity of the bromopyridine, 2-chloro-3-cyanopyridine **114** was converted into 2-bromo-3-cyanopyridine **115** (Scheme 8). The chloride of **114** was displaced with acetate by treatment with boiling acetic acid to give 2-acetoxy-3-cyanopyridine **138**, by the method of Lavecchia *et al*.[185] Hydrolysis of the labile ester with boiling aqueous tetrahydrofuran gave 3-cyanopyridin-2-one **140** quantitatively, *via* its tautomer 3-cyano-2-hydroxypyridine **139**. To convert **140** into the 2-bromopyridine **115**, three methods were investigated. Treatment with phosphorus tribromide in boiling toluene for 6 d and with this reagent in tetrahydrofuran and pyridine at 40 °C for 5 d gave only recovery of the starting material. Similar treatment with the phosphorus(V) reagent $POBr_3$ also failed to effect the conversion. Following the procedure of Takehiro *et al*.,[186] a phosphorus-

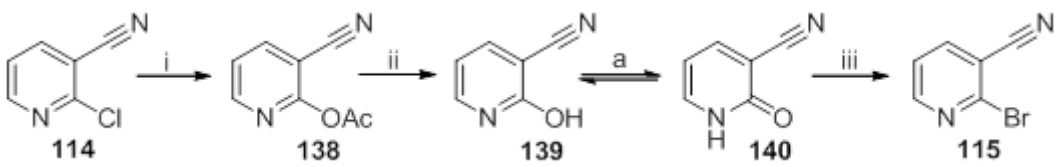

Scheme 8. Conversion of 2-chloro-3-cyanopyridine **114** into 2-bromo-3-cyanopyridine **115** *via* 3-cyano-2-hydroxypyridine **139.** *Reagents & conditions*: i, AcOH, Δ; ii, THF, H_2O, Δ, 100% for two steps; iii, Bu_4NBr, P_2O_5, PhMe, Δ, 94%; a: tautomerism.

bromine reagent was generated *in situ* from phosphorus pentoxide and tetrabutylammonium bromide. This method gave moderate to excellent yields of **115** without any additional purification.

Another route to 2-bromo-3-cyanopyridine **115** was investigated, using 2-bromopyridine-3-carboxylic acid **126** as a starting material.[187] Compound **126** was converted into the corresponding amide **141**, *via* a mixed anhydride formed with ethyl chloroformate (Scheme 9). The amide **141** was then dehydrated with phosphorus oxychloride to give desired bromo derivative **115**.

Following Route B of the synthetic plan above (see Scheme 3), the coupling of 2-bromo-3-cyanopyridine **115** with TMSE was explored using different palladium catalysts (Scheme 10). When $Pd(PPh_3)_4$, which lacks chloride, was used as the catalyst, the major product was the expected trimethylsilylethynylpyridine **136**. However, in some runs when $Pd(PPh_3)_2Cl_2$ was used as catalyst, the desilylated alkyne **137** was obtained directly. Copper(I) chloride has been reported to remove trimethylsilyl groups from alkynes.[188,189] Co-ordination of the copper to the alkyne delivers the chloride to attack the silicon. After loss of the trimethylsilyl group, the copper moves from π-co-ordination to σ-co-ordination in the alkynyl-copper, which hydrolyses on workup to form the terminal alkyne. It was predicted that copper(I) chloride might be formed *in*

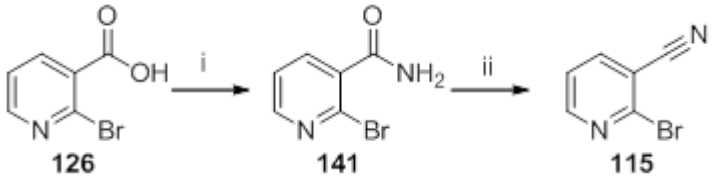

Scheme 9. Alternative approach to synthesis of 2-bromo-3-cyanopyridine **115**. *Reagents & conditions:* i, EtO_2CCl, Et_3N, THF, then NH_3 0 °C, 89%; ii, $POCl_3$, 0 °C, 55%.

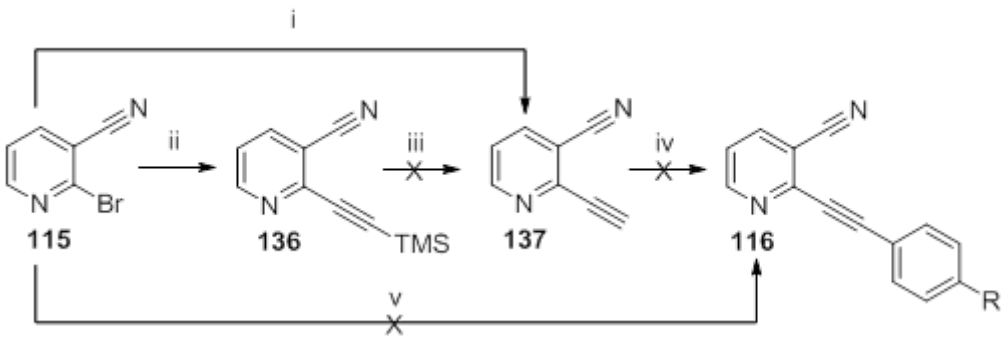

Scheme 10. Studies on the Sonogashira coupling of TMSE with **115**. *Reagents & conditions:* i, $Me_3SiC{\equiv}CH$, $Pd(PPh_3)_2Cl_2$, CuI, Pr^i_2NH, THF, 40 °C, 78%; ii, $Me_3SiC{\equiv}CH$, $Pd(PPh_3)_4$, CuI, Pr^i_2NH, THF, 40 °C, 30%; iii, *e.g.* Bu_4NF, THF; NaOH, EtOH; KOH, MeOH; AgOTf, acetone, $CHCl_3$, water; iv, RC_6H_4I, $Pd(PPh_3)_2Cl_2$, CuI, Pr^i_2NH, THF, 40°C; v, $Me_3SiC{\equiv}CH$, $Pd(PPh_3)_2Cl_2$, CuI, Pr^i_2NH, THF, 40°C, then RC_6H_4I.

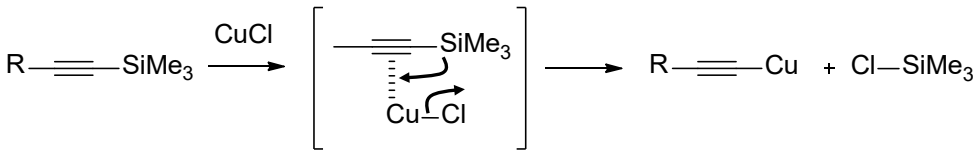

Scheme 11. Possible mechanism of cleavage of the TMS group by CuCl.

situ during the Sonogashira reaction and be responsible for the cleavage of the trimethylsilylalkyne (Scheme 11). However, once isolated, **136** could not be desilylated with copper(I) chloride nor with conventional desilylating agents, including tetrabutylammonium fluoride,[190,191] potassium hydroxide,[192] sodium hydroxide[193] and silver(I) triflate.[100,173] It had been intended that **137** would be a late common intermediate and that the aryl groups in the targets could be introduced through a second Sonogashira coupling with iodoarenes but these second couplings failed. It was also attempted to carry out the two Sonogashira couplings as one-pot reaction: in the first step, **115** was intended to couple with TMSE; $Pd(PPh_3)_2Cl_2$ was used to obtain the deprotected compound **137** directly. Iodobenzene was then added for the second coupling but this experiment gave an unidentifiable mixture of compounds (see Scheme 10).

Investigating alternatives to the trimethylsilyl protecting group, it was decided to examine the Favorskii reaction (not to be confused with the Favorskii rearrangement). This reaction involves protection of a terminal alkyne *via* formation of a propargyl alcohol.[194] The 2-hydroxyprop-2-yl group is commonly used for protection in this reaction.[189] 2-Bromo-3-cyano-pyridine **115** was treated with 2-methylbut-3-yn-2-ol using palladium-on-charcoal as catalyst, by the general method of Swindell *et al.* (Scheme 13).[195] However, the yield of **142** was very low (6%), causing this route to be abandoned. It had been intended to eliminate an acetone unit from **142** with strong base to provide **137**.

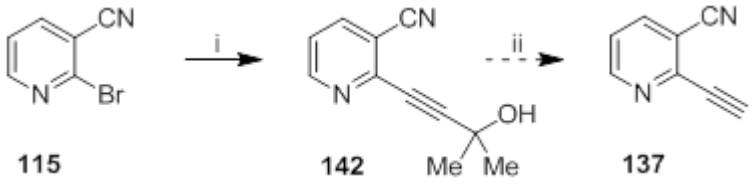

Scheme 12. An alternative route to **137**. *Reagents & conditions*: i, $HC{\equiv}CCMe_2OH$, Pd/C, PPh_3, CuI, K_2CO_3, $(MeOCH_2)_2$, water, 6%; ii, KOH.

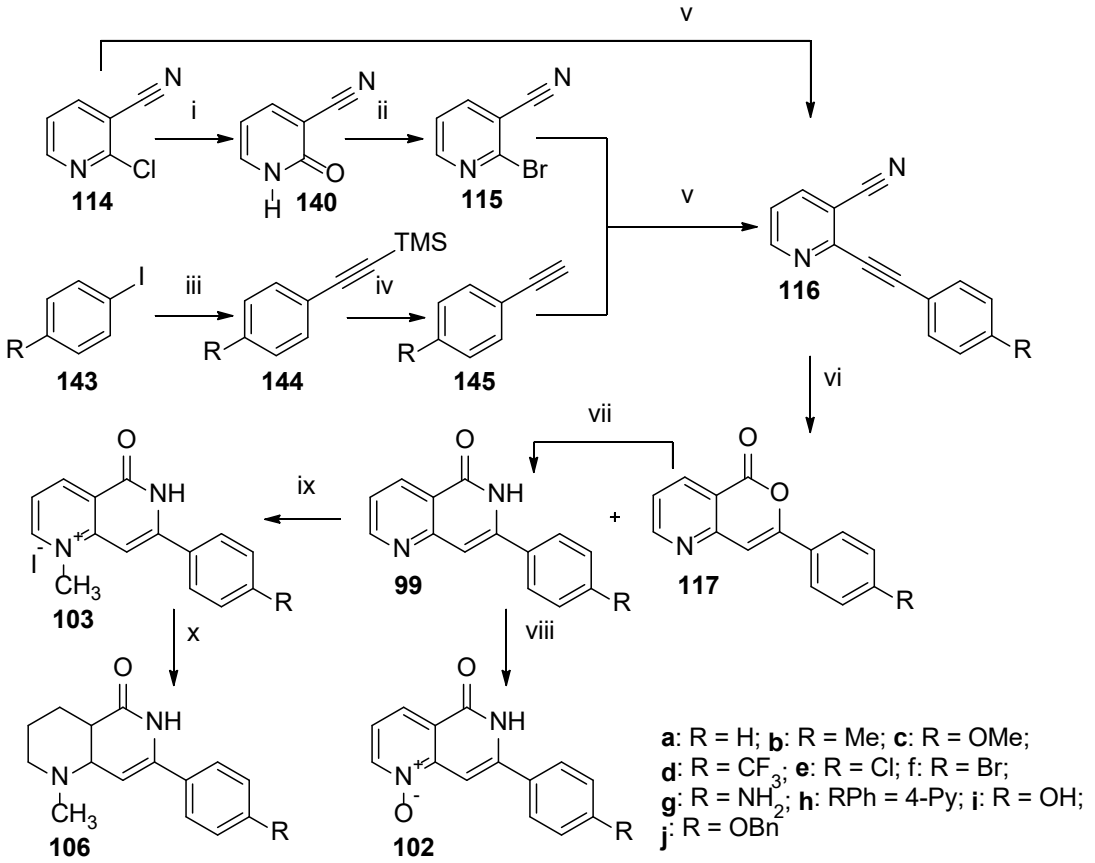

Scheme 13. Synthesis of 7-aryl-1,6-naphthyridin-5-ones and their *N*-oxide and *N*-alkyl derivatives. *Reagents & conditions:* i, AcOH, Δ, then THF, H_2O, Δ, 100%; ii, Bu_4NBr, P_2O_5, PhMe, Δ, 94%; iii, $Me_3SiC{\equiv}CH$, $Pd(PPh_3)_2Cl_2$, CuI, Et_3N, Na ascorbate, THF, 40 °C, 58-96%; iv, Bu_4NF, THF, 42-92%; v, $Pd(PPh_3)_2Cl_2$, CuI, Na ascorbate, Pr^i_2NH, THF, 40 °C, 25-87%; vi, aq. H_2SO_4 (9 M), Δ; vii, NH_3, $MeO(CH_2)_2OH$, 100 °C, pressure, 10-75% for two steps; viii, H_2O_2.urea, $(F_3CCO)_2O$, DMF, 29-50%; ix, MeI, DMF, 4-90%; x, pyridine.BH_3, HCOOH, 3-47%.

Sonogashira couplings were also used to synthesise the phenylethynes **145** needed for Route C (Scheme 13). In this route, the ethyne is attached to the aryl unit before coupling to the 3-cyano-2-halopyridines. The conversion of iodobenzenes **143** into ethynylbenzenes **145** was chosen because commercially available ethynylbenzenes are relatively expensive. However, phenylethyne **145a** and 4-methylphenylethyne **145b** were purchased. Iodobenzenes **143** and TMSE were used as educts in these coupling reactions, for which the following conditions were chosen: $(Ph_3P)_2PdCl_2$ as the palladium catalyst / ligand system, copper(I) iodide as the copper(I) co-catalyst and triethylamine as the base and the solvent. The reactions were performed under argon. This method resulted in moderate to good yields, providing a variety of trimethylsilylethynylbenzenes **144c-e,g-i** (see Scheme 13). To improve the yield, the amount of TMSE was increased. However, it did not result in better yields but only in formation of considerable amounts of the competing Glaser-coupling product, 1,4-bis(trimethylsilyl)butadiyne. In the literature,[196] possible ways of avoiding this side

reaction are described, including degassing the reaction flask with argon, nitrogen or hydrogen; however, argon had already been used in these couplings. Bag *et al.*[197] used click chemistry conditions for Sonogashira coupling. Copper(I) was generated *in situ* by reaction of copper(II) salts with sodium ascorbate. The latter was used also as a deoxidising agent. In the present work, addition of a small amount (6 mol%) of sodium ascorbate as a reducing agent, together with a direct copper(I) source, led to excellent yields of the desired trimethylsilylethynylbenzenes **144c-e,g-i**, with very low levels of Glaser side-reactions. The trimethylsilylethynylbenzenes **144c-e,g-i** were deprotected with tetrabutylammonium fluoride (TBAF) in THF, to give ethynylbenzenes **145** in moderate to excellent yields. Commercially available phenylethyne **145a**, 4-methylphenylethyne **145b** and the synthesised ethynylbenzenes **145c-e,g-i** were then introduced into the second Sonogashira coupling with 2-bromo-3-cyanopyridine **115**.

The general conditions for this second coupling included bis(triphenylphosphine)palladium(II) dichloride, copper(I) iodide, sodium ascorbate and THF. Diisopropylamine was used as the base instead of the less polar triethylamine used in the first Sonogashira coupling. Other conditions were also investigated. Absence of sodium ascorbate led to formation of major amounts of oxidative side-products (1,4-diarylbutadiynes). Use of tetrakis(triphenylphosphine)palladium(0) increased the yield of 3-cyano-2-(phenylethynyl)pyridine to 98% but dramatically slowed the reaction rate. Surprisingly, in one run, 2-chloro-3-cyanopyridine **114** gave better yields than the 2-bromo analogue **115** in the formation of 3-cyano-2-(phenylethynyl)pyridine **116a** but the origin of this effect is not clear. Freshly prepared bis(triphenylphosphine)palladium(II) dichloride improved yields and decreased the reaction time in comparison to the commercially available catalyst. The 2-arylethynylpyridines **116a-e,g-i** were obtained in moderate-to-good yields. Synthesis of a 4-hydroxyphenyl derivative was also investigated. However, 4-ethynylphenol **145i** failed to couple under Sonogashira conditions with **115**; after 5 d, an unidentifiable mixture of

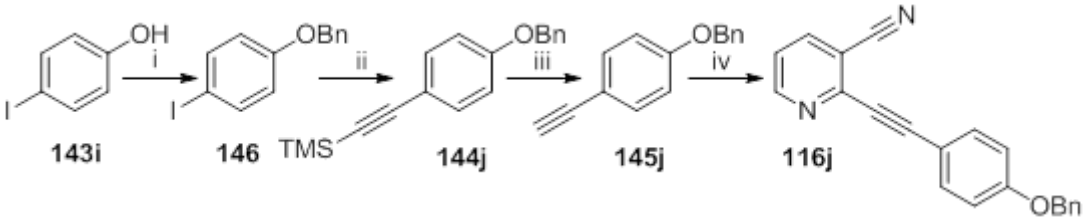

Scheme 14. Protection and following coupling of 4-iodophenol **143i**. *Reagents & conditions*: i, BnBr, Cs_2CO_3, DMF, r.t., 82%; ii, $Me_3SiC{\equiv}CH$, $Pd(PPh_3)_2Cl_2$, CuI, Na ascorbate, Et_3N, THF, 40 °C, 92%; iii, Bu_4NF, THF, r.t., 72%; iv, **115**, $Pd(PPh_3)_2Cl_2$, CuI, Na ascorbate, Pr^i_2NH, THF, 40 °C, 29%.

compounds was observed. This might be explained by deprotonation of the phenolic hydroxy group by the strongly basic diisopropylamine (pKa of conjugate acid = 11.07[198]), which disfavours the generation of the alkynyl-copper intermediate. To avoid this, a protective *O*-benzyl group was introduced (Scheme 14). 4-Iodophenol **143i** was treated with benzyl bromide under basic conditions in anhydrous dimethylformamide to give **146** in good to excellent yields, depending on the base used. Caesium carbonate, possessing non-coordinating caesium cation, proved to be the best option, giving 82% yield, compared to sodium hydride (76%) and potassium carbonate (55%). 1-(Benzyloxy)-4-iodobenzene **146** was coupled with TMSE under the usual conditions in triethylamine. Deprotection of the resulting alkyne **144j** with TBAF gave an excellent yield of 1-(benzyloxy)-4-ethynylbenzene **145j**. The latter was then coupled under Sonogashira conditions with **115** to give **116j** in 29% yield (see Scheme 14).

The 2-arylethynyl-3-cyanopyridines **116a-e,g-j** were cyclised to obtain the desired 7-aryl-1,6-naphthyridin-5-ones **99a-e,g-j** as a mixture with the corresponding pyrano-pyridinones **117**. The cyclisation of arylalkynes carrying nucleophilic groups *ortho* to the alkyne, triggered by electrophiles, has been extensively studied.[173,199-208] Using the example of cyclisation of 2-alkynylbenzoic acids (Scheme 15), there are two possible modes of cyclisation – 5-*exo*-dig and 6-*endo*-dig (Figure 37). Both of these are favoured under Baldwin's Guidelines.[209] The balance of electron-densities of the two aromatic rings has a major influence on the direction of cyclisation. If the ring carrying the nucleophile carries a further electron-withdrawing group, then the 6-*endo*-dig route is favoured. For example, cyclisation of methyl 3-nitro-2–phenylethynylbenzoate with Hg^{2+} / H_2SO_4, iodine monochloride or phenylselenenyl chloride gives 5-nitro-3-phenyl-isocoumarin, 4-iodo-5-nitro-3-phenylisocoumarin or 5-nitro-3-phenyl-4-phenylselenyl-isocoumarin, respectively.[173] It was predicted that the electron-deficient pyridine in **116a-e,g-j,** would drive the 6-*endo*-dig cyclisation during reaction with a proton or heavy metal cations.[173]

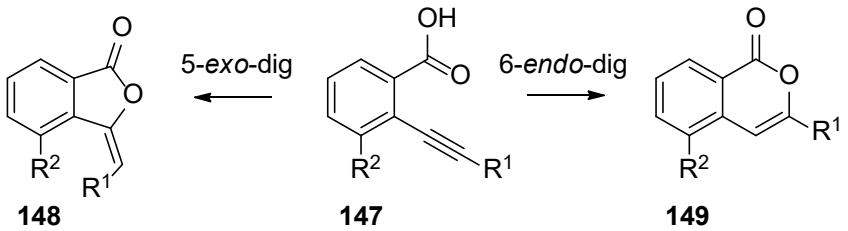

Scheme 15. Possible modes of cyclisation of arylethynes carrying potential nucleophiles *ortho* to the alkyne.

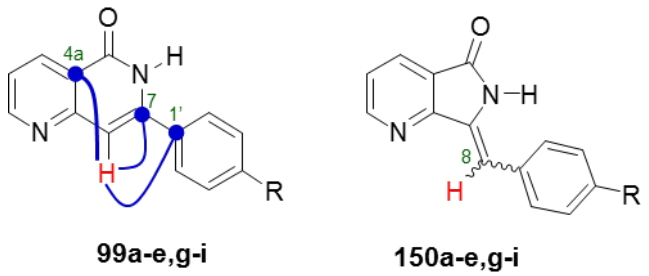

Figure 37. Left: HMBC correlations between 8-HH and 4a-C, 7-C and 1'-C in a molecule of **99a-e,g-i**, confirming the naphthyridinone structure **Right**: structure of putative 7-arylidinepyrrolo[3,4-*b*]pyridin-5-one isomers from 5-*exo*-dig cyclisation.

Nishiwaki *et al.*[174] reviewed procedures for the cyclisation of 2-arylethynyl-3-cyanopyridines. Reflux of **116a** for 1 h with 1 M sodium hydroxide in methanol gave a small amount of 1,6-dihydro-1,6-naphthyridin-5-one **99a** from 6-*endo*-dig cyclisation but the main component was 7-benzylidenepyrrolo[3,4-*b*]pyridine **150a** from the 5-*exo*-dig reaction. Reflux of **116a** in 4.5 M aq. sulfuric acid with 20 mol% mercury(II) chloride gave 2-phenacylpyridine-3-carboxylic acid through 6-*endo*-dig cyclisation, followed by hydrolysis of the intermediate lactone. By contrast, reaction of **116a** with 9 M aq. sulfuric acid alone gave 7-phenyl-1,6-naphthyridin-5-one **99a** and 7-phenylpyrano[4,3-*b*]pyridin-5-one **117a** in a 1:1 molar ratio, both through 6-*endo*-dig cyclisations.[174] In the present work, 2-(arylethynyl)-3-cyanopyridines **116a-e,g-j** were treated with hot 9 M aq. sulfuric acid in the absence of mercury (Scheme 16). Interestingly, the mechanism of this cyclisation could imply that the driving force of the reaction is the

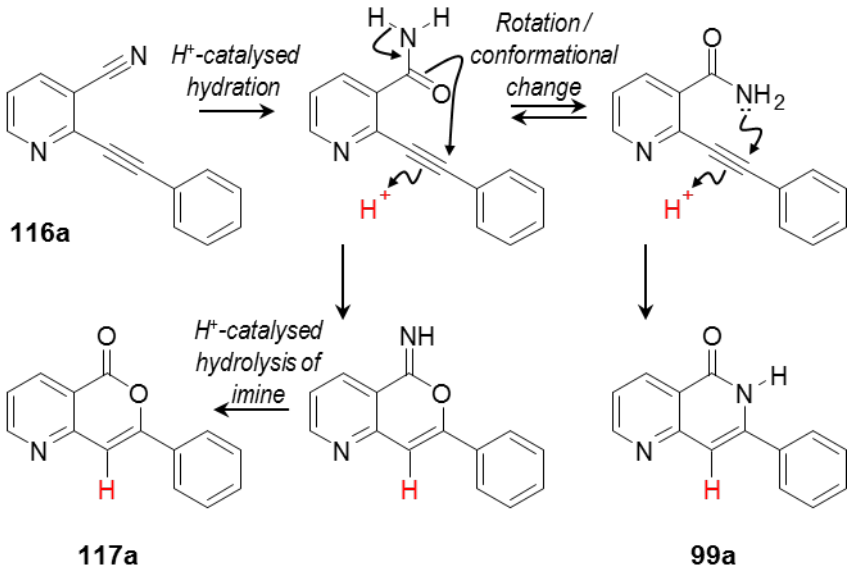

Scheme 16. Mechanism of 6-*endo*-dig cyclisation of 3-cyano-2-phenylethynylpyridine **116a** with 9 M aq. H_2SO_4 to give 7-phenyl-1,6-naphthyridin-5-one **99a** and 7-phenyl-5*H*-pyrano[4,3-*b*]pyridin-5-one **117a.**

protonation of an electron-rich triple bond. Subsequently, the triple bond would be converted into a double bond with sp^2-hybridised carbons, one of which would experience the attack of electron-rich carbonyl double bond or a lone pair of the nitrogen atom (depending on the conformation of the alkyne **116**), giving a 5-*exo*-trig or 6-*endo*-trig product. Alternatively, the attack of the sp-hybridised carbon atom by the carbonyl double bond or a lone pair of the nitrogen atom might happen firstly, providing 5-exo-dig or 6-endo-dig cyclisation pattern. Further mechanistic studies should be carried out to investigate the first step of this cyclisation (see Scheme 16). This method gave mixtures of 7-arylphenylpyrano[4,3-*b*]pyridin-5-ones **117a-e,g-i** and the desired compounds **99a-e,g-i**, which could be separated by chromatography. To ensure that the products were 6-*endo*-dig cyclised and were indeed 7-aryl-1,6-naphthyridin-5-ones **99** and not the 5-*exo*-dig products (7-arylidinepyrrolo[3,4-*b*]pyridin-5-ones) **150**, their structures were primarily confirmed by NMR.

In the ^{1}H NMR spectra, the 8-H (shown in red in Figure 37) resonated as a singlet at *ca.* δ 7, consistent with either structure **99** or **150**. The ^{1}H-^{13}C HMBC NMR spectrum of **99d** (Figure 38) showed a two-bond correlation between 8-H and 7-C; this is not diagnostic, as it could have been a two-bond correlation between 8-H and 7-C in the 7-arylidenepyrrolo[3,4-*b*]pyridin-5-ones **150**. The three-bond correlation between 8-H and 1'-C was revealed; however, it could have been a two-bond correlation between 8-H and 1'-C in the 5-*exo*-dig product **150**. A three-bond correlation between 8-H and 4a-C was also evident: the corresponding relationship in the 5-*exo*-dig cyclised products would be 8-H to 4a-C, *i.e.* through four bonds, which is unlikely (see Figure 37). The second proof was revealed when the product of the cyclisation was introduced into subsequent steps of the synthesis, alkylation and reduction (these will be discussed further). NMR studies of the products of the reactions of alkylation and reduction showed the structures, which would be only possible to obtain from 6-*endo*-dig products of cyclisation. Moreover, some crystal structures were obtained of derivatives bound into the tankyrase-2 protein (discussed later), unequivocally showing the structure of the compounds that could only be obtained from 6-*endo*-dig cyclised material.

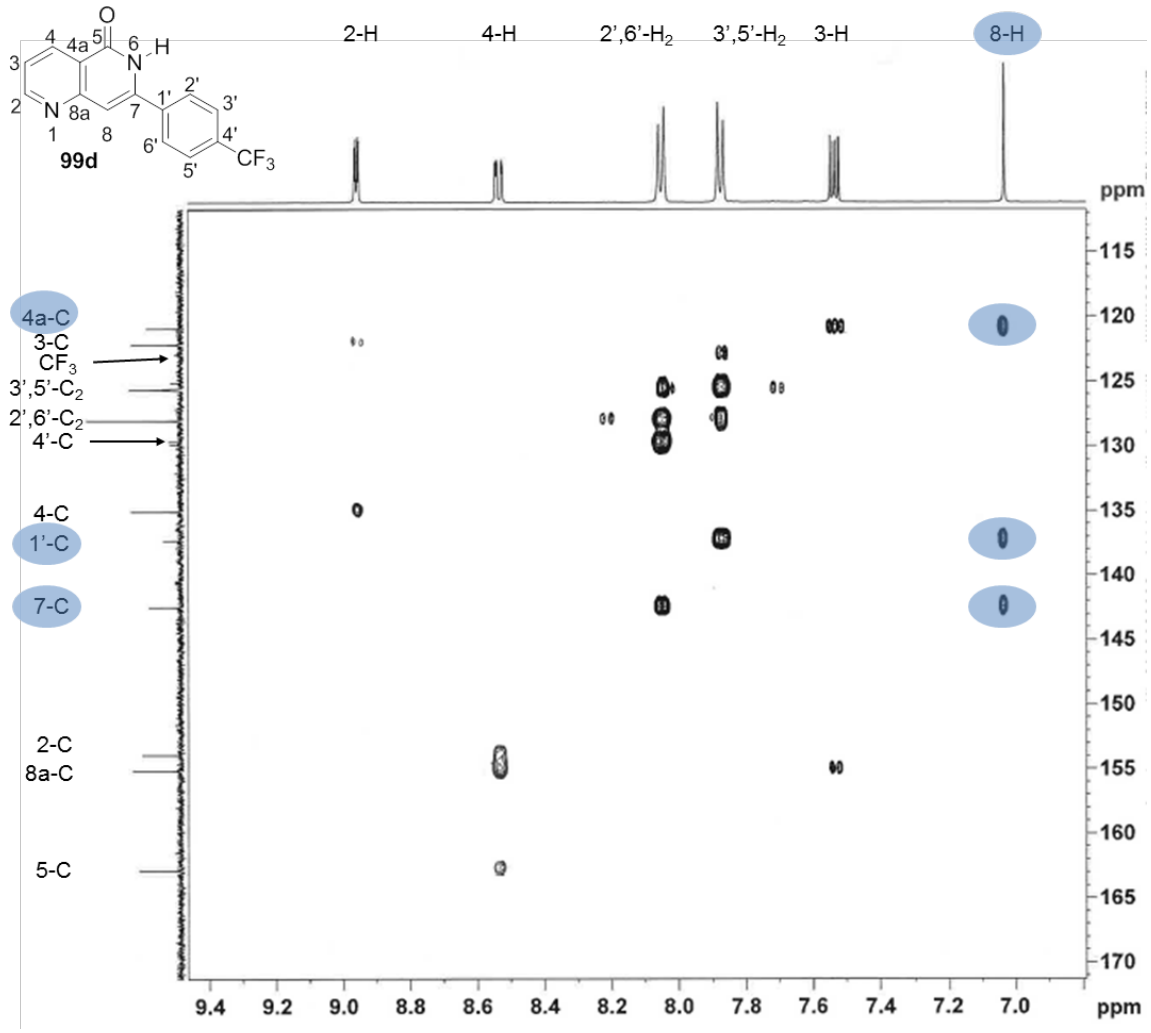

Figure 38. Parts of ^{1}H-^{13}C HMBC NMR spectrum of 7-(4-trifluoromethylphenyl)-1,6-naphthyridin-5-one **99d**. The highlighted ellipses indicate important correlations.

Firm establishment of the course of the cyclisation was critical at this stage, as Hellal and Cuny obtained 7-benzylidenepyrrolo[3,4-*b*]pyridin-5-one from a one-pot tandem Sonogashira coupling of 2-chloropyridine-3-carboxamide with phenylethyne and cyclisation under forcing conditions under prolonged microwave irradiation.[210] For most examples, the pyranopyridin-5-ones **117** were more abundant in the mixtures. However, for further synthesis, separation of these two cyclised products was not essential. Interestingly, when polyphosphoric acid was used instead of 9 M aq. sulfuric acid for the cyclisation of **116g**, it provided a better yield. However, the major product was the corresponding pyranopyridin-5-one **117g**. Unfortunately, the cyclisation of **116h** failed after multiple attempts with various electrophiles, giving an unidentifiable mixture of compounds. Some difficulties in the synthesis and isolation of **99h** were, however, expected, since this molecule contained two pyridine rings, which provided an even electron-density. Also, in the highly acidic conditions of the cyclisation, protonation of both heterocyclic nitrogen atoms in the molecule of **116h** is likely to happen. This protonation would deplete the electron density of the triple bond and prevent it from binding to the acidic proton, thereby stopping the cyclisation. According to the Baldwin Guidelines, both 5-*exo* and 6-*endo* cyclisation patterns would be feasible.[209] The 5-*exo* product would also be of *E*- or *Z*-geometry. Therefore, at least three products were expected. However, an unidentifiable mixture of compounds was detected after multiple attempts. Intriguingly, when an attempt was made to cyclise **116j** with 9 M aq. sulfuric acid, it resulted in loss of the benzyl group, providing a mixture of **99i** and **117i** (*ca.* 20 : 80).

The pyranopyridin-5-ones **117a-e,g-i** were converted readily into the desired naphthyridinones **99a-e**. Modifying a method developed in our laboratory for the conversion of

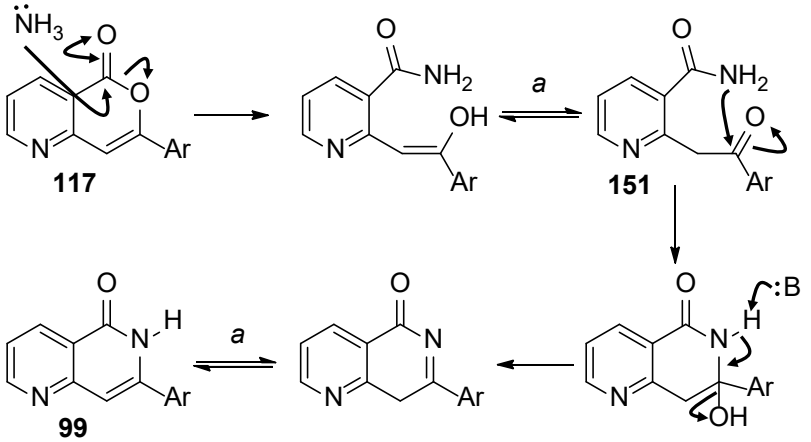

Scheme 17. Mechanism of conversion of 7-phenyl-5*H*-pyrano[4,3-*b*]pyridin-5-ones **117** into 7-phenyl-1,6-naphthyridin-5(6*H*)-ones **99.** *a*: tautomerism

3- and 4-substituted 5-nitroisocoumarins to the corresponding 5-nitroisoquinolin-1-ones (including an optimised route to 5-AIQ **48a**),[12] ammonia was passed through solutions of **117a-e,g-i** in the high-boiling protic solvent 2-methoxyethanol and the solutions were then heated under pressure (Scheme 17). It was observed that the presence of an electron-neutral or electron-donating group, such as methyl, methoxy, or amino in the 4-position of the 7-aryl moiety decreased the reaction rate markedly. This could be due to decreased electrophilicity of the ketone carbonyl of the intermediate **151** (see Scheme 17), caused by the electron-donating groups. Alternatively, the effect may be due to the electron-donating groups making the lactone carbonyl group less electrophilic by increasing electron-density at the carbon.

To provide a less basic bicyclic heterocycle (pKa of pyridine (conjugate acid) 5.25)[211] and an alternative hydrogen-bonding group, the 1-N in 7-aryl-1,6-naphthyridin-5-ones **99a,b** was oxidised to the corresponding *N*-oxide **102a,b** (pKa of pyridine-*N*-oxide (conjugate acid) 0.79).[212] Electron-poor pyridines are relatively difficult to oxidise to their *N*-oxides. Previous procedures[100,213,214] used different strong oxidising agents (all peroxyacids) for forming (fused) pyridine-*N*-oxides. Caron *et al.*[213] developed a procedure of oxidation of pyridines carrying electron-withdrawing groups with peroxytrifluoroacetic acid, generated *in situ* from urea.H_2O_2 and trifluoroacetic anhydride, instead of the previously used trifluoroacetic acid and 90% H_2O_2 (a very dangerous reagent) (Scheme 18). This method gave excellent yields of the corresponding *N*-oxides **153**. Later Lord *et al.*[100] used urea.H_2O_2 complex and trifluoroacetic anhydride in dichloromethane to generate anhydrous peroxytrifluoacetic acid for *N*-oxidation of 8-cyano-3-phenylquinoline, which gave a modest yield of

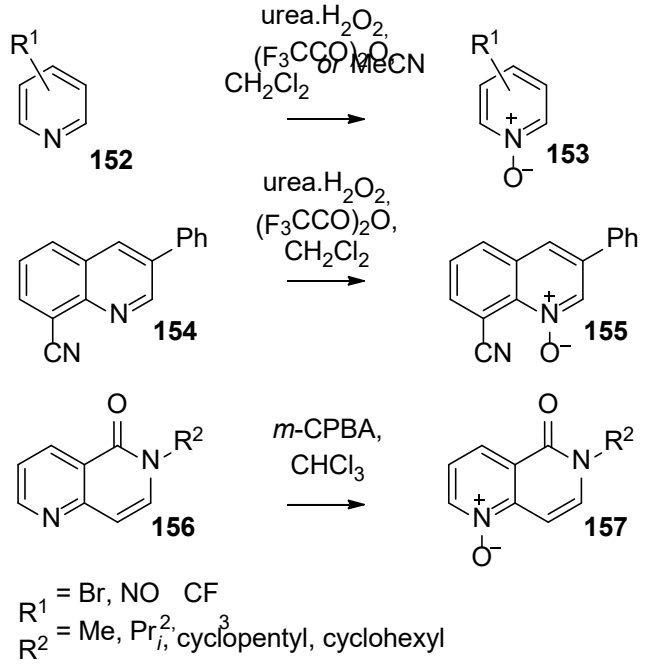

Scheme 18. *N*-oxidation of (fused)pyridines carrying electron-withdrawing groups: **Top**: *N*-oxidation of pyridine rings carrying electron-withdrawing groups.[213] **Middle**: *N*-oxidation of 8-cyano-3-phenylquinoline.[100] **Bottom**: *N*-oxidation of 6-alkyl-1,6-naphthyridin-5-ones.[214]

oxidised product **155** (see Scheme 18). Very recently, a procedure for oxidation of substituted 6-alkylnaphthyrid- in-5-ones was developed, using 3-chloroperoxybenzoic acid, which gave excellent yields of the N^1-oxides.[214] However, our 7-arylnaphthyridin-5-ones **99a,b** were poorly soluble in dichloromethane, owing to intermolecular hydrogen bonding of the lactam N-H and C=O, and treatment with urea.H_2O_2 complex and trifluoroacetic anhydride in this solvent did not give the desired *N*-oxides. However, a change of solvent to DMF allowed the reactions to go to completion (see Scheme 13).

The structures of the *N*-oxides were proven by ^{1}H-^{15}N HMBC NMR (Figures 39 and 40), which showed two- and three-bond correlations between hydrogen and nitrogen atoms and allowed the assignment of the two ^{15}N signals for the naphthyridinones. Starting from the analysis of the ^{1}H NMR spectra, it was revealed that the signal for 2-H in both molecules **99** and **102** was in the downfield region: δ (2-H) in **99a** was 8.89; δ (2-H) in **102a** was 8.62. For the naphthyridinone **99a**, the relative downfield chemical shift of 2-H might be due to electron-withdrawing effect of the nitrogen atom, which is two bonds away from 2-H. The doublet for 2-H in the *N*-oxide molecule **102a** was 0.27 ppm upfield, compared to the doublet for 2-H in **99a**. Considering the formal change of charge on the nitrogen atom and the influence of the formally negatively charged oxygen atom, which is three bonds away from 2-H, this upfield shift is feasible. For instance, previous NMR studies of pyridine-*N*-oxide revealed a similar change in chemical shift of 2-H: δ (2-H) in pyridine is 8.50,[215] when δ (2-H) in pyridine *N*-oxide is 8.29[216] or, according to more recent data, 7.97-7.96.[217] Slightly lesser change of charge is present in quinolines: δ (2-H) in quinoline is 8.88,[215] when δ (2-H) in quinoline-*N*-oxide is 8.77.[217] By contrast, the singlet for 8-H in both molecules was further upfield (δ (8-H) in **99a** was 6.98; δ (8-H) in **102a** was 7.31) as 8-C can be considered as part of an enamine system with 7-C and 6-N. The singlet for 6-H appears at *ca*. δ 11 and should be an important parameter of changes at 6-N. However, it is often broad and its precise chemical shift will also depend on hydrogen-bonding to solvent, *etc*. This does not allow it to be a reliable characteristic of the product of *N*-oxidation. The expected outcome for this reaction was the oxidation of 1-N, since it is expected to be more nucleophilic than is 6-N and, therefore, is more likely to react with the electrophilic oxidising agent (peroxytrifluoroacetic acid). For the starting naphthyridinone **99a**, the NMR signal for 1-N is at δ 278.87, with HMBC correlations to 2-H and 8-H (see Figure 39). The signal for 6-N is at δ 124.89, with HMBC correlation to 8-H only. A dramatic

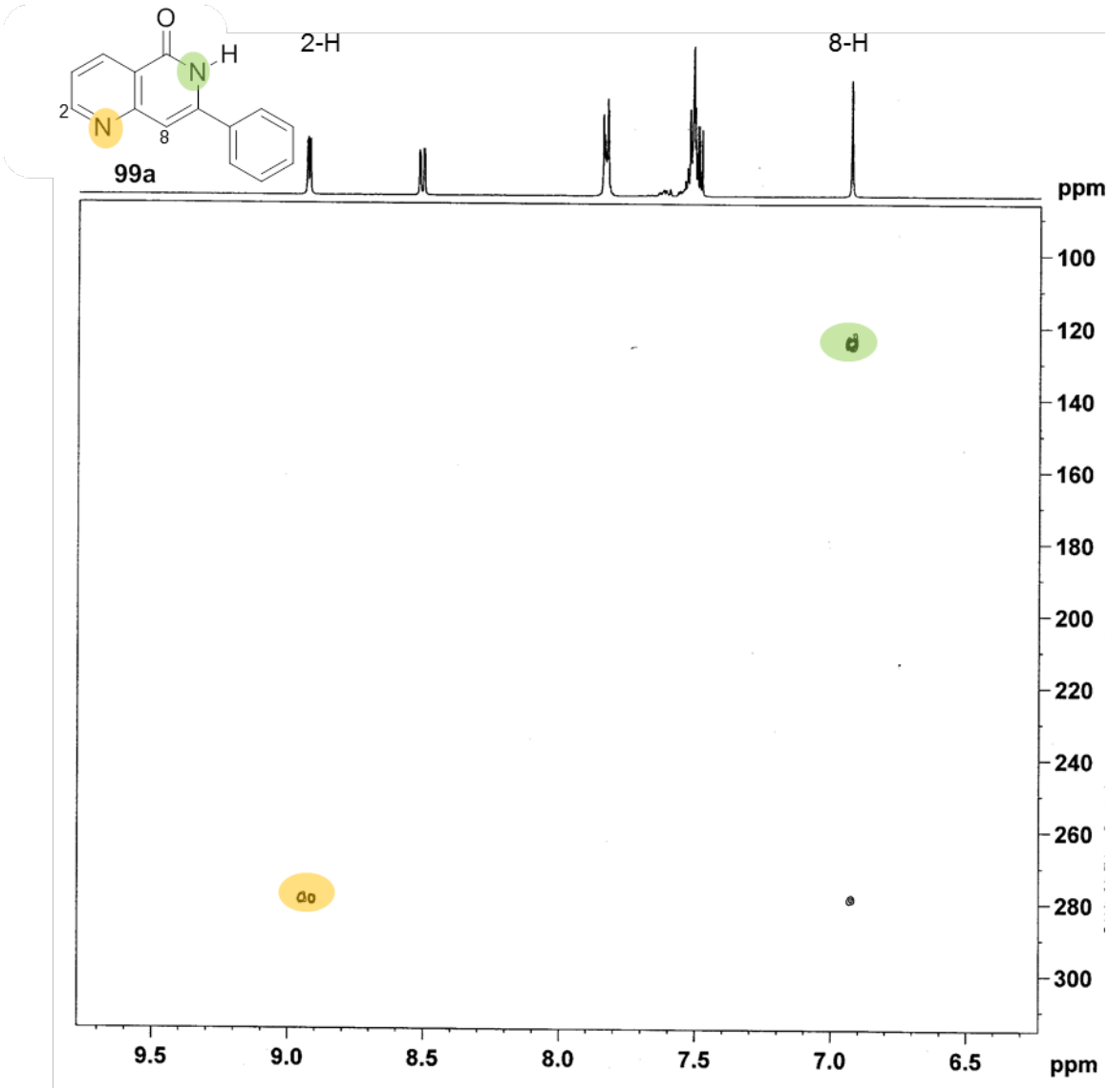

Figure 39. Parts of ^{1}H-^{15}N HMBC NMR spectra of 7-phenyl-1,6-naphthyridin-5-one **99a**. The highlighted ellipses indicate important correlations.

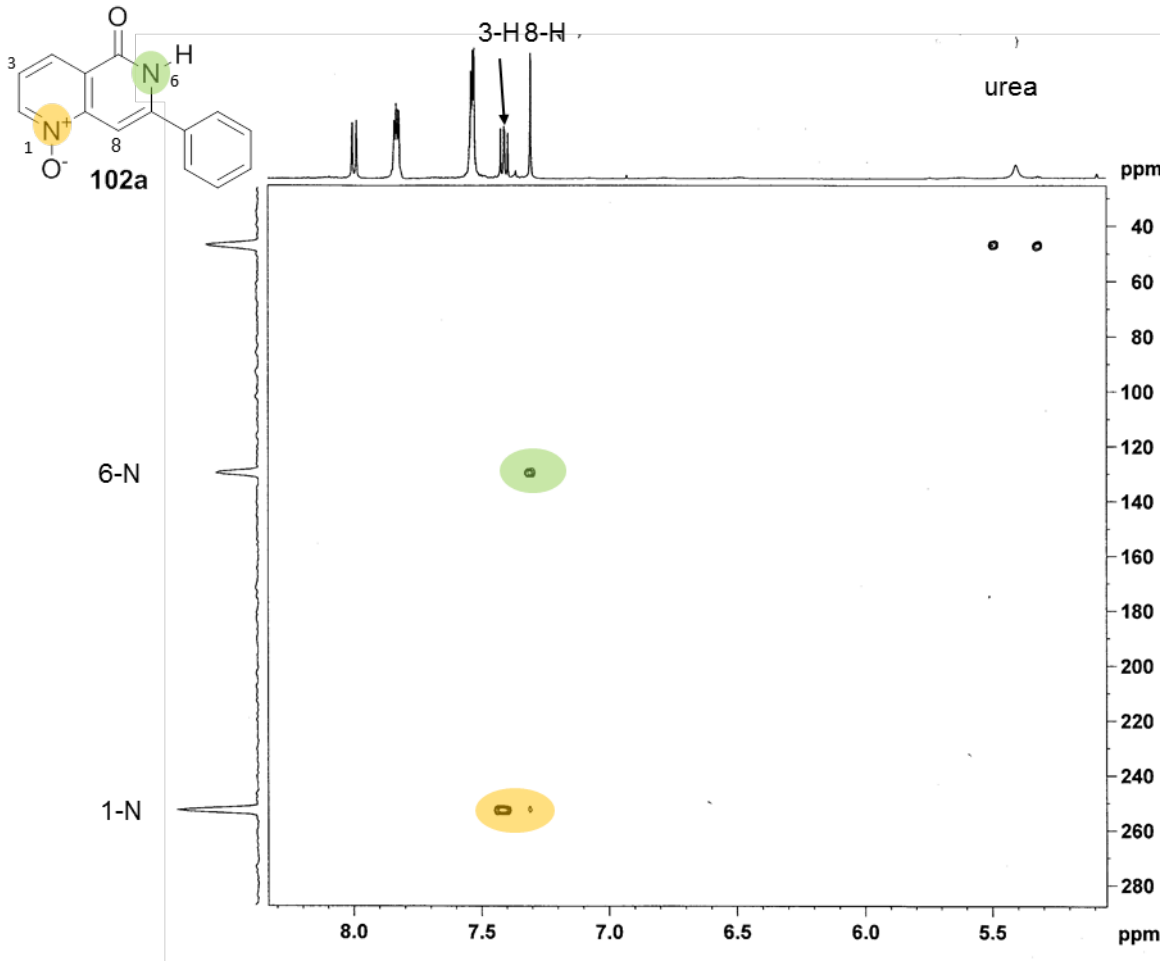

Figure 40. Parts of ^{1}H-^{15}N HMBC NMR spectrum of 5-oxo-7-phenyl-5,6-dihydro-1,6-naphthyridine 1-oxide **102a**. The highlighted ellipses indicate important correlations.

change of chemical shift of the 1-N signal (δ (1-N) in **102a** is 252.76) can be seen in the ^{1}H-^{15}N HMBC NMR spectrum of *N*-oxide **102a** (see Figure 40), whereas that of 6-N changed only slightly (δ (6-N) in **102a** is 129.56). The small amount of urea contaminating the sample of **102a** was then easily removed by washing the product with water.

Other derivatives of 7-aryl-1,6-naphthyridin-5-ones were synthesised through methylation at 1-N. Under neutral conditions, this should be the more nucleophilic of the two nitrogen atoms, although Sunderland has shown that 5-AIQ is alkylated at the exocyclic 5-NH_2 under mildly basic conditions but at 2-N in the presence of sodium hydride.[110] Under mildly basic conditions, the molecule of 5-AIQ is neutral and the exocyclic amino group is more nucleophilic than 2-N. However, when a strong base, *e.g.* sodium hydride, is employed, it deprotonates 2-N, making a monoanion, which is more nucleophilic than the exocyclic amino group and thus undergoes the alkylation. Adapting the method of Showalter,[218] compounds **99a-e,g** were treated with iodomethane in dry DMF. Similarly to the *N*-oxidation, it was expected that the alkylation would happen at 1-N. Indeed, the reaction gave the corresponding 1-methyl-5-oxo-7-aryl-5,6-dihydro-1,6-naphthyridin-1-ium iodides **103a-e,g** (see Scheme 13). The structures of these compounds were proven by ^{1}H NMR and ^{1}H-^{13}C HMBC NMR. Firstly, the broad singlet of 6-H was conserved in the products of alkylation, indicating that changes at 6-N were unlikely. The signal for 2-H correlated in the HMBC spectrum with the signal for a carbon at *ca.* δ 45. This signal was shown also to correlate with the methyl protons in the HSQC spectrum. At the same time, the singlet for the N-Me at *ca*.δ 4.5 correlated with 2-C and 8a-C. Taken together, these indicate that the alkylation happened on 1-N, not on 6-N, as it was predicted.

1-Methyl-5-oxo-7-aryl-5,6-dihydro-1,6-naphthyridin-1-ium iodides **103a-e,g** were subjected to reduction with the borane-pyridine complex to give the corresponding compounds **106** (see Scheme 13). This reagent is known as a mild reducing agent suitable for the reduction of naphthyridinium salts.[218] Formic acid was used as a polar solvent in this reaction. However, formic acid was also undergoing the reduction induced by the borane-pyridine complex, causing a partial loss of the reducing agent. Bearing that in mind, a significant excess of the reducing agent was used. Interestingly, the addition of borane-pyridine complex in one portion did not lead to the complete reduction of the starting **103a-e,g**, leaving a significant amount of the starting material. However, when added dropwise in a few portions, borane-pyridine complex fully

reduced the 1-methyl-5-oxo-7-aryl-5,6-dihydro-1,6-naphthyridin-1-ium iodides **103** into 1-methyl-7-aryl-1,2,3,4-tetrahydro-1,6-naphthyridin-5-ones **106**.

Overall, a variety of 7-phenyl-1,6-naphthyridin-5-ones **99**, 7-aryl-5,6-dihydro-1,6-naphthyridin-5-one 1-oxides **102**, 1-methyl-5-oxo-7-aryl-5,6-dihydro-1,6-naphthyridinium iodides **103** and 1-methyl-7-aryl-1,2,3,4-tetrahydro-1,6-naphthyridin-5-ones **106** was synthesised through a modified Sonogashira pathway, providing a library of candidate tankyrase-1/2 inhibitors for biological evaluation (Figure 41).

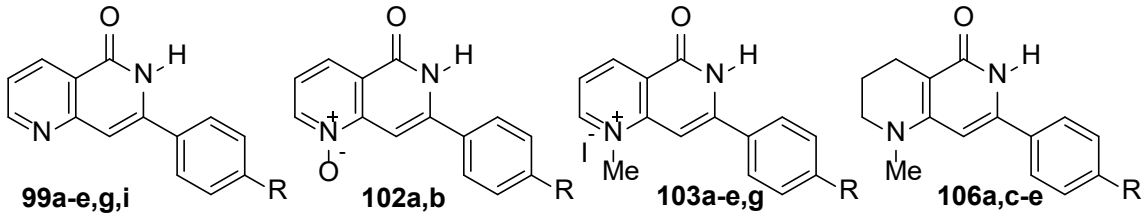

a: R = H; b: R = Me; c: R = OCH_3; d: R = CF_3; e: R = Cl; f: R = Br; g: R = NH_2; h: RPh = 4-Py; i: R = OH; j: R = OBn

Figure 41. Summary of 7-phenyl-1,6-naphthyridin-5-ones **99** and their derivatives, synthesised through a modified Sonogashira pathway.

2.3 Synthesis of 3-aryl-2,7-naphthyridin-1-ones and their derivatives.

In order to investigate further SAR of the tankyrase-1/2 inhibitors, it was decided to make various regioisomers of arylnaphthyridinones **99**. 3-Aryl-2,7-naphthyridin-1-ones **101** are of particular interest for the SAR studies, since the nitrogen atom in these molecules is in the position where no bulky substituents are predicted to be tolerated. The synthesis of 7-aryl-1,6-naphthyridin-5-ones **99** and their derivatives became the first step towards the investigation of the influence of the location of the heterocyclic nitrogen atom on the activity of the tankyrase-1/2 inhibitors. The series of compounds **99** revealed several synthetic possibilities, *e.g.* Sonogashira coupling of cyanohalopyridines with ethynylbenzenes with subsequent electrophilic cyclisation and conversion of the resulting mixture into the lactam, as well as derivatisation of lactams **99** into *N*-oxides **102**, *N*-methyl iodides **103** and tetrahydronaphthyridinones **106**.

Moving towards the synthesis of 3-aryl-2,7-naphthyridin-1-ones **101**, it was decided to try the same approach as for 7-phenyl-1,6-naphthyridin-5-ones **99**: Sonogashira coupling, followed by electrophilic cyclisation and conversion of the lactone into the lactam (Scheme 19). Commercially available 4-bromo-3-cyanopyridine **123** was proposed to be used as the haloarene in the Sonogashira couplings, since the chloro derivative would be unreactive, as the halogen in the 4-position is only weakly activated by the pyridine

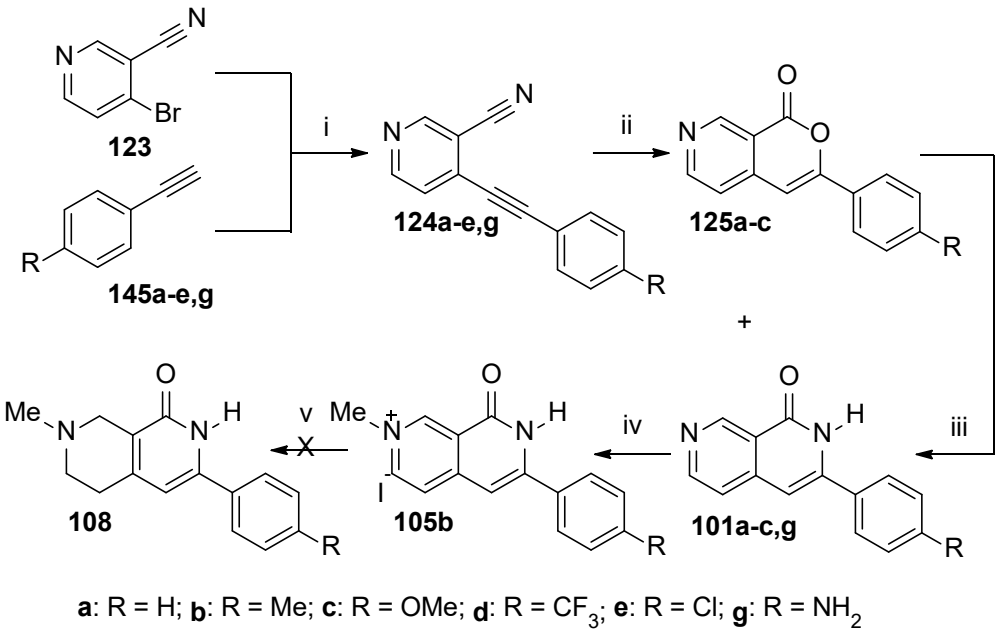

Scheme 19. Synthesis of 3-aryl-2,7-naphthyridin-1-ones **101** and their derivatives. *Reagents & conditions:* i, $Pd(PPh_3)_4$, CuI, Na ascorbate, Et_3N, THF, 40 °C, 35-78%; ii, aq. H_2SO_4 (9 M), Δ, ; iii, NH_3, $MeO(CH_2)_2OH$, 100°C, pressure; iv, MeI, DMF; v, pyridine.BH_3, HCOOH

nitrogen and again, the iodopyridines were expected to be labile to light.[184] The variety of arylethynes **145** was made *via* the two-step pathway from the corresponding iodoarenes, as for the earlier pathway. Therefore, the first step of this synthetic route involved sodium ascorbate-moderated Sonogashira coupling of **123** with arylethynes **145a,c-e,g**. This choice of arylethynes was determined by different electronic and steric effects of their substituents. Interestingly, when bis(triphenylphosphine)palladium(II) dichloride was used as a catalyst, the yield of the coupled product **124a** from **123** and phenylethyne **145a** was only 10%. However, substitution of the catalyst with tetrakis-(triphenylphosphine)palladium(0) resulted in a dramatic improvement of the yield of the reaction to 78%. This might be explained by the oxidation state of palladium; in tetrakis(triphenylphosphine)palladium(0), the palladium is already in the oxidation state which is necessary for the coupling. Triethylamine was used as a base in these coupling reactions, providing similar results to those reactions where diisopropylamine was utilised, *e.g.* the coupling of 2-bromo-3-cyanopyridine **115** with arylethynes **145**.

3-Cyano-4-(arylethynyl)pyridines **124a,c-e,g** were subjected to the cyclisation reaction and the conversion of lactone into lactam to obtain the target 3-aryl-2,7-naphthyridin-1-ones **101**. However, this sequence only gave the desired products in four cases: 3-phenyl-2,7-naphthyridin-1-one **101a**, 3-(4-methylphenyl)-2,7-naphthyridin-1-one **101b**, 3-(4-methoxyphenyl)-2,7-naphthyridin-1-one **101c** and 3-(4-aminophenyl)-2,7-naphthyridin-1-one **101g**. Interestingly, the 4-aminophenyl analogue **124g** was cyclised to form the lactam **101g** only, with no evidence for the corresponding lactone during the electrophilic cyclisation step. Thus, for this analogue, the subsequent treatment with ammonia was unnecessary. Therefore, it should be the conformation of the intermediate amide during the electrophilic cyclisation step which favoured the formation of **101g** (refer to Scheme 17). It can be noticed that 3-cyano-4-(arylethynyl)pyridines **124**, which carry –M electron-withdrawing substituents, failed to cyclise, giving an unidentifiable mixture of compounds. A possible explanation of this failure might be the effect of the electron-withdrawing group during the electrophilic cyclisation. It is probable that the electron-withdrawing substituent on the aryl ring depletes the electron-density of the triple bond, not allowing it to bind a proton and thus arresting electrophilic cyclisation. At the same time, electron-donating substituents of the aryl ring should increase the basicity of the triple bond, favouring the ring closure. However, this argument does not explain why the amino derivative readily provided a lactam, considering that, in the strongly acidic conditions of the cyclisation, the amino group would be protonated and,

therefore, would attain electron-withdrawing properties through the negative inductive effect.

The low-to-modest yields of the 3-aryl-2,7-naphthyridin-1-ones **101** did not provide enough material for further conversion in many cases. Following the example from the 1,6-naphthyridin-5-one series, methylation of 2,7-naphthyridin-1-ones **101a-c,g** with iodomethane was investigated, aiming for 6-aryl-2-methyl-8-oxo-7,8-dihydro-2,7-naphthyridin-2-ium iodides **105**. As before, it was expected that the nitrogen which underwent the alkylation would be 7-N and not 2-N, due to the higher nucleophilicity of 7-N. However, only **101a** could be converted into the corresponding 2,7-naphthyridin-2-ium iodide **105a**, with a yield of 11%. The structure of **105a** was proved by the same method as for the 1,6-naphthyridin-5-one series, using ^{1}H NMR and ^{1}H-^{13}C HMBC NMR. It revealed that the broad singlet for 2-H at δ 12.75 was conserved in the product of alkylation. A new singlet at *ca.* δ 4.4 appeared in the ^{1}H NMR spectrum, correlating in the HMBC spectrum with the signals of 6-C and 8-C. Together, these indicated that the alkylation indeed happened on 7-N and not on 2-N.

Compound **105a** was subjected to reduction with borane-pyridine complex in order to obtain 7-methyl-3-phenyl-5,6,7,8-tetrahydro-2,7-naphthyridin-1-one **108a**. The same procedure as for 1,6-naphthyridin-6-ium salts **103** was implemented, using borane-pyridine complex as a reducing agent and formic acid as a solvent. However, after multiple attempts, compound **105** could not be reduced to the tetrahydro-derivative **108** with borane-pyridine complex; the starting material **105** was isolated after 21 days of stirring. The reasons for this failure need to be investigated. However, it might be possible that, due to a different distribution of electron-density in the molecule of **105a** compared to the molecule of **99a**, the reduction became more challenging.

To sum up, despite the electronic effects of the substituents, which might have disfavoured the formation of target 3-aryl-2,7-naphthyridin-1-ones **101**, four examples of these molecules were synthesised *via* a Sonogashira pathway (Figure 42). Due to unknown reasons, only one compound, **101a**, resulted in the corresponding pyridinium salt **105a** during the alkylation. The reduction of **105a** did not lead to the desired

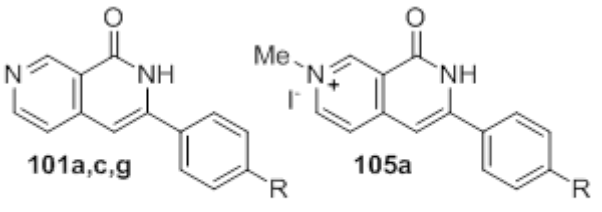

a: R = H; b: R = OCH_3; c: R = NH_2

Figure 42. Summary of 3-phenyl-2,7-naphthyridin-1-ones **101** and their derivatives, synthesised through a modified Sonogashira pathway.

product **108a**, leaving only the starting material only after multiple attempts. Further investigation might be necessary in order to establish a thorough understanding of the reasons of such poor reactivity of the series.

2.4 Synthesis of 3-aryl-2,6-naphthyridin-1-ones and their derivatives.

Having obtained 7-aryl-1,6-naphthyridin-5-ones **99** and 3-aryl-2,7-naphthyridin-1-ones **101**, the investigation of the influence of heterocyclic nitrogen on the activity of tankyrase-1/2 inhibitors was planned to be continued by the synthesis of another arylnaphthyridinone regioisomer. No information is available about the effect of substituents at the position-6 of 3-aryl-2,6-naphthyridin-1-ones on the inhibitory activity against tankyrase-1/2. Thus, 3-aryl-2,6-naphthyridin-1-ones **100** were of particular interest in order to investigate the SAR further.

A similar approach to that used for the previous syntheses of 7-aryl-1,6-naphthyridin-5-ones **99** and 3-aryl-2,7-naphthyridin-1-ones **101** was investigated. Some difficulty was anticipated in using 3-bromo-4-cyanopyridine **119** as a coupling partner in the Sonogashira reaction, since the 3-position is not activated by the ring-nitrogen, as it is in 2-bromo-3-cyanopyridine **115** (greatly) and in 4-bromo-3-cyanopyridine **123** (to a lesser extent). Firstly, as it was not commercially available, it was planned to synthesise starting 3-bromo-4-cyanopyridine **119**. Several pathways were planned (Scheme 20): (i) formylation of 3-bromopyridine **158**[219] with subsequent conversion of **159** into an oxime **160** and dehydration of the latter (shown in blue);[220] (ii) carboxylation of an anion formed from 3-bromopyridine **158**, followed by formation of the primary amide **162** and dehydration (shown in green);[187] (iii) direct bromination of an anion derived from 4-cyanopyridine **163** (shown in red).[221]

The first approach (see Scheme 20, blue) started with lithiation of 3-bromopyridine **158** and reaction of the anion with DMF as an electrophilic formylating agent. Lithium diisopropylamide (LDA) was chosen as the base, as it should act purely as a sterically hindered base and not indulge in lithium-bromine exchange (as would butyllithium).

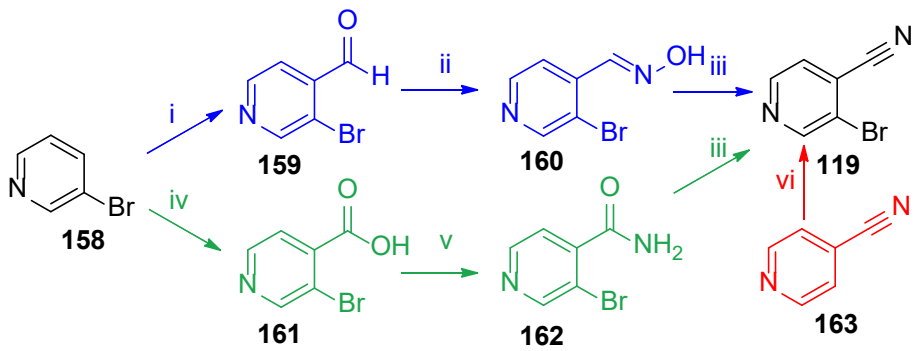

Scheme 20. Possible routes of synthesis of 3-bromo-4-cyanopyridine **119**. i, formylation; ii, formation of oxime; iii, dehydration; iv, carboxylation; v, formation of amide; vi, bromination

The 4-H is the most acidic proton in substrate **158**, not being adjacent to the heterocyclic nitrogen. Nucleophilic attack of the resulting anion on DMF gave the tetrahedral oxyanion intermediate, which is stable in anhydrous media but which collapses to the aldehyde upon aqueous work-up. The required aldehyde **159** was formed in 40% yield. There was no evidence for competing lithium-bromine exchange but, in some runs, 3-(diisopropylamino)pyridine **164** (Figure 43) was isolated, having been formed either in an S_NAr reaction or through a pyridyne as an intermediate.[222] The intermediacy of 2,3-pyridyne can be discounted, as Fang and Larock have shown that this pyridyne reacts with amine nucleophiles only at the 2-position.[223] By contrast, 3,4-pyridyne is claimed to be promiscuous between reactivity at the 3- and 4-positions.[224] 3-Bromopyridine-4-carboxaldehyde **159** was then converted with hydroxylamine into the corresponding oxime **160**, which was crystalline. However, the last step, dehydration of 3-bromopyridine-4-carboxaldehyde oxime **160** with phosphorus oxychloride, resulted in an unidentifiable mixture of compounds after multiple attempts.

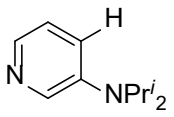

164

Figure 43. 3-(Diisopropylamino)pyridine **164,** a side-product of formylation of 3-bromopyridine **158.**

The second pathway (Scheme 20, sgreen; Scheme 21) also started with 3-bromopyridine **158** but involved the carboxylation, not formylation, of it. The benefit of this reaction was the formation of a stable carboxylic acid **161**, which would not undergo further oxidation, as would an aldehyde. The reaction was quite difficult to handle and resulted in a poor yield (10%) of **161**. At this point in the work, the carboxylic acid **161** became commercially available. Following the procedure of Dunn,[187] it was converted into a mixed anhydride with ethyl chloroformate. This mixed anhydride was used without isolation in a reaction with ammonia to give the amide **162**.

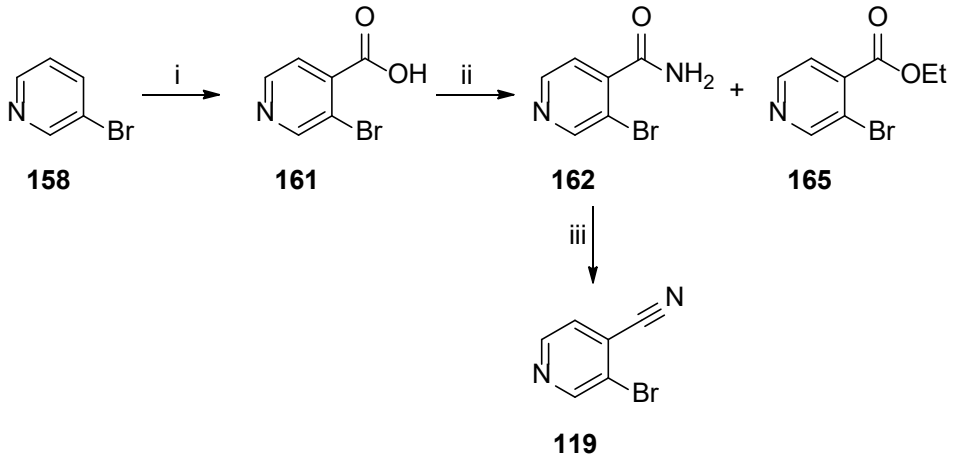

158 **161** **162** **165**

119

Scheme 21. Synthesis of 3-bromo-4-cyanopyridine **119** from 3-bromopyridine **158** *via* carboxylation of the latter. *Reagents & conditions*: i, *n*-BuLi, Pr$^i_2$NH, CO_2, -78 °C → r.t., 10%; ii, EtO_2CCl, NH_3, THF, 0 °C, 78% (**162**), 4.8% (**165**); iii, $POCl_3$, Δ, 42%.

Table 12. Optimisation of the synthesis of 3-bromo-4-cyanopyridine **119**[a].

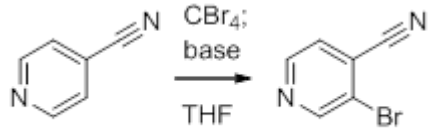

163 **119**

Entry	Base	Temperature, °C	Time, s	Yield, %
1	LTMP (*in situ*)	-95	10	5
2	LTMP (commercial)	-95	10	0
3	LDA (*in situ*)	-85	30	0
4	LDA (commercial)	-85	30	0
5	LiHMDS	-78	60	0

[a] The reactions were carried out in anhydrous THF at 2 M concentration of **163** with 2 equivalents of base and 1.2 equivalents of tetrabromomethane.

In some cases, the product formed was not the amide **162** but the ester **165** (see Scheme 21), formed by reaction of the mixed anhydride with ethanol during the desired reaction with ammonia. Subsequent dehydration of the amide of **162** with phosphorus oxychloride resulted in formation of desired 3-bromo-4-cyanopyridine **119** in 42% yield.

The third route (Scheme 20, red) resulted in a very poor yield (5%) of the desired 3-bromo-4-cyanopyridine **119** from 4-cyanopyridine **163** when following the literature procedure (lithium 2,2,6,6-tetramethylpiperidide (LTMP) prepared *in situ*, anhydrous THF, -95°C, 10 s, quench with tetrabromomethane).[221] A series of experiments was undertaken in an attempt to optimise the yield by varying the conditions (Table 12). Freshly prepared lithium tetramethylpiperidide (LTMP) was substituted with commercially available LTMP; lithium diisopropylamide (LDA) and lithium hexamethyldisilazide (LiHMDS) were also investigated (the apparent pK_a of the conjugate acid of LiHMDS in THF is 30.0,[225] the apparent pK_a of the conjugate acid of LDA in THF is 35.7 and the apparent pK_a of the conjugate acid of LTMP in THF is 37.3);[226] different sources of tetrabromomethane were used. The time and temperature of the reaction also were altered. These changes did not improve the reaction outcome; in fact, some of them led to complete degradation of the starting material. It is probable that the 4-cyanopyridin-3-ide anion was not stable enough to survive, even at -95°C.

3-Bromo-4-cyanopyridine **119** was involved in a Sonogashira coupling with arylethynes **145a-e**. Following the procedure previously optimised for other regioisomers, tetrakis-(triphenylphosphine)palladium(0) was used as the catalyst, copper(I) iodide as co-catalyst and diisopropylamine as base and solvent. Sodium ascorbate was used as a deoxidant as before. Interestingly, despite the deactivating position of the heterocyclic nitrogen, the coupled products **120a-e** were obtained in moderate (41%, **120e**) to good (72%, **120c**) yields (Scheme 22), in contrast to the previous regioisomer **123**.

Multiple attempts to cyclise the 3-(arylethynyl)-4-cyanopyridines **120a-e**, following our previously established procedure (9 M aqueous sulfuric acid), did not result in the desired mixtures of cyclised products **100** and **121** but in an unidentifiable mixture of compounds. The origin of the sensitivity of this particular regioisomer to sulfuric acid is not clear. However, changing to polyphosphoric acid for the cyclisation led to the formation of the expected mixtures of a lactam and a lactone. Polyphosphoric acid, although as strong as sulfuric acid, is not as oxidising as the latter and this may have led to preservation of the products of cyclisation under the reaction conditions. The lactones **121** were converted into the lactams **100** by the usual procedure with ammonia in 2-methoxyethanol under pressure. However, it was not possible to isolate the trifluoromethylphenyl derivatives **100d** and **121d**. Attempted cyclisation of the trifluoromethylphenylethynylpyridine **120d** gave an unidentifiable mixture of compounds. Possibly, the electron-withdrawing effect of the trifluoromethyl substituent on the aryl ring of **120d**

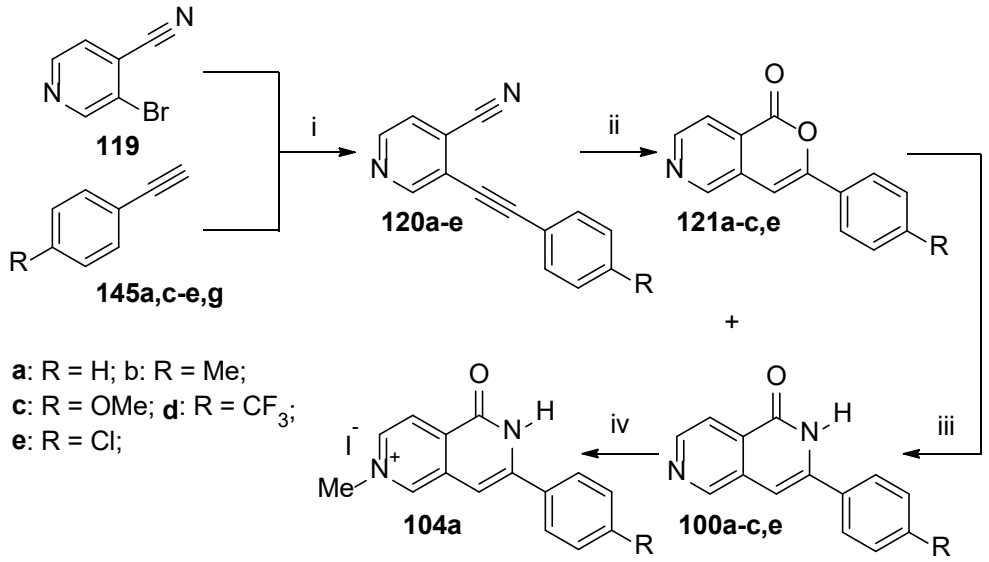

Scheme 22. Synthesis of 3-aryl-2,6-naphthyridin-1-ones **100** and their derivatives *via* modified Sonogashira pathway. *Reagents & conditions:* i, $Pd(PPh_3)_4$, CuI, Na ascorbate, Et_3N, THF, 40 °C, 41-72%; ii, aq. H_2SO_4 (9 M), Δ; iii, NH_3, $MeO(CH_2)_2OH$, 100 °C, pressure, 6-56%; iv, MeI, DMF, 52%.

diminished the electron-richness of the triple bond in this system, preventing the cyclisation from happening and leading to degradation of the starting materials.

One intermediate, **100c**, was converted into 7-(4-methoxyphenyl)-2-methyl-5-oxo-5,6-dihydro-2,6-naphthyridin-2-ium iodide **104c**, applying the general method described by Showalter.[218] Other compounds failed to result in the desired salts after multiple attempts, despite being fully dissolved in DMF. The reasons for this are not clear and yet need to be investigated. An attempt to reduce **104c** into 5,6,7,8-tetrahydro-2,6-naphthyridinone **107c** with borane-pyridine complex in formic acid failed, giving the starting material only even after twenty-one days. Considering that the formic acid also undergoes reduction with borane.pyridine complex, the problem might be referred to the loss of the reducing agent. However, a significant excess of borane-pyridine complex did not result in any improvement of the reaction outcome. Notably, similar problems were experienced when the alkylation and subsequent reduction of 2,7-naphthyridinones **101** was attempted under the same conditions. This might point to the dependence of these reactions on the distribution of electron-density in the pyridine ring.

Overall, the synthesis of 2,6-naphthyridinones **100** and their derivatives *via* a Sonogashira pathway became rather challenging. The heterocyclic nitrogen did not activate the 3-bromo position of **119** for the Sonogashira coupling with arylethynes **145** in the first place, resulting in moderate yields of coupled compounds **120**. The scope of the electrophilic cyclisation step was limited to the coupled compounds **120** bearing electron-neutral and electron-donating groups. Lastly, the alkylation step resulted in one compound only and the reduction step failed. However, despite the limitations, a series of compounds ready for biological evaluation was synthesised.

2.5 An alternative approach for the synthesis of naphthyridinones: Hurtley reaction – intramolecular cyclisation.

Having obtained only three examples of 3-aryl-2,6-naphthyridin-1-ones **100** by the Sonogashira / acid-catalysed cyclisation route, other synthetic pathways were investigated in order to obtain more compounds in this series. A tandem Hurtley-intramolecular cyclisation was proposed for a synthesis of the corresponding lactones from a variety of bromopyridinecarboxylic acids and β-diketones, followed by conversion of the product lactones into lactams (Scheme 23). This strategy has been applied in our laboratory earlier to obtain 3-substituted 5-nitro- and 5-aminoisoquinolines.[166,227] These compounds were designed as inhibitors of PARP-1 and PARP-2. 5-Nitroisoquinolin-1-ones were synthesised from 2-bromo-3-nitrocarboxylic acid and a variety of β-diketones through tandem Hurtley-retro-Claisen condensation under basic conditions with copper catalysis, followed by conversion of the isocoumarin into the isoquinolinone. Hurtley-retro-Claisen condensation was also used by Ames and Ribeiro to obtain 3-substituted isocoumarins from 2-bromobenzoic acid and pentane-2,4-dione or 1,3-diphenylpropane-1,3-dione at 170 °C.[228] Another approach to make 3-substituted isocoumarins was performed by Cai *et al.*, who developed a one-pot synthesis of isocoumarins from 2-iodo- or

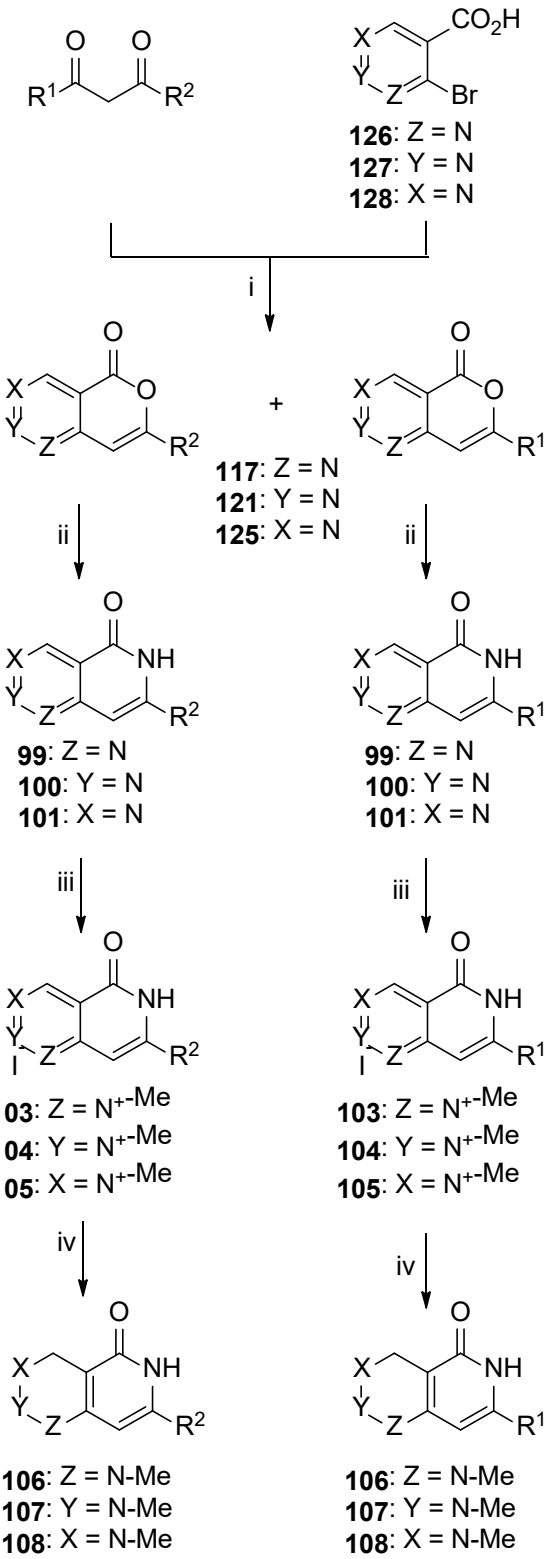

Scheme 23. Proposed route of synthesis of target naphthyridinones **99-101** and their derivatives **103-108** *via* Hurtley couplings. i, Hurtley coupling; ii, ammonia, pressure; iii, *N*-alkylation; iv, reduction.

2-bromobenzoic acid and β-diketones under basic conditions (potassium phosphate) and copper catalysis (copper(I) iodide) in dimethylformamide.[229]

The Hurtley reaction, or coupling, is a variation of the Ullmann condensation (not to be confused with the Ullmann reaction). In the Ullmann condensation, a nucleophilic phenol couples with an aryl halide at a very high temperature (*ca.* 150 °C) in the presence of a copper-bronze catalyst to form a diaryl ether. When a β-diketone acts as the nucleophile, the reaction is called the Hurtley coupling. Originally, the reaction was performed on 2-bromobenzoic acid, acetylacetone (pentane-2,4-dione, the enolate of which acted as the nucleophile), sodium ethoxide as a base (obtained *in situ* from sodium and ethanol) and copper bronze.[230] This was the first attempt to investigate the reactivity of *ortho*-halobenzoic acids and dicarbonyl compounds in the presence of a copper catalyst. Subsequent studies of the Hurtley reaction revealed the following observations:[231]

1. 2-Bromobenzoic acid gives the best results, compared to other 2-halobenzoic acids.
2. Only the carboxylic acid is tolerated; replacement of the carboxylic group by any other groups (*e.g.* ester) arrests the reaction.
3. Copper is crucial for the catalysis of the reaction.

Despite the eighty-four years history of this reaction, there is still no evidence of a certain mechanism. However, numerous studies have been performed in order to investigate it. Thus, Setsune *et al*. proposed that the coupling was catalysed by copper(I) gen-

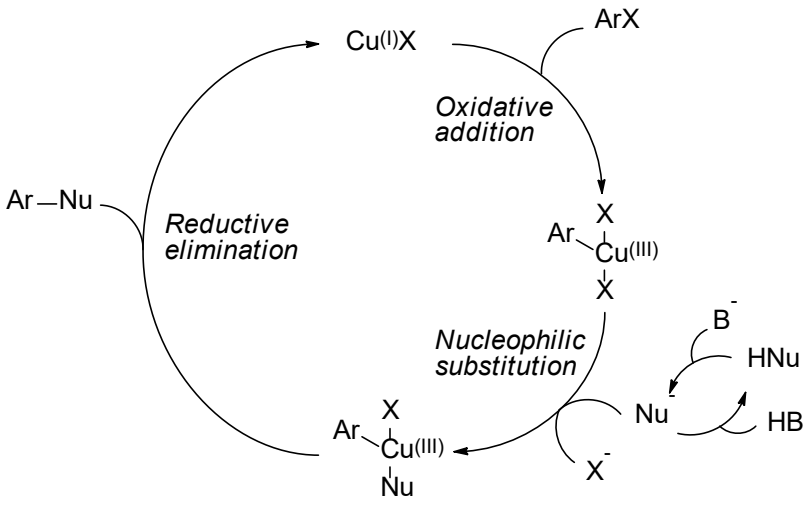

Scheme 24. Mechanism of Hurtley coupling based on the concept of oxidative addition / reductive elimination.[233,234]

erated *in situ*, which reacted firstly with the aryl halide and therefore induced halide atom transfer.[232] Cohen *et al.* suggested a copper(I)-copper(III) oxidative addition / reductive elimination mechanism (Scheme 24).[233,234] This pathway involves three major steps:

- *Oxidative addition*, when copper(I) reacts with the aryl halide, forming a copper(III) intermediate.
- *Nucleophilic substitution* of the copper halide by the nucleophile (*i.e.* the enolate of the β-diketone).
- *Reductive elimination*, during which the copper catalyst is re-generated and the coupled product is formed.

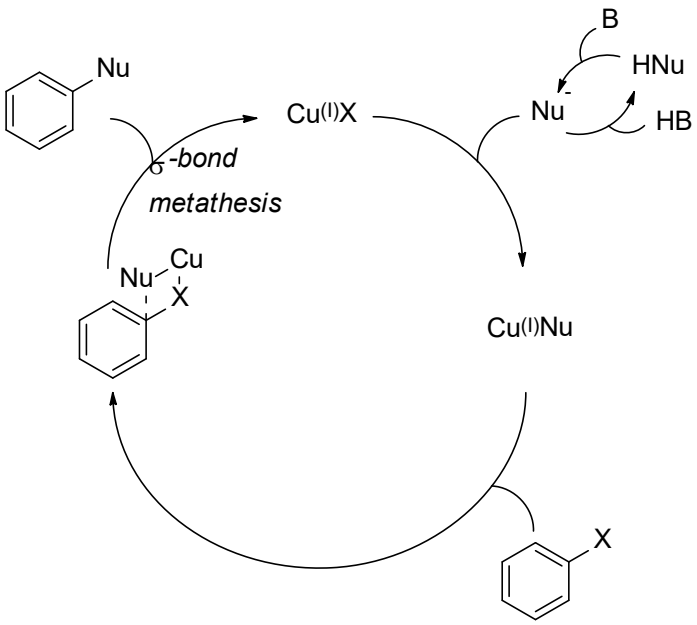

Scheme 25. σ-Bond metathesis mechanistic pathway of Hurtley coupling.[231,234]

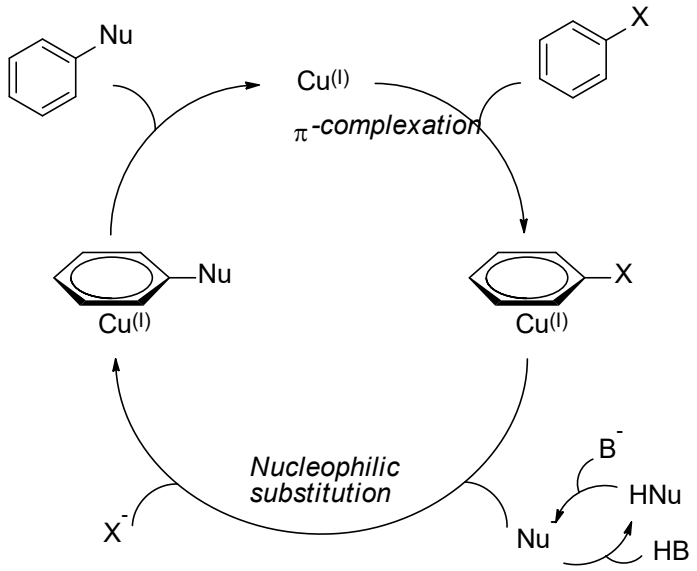

Scheme 26. π-Complexation mechanistic pathway of Hurtley coupling.[231]

However, unlike the palladium-catalysed cross-couplings, there might be two possible sequences of the stages of this mechanism. There were some suggestions that the nucleophilic substitution might be the initial step and the oxidative addition would follow it.[234] Recently, Ribas *et al.* used UV monitoring to demonstrate that the oxidative addition would indeed be the first stage of a copper(I)-copper(III)-associated mechanism.[235]

Both the aryl halide transfer and the copper(I)-copper(III)-associated mechanisms involve a change in the oxidation state of copper. There are other two proposed mechanisms, which suggest that the oxidation state of copper remains unchanged: σ-bond metathesis and a π-complexation of copper with the aryl halide. σ-Bond metathesis is believed to occur through the formation of an intermediate containing a four-membered ring (Scheme 25). Firstly, substitution of the copper halide by a nucleophile (*i.e.* the enolate of the diketone) provides a copper(I)-Nu species, which forms a four-bond intermediate with aryl halide in the next step. Lastly, σ-bond metathesis gives ArNu and recovers copper halide catalyst.[231,234]

The π-complexation pathway suggests initial formation of a π-complex of copper and the aryl halide with subsequent nucleophilic substitution on aryl halide (Scheme 26). In the π-complex, the copper withdraws electron-density from the aromatic ring, favouring the attack of a nucleophile. In the last step, ArNu is formed and the copper catalyst is recovered through the destruction of the π-complex.[231]

2.5.1 Synthesis of symmetrical and unsymmetrical β-diketones.

Approaching the proposed synthetic pathway, it was necessary to make symmetrical 1,3-diarylpropane-1,3-diones or unsymmetrical 1-alkyl-3-arylpropane-1,3-diones. These compounds are commonly referred to as β-diketones, since they possess an α-carbon and two carbonyl groups in β-positions. β-Dicarbonyl compounds are readily deprotonated to form a conjugated enolate, which acts as a good nucleophile in the Hurtley coupling. Symmetrical 1,3-diarylpropane-1,3-diones were the more desired option, since, in the next step, they should give only one coupled product. At the same time, Hurtley coupling with unsymmetrical β-diketones would result in two products, hopefully separable by chromatography. Aiming to avoid this separation and to increase the yield of desired product, it was decided to investigate the synthesis of symmetrical β-diketones. Since the synthesis of 7(3)-pyridyl derivatives of naphthyridinones had not been achieved, it was proposed to start with the synthesis of 1,3-di(pyridin-4-yl)-propane-1,3-dione **166** and to involve it in the subsequent steps (see Scheme 23). Following the general procedure of Andrews *et al.*,[236] 4-acetylpyridine **168** was introduced into Claisen condensation with ethyl pyridine-4-carboxylate **169** in anhydrous THF, using an excess of sodium hydride as a base (Scheme 27). The excess base was used to fully deprotonate 4-acetylpyridine and generate the enol form of the product β-diketone.

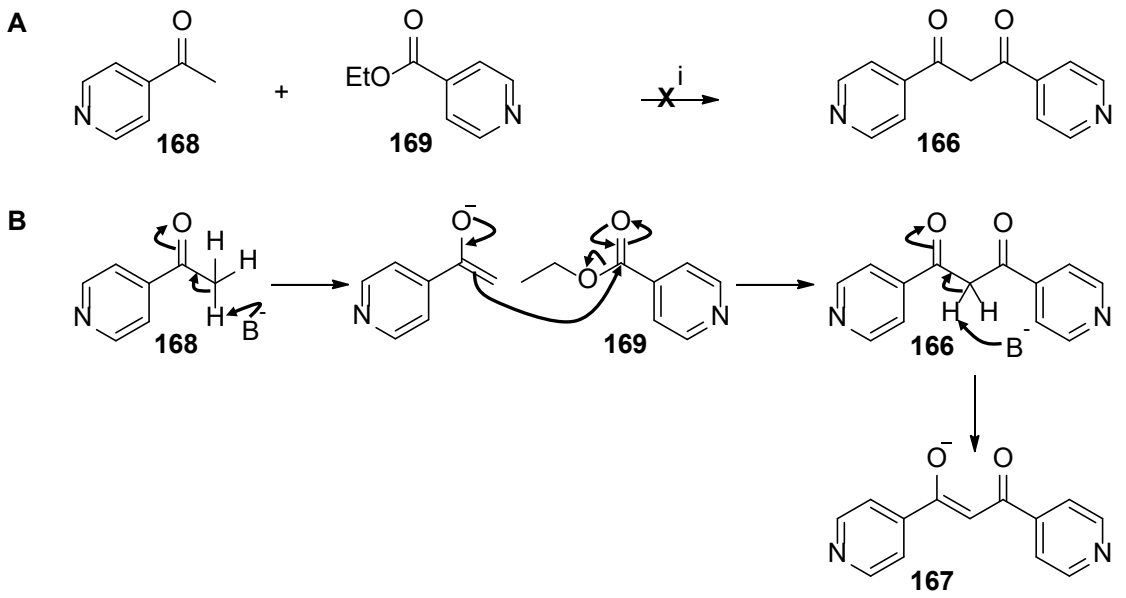

Scheme 27. A: Initial attempt to make 1,3-di(pyridin-4-yl)propane-1,3-dione **166**. *Reagents & conditions*: i, NaH, THF anhydrous, Δ. **B**: Mechanism of formation of 1,3-di(pyridin-4-yl)-propane-1,3-dione **166**.

Stirring the reaction mixture under reflux for 16 hours did not lead to any sign of a product on TLC. A mixture of starting materials and products of degradation were observed by ^{1}H NMR spectroscopy. After multiple attempts, it was decided to modify the reaction conditions and, at the same time, to try other strategies to obtain unsymmetrical β-diketones. It was predicted that the unsymmetrical β-diketones might be easier to make, compared to the symmetrical analogues. Moreover, the synthesis of unsymmetrical β-diketones has been studied in our group before.[227] Together with a number of procedures found in the literature,[237,238] it was decided to attempt the synthesis of unsymmetrical β-diketones and to involve these in the Hurtley condensation / cyclisation.

Firstly, a procedure used by Woon was repeated.[227] 4-Acetylpyridine **168** was treated with sodium amide to form an anion. The latter was condensed with ethyl acetate at 40 °C to form a β-diketone. The product was intended to be isolated through the formation of a copper-pyridine complex, which would be subsequently removed with EDTA. However, this reaction did not provide the desired product **170** after multiple attempts, unlike the original procedure. Substituting the base with lithium hexamethyldisilazide (LiHMDS) did not change the outcome of the reaction.

Acid-catalysed conditions were also investigated. 1-(4-Methylphenyl)ethanone **171** was introduced into reaction with acetic anhydride, mediated by a boron trifluoride - acetic acid complex as a Lewis acid, following the procedure developed by Woon (Scheme

28).[227] However, only an inseparable mixture of starting materials was detected by ^{1}H NMR. The same result was obtained for 1-(4-nitrophenyl)ethanone **173**, when introduced into a coupling under the same conditions.

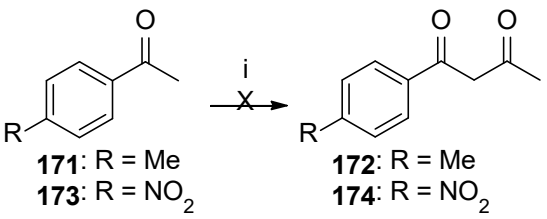

Scheme 28. Synthesis of 1-(4-aryl)butane-1,3-diones **172, 174**. *Reagents & conditions*: i, $BF_3(AcOH)_2$, NaOAc, Ac_2O, Δ.

The second strategy, also involving a Claisen condensation, used acetone as a nucleophile and a corresponding ester as an electrophile (Scheme 29, A). The initial attempt to treat ethyl pyridine-4-carboxylate **169** with acetone using potassium *tert*-butoxide at 40 °C did not lead to formation of 1-(pyridin-4-yl)butane-1,3-dione **170**, probably because of moisture in the base, which led to the formation of potassium hydroxide. However, neither the change of the base to LiHMDS nor the change of the leaving group in the substrate into methoxy group led to the desired product **170**. Notably, when sodium

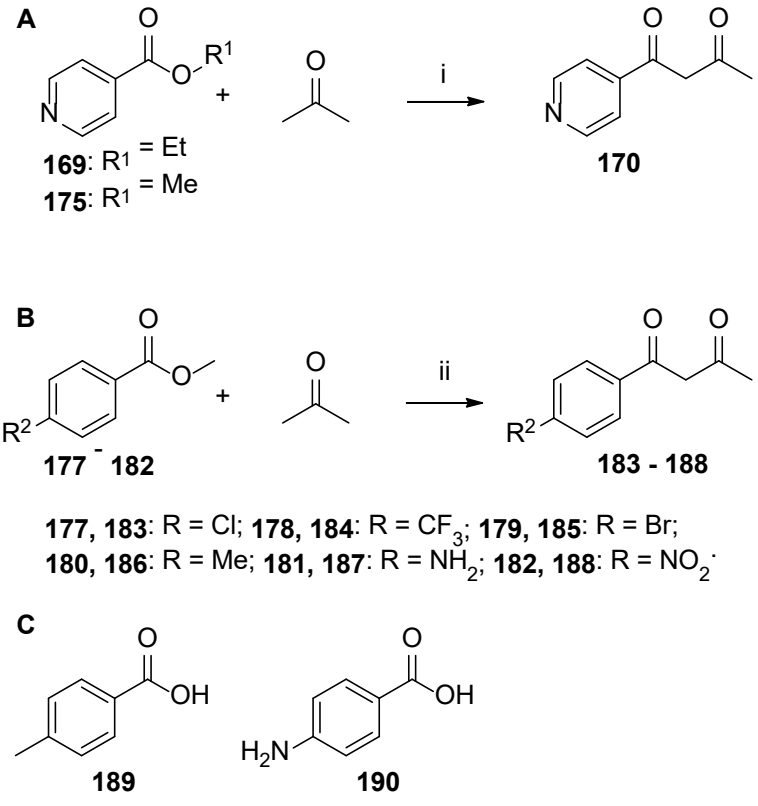

Scheme 29. A: Synthesis of 1-(pyridin-4-yl)butane-1,3-dione **170**. **B**: Synthesis of 1-arylbutane-1,3-diones **183-188**. **C**: Structures of 4-substituted benzoic acids **189** and **190**. *Reagents & conditions*: i, R^1 = Me, NaOMe, THF, Δ, 27%; ii, R^1 = Me, NaH, THF, Δ, 33-51%.

methoxide was used as a base, it resulted in 27% yield of 1-(pyridin-4-yl)butane-1,3-dione **170**. Despite the modest yield, the optimised procedure was employed in the synthesis of other derivatives. Methyl 4-chlorobenzoate **177** was investigated in order to form 1-(4-chlorophenyl)butane-1,3-dione **183** (Scheme 29, B). Using the same conditions as for 1-(pyridin-4-yl)butane-1,3-dione **170**, it was not possible to isolate the desired product **183**. Driven by this fact, it was decided to optimise the reaction conditions further. When sodium hydride was used as a base and all reagents were dry, the coupled product **183** was obtained in 51% yield. Dry methyl 4-trifluoromethylbenzoate **178** reacted with acetone and sodium hydride to give an exceptional 94% yield of β-diketone **184**, whereas dry methyl pyridine-4-carboxylate **175** gave 62% yield of 1-(pyridine-4-yl)butane-1,3-dione **170**.

Table 13. Optimisation of the synthesis of 1-(pyridin-4-yl)butane-1,3-dione **166**[a] and synthesis of symmetrical β-diketones **197-201**.

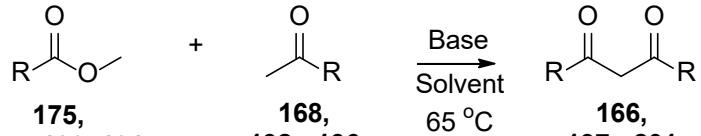

175, 177 - 180, 191 | **168, 192 - 196** | **166, 197 - 201**

Entry	Starting materials	Base	Solvent[b]	Time, h	Yield, %
1	**168**, **175** (R = 4-Py)	NaH	THF	16	0 (**166**)
2	**168**, **175** (R = 4-Py)	NaOMe	MeOH	24	27 (**166**)
3	**168**, **175** (R = 4-Py)	NaH washed with hexane	THF	16	42 (**166**)
4	**177**, **192** (R = 4-ClPh)	NaH washed with hexane	THF	16	68 (**197**)
5	**178**, **193** (R = 4-F_3CPh)	NaH washed with hexane	THF	16	57 (**198**)
6	**179**, **194** (R = 4-BrPh)	NaH washed with hexane	THF	16	30 (**199**)
7	**180**, **195** (R = 4-MePh)	NaH washed with hexane	THF	16	50 (**200**)
8	**191**, **196** (R = 4-MeOPh)	NaH washed with hexane	THF	16	46 (**201**)

[a] The reactions were carried out at 1 M concentration of starting materials with 2 equivalents of base.

[b] All solvents used were anhydrous.

Dry methyl 4-bromobenzoate **179** provided 51% yield of coupled product **185** in a reaction mediated by sodium hydride, when non-dried **179** gave 33% yield of **185**. Notably, these conditions failed to provide β-diketones **186** and **187** from methyl 4-methylbenzoate **180** and methyl 4-aminobenzoate **181**, giving instead the corresponding benzoic acids **189** and **190**, respectively (Scheme 29, C). For unknown reasons, methyl 4-nitrobenzoate **182** did not result in the desired product **188** under these conditions. Popic *et al.* used a catalytic amount of 18-crown-6 crown ether together with sodium hydride to accelerate the Claisen condensation between a variety of methyl ketones and esters. Despite the fact that 18-crown-6 has less affinity to sodium ions than does 15-crown-5, it provided good-to-excellent yields of β-diketones.[237] However, addition of 18-crown-6 or 15-crown-5 did not lead to the formation of desired β-diketone from methyl 4-nitrobenzoate **182**; only starting material was isolated after 1 d of stirring.

Moving towards the synthesis of more suitable symmetrical β-diketones, it was decided to improve the reaction conditions, changing the base and the solvent, together with the temperature and time of the reaction. Various bases, *e.g.* potassium *tert*-butoxide, sodium amide and lithium hexamethyldisilazide were investigated, providing no desired product **166**. After multiple attempts, it was discovered that the use of sodium hydride only gave coupled β-diketone **166** when washed free from oil before the addition of other reagents. These conditions provided a moderate yield (42%; Table 13, entry 3) of 1,3-di(pyridin-4-yl)propane-1,3-dione **166**. The same technique was used for other derivatives, providing a variety of symmetrical β-diketones **197-201** in moderate-to-excellent yields (see Table 13, entries 4-8). Interestingly, the ^{1}H NMR spectra of these products revealed that the enol form was by far the major tautomer of the β-diketone, showing a characteristic singlet for the hydroxy group at *ca.* δ 16 and a singlet for the olefinic proton at *ca.* δ 6. Since the enol tends to form intramolecular hydrogen bonds, this equilibrium seems feasible.

2.5.2 Hurtley coupling and intramolecular cyclisation.

The Hurtley coupling is a special case of the Ullmann condensation.[230] Following the σ-bond metathesis mechanistic pathway for Hurtley coupling, a nucleophile in this reaction would be an enolate, generally formed by deprotonation of a dicarbonyl β-dike-

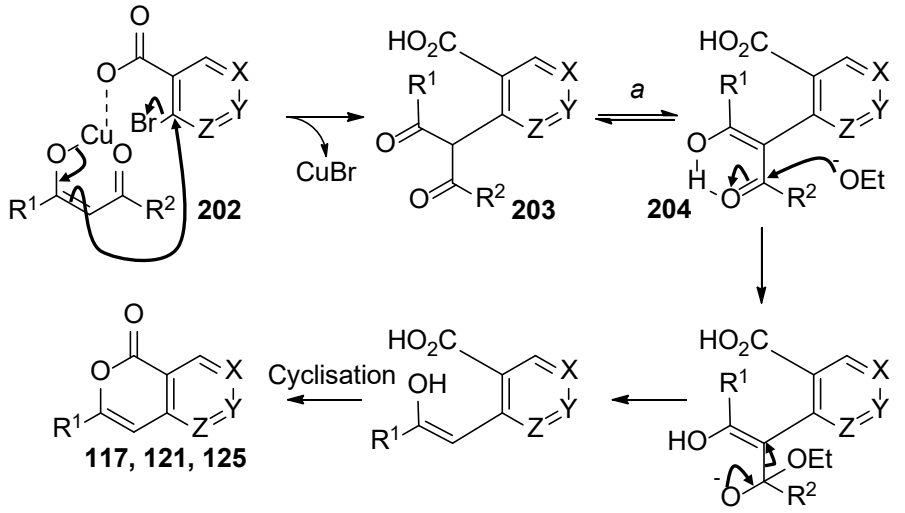

Scheme 30. Probable mechanism of Hurtley-intramolecular cyclisation catalysed by Cu in basic media. *a* – tautomerism; X *or* Y *or* Z = N; R^1 *and/or* R^2 = Ar.

tone with a base, *e.g.* sodium methoxide or ethoxide (Scheme 30). Under copper catalysis in basic conditions, intermediate **204** undergoes an intramolecular cyclisation giving a lactone **117** or **121** or **125**.

Initially, the coupling between 4-bromopyridine-3-carboxylic acid **128** and a variety of unsymmetrical β-diketones **170**, **183** – **186** was investigated. However, none of the conditions applied resulted in the desired pyranopyridinone **125**. Only in one case, 3-methyl-2,7-naphthyridin-1-one **206** was obtained.

In light of this, it was clear that symmetrical β-diketones were essential for the Hurtley coupling to form the desired pyranopyridinones. However, the first attempt to obtain 7-(4-methylphenyl)pyrano[4,3-*b*]pyridin-5-one **117b** from the acid **128** and 1-(4-methyl-

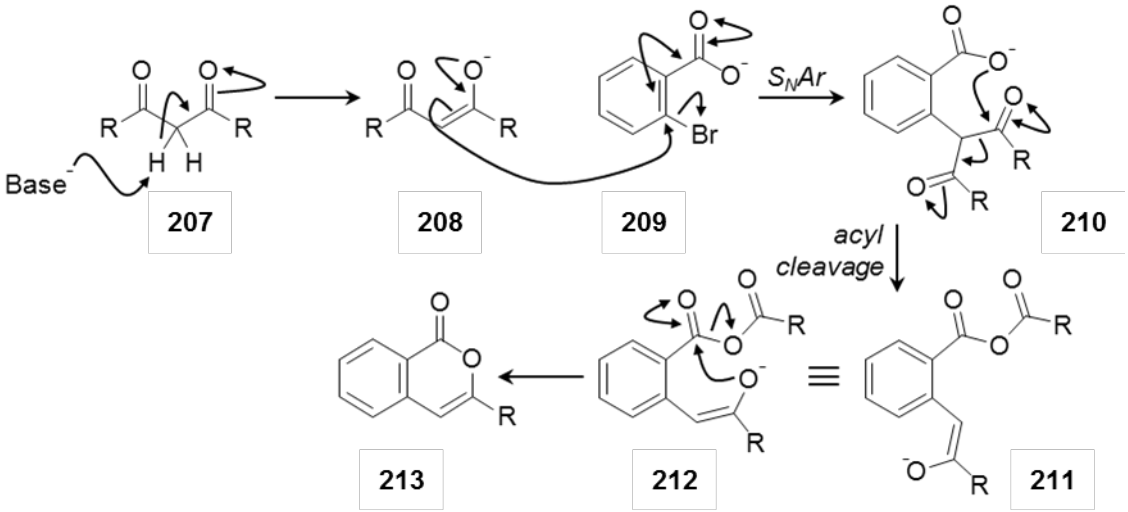

Scheme 31. Probable mechanism of copper-free Ullmann-type intramolecular condensation (modification from ref. 240).

phenyl)butane-1,3-dione **200** using potassium *t*-butoxide and copper powder failed, providing no signs of reaction after three days.

Recently, interesting transition-metal-free intramolecular cyclisation reaction procedures for the synthesis of chromones[239] and isocoumarins[240] have been published. Liu *et al.*[240] described an intramolecular Ullmann-type tandem reaction between 2-iodo- or 2-bromobenzoic acids and β-diketones, which involved caesium carbonate as the base and acetonitrile as the solvent. Notably, no copper catalyst was involved in this reaction. A modification of the mechanism proposed by Liu[240] is shown in Scheme 31.

Deprotonation of the β-diketone **207** by the base (*e.g.* Cs_2CO_3, Bu^{t}OK) gives the conjugated enolate **208**. This anionic nucleophile then carries out an S_NAr reaction on the 2-bromobenzoate **209**, activated by the adjacent carbonyl. The carboxylate nucleophile in the first coupled product **210** is then appositely placed as a nucleophile to facilitate the required acyl cleavage, transferring one acyl group (RC=O) onto the carboxylate and generating the lower enolate in **211**, through six-membered cyclic transition states and an intermediate. After rotation of a σ-bond, the oxygen of the enolate **211** is well placed to attack the benzoyl carbonyl, which is now part of an anhydride and thus a highly reactive electrophile. This reaction then affords the product isocoumarin **213**.

When using these conditions to couple 2-bromopyridine-3-carboxylic acid **126** with 1,3-bis(4-methoxyphenyl)propane-1,3-dione **201**, the desired 7-(4-methoxyphenyl)pyrano-[4,3-*b*]pyridin-5-one **117c** was obtained in a good yield (71%). Other couplings of different β-diketones with 2-bromopyridine-3-carboxylic acid **126** resulted in moderate-to-excellent yields of pyranopyridinones (Table 14, entries 2-9).

Despite the initial success of this strategy, there were several disadvantages. Symmetrical β-diketones with strong electron-withdrawing groups, *e.g.* 4-trifluoromethylphenyl or pyridin-4-yl-, failed to couple with *ortho*-bromobenzoic acids **126-128** under the standard or modified conditions (modified conditions included propionitrile as a solvent with a higher boiling point and, subsequently, a higher temperature of the reaction).

Table 14. Optimisation of intramolecular cyclisation reaction of bromopyridinecarboxylic acids **126-128** and symmetrical β-diketones **166, 197 – 201, 214**.

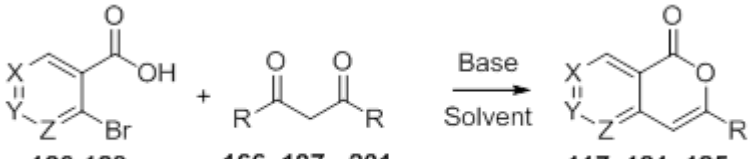

126-128 166, 197 - 201, 214 117, 121, 125

Entry	R	X, Y, Z (compound number)	Base	Cu catalyst	Solvent	t°C	Yield, % (compound number)
1	4-MePh (**200**)	Z = N; X = Y = CH (**126**)	Bu^{t}OK	Cu[b]	DMF	150	0[§] (**117b**)
2	4-MeOPh (**201**)	Z = N; X = Y = CH (**126**)	Cs_2CO_3	-	MeCN	80	71 (**117c**)
3	4-MePh (**200**)	Z = N; X = Y = CH (**126**)	Cs_2CO_3	-	MeCN	80	93 (**117b**)
4	4-BrPh (**199**)	Z = N; X = Y = CH (**126**)	Cs_2CO_3	-	MeCN	80	93 (**117f**)
5	4-ClPh (**197**)	Z = N; X = Y = CH (**126**)	Cs_2CO_3	-	MeCN	80	63 (**117e**)
6[c]	Ph (**214**)	Y = N; X = Z = CH (**127**)	K_3PO_4	CuI[b]	DMF	150	17 (**121a**)
7	4-MePh (**200**)	X = N; Y = Z = CH (**128**)	Cs_2CO_3	-	MeCN	80	32 (**125b**)
8	4-MeOPh (**201**)	X = N; Y = Z = CH (**128**)	Cs_2CO_3	-	MeCN	80	71 (**125c**)
9	4-ClPh (**197**)	X = N; Y = Z = CH (**128**)	Cs_2CO_3	-	MeCN	80	6.6 (**125e**)

[a] The reactions were carried out at 0.1 M concentration of substrates and 2 equivalents of base.

[b] 0.1 equivalent of copper catalyst.

[c] The reaction was carried out under Ar.

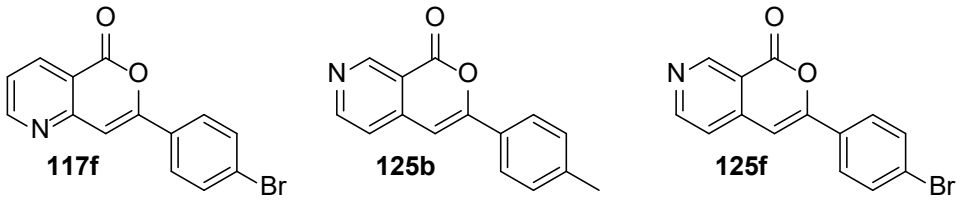

Figure 44. Pyranopyridinones, obtained solely *via* the Hurtley pathway.

It was possible that this might be due to the electron-withdrawing properties of these groups, which change the electron-density of the β-diketone, making the enolate easier to form but less reactive as a nucleophile. The isomeric 3-bromopyridine-4-carboxylic acid **127** provided a coupled product with 1,3-diphenylpropane-1,3-dione **214** only under copper-induced Hurtley coupling conditions. Whereas the 2-position in **126** is strongly activated as an electrophile by the adjacent ring-nitrogen, the 3-position of **127** is not activated in this way. Hence, the reactivity of **127** in Hurtley-intramolecular cyclisation was likely to be low.

A variety of pyranopyridinones was made following this protocol. More importantly, this approach provided those derivatives (Figure 44) which could not be obtained *via* the Sonogashira pathway.

2.5.3 Conversion of lactones to lactams and synthesis of derivatives of the naphthyridinones.

The reaction of pyranopyridinones **117**, **121** and **125** with ammonia under pressure in a high-boiling solvent (2-methoxyethanol) provided a ready conversion of the lactone moiety into a lactam (see Scheme 17). This *modus operandi* was applied to the derivatives obtained during the modified Hurtley-intramolecular cyclisation and resulted in the corresponding naphthyridinones **99**, **100** and **101**. Notably, 7-(4-bromophenyl)-1,6-naphthyridin-5-one **99f** was synthesised, providing an opportunity for further couplings at the 4-bromophenyl position of the naphthyridinone to extend the candidate inhibitors to probe further the hydrophobic binding pocket (Scheme 32). Initially, a Sonogashira coupling of **99f** with phenylethyne in diisopropylamine / THF (1:1) using $Pd(PPh_3)_4$ and copper(I) iodide as metal catalyst was planned to give **99k**. However, it failed, most probably due to the insolubility of **99f**, caused by the H-bonding characteristics of the lactam.

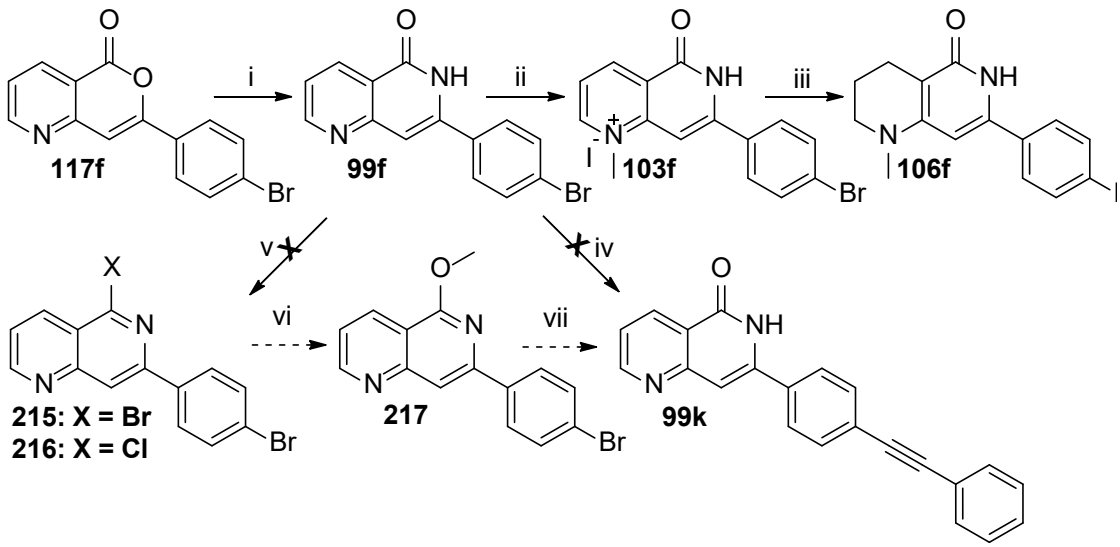

Scheme 32. Planned synthesis of 7-(4-bromophenyl)-1,6-naphthyridin-5-one **99f** derivatives. *Reagents & conditions:* i, NH_3, $MeO(CH_2)_2OH$, 120 °C, pressure, 75%; ii, MeI, DMF, r.t., 52%; iii, BH_3.pyridine, HCO_2H, r.t., 47%; iv, PhC≡CH, $Pd(PPh_3)_2Cl_2$ *or* $Pd(PPh_3)_4$ CuI, Pr^i_2NH, Na ascorbate, DMF, 40°C; v, $POBr_3$, Δ *or* $POCl_3$, Δ; vi, NaOMe, MeOH, rt.; vii, PhC≡CH, $Pd(PPh_3)_2Cl_2$ *or* $Pd(PPh_3)_4$, CuI, Pr^i_2NH, Na ascorbate, DMF, 40°C, then HBr in AcOH.

In the light of this failure, it was decided to mask the lactam group and, therefore, to increase the solubility of the haloarene in solvents compatible with Sonogashira coupling. The most common strategy of protecting a lactam group is a two-step conversion into an imino ester.[189] This strategy was implemented in the Threadgill group before to obtain 5-(acylamino)isoquinolin-1-ones[110] and 3- and 4-substituted 5-aminoisoquinolin-1-ones.[‡] 5-Nitroisoquinoline-1,3-dione **218** was treated with phosphorus oxybromide, giving 1,3-dibromo-5-nitroisoquinoline **219** (Scheme 33). The latter was stirred with sodium methoxide in methanol at room temperature to give 3-bromo-1-methoxy-5-nitroisoquinoline **220** in good yield ready for further synthesis. Interestingly, sodium methoxide selectively substituted at the 1-position, without engaging the 3-Br, even after 12 h of stirring. The position 1-C, being more electrophilic, was more likely to react with sodium methoxide before 3-C; however, the

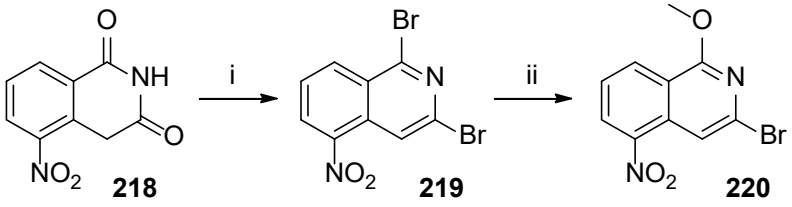

Scheme 33. Protection (i) and selective deprotection (ii) of the lactam group in 5-nitroisoquinoline-1,3-dione **218**, performed by Paine (unpublished results). *Reagents & conditions*: i, $POBr_3$, r.t. → 100°C; ii, NaOMe, MeOH, r.t.

[‡] H. A. Paine, unpublished results

complete selectivity of this reaction towards 1-C was not expected. The methoxy group was chosen for the protection, since it could easily be removed by hydrobromic acid.

In the present work, introducing the methoxy group by alkylation with iodomethane was not suitable, as this reagent has already been shown to methylate exclusively at the pyridine nitrogen (see above and ref. 218). Moreover, alkylation of anions derived from isoquinolin-1-ones usually takes place at the 2-nitrogen,[110,241-247] rather than the exocyclic oxygen, although Ferrer *et al*. showed some alkylation at exocyclic oxygen with primary alcohols under Mitsunobu conditions.[248] Attempting to apply Paine's procedure to the naphthyridinones, lactam **99f** was treated with phosphorus oxybromide initially at room temperature with subsequent increase of temperature to 100 °C. However, an unidentifiable mixture of compounds was observed on the ^{1}H NMR spectrum. The same result was obtained, after multiple attempts, when phosphorus oxychloride was used in the same temperature range. The reasons for this outcome are unknown but the failure to form the halonaphthyridines forced abandonment of this route to extended substitution in this region.

Implementing the previously described method of *N*-alkylation with iodomethane in DMF at room temperature, compound **99f** was selectively alkylated at 1-N, providing the salt **103f** (see Scheme 32). The salt **103f** was subsequently reduced with borane-pyridine complex under the conditions described above in section 2.2. The reaction resulted in reduced compound **106f** ready for biological evaluation.

2.6 Synthesis of pyridopyrimidinones.

In order to investigate the structure-activity relationships of the tankyrase-1/2 inhibitors further, it was decided to examine the influence of additional nitrogen atoms by replacing one of the carbons in the lactam ring with a heterocyclic nitrogen. A pyrimidinone core structure has been used before in the inhibitors of the tankyrases, *e.g.* 2-(4-trifluoromethyl)phenyl-7,8-dihydrothiopyrano[4,3-*d*]pyrimidin-4-one (XAV939) **47** (IC_{50} (TNKS-1) 11 nM; IC_{50} (TNKS-2) 4 nM).[60] 2-Arylquinazolin-4-ones **75-86** (see Figure 33), also containing a pyrimidinone ring, showed very promising results in selective inhibition of the tankyrases.[166] For example, 2-(4-bromophenyl)-8-methylquinazolin-4-one **81** inhibited 50% of tankyrase-1 activity at 32 nM and tankyrase-2 activity at 9 nM, without affecting PARP-1 even at 5 μM.[166] However, there are no reports in the literature on the activity of the pyridopyrimidinones against the tankyrases.

Approaching the synthesis of pyridopyrimidinones **109-111**, three possible routes of

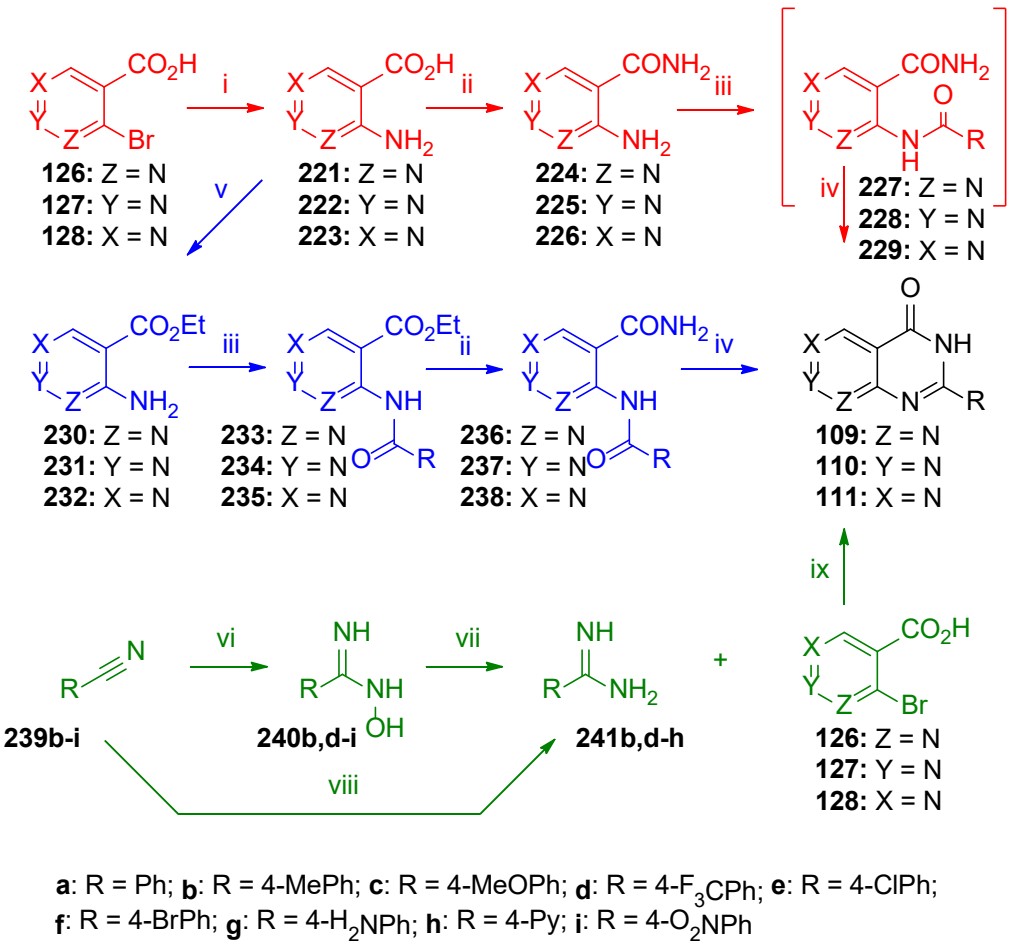

Scheme 34. Possible routes of synthesis of arylpyridopyrimidinones **109-111**. i, amination; ii, formation of an amide; iii, acylation; iv, cyclisation; v, esterification; vi, formation of a benzimidamide; vii, reduction; viii, formation of a benzamidine; ix, Ullmann-type coupling.

synthesis were considered (Scheme 34). The first route (see Scheme 34, red) involved acylation of aminopyridinecarboxamides and cyclisation of the intermediate acylaminopyridinecarboxamides. The second pathway (see Scheme 34, blue) employed acylation of ethyl aminopyridinecarboxylates, followed by condensation and cyclisation with ammonia. The third strategy (see Scheme 34, green) involved Ullmann-type coupling of a variety of benzamidines with bromopyridinecarboxylic acids.

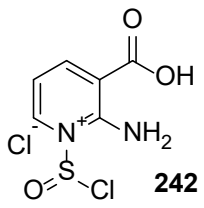

242

Figure 45. Structure of the salt **242**.

The first route (see Scheme 34, red) involved a modification of a well-known procedure for the synthesis of quinazolin-4-ones. For example, Griffin acylated 2-amino-benzamides with aroyl chlorides to obtain intermediate 2-acylaminobenzamides, which were cyclised under basic conditions to give 2-arylquinazolin-4-ones, claimed to be modest inhibitors of PARP-1.[249] A similar procedure was developed by Nathubhai *et al.* to obtain a series of 2-arylquinazolin-4-ones as potent inhibitors of the tankyrases.[166] However, treatment of commercially available aminopyridinecarboxylic acid **221** with thionyl chloride, followed by ammonia, failed to provide amide **224**. This unfortunate result might be due to the effect of the lone pair of the heterocyclic nitrogen atom, which might have attacked sulfur in thionyl cloride, forming a salt **242** (Figure 45). After multiple attempts, the strategy was abandoned.

Ismail and Wibberley acylated the amino group in the corresponding ester **230** with aroyl chlorides to obtain the 2-acetamidopyridine-3-carboxylates **233** (Scheme 34, blue).[250] The latter was converted into an amide **236**, which was cyclised under basic conditions, providing pyrido[2,3-*d*]pyrimidin-4-ones **109**. However, this pathway, consisting of four different steps, is rather time-consuming.

At the same time, a slightly shorter pathway was proposed (Scheme 34, green). It was found that benzamidines **241** could couple to 2-halobenzoic acids **243** under copper-mediated conditions in basic media (Scheme 35, A).[251] This novel Ullmann-type coupling has been described as a convenient way of obtaining quinazolinones.[252] The mechanism, proposed by Liu *et al.*,[251] involves several steps (Scheme 35, B):

- *Coordination* of copper to halobenzoic acid **126** under basic conditions.
- *Oxidative addition* of formed product and complexation of benzamidine **241a** with copper.

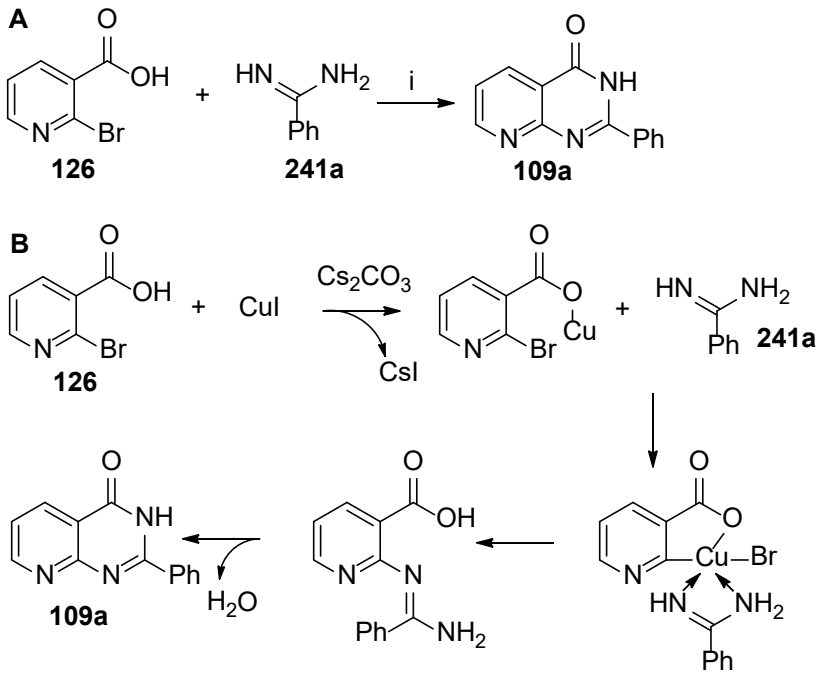

Scheme 35. A, First attempt to couple **126** with **241a**. *Reagents & conditions:* i, CuI, Cs_2CO_3, DMF, 80 °C, 53%; **B**, Proposed mechanism of the coupling, based on work by Liu *et al*.[251]

- *Reductive elimination* and recovery of copper catalyst.
- *Condensation* and formation of the product **109a**.

It was decided to try this approach in order to make target pyridopyrimidinones **109-111**. Initially, 2-bromopyridine-3-carboxylic acid **126** was to be coupled with commercially available benzamidine **241a**. 0.2 Equivalents of copper iodide were used as the catalyst and two equivalents of caesium carbonate served as the base. Using DMF as a solvent, the desired pyridopyrimidinone **109a** was obtained in 53% yield (see Scheme 35). Extension of this route to other examples required a selection of benzamidines **241**.

Several strategies were considered for the synthesis of the range of 4-substituted benzamidines **241**. A two-step synthesis of benzamidines **241** was planned, which involved initial formation of *N*-hydroxybenzimidamides **240** from 4-substituted benzonitriles **239**, followed by hydrogenolysis (Scheme 36, green).[253] 4-Substituted benzonitriles **239** could be treated with hydroxylamine, providing the corresponding *N*-hydroxybenzimidamides **240**. Next, hydrogenolysis of the N-O bond should give the desired benzamidines **241**. Interestingly, Anbazhagan *et al.* showed the possibility of hydrogenolysis of *N*-methoxybenzimidamides **248** under the same conditions as for *N*-hydroxybenzimidamides **240**.[253] Speculating that the *N*-methoxybenzimidamides **248** might give better results in a hydrogenolysis step, it was decided to make a selection of compounds

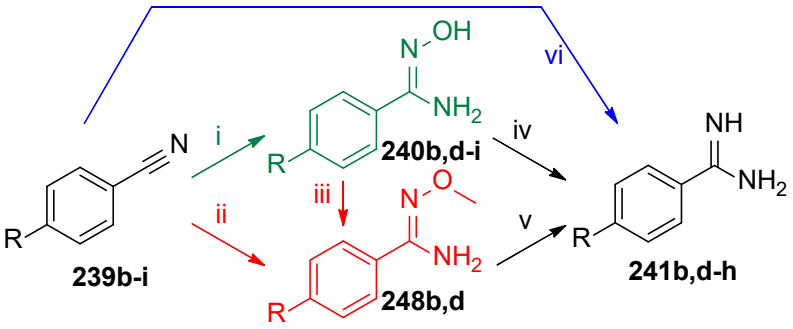

a: R = H; **b**: R = CH_3; **c**: R = OCH_3; **d**: R = CF_3; **e**: R = Cl; **f**: R = Br; **g**: R = NH_2; **h**: RPh = 4-Py; **i**: R = NO_2

Scheme 36. Synthetic routes for preparing benzamidines **241**. *Reagents & conditions:* i, $NH_2OH{\cdot}HCl$, Na_2CO_3, EtOH, water, Δ, 15-98%; ii, $NH_2OMe{\cdot}HCl$, Na_2CO_3, EtOH, water, Δ, 3% (**248b**), 20% (**248d**); iii, $(CH_3)_2SO_4$, NaOH, 1,4-dioxane, water, Δ; iv,v, Pd/C *or* Pt/C, $HCOONH_4$, AcOH, yields for iv: 25-92%; vi, NaOMe, NH_4Cl, MeOH, Δ, 22-68%.

248. Two possible ways to synthesise *N*-methoxybenzimidamides **248** were proposed. One approach to **248** (Scheme 36, iii) involved methylation of *N*-hydroxybenzimidamides **240** with a suitable hard-electrophile methylating agent, *e.g.* dimethyl sulfate.[254] Another approach, having advantages of being a single step and not involving highly toxic methylating reagents, consisted of a reaction of benzonitriles **239** with methoxylamine (Scheme 36, red). Initially, a procedure by Barros *et al.* was implemented.[255] According to it, a mixture of sodium carbonate, methoxylamine hydrochloride and benzonitrile **239b** in dichloromethane was treated with ultrasonic irradiation to dissolve and disperse the reagents. However, only starting materials were isolated after 1 hour of sonication and 24 hours of stirring under reflux. The attempt was repeated without the sonication: the reaction mixture was stirred under reflux for three days. The desired product **248b** was obtained in a very poor yield (3.1%). A better yield (20%) was obtained when the same conditions were applied to 4-trifluoromethylbenzonitrile **239d**. 4-Chlorobenzonitrile **239e** failed to give the desired 4-chloro-*N*-methoxybenzimidamide **248e** under these conditions. As this *N*-methoxybenzamidine route was unreliable, the analogous *N*-hydroxybenzamidine pathway was investigated. The conversion of benzonitriles **239** into *N*-hydroxybenzamidines **240** with hydroxylamine occurred in moderate to excellent yields (Table 15).[256-258] Notably, electron-donating substituents dramatically decreased the yield of the reaction (Table 15, entries 2,3), as the reaction mechanism predicted (Scheme 37). Electron-donating substituents change the electron-density at the nitrile carbon (C≡N) in the benzonitrile **239** and hence decrease its electrophilicity. Therefore, the nucleophilic attack of this carbon by the nitrogen of

hydroxylamine became less likely. Indeed, 4-methoxybenzonitrile **239c** failed to give expected *N*-hydroxy-4-methoxybenzimidamide **240c** after multiple attempts.

Table 15. Conversion of benzonitriles **239** into *N*-hydroxybenzimidamides **240**.

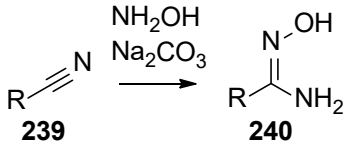

b: R = 4-MePh; **c**: R = 4-MeOPh; **d**: R = 4-F_3CPh; **e**: R = 4-ClPh; **f**: R = 4-BrPh; **g**: R = 4-H_2NPh; **h**: 4-Py; **i**: R = 4-O_2NPh

Entry	R	Yield, %
1[a]	4-MePh	78
2	4-H_2NPh	15
3	4-MeOPh	0
4	4-F_3CPh	98
5	4-ClPh	95
6	4-BrPh	90
7	4-O_2NPh	97
8	4-Py	83

[a] The reactions were carried out in EtOH / water (1:1) at 0.1 M concentration of **239**; 6 eq. of $NH_2OH \cdot HCl$ and 3 eq. of Na_2CO_3 were used.

The next step was the hydrogenolysis of the N-O bond but, even after 7 days' treatment with hydrogen and palladium-on-carbon, the *N*-methoxybenzimidamides **248** failed to give the desired benzamidines, despite the report in the literature.[253] At the same time, the *N*-hydroxybenzimidamides **240** were reduced to corresponding benzamidines in

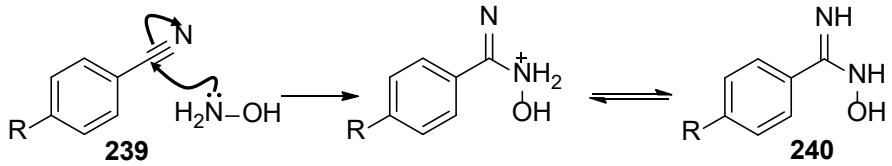

Scheme 37. Mechanism of formation of *N*-hydroxybenzimidamides **240** from benzonitriles **239** and hydroxylamine.

good yields (Table 16). However, the palladium-mediated hydrogenolysis was not suitable for 4-halo-*N*-hydroxybenzamidines **240e,f**, since it would cause cleavage of the halogen from the aryl ring. To demonstrate this, palladium-on-carbon was used for the reduction of 4-chloro-*N*-hydroxybenzimidamide **240e** and, indeed, the benzamidine **241a** was obtained. To avoid the cleavage of halogens from the aryl ring, platinum-mediated hydrogenolysis was proposed. It is known that platinum catalyses this type of reaction differently than palladium and, unlike palladium, it is suitable for hydrogenolysis of halogen-containing compounds.[187] However, when 1% platinum-on-carbon was used as catalyst for the hydrogenolysis, it did not provide desired benzimidamides **241e,f** and the starting 4-halo-*N*-hydroxybenzimidamides **240e,f** were recovered after 7 d of stirring. When 5% platinum-on-carbon was used, 4-chloro- and 4-bromobenzamidines **241e** and **241f** were obtained in good yields (Table 16, entries 4, 5).

Table 16. Hydrogenolysis of *N*-hydroxybenzimidamides **240**.

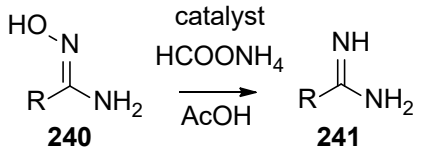

240 **241**

b: R = 4-MePh; **d**: R = 4-F_3CPh; **e**: R = 4-ClPh;
f: R = 4-BrPh; **h**: 4-Py; **I**: R = 4-O_2NPh

Entry	R in starting material	R in product	Catalyst	Yield, %
1[a]	4-MePh, **240b**	4-MePh, **241b**	Pd/C[b]	61
2	4-O_2NPh, **240l**	4-H_2NPh, **241g**	Pd/C	59
3	4-F_3CPh, **240d**	4-F_3CPh, **241d**	Pd/C	92
4	4-ClPh, **240e**	4-ClPh, **241e**	Pt/C[c]	70
5	4-BrPh, **240f**	4-BrPh, **241f**	Pt/C	68
6	4-Py, **240h**	4-Py, **241h**	Pd/C	25

[a] The reactions were carried out in AcOH at 0.2 M concentration of **240**; 6 eq. of $HCOONH_4$ and equal mass of the metal catalyst were used.

[b] 10% Pd/C was used.

[c] 5% Pt/C was used.

Later, a more convenient strategy for the synthesis of benzamidines **241** was found. It was reported that the treatment of 4-cyanopyridine **239h** with sodium methoxide and ammonium chloride resulted in good yield of 4-pyridylamidine **241h** (Scheme 36, blue).[259] This procedure was repeated in the present work, giving 25% yield of the desired 4-pyridylamidine **241h**. The same approach was applied to the synthesis of 4-trifluoromethylbenzamidine **241d**, resulting in 30% yield of the compound. Despite the apparently lower yields, this approach had an advantage of being one step and overall resulted in better yield.

The next step comprised the copper-mediated Ullmann-type coupling of the benzamidines **241b,d-h** with the corresponding bromopyridinecarboxylic acids **126-128**. The conditions as used by Liu *et al.*[251] were applied (see Scheme 35): copper iodide as the copper catalyst, caesium carbonate as the base and DMF as the solvent. This approach resulted in a variety of pyridopyrimidinones (Table 17), obtained in moderate to good yields. Several patterns of reactivity were detected. Notably, benzamidines **241** with electron-donating substituents (Table 17, entries 6, 9, 13, 20, 21) failed to couple with bromopyridinecarboxylic acids **126-128**, giving an unidentifiable mixture of compounds. At the same time, 4-bromobenzamidine **241f**, having an electron-neutral bromine substituent, failed to couple to any of the bromopyridine-carboxylic acids. The starting materials were fully recovered after 3 days of stirring (Table 17, entries 5, 12, 18). 4-Chlorobenzamidine **241e**, also having a halogen as a substituent, provided poor yields of the coupled pyridopyrimidinones **109e** (8%) and **111e** (13%) and failed to couple with 3-bromo-pyridine-4-carboxylic acid **127** (Table 17, entries 4, 11, 17, respectively). This may be due to unwanted reactions of the copper at the halogen atoms in the benzamidines, with bromine being more susceptible than chlorine. The best yields of pyridopyrimidinones **109-111** were obtained when the corresponding benzamidine **241** had an electron-neutral or electron-withdrawing substituent, *e.g.* H or CF_3 (Table 17, entries 1, 3, 8, 10, 15, 19). It could be pointed out that pyridine-4-amidine **241h**, being electron-deficient, failed to couple with any of the bromopyridinecarboxylic acids **126-128** (Table 17, entries 7, 14, 21). This is more likely to happen due to inappropriate coordination of the nitrogen at the pyridine ring to the copper, which halted the coupling.

At the same time, the influence of the heterocyclic nitrogen in the bromopyridinecarb-oxylic acids **126-128** on the coupling outcome was explored. It appeared that the hetero-cyclic nitrogen (Table 17, Y = N) weakened the ability of the bromopyridinecarboxylic

Table 17. Ullmann-type copper-mediated coupling of bromopyridinecarboxylic acids **126-128** with benzamidines **241**.[a]

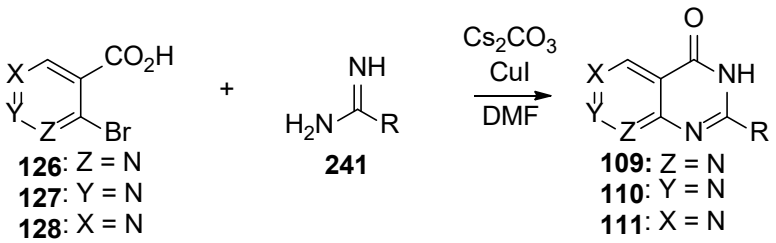

a: R = Ph; **b**: R = 4-MePh; **c**: R = 4-MeOPh; **d**: R = 4-F_3CPh; **e**: R = 4-ClPh; **f**: R = 4-BrPh; **g**: R = 4-H_2NPh; **h**: 4-Py

Entry	X/Y/Z	R	Yield, %
1	Z = N, X = Y = CH (**126**)	Ph (**241a**)	53
2	Z = N, X = Y = CH (**126**)	4-MePh (**241b**)	35
3	Z = N, X = Y = CH (**126**)	4-F_3CPh (**241d**)	45
4	Z = N, X = Y = CH (**126**)	4-ClPh (**241e**)	8
5	Z = N, X = Y = CH (**126**)	4-BrPh (**241f**)	0[§]
6	Z = N, X = Y = CH (**126**)	4-H_2NPh (**241g**)	0[§]
7	Z = N, X = Y = CH (**126**)	4-Py (**241h**)	0[§]
8	Y = N, X = Z = CH (**127**)	Ph (**241a**)	13
9	Y = N, X = Z = CH (**127**)	4-MePh (**241b**)	0[§]
10	Y = N, X = Z = CH (**127**)	4-F_3CPh (**241d**)	2.4
11	Y = N, X = Z = CH (**127**)	4-ClPh (**241e**)	0[§]
12	Y = N, X = Z = CH (**127**)	4-BrPh (**241f**)	0[§]
13	Y = N, X = Z = CH (**127**)	4-H_2NPh (**241g**)	0[§]
14	Y = N, X = Z = CH (**127**)	4-Py (**241h**)	0[§]
15	X = N, Y = Z = CH (**128**)	4-F_3CPh (**241d**)	50
16	X = N, Y = Z = CH (**128**)	4-MePh (**241b**)	42
17	X = N, Y = Z = CH (**128**)	4-ClPh (**241e**)	13
18	X = N, Y = Z = CH (**128**)	4-BrPh (**241f**)	0[§]
19	X = N, Y = Z = CH (**128**)	Ph (**241a**)	44
20	X = N, Y = Z = CH (**128**)	4-H_2NPh (**241g**)	0[§]
21	X = N, Y = Z = CH (**128**)	4-Py (**241h**)	0[§]

[a] The reactions were carried out in DMF at 0.1 M concentration of **126-128** and **241**; 2 eq. of caesium carbonate and 0.2 eq. of copper(I) iodide in DMF at 80 °C. [§] The reaction was stirred for 3 d.

acid **127** to couple to the benzamidines **241**, particularly to those carrying electron-neutral groups (Table 17, entries 9, 11) and electron-donating groups (Table 17, entry 13). As discussed before, the relative electrophilicity of the carbon at C-Br depends on the position of the heterocyclic nitrogen in the ring. When Y = N (Table 17), the corresponding carbon at position-3 is the least electrophilic, compared to the respective carbons in molecules where X = N (**128**) or Z = N (**126**). The carbon at position-2 in 2-bromopyridine-3-carboxylic acid **126** (Table 17, Z = N) is the most electrophilic and, hence, the most reactive, compared to the carbon at position-3 in **127** and the carbon at position-4 in **128**. Indeed, the unsubstituted benzamidine **241a** coupled to all bromo-pyridinecarboxylic acids **126**-**128**, providing the best yield (53%; Table 17, entry 1) of the pyridopyrimidinone **109** (Z = N), and the lowest yield (13%; Table 17, entry 8) of the pyridopyrimidinone **110** (Y = N). Apparently, the more electrophilic is the carbon at C-Br in the bromocarboxylic acids **126**-**128**, the more readily available it is to be involved in the coupling with benzamidines **241** under the described conditions.

To test the reactivity of *N*-hydroxybenzamidines **240** in the copper-catalysed Ullmann-type coupling, possibly leading to 3-hydroxy-2-phenylpyrido[2,3-*d*]pyrimidin-4-one **249** or 1-hydroxy-2-phenylpyrido[2,3-*d*]pyrimidin-4-one **250**, the reaction of 2-bromo-pyridine-3-carboxylic acid **126** with *N*-hydroxy-4-methylbenzimidamide **240b** was investigated (Scheme 38). It was planned that, after the coupling of **240b** with **126**, the product *N*-hydroxy-2-(4-methylphenyl)pyrido[2,3-*d*]pyrimidin-4-one **249b** or **250b** could be converted into the target pyridopyrimidinone **109b** by hydrogenolysis of the N-O bond to remove the hydroxy group. Therefore, the order of steps in the pathway would be changed. As no information on the reaction of *N*-hydroxybenzimidamides **240**

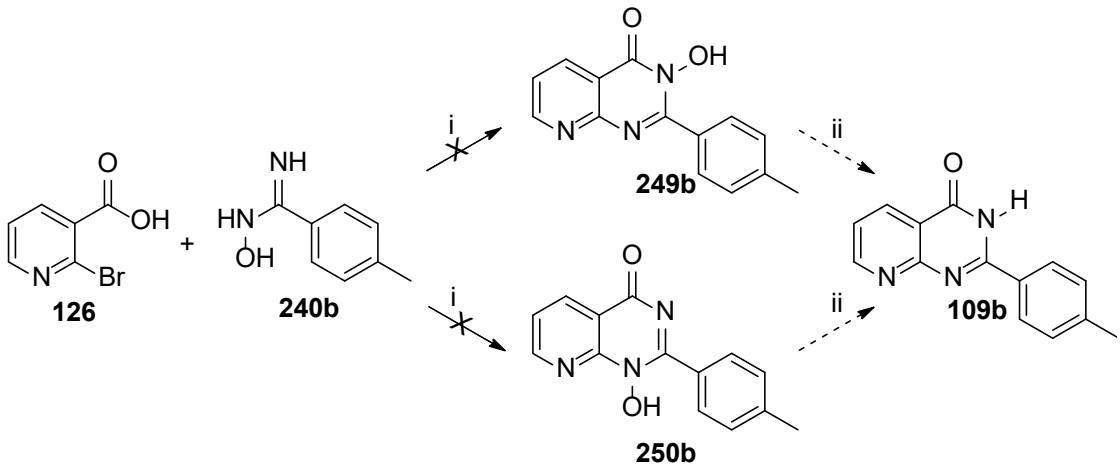

Scheme 38. Alternative pathway to synthesise pyridopyrimidinones **109**-**111**. *Reagents & conditions*: i, CuI, Cs_2CO_3, DMF, 80 °C; ii, 10% Pd/C, $HCOONH_4$, AcOH, Δ.

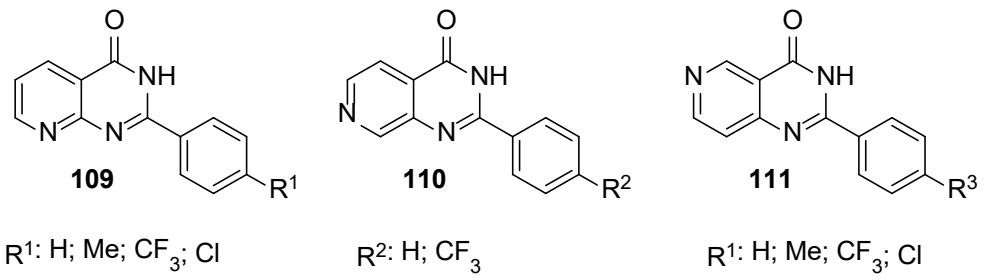

Figure 46. The range of synthesised pyridopyrimidinones **109-111**.

with haloarenecarboxylic acids under copper catalysis was found in the literature, the same conditions as for Ullmann-type coupling with benzamidines **241** were implemented: 0.2 equivalents of copper iodide, two equivalents of caesium carbonate and DMF as the solvent. However, none of the desired pyridopyrimidinone **249b** or **250b** was observed after seven days. It might be the benzamidine $NH(C)NH_2$ group is essential for this type of coupling.

Overall, a variety of target novel pyridopyrimidinones **109-111** was synthesised, using a fairly short pathway of one to three reactions (Figure 46). The range of obtained compounds allowed investigation of the pyrimidine core structure fused to the pyridine ring and the effect of this structure on the inhibition of the tankyrases.

2.7 Synthesis of tetrahydropyridopyrimidinones.

So far, most of the target compounds which have been synthesised have had aromatic pyridine rings fused to the lactam. The known inhibitor of the tankyrases, XAV939 **47**, has a partly saturated dihydrothiopyran in this position. It was therefore of interest to study the effect of a flexible partly saturated ring but with a basic secondary aliphatic amine. The tetrahydropyridopyrimidinones **112** and **113** were synthesised to address the question of isosteric replacement of lipophilic sulfur in XAV939 **47** with a polar cationic protonated secondary nitrogen. The saturated aliphatic ring was expected to be flexible and therefore to accomodate different conformations, whereas the aromatic ring of **109-111** is flat. Also, the heterocyclic nitrogen atom is sp^3-hybridised in **113**, but in **109-111** it is sp^2-hybridised. The structure of tetrahydropyridopyrimidinones **113** bears resemblance to the structure of XAV939 **47** (see Scheme 2); both consist of a partly saturated ring with a heteroatom in position-6 and a pyrimidinone ring. However, different heteroatoms in the structures of **47** and **113** should bring certain dissimilarities to their chemical and biological properties. Nitrogen-containing tetrahydropyridopyrimidinones **113** are expected to be more basic compared to sulfur-containing XAV939 **47**. The (potentially protonated) NH moiety in the saturated ring of **113**, being a hydrogen-bond donor, is able to form hydrogen bonds with the residues of amino acids in the enzyme, while the sulfur atom in **47** is not. Taking into account both differences and similarities of tetrahydropyrimidinones **113**, XAV939 **47** and pyridopyrimidinones **109-111**, it was of interest to explore the inhibitory activity of **113**. Since the structure of designed compounds **113** differs from the structure of compound **47** by the heteroatom only, a synthetic approach similar to that for synthesis of XAV939 **47** was implemented: condensation of a β-ketoester product of Dieckmann condensation with a variety of benzamidines.[260] The advantage of this method was the fact that the

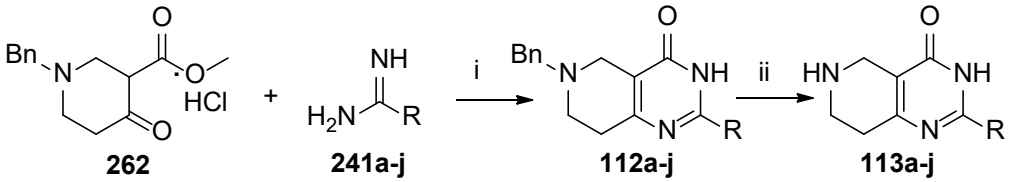

262 **241a-j** **112a-j** **113a-j**

a: R = Ph; **b**: R = MePh; **c**: R = MeOPh; **d**: R = F_3CPh; **e**: R = ClPh;
f: R = BrPh; **g**: R = H_2NPh; **h**: R = 4-Py; **j**: R = 4-phenylethynylphenol

Scheme 39. Proposed synthesis of target tetrahydropyridopyrimidinones **112** and **113**. *Reagents & conditions*: i, NaOMe, MeOH, Δ, 43-86%; ii, Pd/C, H_2, MeOH, Δ, 34-89%.

selection of benzamidines **241** had already been made for the previous synthesis of pyridopyrimidinones **109-111**. However, the only commercially available appropriate product of a Dieckmann condensation was methyl 1-benzyl-4-oxopiperidine-3-carboxylate hydrochloride **262**, a *N*-benzyl-protected piperidine ketoester. Therefore, after the condensation of **262** with benzamidines **241**, an extra step of removal of the benzyl group from the products of condensation, 6-benzyl-2-aryl-5,6,7,8-tetrahydropyrido[4,3-*d*]pyrimidin-4-ones **112**, would be necessary. It was decided to introduce protected intermediates **112** into biological evaluation together with target compounds **113**, despite the fact that compounds **112** possessed a bulky substituent at position-6, which generally should not be tolerated for the inhibitors of the tankyrases.[146] Firstly, the starting material **262** was to be condensed with benzamidines under basic conditions, as described for the synthesis of XAV939 **47** (Schemes 39, 40).[260] The benzyl protecting group in the constructed 6-benzyl-2-aryl-5,6,7,8-tetrahydropyrido[4,3-*d*]pyrimidin-4-ones **112** was to be removed by palladium-catalysed hydrogenolysis, resulting in 2-phenyl-5,6,7,8-tetrahydropyrido[4,3-*d*]pyrimidin-4-ones **113** (see Scheme 39).

Following this strategy, a variety of compounds **112** was synthesised (Table 18). However, the same problem was observed as for the synthesis of pyridopyrimidinones **109-111**; benzamidines **241** with electron-donating substituents, when condensed with compound **262**, gave an unidentifiable mixture of compounds (Table 18, entries 3, 6). Unlike the previous experience with the synthesis of pyridopyrimidinones **109-111**, halo-substituted benzamidines **241e,f** provided good yields of condensed products **112e,f** (Table 18, entries 5, 7), proving the unfavourable effect of copper on the halo-

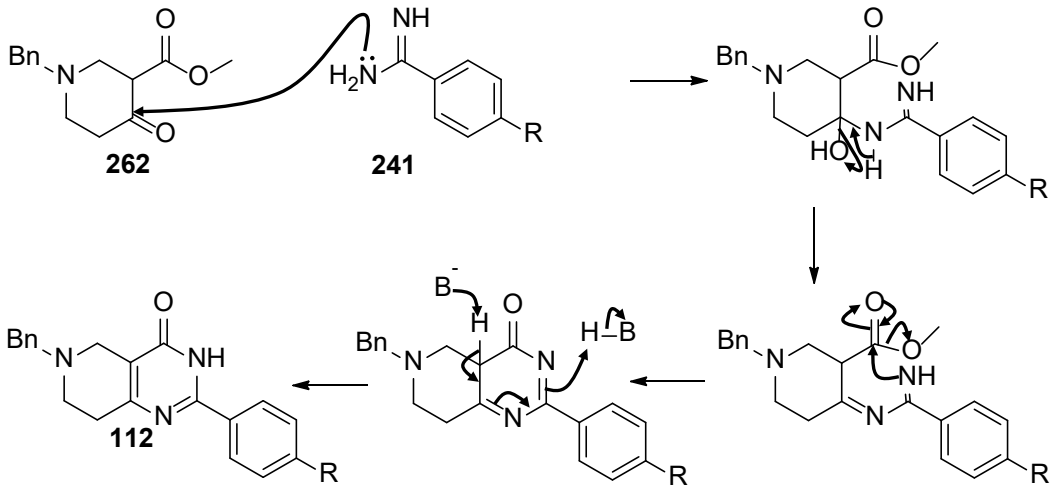

Scheme 40. Mechanism of formation of compounds **112.**

substituted benzamidines. Pyridin-4-imidamide **241h**, also unlike the failure of the previous copper-catalysed coupling with all three bromopyridinecarboxylic acids **126-128**, when condensed to compound **262** under copper-free conditions provided the desired product **112h** (Table 18, entry 8). This result supports the concept of the inappropriate ligation of the copper catalyst to the heterocyclic nitrogen atom in pyridin-4-imidamide **241h**, which hindered the reaction and thus synthesis of **109h-111h**.

Table 18. Condensations of the ketoester **262** with benzamidines **241a-h** under basic conditions.[a]

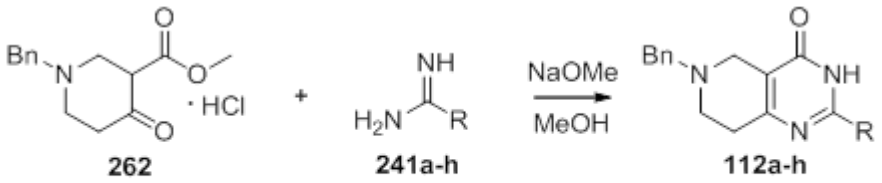

262 **241a-h** **112a-h**

a: R = Ph; **b**: R = 4-MePh; **c**: R = 4-MeOPh; **d**: R = 4-F_3CPh; **e**: R = 4-ClPh; **f**: R = 4-BrPh; **g**: R = 4-H_2NPh; **h**: R = 4-Py

Entry	R	Yield, %
1	Ph	53
2	4-MePh	56
3	4-MeOPh	0
4	4-F_3CPh	60
5	4-ClPh	58
6	4-H_2NPh	0
7	4-BrPh	43
8	4-Py	86

[a] The reactions were carried out in DMF at 0.5 M concentration of **262** and **241**; 6 eq. of NaOMe.

The next step, a palladium-mediated reductive removal of the benzyl group, proposed by Huber *et al.*,[261] involved stirring the reaction mixture under reflux in methanol under an atmosphere of hydrogen. In light of safety issues, it was decided to use an alternative source of hydrogen (or reducing equivalents) (Table 19). Initially, ammonium formate was used, resulting in no deprotection after seven days (Table 19, entry 1).

Table 19. Palladium-mediated reductive deprotection of compounds **112**.[a]

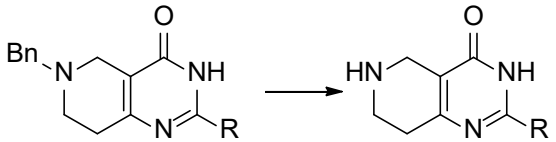

112a-h,k **113a-h,k**

a: R = Ph; **b**: R = 4-MePh; **c**: R = 4-MeOPh; **d**: R = 4-F_3CPh; **e**: R = 4-ClPh; **f**: R = 4-BrPh; **g**: R = 4-H_2NPh; **h**: R = 4-Py; **k**: R = 4-phenylethynylphenol

Entry	R	Catalyst	Reductant	Solvent	Yield
1	Ph	Pd/C	$HCOONH_4$[b]	HCl/MeOH[c]	0[§]
2[d]	Ph	Pd/C	HCOOH	MeOH	89
3	4-MePh	Pd/C	HCOOH	MeOH	86
4	4-F_3CPh	Pd/C	HCOOH	MeOH	68
5	4-Py	Pd/C	HCOOH	MeOH	80
6	4-Ph-ethynyl-Ph	Pd/C	HCOOH	MeOH	34[e]

[a] The reactions were carried out at 0.01 M concentration of **112a-j**. [§] The reaction was stirred for 7 d.

[b] 14 eq. of $HCOONH_4$ were used.

[c] 1 mL of conc. HCl and 10 mL of anhydrous MeOH were used.

[d] 1 eq. (w/w) of 10% Pd/C, 1 mL of conc. HCOOH and 10 mL of anhydrous MeOH were used.

[e] As a hydrochloride salt.

However, when formic acid was used, the reaction provided an excellent yield of the deprotected compound **113a** as the formate salt (Table 19, entry 2). This success might be due to protonation of the benzylamines facilitating reductive cleavage as the leaving group is improved. By contrast, neutral ammonium formate cannot protonate 6-N and therefore the putative leaving group, R'N^-, is less likely to cleave.

The reaction mixture caught fire during the addition of palladium on charcoal; there were methanol vapours in the flask, which were likely to be ignited by palladium. Despite the dangers of the method, the same conditions were applied to deprotect other derivatives, excluding halogen-substituted **112e** and **112f**. Alternative debenzylation methods were investigated for the haloaryl compounds. Initially, 5% platinum-on-carbon was used, failing to deprotect both compounds **112e** and **112f**, even after 7 d of stirring. Non-reductive methods of deprotection were studied. Acid-catalysed debenzylation with strong Brønsted acids, such as hydrobromic acid, and Lewis acids, such as boron tribromide, was explored. Despite the well-known debenzylation

properties of hydrobromic acid and boron tribromide,[187] they did not provide the desired compounds **113e,f**, giving an unidentifiable mixture of compounds. Hydrobromic acid as a strong Brønsted acid (pKa = -9),[262] was expected to protonate 6-N, generating a good leaving group, R'NH. Thus, it was rather surprising that it failed to deprotect **112e** and **112f**. Boron tribromide, being a strong Lewis acid and not being able to protonate 6-N, was expected to coordinate to the lone pair on the nitrogen atom, generating, after appropriate work-up, R'NH and several by-products: benzyl bromide, hydrobromic acid and boric acid. Oxidative reagents, *e.g. N*-iodosuccinimide[263] and *m*-CPBA[264] did not lead to deprotection either. Debenzylation with *N*-iodosuccinimide is believed to go through the oxidative formation of the benzyliminium ion, followed by hydrolysis.[263] The deprotection of the benzyl group with *m*-CPBA consists of two steps: firstly, *m*-CPBA oxidises the nitrogen at the benzyl group to a *N*-oxide; then the *N*-oxide is treated with catalytic amounts of Fe^{2+} ion to give R'NH and an aldehyde.[264] It was decided to postpone the deprotection and to explore it further only if biological evaluation of other deprotected compounds would provide promising results. The bromo derivative **112f** provided an interesting opportunity for further coupling reactions. Initially, a Sonogashira coupling of **112f** with phenylethyne **145a** was attempted (Scheme 41, A). Despite signs of a product on TLC, isolation did not lead to the desired product **113k**. Considering that this compound is highly polar and poorly soluble, another strategy was suggested (Scheme 41, B), which involved a change in the order of steps, that is, to perform the Sonogashira coupling before the condensation. Thus, Sonogashira coupling would be performed on less polar and more soluble compounds. Firstly, 4-phenylethynylbenzonitrile **239k** was synthesised *via* a sodium-ascorbate-modified Sonogashira coupling from 4-bromobenzonitrile and phenylethyne. Next, the nitrile **239k** was converted into a benzamidine **241k** with sodium methoxide and ammonium chloride, using the procedure applied previously (see Section 2.6).[259] Condensation with methyl 1-benzyl-4-oxopiperidine-3-carboxylate **262** provided the benzyl-protected compound **112k**. Finally, the palladium-mediated hydrogenolysis was performed. It was taken into account that there was a high possibility of reduction of the triple bond instead of (or together with) cleavage of the benzyl group. However, quite remarkably, the triple bond remained untouched and the benzyl group was cleaved. The deprotected compound **113k**, obtained as a formate salt, surprisingly had an aspect of a buff gum. For handling purposes, compound **113k** was converted into a crystalline hydrochloride salt by treatment with hydrogen chloride in 1,4-dioxane.

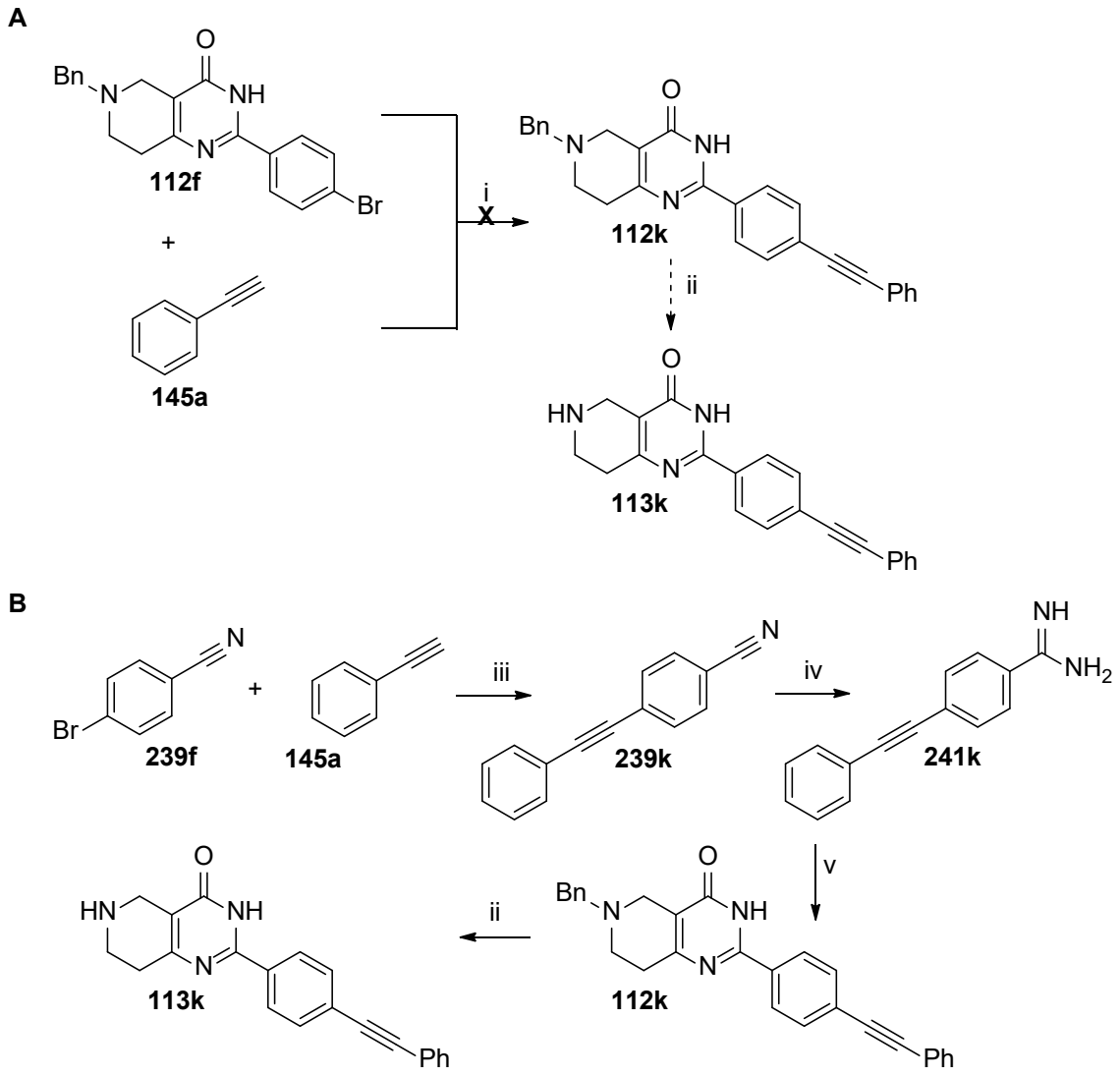

Scheme 41. A, Proposed synthesis of **113k** *via* Sonogashira coupling; **B**, Synthesis of **113k** *via* a coupling with specially made benzamidine **241k**. *Reagents & conditions*: i, $Pd(Ph_3)_4$, CuI, Na ascorbate, $^{i}Pr_2NH$, THF, 40 °C; ii, Pd/C, HCOOH, MeOH, Δ, 34%; iii, $Pd(Ph_3)_4$, CuI, Na ascorbate, $^{i}Pr_2NH$, THF, 40 °C, 87%; iv, NaOMe, NH_4Cl, MeOH, Δ, 68%; v, NaOMe, MeOH, Δ, 57%.

Altogether, a variety of benzyl-protected and deprotected tetrahydropyridopyrimidinones **112** and **113** was synthesised, providing an opportunity to investigate the significance of a range of factors for the inhibition of tankyrases. Compared with the known tankyrase-1/2 inhibitor XAV939 **47**, it would be possible to explore the influence of heterocyclic atoms, *i.e.* nitrogen and sulfur, and their hybridisation. At the same time, comparison of tetrahydropyrimidinones **112** and **113** with the pyridopyrimidinones **109-111** provides an opportunity to investigate the importance of the basicity of the compounds, the flexibility of the ring and the influence of conformations. Moreover, compounds **112** also would confirm if bulky substituents were tolerated at the 6-position.

2.8 Synthesis of XAV939.

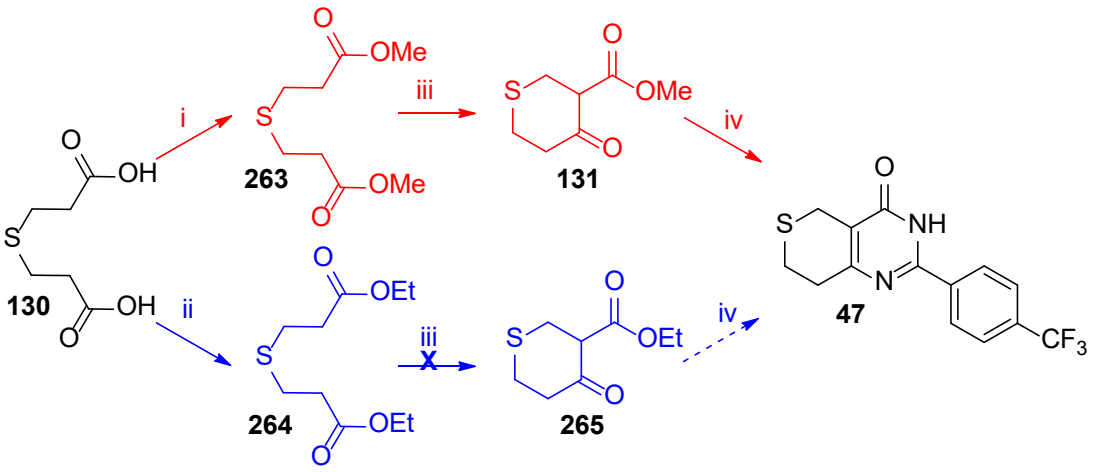

Scheme 42. Patented synthesis of XAV939 **47** (red); proposed modification of the synthesis of XAV939 **47** (blue). *Reagents & conditions:* i, MeOH, conc. H_2SO_4, Δ, 99%; ii, EtOH, conc. H_2SO_4, Δ, 26%; iii, NaOMe, MeOH, THF, r.t., 95%; iv, **241d**, K_2CO_3, MeOH, Δ, 61%.

To obtain large quantities of the tankyrase-1/2 inhibitor XAV939 **47**,[60] which would serve as a positive control in the tankyrase-1/2 enzyme assays, it was planned to optimise the existing method.[260] The patented strategy of synthesis of XAV939 **47** involved potassium-carbonate-mediated reaction of Dieckmann condensation product **131** with 4-trifluoromethylbenzamidine **241d** (Scheme 42, red). It was decided to investigate if the condensation of ethyl 4-oxotetrahydro-2*H*-thiopyran-3-carboxylate **265** with the same benzamidine **241d** would give better results (Scheme 42, blue). For this purpose, diethyl 3,3'-thiodipropanoate **264** was made from the corresponding acid **130** by Fischer-Speier esterification (the reaction of a carboxylic acid with an aliphatic alcohol (primary or secondary) under acid catalysis at high temperature).[265]

The diethyl diester **264** was then subjected into the base-mediated Dieckmann

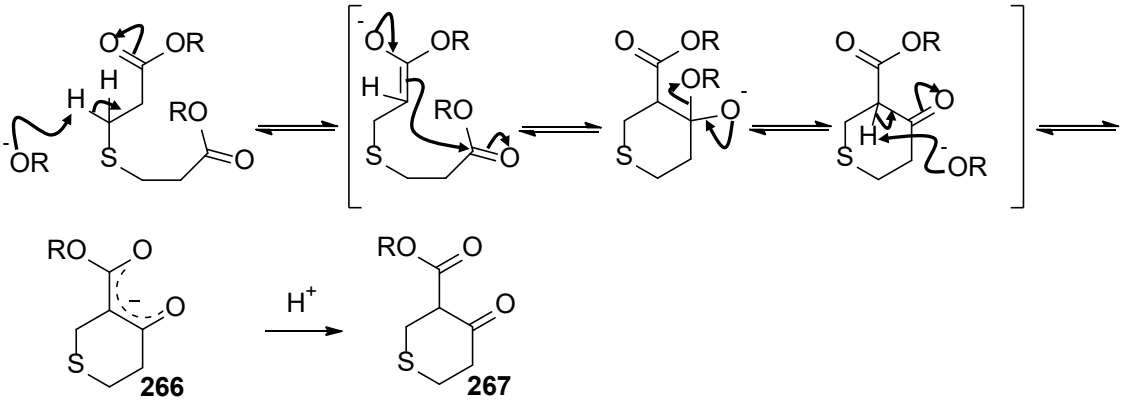

Scheme 43. Mechanism of Dieckmann cyclisation.

cyclisation. The Dieckmann cyclisation or condensation is an intramolecular type of Claisen condensation, in which the ester groups are tethered.[179] The driving force for this reaction is the formation of a stable enolate **266** of the β-ketoester **267** (Scheme 43). If this structure fails to form, the reaction is readily reversible. Approaching the Dieckmann condensation of **264**, a literature search revealed several procedures. Bennett *et al*. used sodium ethoxide prepared *in situ* using dry ethanol.[266] This approach did not lead to the formation of the desired cyclised product **265**. The same unfortunate result was obtained when sodium hydride in THF with a catalytic amount of dry ethanol was implemented, following the procedure of Cross *et al.*[267] The use of potassium *tert*-butoxide did not result in the desired product **265** either. Since an ethoxy group is more bulky than methoxy, it might be possible that the ethoxy group at the electrophilic carbonyl prevented nucleophilic attack. In light of this, it was decided to return to the published strategy. The dimethyl diester **263** was made using from **130** the same procedure as for the diethyl analogue **264**, resulting in an excellent yield (99%) of **263**.

The esterification product **263** was introduced into Dieckmann cyclisation. Firstly, the procedure published by Ward *et al.* was repeated: dimethyl 3,3'-thiobispropanoate **263** was treated with sodium methoxide (generated *in situ*) in THF solution.[268] Surprisingly, it did not provide the cyclised β-ketoester **131** at room temperature nor under reflux. Since an excess of methanol was used in this reaction, it was possible that it made sodium methoxide a weaker base. Sodium hydride was investigated as a base in this reaction.[269] However, both the 60% dispersion of sodium hydride in oil and sodium hydride washed free from oil did not provide the desired product **131**. Notably, only when commercially available sodium methoxide was used instead of reagent made *in situ*, the reaction yielded 95% of the cyclised product **131**. Since the commercially available solid sodium methoxide is not weakened by the excess of methanol, such an outcome was feasible.

Methyl 4-oxotetrahydro-2*H*-thiopyran-3-carboxylate **131** was condensed with 4-tri-

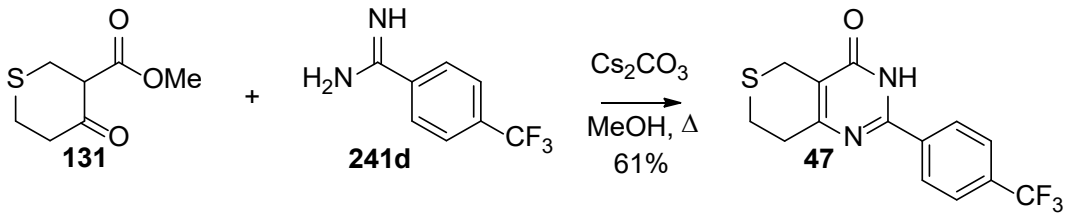

Scheme 44. Formation of XAV939 **47.**

fluoromethylbenzamidine **241d**. The patented procedure involved the use of potassium carbonate in methanol. However, when these conditions were applied, the condensation did not happen after 3 d. A stronger base, caesium carbonate, was investigated. Caesium carbonate possesses a cation with larger radius of atom, compared to potassium carbonate; therefore, caesium carbonate dissociates and provides basic carbonate anion more easily. When caesium carbonate was used, it provided 64% of target XAV939 **47**. The mechanism of this condensation is believed to be similar to that of methyl 1-benzyl-4-oxopiperidine-3-carboxylate **262**, which was discussed in the previous section (see Scheme 40). The modified procedure for the synthesis of XAV939 **47** resulted in good yields of the target compound, providing plenty of material for biological evaluation.

2.9 Conclusions.

A summary of synthesised compounds is represented in Figure 47. Specially designed synthesis (see Scheme 2) resulted in a selection of target nitrogen-containing bicyclic lactams ready for biological evaluation.

A series of 7-substituted 1,6-naphthyridinones **99** was synthesised *via* Sonogashira coupling and electrophilic cyclisation, giving material for the investigation into the effect of the heterocyclic nitrogen atom at the position-1 on the inhibitory activity against tankyrase-1/2. Two examples of compounds **99** were *N*-oxidised, giving *N*-oxides **102a,b** and providing an opportunity to investigate the activity of charged species. Compounds **99** were also *N*-methylated to provide salts **103**, which would be interesting to evaluate biologically, since they possess a quaternary nitrogen atom. The *N*-methyl naphthyridinones **103** were reduced, giving tetrahydronaphthyridinones **106**. Compounds **106**, being rather different from the series, make it possible to investigate the effect of a basic partly saturated and, therefore, partly planar, ring on the inhibition of the tankyrases.

A selection of structural isomers of naphthyridinones - 3-aryl 2,6-naphthyridinones **100** and 3-aryl 2,7-naphthyridinones **101** – was made by the same pathway as 1,6-naphthyridinones **99**: Sonogashira coupling followed by electrophilic cyclisation. An interesting reactivity pattern was detected during the synthesis, proving that the heterocyclic nitrogen atom alters the electron-density of the molecules and therefore affects their reactivity. Thus attempted *N*-methylation of the compounds **100** and **101** only resulted in two examples of the quaternised salts **104c** and **105a**. The reduction of these salts did

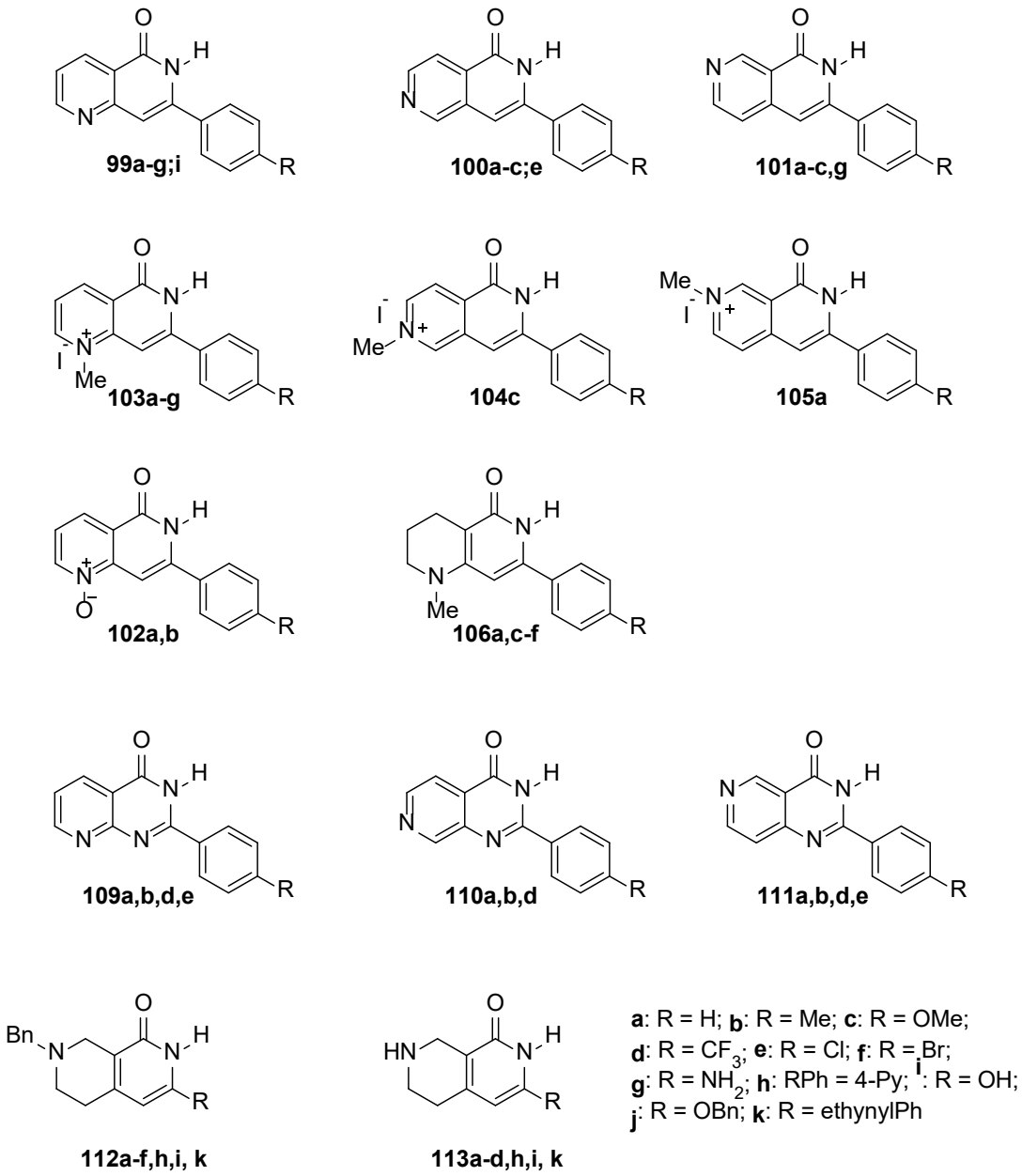

Figure 47. Structures of synthesised target compounds **99-113**.

not provide tetrahydronaphthyridinones **107** and **108**, unlike to the previous series of 1,6-naphthyridinones. Considering the different chemical properties, it would be interesting to explore the biological profile of these compounds, investigating the effect of the position of the heterocyclic nitrogen atom on the inhibitory activity against the tankyrases.

The scope of these series was significantly broadened, when another synthetic strategy was implemented: the Hurtley-intramolecular cyclisation.

A variety of pyridopyrimidinones **109-111** was synthesised *via* an Ullmann-type copper-catalysed coupling. This series would provide information on the effect of a second heterocyclic nitrogen atom in the lactam ring.

Base-mediated condensation of a Dieckmann condensation product **262** with a variety of benzamidines **241** provided benzyl-protected compounds **112**, allowing a test of the expected intolerance of any substituents at the 6-position for the inhibition of tankyrase-1/2. Reductive deprotection of compounds **112** gave the corresponding tetrahydro-pyridopyrimidinones **113**. Compounds **113** are of particular interest for biological evaluation, since they could provide SAR data, being compared to the data for pyrido-pyrimidinones **109-111** and XAV939 **47**.

The variety of synthesised compounds would allow expansion of our knowledge of the structure-activity relationships of inhibitors of the tankyrases.

Chapter 3. Biological evaluation

3.1 Overview of planned biological evaluation.

In order to perform the biochemical evaluation of the inhibitory activity of the synthesised target compounds, a five-step testing system was proposed (Scheme 45). Initially, the target compounds were planned to be screened against the catalytic activity of tankyrase-2 to establish an order of magnitude of their inhibitory activity. For those compounds which showed reasonable activity in the preliminary three-point ranging screening, an exact IC_{50} value against tankyrase-2 and tankyrase-1 would be obtained. To determine the selectivity of the compounds towards tankyrase-1/2 (PARP-5a/b), the most active compounds would be subjected to counter-screening against catalytic

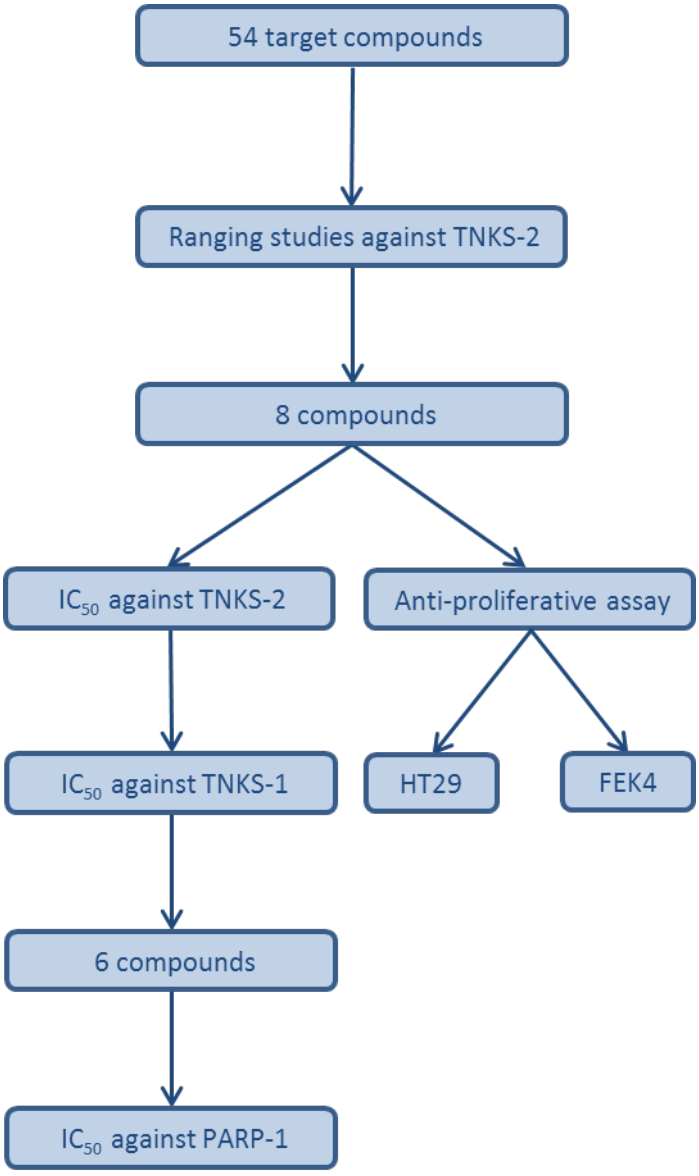

Scheme 45. Flow chart of the general concept for the biological evaluation of the target compounds.

activity of another PARP enzyme, PARP-1. The anti-proliferative activity of the most active compounds was proposed to be measured against the human colon adenocarcinoma cell line HT29, using an MTS assay, since the *Wnt* signalling and, subsequently, the tankyrases, are more active in colorectal cancers.[84-86] Therefore, it would be possible to show the cytotoxicity of the compounds against cancer cells. At the same time, it was important to determine if the compounds are non-toxic towards normal cells. This was also planned to be evaluated using an MTS assay but with a different cell line, human skin fibroblasts FEK4.

3.2 Three-point ranging study against tankyrase-2.

Approaching the preliminary ranging studies to determine if the compounds show any inhibitory activity against the tankyrases, an in-house tankyrase-2 assay was developed. A truncated form of tankyrase-2, containing the catalytic and SAM domains, is commercially available and was therefore employed. A tankyrase-2 assay was established by Dr. Matthew D. Lloyd, Dr. Pauline J. Wood and Dr. Amit Nathubhai in our group.[166] It is a colorimetric assay, which employs the ability of tankyrase-2 to (poly-ADP)ribosylate itself in the SAM domain, using NAD^+ as the source of ADPr. The catalytic activity of the enzyme was measured through the auto-(poly-ADP-ribosyl)ation. In order to measure it, the suspension of the enzyme in the assay buffer was loaded into the wells of a high-binding ELISA-quality 96-well plate and allowed to stand overnight. The non-bound excess of the enzyme was washed away with phosphate-buffered saline solution pH 7.4 [+ 0.05% (v/v) Tween® 20] (PBS-T) and the protein-free areas of the wells were blocked with milk protein to reduce non-specific binding of substrate. The inhibitors were dissolved in DMSO to give stock solutions of appropriate concentrations and then diluted with the assay buffer to obtain a final concentration of 1% DMSO (v/v). After another wash with PBS-T, the wells were loaded with the solutions of the candidate inhibitors, biotinylated NAD^+ and NAD^+ (equimolar) and the assay buffer to give the final reaction volume of 25 μL. Biotinylated NAD^+ was used as a substrate for the reaction and, at the same time, as a detector of the enzyme activity. The active enzyme would use biotin-labelled NAD^+ as a source of ADPr; therefore, measuring the amount of bound biotin would be a measure of the amount of ADPr bound to the tankyrase. Detection of biotin with a commercially available detecting system, which generated a colorimetric signal, would reveal the amount of bound ADPr and, hence, the catalytic activity of the tankyrase-2. Biotinylated NAD^+ was diluted with non-labelled NAD^+, since this mixture gave better

results; when biotinylated NAD^+ was used alone, the colorimetric signal was lower as the detection reagent (streptavidin-peroxidase) could not get access to it because of the overcrowding of biotin residues. The plates were incubated at 30 °C for two hours to allow the reaction of auto(poly-ADPribosyl)ation of tankyrase-2 to happen. The wells were washed with PBS-T and a component of the commercially available biotin detection system, streptavidin-horse-radish peroxidase (HRP) solution, was added to the wells and the plates were left at room temperature for two hours. After another washing with PBS-T, the special substrate solutions A and B were loaded to each well in order to generate the colour. After thirty minutes, the peroxidase reaction was stopped by addition of aq. sulfuric acid (1.0 M) and the absorbance at 450 nm was measured within 20 min.

All synthesised target compounds were studied in this assay to obtain a preliminary measure of their activity against tankyrase-2 at three different concentrations. The concentrations ranged over a factor of 100 for each compound, within the overall range 10 nM to 100 μM. This concentration range was chosen on the basis of the known activity of other tankyrase-1/2 inhibitors, such as XAV939 **47** (TNKS-1 IC_{50} = 0.011 μM; TNKS-2 IC_{50} = 0.004 μM)[60] and the 2-arylquinazolin-4-ones (see Table 10).[166]

3.2.1 Naphthyridinones and their derivatives.

Initially, the series of 7-aryl-1,6-naphthyridinones **99** was screened against catalytic activity of tankyrase-2 (*vide infra*, Table 20), using the three-point assay.

It was necessary to determine an appropriate range of concentrations at which to test the inhibitors. Aiming to make inhibitors with IC_{50} values lying in the nanomolar range, it was initially proposed to test all the compounds at 10 nM, 100 nM and 1 μM. However, after testing compounds **99a** and **99d**, no inhibition was detected at nanomolar concentrations. For **99a**, 42% inhibition was observed at 1.0 μM, indicating that the IC_{50} value should be slightly greater than 1.0 μM. The compound **99f** showed lesser activity at the same concentration range: 14% inhibition was noted at 1.0 μM and 100 nM, suggesting that the IC_{50} value would be at a high micromolar concentration. In light of these results, further testing was performed at higher concentrations. Compounds **99b**, **99c** and **99e** were evaluated at 1.0 μM, 10 μM and 100 μM. Interestingly, the 4-methylphenyl derivative **99b** and the 4-chlorophenyl derivative **99e** completely inhibited the catalytic activity of tankyrase-2 at 10 μM and at 100 μM. The hydrophobic

nature of these groups, together with the small size and electron-neutrality, might cause this beneficial effect. Proving this point, the 4-methoxyphenyl compound **99c**, possessing a hydrophobic but electron-donating and more bulky substituent, showed 50% inhibition at 10 μM and no inhibition at 1.0 μM. Aiming to investigate further the structure-activity relationship of 7-aryl-1,6-naphthyridinones **99**, the last three compounds in this series were tested. It was decided to perform the three-point assay at the middle range of concentrations: 100 nM, 1.0 μM and 10 μM.

Table 20. Data from the three-point assay of 7-aryl-1,6-naphthyridinones **99** against the catalytic activity of tankyrase-2.*

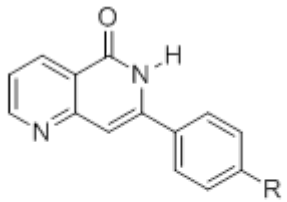

99a: R = H; **99b**: R = Me; **99c**: R = OMe;
99d: R = CF_3; **99e**: R = Cl; **99f**: R = Br;
99g: R = NH_2; **99i**: R = OH

Number of the compound	Concentration of the inhibitor				
	10 nM	**100 nM**	**1.0 μM**	**10 μM**	**100 μM**
	% inhibition				
XAV939	44 ± 7				
99a	< 0	< 0	42 ± 4		
99b			39 ± 3	> 100	97 ± 8
99c			< 0	51 ± 22	93 ± 19
99d	1 ± 10	14 ± 10	14 ± 24		
99e			35 ± 25	94 ± 26	> 100
99f		25 ± 4	47 ± 14	77 ± 8	
99g		< 0	74 ± 5	96 ± 3	
99i		3 ± 13	58 ± 6	96 ± 5	

*The given values are an average for the triplicates ± calculated SD.

The bromo analogue **99f** predictably showed results similar to the 7-(4-chlorophenyl) analogue **99e**. More intriguing results were obtained for the compounds with more polar and hydrophilic substituents, such as hydroxy or amino. Apparently, the electron-donating nature of the substituents at the phenyl ring did not influence on the inhibitory activity of the compounds: the amino compound **99g** showed 74% inhibition at 1.0 μM, whilst the 7-(4-methoxyphenyl) derivative **99c**, which also possessed an electron-donating substituent on the phenyl ring, showed no inhibition at all at this concentration. The lipophilicity of the substituent at the aryl ring also did not seem to be a key factor; the 7-(4-hydroxyphenyl) analogue **99i**, having a hydrophilic hydroxy group on the aryl ring, showed 58% inhibition at 1.0 μM, when the corresponding methoxy compound **99c** was completely inactive at this concentration. Another possible factor that could be important for the inhibition could be the size of the substituent. The methoxy derivative **99c**, carrying the bulkiest substituent in all the series, was noted to be the least active. However, the relative size of the bromine atom in **99f** did not impair the inhibition and the relatively small trifluoromethyl group in **99d** did not improve the activity. Compound **99c**, showing poor inhibitory values, possessed the methoxy substituent, which is a hydrogen-bond acceptor. At the same time, compounds **99i** and **99g**, having, respectively, a hydroxy group, which is both a hydrogen-bond acceptor and donor, and an amino group, which is a hydrogen bond donor, showed better inhibition. Therefore, the hydrogen-bond donating properties of the substituent might be important for the inhibition.

In light of these results, it was particularly interesting to evaluate the N^1-substituted compounds (Table 21). Amongst the N^1-oxides, the 7-(4-methylphenyl)-substituted N^1-oxide **102b** was markedly more active than the 7-phenyl N^1-oxide **102a**; at 1.0 μM, **102b** inhibited 94% of the enzyme activity, when **102a** inhibited just 23%. Compound **102b** was also more active than the corresponding non-oxidised 7-aryl-1,6-naphthyridinones **99b**. These data, together with the information obtained from the non-N^1-substituted 7-aryl-1,6-naphthyridinones **99**, might suggest a small substituent at the position-4 of the phenyl ring of the naphthyridinone filled the hydrophobic nook formed by Phe^{1035} and Ile^{1075}. Similar conclusions were drawn after testing 2-aryl-8-methylquinazolin-4-ones against tankyrase-1/2; the size of the substituent at the 4'-position was more important than its electronic effects and hydrogen-bonding properties.[166]

Table 21. Data from the three-point ranging study of N^1-substituted 7-aryl-1,6-naphthyridinones **102, 103** against the catalytic activity of tankyrase-2.*

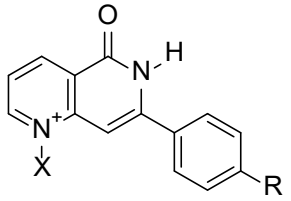

102a: X = O, R = H; **102b**: X = O, R = Me; **103a**: X = Me, R = H; **103b**: X = Me, R = Me; **103c**: X = Me, R = OMe; **103d**: X = Me, R = CF_3; **103e**: X = Me, R = Cl; **103f**: X = Me, R = Br; **103g**: X = Me, R = NH_2.

Number of the compound	Concentration of the inhibitor				
	10 nM	**100 nM**	**1.0 μM**	**10 μM**	**100 μM**
	% inhibition				
102a	< 0	1 ± 6	23 ± 13		
102b		12 ± 15	94 ± 2	106 ± 4	
103a	4 ± 10	24 ± 12	< 0		
103b			83 ± 12	> 100	> 100
103c		0 ± 6	9 ± 5	12 ± 5	
103d		1 ± 28	24 ± 4	< 0	
103e		17 ± 9	8 ± 10	9 ± 6	
103f		23 ± 1	27 ± 5	45 ± 24	
103g		< 0	< 0	2 ± 14	

*The given values are an average for the triplicates ± calculated SD.

To investigate the effect of a quaternising substituent at the heterocyclic nitrogen, further screening was performed. *N*-Methylated compounds **103** were assayed in the three-point ranging studies against the catalytic activity of tankyrase-2. Oddly, **103a**, **103d** and **103e** did not show any dose-response activity, probably because of rather low values of inhibition. Consistent with previous deductions, the 7-(4-methylphenyl) analogue **103b** inhibited 83% of the activity, even at 1.0 μM, which was the best result among the compounds **103**. The 7-(4-methoxyphenyl) derivative **103c** did not appear to be a potent inhibitor, with just 12% inhibition at 10 μM of the inhibitor, again, confirming previous conclusions. Surprisingly, the bromo compound **103f** was more active than the corresponding chloro derivative **103e**; however, the IC_{50} value of **103f** would lie between 10 μM and 100 μM. The amino derivative **103g**, possessing a hydrophilic electron-donating amino group, was significantly less active than other compounds, showing only 2% inhibition at 10 μM.

To secure a structural evidence of the inhibition of tankyrase-2, some crystal structures of tankyrase-2 with selected inhibitors bound to the catalytic site were obtained in the group of our collaborator, Dr. Lari Lehtiö (Åbo Akademi and University of Oulu, Finland). The crystal structures were made using the sitting-drop vapour-diffusion method.[146] The tankyrase-2 solution was mixed with the well solution, containing lithium sulfate, Tris-HCl (pH 8.0) and PEG 3350, in a 96-well plate. The plate was incubated at 4 °C to allow the protein crystals to grow. The obtained crystals of tankyrase-2 were soaked in solutions of the inhibitors. After 24 hours, the crystals were dipped into a cryosolution, consisting of lithium sulfate, Tris-HCl, sodium chloride, PEG 3350, 25% glycerol and the appropriate inhibitor, then flash frozen in liquid nitrogen. Diffraction data were collected at the synchrotron and processed with XDS. The structures were solved by molecular replacement using the apo-tankyrase-2 structure.[146] Pymol™ was used to visualise the structures; Coot™ was used for analysis and manual editing of the structures.

As discussed before, the molecule of an inhibitor of tankyrase-1/2 interacts with the catalytic site of the enzyme through hydrogen-bonding of the lactam or amide NH with the carbonyl of Gly^{1032} and the carbonyl of the inhibitor with NH of Gly^{1032} and with OH of Ser^{1068} and, if applicable, through π-π stacking between the phenyl ring and Tyr^{1050}.[148] The crystal structure of tankyrase-2 with **103b** showed that the inhibitor fitted snugly into the binding pocket and that its lactam moiety was within the hydrogen-bond

interacting distance from Ser[1068] and Gly[1032]; the phenyl ring formed π-π stacking interaction with the phenyl of Tyr[1050] and the lactam ring π-π stacked with Tyr[1071] (Figure 48). The 4-methyl substituent at the phenyl ring fitted neatly into the hydrophobic nook and made hydrophobic interactions with Pro[1034], Phe[1035] and Ile[1075]. However, the structure did not reveal the reasons why the compound showed relatively weak inhibitory activity against the enzyme. The most likely explanation for this poor inhibition might be the ionic nature of the molecule; the formal positive charge at N-1 might not be tolerated by the hydrophobic residues of surrounding amino-acids (Tyr[1060], Tyr[1071], Ile[1075]). Overall, the 4-methylphenyl containing derivatives **99b**, **102b** and **103b** showed significantly higher activity compared to other compounds. N^1-methylated compounds **103** were less active than their non-substituted analogues. Regarding *N*-substitution, N^1-oxides **102** were slightly more potent than N^1-methylated compounds **103**.

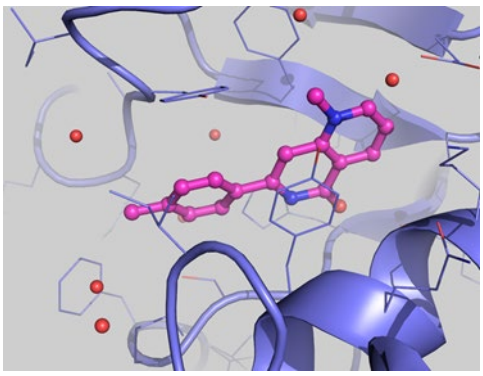

Figure 48. Crystal structure of tankyrase-2 with inhibitor **103b** soaked in (Dr. Lari Lehtiö, unpublished results).

Next, 1-methyl-7-aryl-1,2,3,4-tetrahydro-1,6-naphthyridinones **106** were introduced into the ranging studies against the catalytic activity of tankyrase-2 (Table 22). Unfortunately, the synthesis did not provide the 4-methylphenyl derivative **106b**, so it was impossible to track further the structure-activity relationship of this substituent. These compounds were remarkably more active than the aromatic analogues. Methoxy analogue **106c** and the trifluoromethyl analogue **106d** completely inhibited the enzyme activity, even at 100 nM. Non-substituted compound **106a** inhibited 43% of the enzyme activity at 10 nM, suggesting that the IC_{50} value should be around this concentration. Interestingly, the chloro derivative **106e** was much less active at 100 nM as was the bromo derivative **106f**. These remarkable results provoked further investigations of 1-methyl-7-aryl-1,2,3,4-tetrahydro-1,6-naphthyridinones **106**.

The reduced ring seemed to have a very positive influence on the activity of the compounds, considering that the best tankyrase inhibitor known, XAV939 **47**, had potency. These results might be explained by the presence of a partly saturated ring; this ring is largely planar because of the presence of a double bond and the heterocyclic nitrogen. However, just one CH_2 group of this ring appears to be above the plane and, therefore, this is not purely twisted chair conformation, where one CH_2 group is above

the plane, whilts another CH_2 group is below the plane.[180] Such a twisted conformation of the molecules **106** might have favoured the hydrophobic interactions of C-3 with the hydrophobic side-chains of amino-acids (Ile^{1112}, Ile^{1114}, Leu^{1116}, Pro^{1118}) in this region.

Table 22. Data from the three-point ranging study of 1-methyl-7-aryl-1,2,3,4-tetrahydro-1,6-naphthyridinones **106** against the catalytic activity of tankyrase-2.*

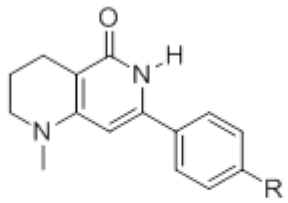

106a: R = H; **106c**: R = OMe; **106d**: R = CF_3;
106e: R = Cl; **106f**: R = Br

Number of the compound	Concentration of the inhibitor				
	10 nM	**100 nM**	**1.0 μM**	**10 μM**	**100 μM**
	% inhibition				
106a	43 ± 9	78 ± 3	99 ± 4		
106c		93 ± 23	82 ± 7	100 ± 4	
106d		82 ± 19	86 ± 5	95 ± 3	
106e		24 ± 12	89 ± 11	91 ± 14	
106f		49 ± 7	89 ± 6	97 ± 3	

*The given values are an average for the triplicates ± calculated SD.

Molecular modelling of the selected inhibitors **106** bound to the catalytic site of tankyrase-1/2 was performed using SYBYL™ and Chimera™ software. Ligands were constructed and charged using the structure of XAV939 **47**. The structure of the TNKS-2 enzyme was generated by removing the XAV939 ligand from the published structure (PDB code: 3KR7).[148] Ligands were then manually docked to the enzyme using the lactam as a beacon. The receptor / ligand complex with established binding

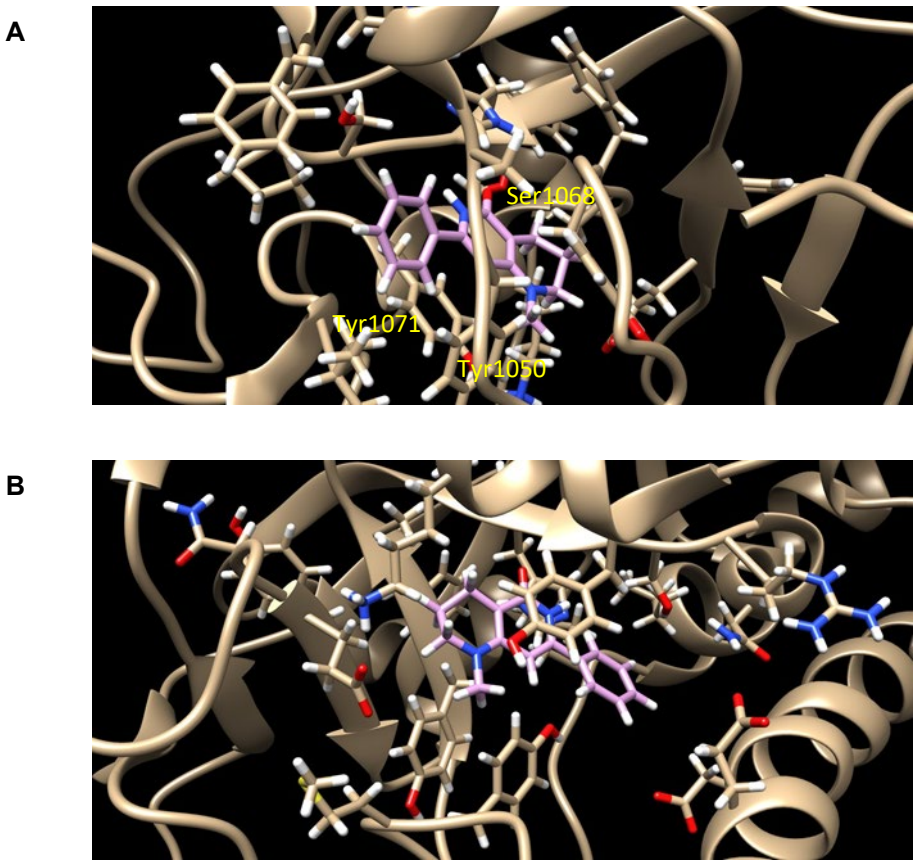

Figure 49. A: Molecular model of compound **106a** with tankyrase-2; **B:** Docking of compound **106a** with PARP-1. Performed using Sybyl^{TM} and Chimera^{TM} software.

conformation of the ligand was then minimised to give the final structures. Molecular modelling of compound **106a** bound to tankyrase-2 confirmed several aspects (Figure 49):

1. Three crucial hydrogen-bond interactions were present between the lactam moiety and Ser^{1068} and Gly^{1032}. The carbonyl accepted two hydrogen bonds, one from OH of Ser^{1068} and another from NH of Gly^{1032}. The lactam NH formed a hydrogen bond with the carbonyl of Gly^{1032}.
2. The planar phenyl ring formed π-π stacking interactions with the phenyl residue of Tyr^{1050} and the lactam ring π-π stacked with Tyr^{1071}.
3. The saturated ring of **106a** was buckled; according to the docking results, C-3 was out of the plane in the same way as the sulfur atom was out of the plane in the crystal structure containing XAV939.[148] Such a conformation probably would fit better into the pocket.

The model showed the π–π stacking interactions between the lactam ring of the inhibitor and phenyl ring of Tyr^{1071}. Interestingly, docking of the same compound with

the structure of the catalytic domain of PARP-1 showed the same possibility of π–π interactions (Figure 49, B).

Dr. Lari Lehtiö (Åbo Akademi and University of Oulu) determined the crystal structure of tankyrase-2 with **106a** soaked in (Figure 50), using the technique described above. The structure confirmed the presence of hydrogen-bond interactions between the lactam moiety of **106a** and Ser^{1068} and Gly^{1032}. These interactions are of great importance for the tankyrase-1/2 inhibition and are characteristic for the known tankyrase-1/2 inhibitor XAV939 **47**.[148] The obtained structure, agreeing with the molecular modelling, corroborated that C-3 of **106a** was out of the plane. Also, the crystal structure showed the π-π stacking interaction between the planar lactam ring of **106a** and the phenyl of Tyr^{1071} as it was seen in the crystal structure of tankyrase-2 with **103b** (see Figure 48). Interestingly, it can be seen that the hydroxy group of Tyr^{1071} is within the interacting distance of the nitrogen of the tetrahydropyridine ring. Thus, it might be possible that an additional hydrogen bond is formed between the compounds **106** and the enzyme, explaining the high potency of the compounds in this series. However, such a hydrogen bond would require this nitrogen to be sp^3 hybridised.

Molecular modelling of other derivatives of **106** with tankyrase-1/2 and PARP-1 was performed in order to provide a possible explanation of such behaviour. The same technique as described above was used to obtain the models. Compound **106c** was docked into the catalytic site of tankyrase-2 (Figure 51). The obtained structure corroborated the results deduced from the crystal structure (see Figure 50) and from the docking of compound **106a** into the nicotinamide-binding site of tankyrase-2 (see Figure 49):

1) Three characteristic hydrogen bonds between the lactam moiety of **106c** and Gly^{1032} and Ser^{1068} were present.
2) π-π Stacking interactions between the phenyl ring and Tyr^{1050} and between the lactam ring and Tyr^{1071} were observed.
3) N-1 and the hydroxy group of Tyr^{1071} were revealed to be within the interaction distance (3.87 Å). However, this interaction, if indeed existed,

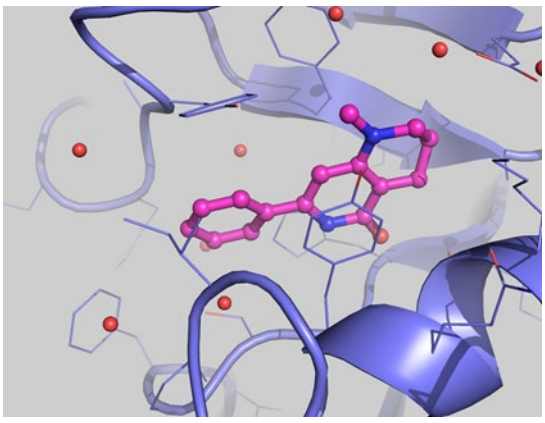

Figure 50. Crystal structure of tankyrase-2 with inhibitor **106a** (Dr. Lari Lehtiö, unpublished results).

would require the nitrogen atom to be sp^3 hybridised.

Moving towards the investigation of the effect of the position of the heterocyclic nitrogen in the ring, further series of 3-aryl-2,6-naphthyridinones **100** and 3-aryl-2,7-naphthyridinones **101** were evaluated (Table 23).

3-Aryl-2,6-naphthyridinones **100** showed similar values at 100 nM, 1.0 μM and 10 μM. The IC_{50} values for these compounds would lay around 1.0 μM (see Table 23). Non-substituted 3-phenyl-2,7-naphthyridin-1-one **101a** and the 4-methoxyphenyl analogue **101c** showed 71% and 78% inhibition at 1.0 μM, respectively. Interestingly, the methyl derivative **101b** had slightly weaker activity, showing 52% inhibition at 1.0 μM. 3-(4-Aminophenyl) derivative **101g**, holding a hydrophilic amino group, appeared to be the weakest inhibitor in this series, with 34% inhibition at 1.0 μM.

Overall, the activity of 3-aryl-2,6-naphthyridinones **100** and 3-aryl-2,7-naphthyridinones **101** appeared to be slightly higher than the activity of their analogues in the series of 7-aryl-1,6-naphthyridinones **99**. However, the amino compound **101g** was an exception, showing 33% inhibition at 1.0 μM, when its 7-aryl-1,6-naphthyridinone analogue **99g** showed 74% inhibition at the same concentration. This is an interesting observation, since it might point to some new interactions between the heterocyclic nitrogen and the enzyme.

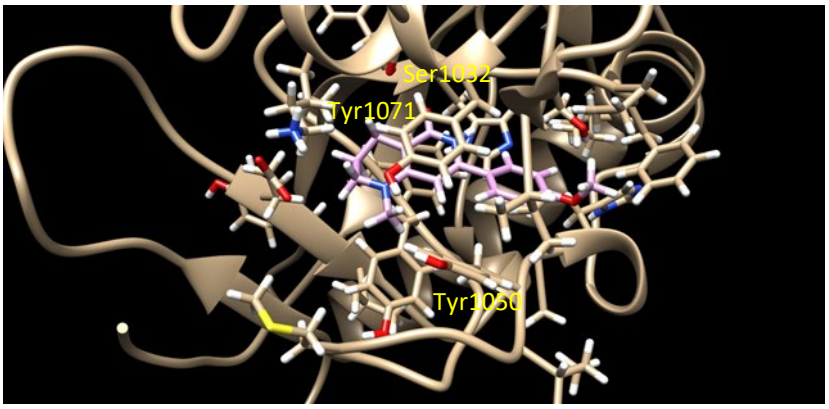

Figure 51. Molecular model of compound **106c** bound to tankyrase-2.

Table 23. Data from the three-point ranging study of 3-aryl-2,6-naphthyridinones **100** and 3-aryl-2,7-naphthyridinones **101** against the catalytic activity of tankyrase-2.*

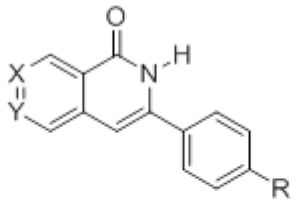

100b: Y = N, R = Me; **100c**: Y = N, R = OMe; **100e**: Y = N, R = Cl;
101a: X = N, R = H; **101b**: X = N, R = Me; **101c**: X = N, R = OMe;
101g: X = N, R = NH_2.

Number of the compound	Concentration of the inhibitor				
	10 nM	**100 nM**	**1.0 μM**	**10 μM**	**100 μM**
	% inhibition				
100b		13 ± 10	51 ± 8	92 ± 4	
100c		9 ± 15	50 ± 13	97 ± 1	
100e		< 0	37 ± 15	84 ± 7	
101a	1 ± 15	18 ± 8	71 ± 8		
101b		1 ± 23	52 ± 20	85 ± 6	
101c	8 ± 38	31 ± 11	78 ± 3		
101g	< 0	14 ± 20	34 ± 15		

*The given values are an average for the triplicates ± calculated SD.

Table 24. Data from the three-point ranging study of 7-(4-methoxyphenyl)-2-methyl-5-oxo-5,6-dihydro-2,6-naphthyridin-2-ium iodide **104c** and 2-methyl-8-oxo-6-phenyl-7,8-dihydro-2,7-naphthyridin-2-ium iodide **105a** against the catalytic activity of tankyrase-2.*

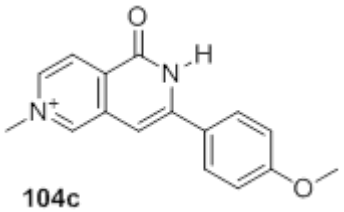

104c

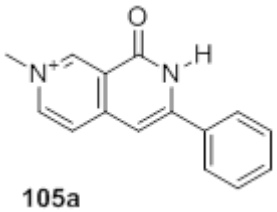

105a

Number of the compound	Concentration of the inhibitor				
	10 nM	**100 nM**	**1 μM**	**10 μM**	**100 μM**
	% of inhibition				
104c		2 ± 7	8 ± 13	< 0	
105a		15 ± 5	14 ± 14	< 0	

*The given values are an average for the triplicates ± calculated SD.

Two examples of 3-aryl-2,6-naphthyridinones **100** and 3-aryl-2,7-naphthyridinones **101** were methylated to give the salts **104c** and **105a**, respectively. These compounds were also evaluated against the catalytic activity of tankyrase-2 (Table 24). However, the results of the three-point ranging study were not truly consistent; no dose response was observed at 100 nM, 1.0 μM and 10 μM, probably because of low inhibition values. Compared to other methylated derivatives **103**, these compounds were also less active. It might be due to their cationic nature, which is not quite suitable for the nook of tankyrase-2, where positively charged Lys^{1121} is present.

3.2.2 Pyridopyrimidinones and tetrahydropyridopyrimidinones.

In order to investigate further the influence of heterocyclic nitrogen atoms on the inhibition of tankyrase-2, the series of pyridopyrimidinones **109-111** and tetrahydropyridopyrimidinones **112** and **113** were introduced into the ranging studies against the catalytic activity of tankyrase-2 (Tables 25-27).

Table 25. Data for the three-point ranging study of pyridopyrimidinones **109-111** against the catalytic activity of tankyrase-2.*

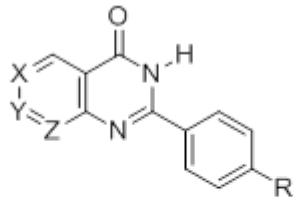

109a: Z = N, R = H; **110a**: Y = N, R = H; **111a**: X = N, R = H;
109b: Z = N, R = Me; **110b**: Y = N, R = Me; **111b**: X = N, R = Me;
109d: Z = N, R = CF_3; **110d**: Y = N, R = CF_3; **111d**: X = N, R = CF_3;
109e: Z = N, R = Cl; **111e**: X = N, R = Cl

Number of the compound	Concentration of the inhibitor				
	10 nM	**100 nM**	**1.0 μM**	**10 μM**	**100 μM**
	% of inhibition				
109a			< 0	< 0	4 ± 16
110a		3 ± 9	20 ± 4	15 ± 9	
111a		47 ± 5	29 ± 6	80 ± 14	
109b			17 ± 35	37 ± 20	71 ± 16
110b			43 ± 19	62 ± 11	86 ± 1
111b		4 ± 17	18 ± 18	93 ± 7	
109d		21 ± 37	20 ± 9	43 ± 9	
110d		3 ± 15	17 ± 14	65 ± 5	
111d		< 0	19 ± 13	57 ± 6	
109e		3 ± 15	3 ± 14	15 ± 3	
111e		9 ± 4	9 ± 6	81 ± 9	

*The given values are an average for the triplicates ± calculated SD.

The variety of pyridopyrimidinones **109-111** was of particular interest, because it would allow monitoring of the effect of the different position of heterocyclic nitrogen on the inhibitory activity of these compounds, as well as the effect of different substituents. 2-Arylpyrido[2,3-*d*]pyrimidin-4-ones **109** turned out to be the least active compounds of all the series (Table 27). For example, 2-phenylpyrido[2,3-*d*]pyrimidin-4-one **109a** was the least potent compound, showing just 4% inhibition at 100 μM. However, this was not true for the trifluoromethyl derivatives **109d**, **110d** and **111d**: all three compounds showed similar inhibitory activities and the compound **109d** showed the best inhibitory value at 100 nM. The methyl-substituted derivatives **109b**, **110b** and **111b** were the best from the series. This is an important proof of the role of small hydrophobic substituent at the position-4 of the phenyl ring for inhibitory activity against tankyrase-2 and it is consistent with previously observed effects[166] (however, in the series of 7-aryl-1,6-naphthyridinones **99**, in contrast, hydrophilic substituents showed better results). Interestingly, no obvious correlations between the activity of compounds **110** and **111** were found, suggesting that both positions of the heterocyclic nitrogen could be tolerated. However, the overall activity of pyridopyrimidinones **109-111** was very weak, compared to the previous series.

The intermediates **112** were investigated in the three-point ranging studies against the catalytic activity of tankyrase-2, mainly to test whether the substituent at position-6 was not favourable for the inhibition of tankyrase-2 (Table 26). The features of the compounds **112** also included a saturated N^6-benzyl-substituted 1,2,3,4-tetrahydropyridine ring with a basic nitrogen. Apart from the effect of the benzyl group and the N^6-substitution, it was possible to assess the effect of the basic nitrogen, which could be protonated at physiological pH, and to confirm the beneficial influence of the partly saturated ring. The activity of the compounds **112** was very weak and no dose response was noted, which usually pointed to the total absence of inhibition. However, this is an important contributor to structure-activity relationship for inhibitors of the tankyrases.

N^6-Unsubstituted tetrahydropyridopyrimidinones **113**, as the formate or hydrochloride salts, were screened against the catalytic activity of tankyrase-2 (Table 27). These structures were of particular interest, as they mimicked closely the structure of the known tankyrase-1/2 inhibitor, XAV939 **47**. The heterocyclic sulfur in XAV939 was replaced by the basic nitrogen atom in order to investigate the influence of the potentially cationic nitrogen atom on the inhibitory activity of the compounds.

Clearly, the replacement of sulfur with nitrogen led to a dramatic decrease of the inhibitory activity. For compounds **113a** and **113h**, no inhibition was observed at 1.0 μM. The nitrogen-containing analogue of XAV939 **47**, **113d**, did not show any dose-response at these concentrations. However, even at 100 nM, it showed only 19% inhibition. These surprising results were of crucial importance for establishing the structure-activity relationship for tankyrase inhibitors.

Table 26. Data from the ranging study of 2-aryl-6-benzyl-5,6,7,8-tetrahydropyrido-pyrimidinones **112** against the catalytic activity of tankyrase-2.*

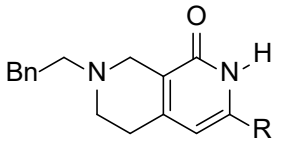

112a: R = Ph; **112b**: R = 4-MePh; **112d**: R = 4-F_3CPh;
112e: R = 4-ClPh; **112f**: R = 4-BrPh; **112h**: R = 4-Py;
112k: R = 4-phenylethynylphenyl.

Number of the compound	Concentration of the inhibitor				
	10 nM	**100 nM**	**1.0 μM**	**10 μM**	**100 μM**
	% of inhibition				
112a		< 0	< 0	< 0	
112b		< 0	< 0	7 ± 18	
112d		< 0	25 ± 35	< 0	
112e		60 ± 7	18 ± 5		
112f		< 0	< 0	< 0	
112h		< 0	< 0	39 ± 9	
112k		29 ± 20	7 ± 8	17 ± 15	

*The given values are an average for the triplicates ± calculated SD.

Interestingly, unlike sulfur, the nitrogen atom was not tolerated at position-6. The NH group, in contrast to sulfide sulfur, is a hydrogen-bond acceptor and donor; the most likely interaction of NH would be with the hydroxy group of Phe[1061]. However, being a secondary amine NH would be protonated at physiological pH, thus losing the ability of accepting hydrogen bonds. Moreover, the positively charged residue of Lys[1121] located in close vicinity to NH (6.02 Å) would not tolerate the positively charged secondary ammonium. This fact was also corroborated by the low efficiency of charged compound **105a** (discussed above). Thus, the charged species in the position-6 were shown to be maleficent for the inhibition of the tankyrases.

Table 27. Data from the three-point study of 2-aryl-5,6,7,8-tetrahydropyridopyrimidin-ones **113** against the catalytic activity of tankyrase-2.*

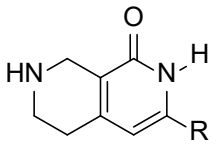

113a: R = Ph; **113b**: R = 4-MePh; **113d**: R = 4-F_3CPh; **113h**: R = 4-Py; **113k**: R = 4-phenylethynylphenyl.
Compounds **113a**-**113h** were used as a formate salts; compound **113k** was used as a hydrochloride salt.

Number of the compound	Concentration of the inhibitor				
	10 nM	100 nM	1.0 μM	10 μM	100 μM
	% of inhibition				
113a		< 0	< 0	11 ± 14	
113b		< 0	33 ± 52	35 ± 42	
113d		19 ± 10	7 ± 11	7 ± 10	
113h		5 ± 10	< 0	< 0	
113j		1 ± 19	28 ± 9	36 ± 7	

*The given values are an average for the triplicates ± calculated SD.

3.2.3 Conclusion.

After the ranging studies of all synthesised target compounds and some intermediates, based on the obtained activity ranges and chemical diversity, it was decided to proceed to fuller biological evaluation for eight compounds: 7-aryl-1-methyl-1,2,3,4-tetrahydro-1,6-naphthyridinones **106a,c-f**; 7-phenyl-1,6-naphthyridinone **99a**; 3-(4-methylphenyl)-2,6-naphthyridinone **100b** and 3-phenyl-2,7-naphthyridinone **101a**. For these compounds, it was planned to determine the IC_{50} values against the catalytic activity of tankyrase-2 and tankyrase-1 and PARP-1 and to evaluate their cytotoxicity against cancer and normal cells.

3.3 Determination of IC_{50} values against tankyrase-2.

In order to determine the IC_{50} values against the catalytic activity of tankyrase-2 for the selected compounds, the same biochemical assay as for the three-point ranging studies was used. However, to obtain the valid IC_{50} curves, not three but six-ten concentration points were employed. The IC_{50} values were calculated using SigmaPlot® 12 software

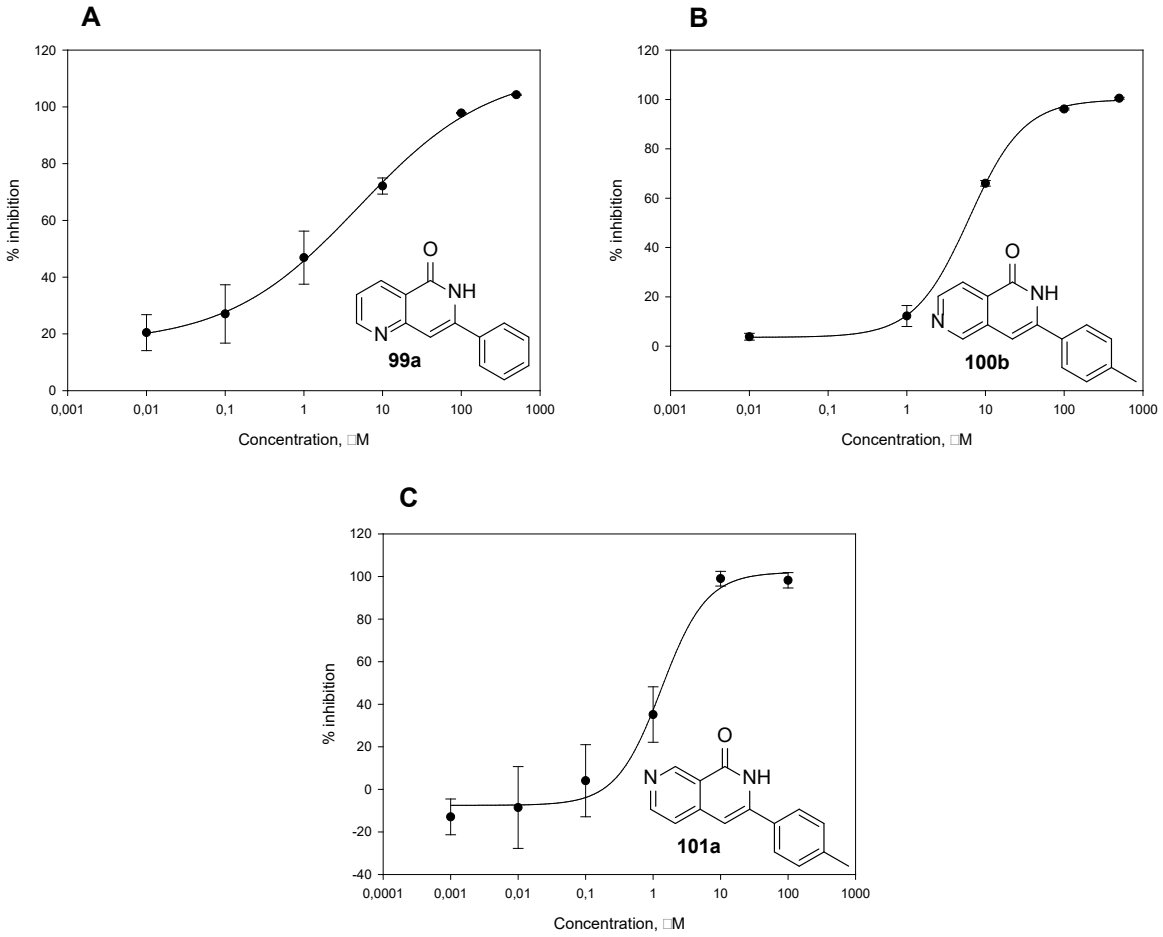

Figure 52. Tankyrase-2 IC_{50} curves obtained for compounds **99a** (**A**), **100b** (**B**) and **101a** (**C**). Error bars indicate ±1SD.

based on the four-parameter logistic sigmoidal curve.

Confirming the data obtained in the ranging studies, the highest IC_{50} values were noted for the compounds **99a**, **100b** and **101a**. All of them inhibited 50% of the enzyme activity in the micromolar range (Figure 52, Table 28).

More encouraging results were obtained for the partly saturated compounds **106** (Figure 53, Table 28). All of them showed nanomolar activity against tankyrase-2, with **106c**

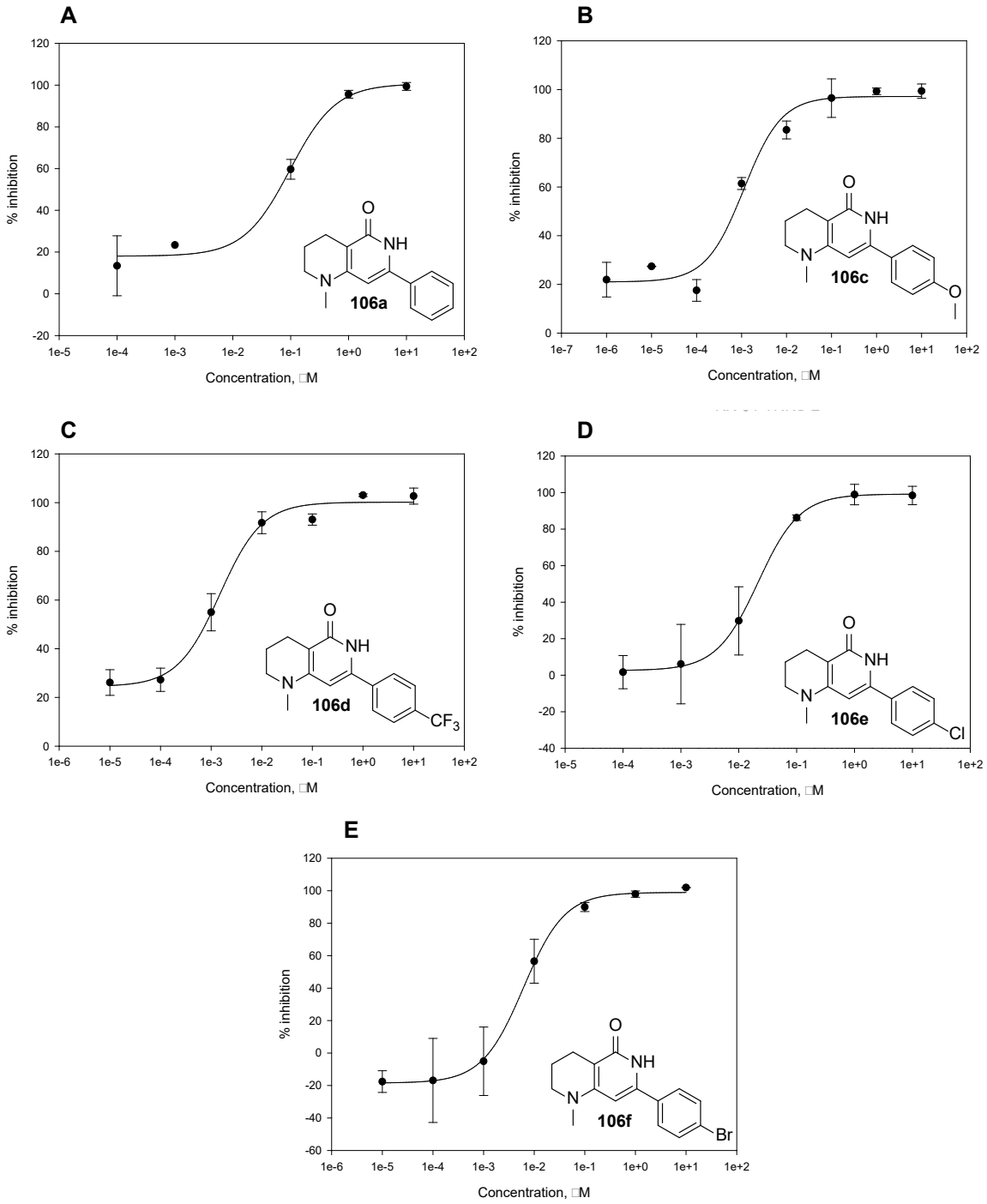

Figure 53. Tankyrase-2 IC_{50} curves obtained for compounds **106**: **106a** (**A**), **106c** (**B**), **106d** (**C**), **106e** (**D**), **106f** (**E**). Error bars indicate ±1SD.

and **106d** being the lead compounds. The methoxy derivative **106c** and the trifluoromethyl analogue **106d** inhibited 50% of the catalytic activity of tankyrase-2 at 1.1 nM and 1.5 nM, respectively, making them more potent than XAV939 **47**. Interestingly, compounds **106c** and **106d**, holding rather different substituents in terms of electronic effects and size, showed similar potent values of the inhibition. At the same time, phenyl compound **106a** and the 4-chlorophenyl derivative **106e** appeared to be slightly less potent. Further investigations are required to establish structure-activity relationship for the inhibitory activity of these molecules.

Table 28. Tankyrase-2 IC_{50} values obtained for compounds **99a, 100b, 101a** (n = 1).

Compound	IC_{50}, μM	$logIC_{50}$ ± SD
99a	5	0.70 ± 0.04
100b	6	0.79 ± 0.39
101a	1	0.12 ± 0.39

Table 29. Tankyrase-2 IC_{50} values obtained for compounds **106** (n = 1).

Compound	IC_{50}, nM	$logIC_{50}$ ± SD
106a	97	-1.01 ± 1.45
106c	1	-2.96 ± 3.39
106d	2	-2.82 ± 3.39
106e	20	-1.67 ± 2.85
106f	6	-2.22 ± 3.15

3.4 Determination of IC_{50} values against tankyrase-1.

In order to evaluate the inhibitory activity of the selected compounds against tankyrase-1, a commercial kit was purchased. A full-length enzyme was used in this assay, in contrast to the tankyrase-2 assay, where a truncated form (catalytic domain and SAM domain) was employed. The assay involved an ELISA colorimetric quantitative detection of ADP-ribosylated immobilised histone proteins with a system of labelled antibodies. Importantly, this assay used the ability of tankyrase-1 (in solution) to poly(ADP-ribosyl)ate other proteins, rather than itself. Firstly, a pre-hydrated histone-coated plate was loaded with the solution of the enzyme, the substrate and the inhibitor solution in the assay buffer to make a total reaction volume 50 μL. The inhibitors were initially dissolved in DMSO to give stock solutions of appropriate concentrations and then diluted with assay buffer to obtain the final concentration of inhibitor with DMSO at 1% (v/v). The plates were incubated at 25 °C for thirty minutes to allow the tankyrase-1-catalysed reaction of poly(ADP-ribosyl)ation of the histones to happen. After washing with PBS-T and PBS, the plate was loaded with mouse anti-poly(ADP)-ribose monoclonal antibody. The plate was incubated for thirty minutes at 25 °C to allow the immunochemical reaction of antigen-antibody to happen; the mouse antibody would bind to the poly(ADP-ribose) units of the poly(ADP-ribosyl)ated histones. After the second washing with PBS-T and PBS, a goat anti-mouse IgG-horseradish peroxidase conjugate was added, with a horseradish peroxidase substrate. This labelled antibody would bind to the mouse antibody and would enable the quantitative determination of poly(ADP-ribosyl)ated histones. After the last washing with PBS-T and PBS, a pre-warmed (30 ºC) TACS-Sapphire™ was loaded into each well in order to generate the colour. After fifteen minutes, the reaction was stopped by addition of aq. hydrochloric acid (0.2 M) and the absorbance at 450 nm was read immediately. The IC_{50} values were calculated using SigmaPlot® 12 software based on the four-parameter logistic sigmoidal curve.

The difference in the concept of the two assays was taken into account. XAV939 **47** was used as a positive control in the two assays and the obtained results proved that this difference was insignificant. For the majority of compounds, the IC_{50} values obtained for tankyrase-1 did not differ much from those obtained for tankyrase-2 (Table 30, Figure 54). However, some notable data were observed. Chloro-substituted 1,2,3,4-tetrahydro-1,6-naphthyridin-5-one **106e** appeared to be 6-fold less active against tankyrase-1 than against tankyrase-2 and bromo analogue **106f** was 69-fold less active

against tankyrase-1. It might be possible that the halogen substituents somehow enhanced the cross-isoform selectivity of the inhibitors. To prove this, it would be necessary to synthesise and evaluate fluorophenyl- and iodophenyl derivatives of 1-methyl-7-aryl-1,2,3,4-tetrahydro-1,6-naphthyridin-5-ones **106**. It was attempted to investigate the reasons for the unusual selectivity of compounds **106e** and **106f** towards tankyrase-1 using molecular modelling (Figures 55 and 56). The models showed:

1. Three characteristic hydrogen bonds between the lactam moiety and Gly^{1032} and Ser^{1068};
2. π-π Stacking interactions between the phenyl ring and Tyr^{1050} and between the lactam ring and Tyr^{1071};
3. N-1 and the hydroxy group of Tyr^{1071} were revealed to be within the interaction distance (3.92 Å for **106e** and 3.59 Å for **106f**), as it was seen in the molecular model of **106c** (see Figure 51). However, this interaction, if indeed existed, would require the nitrogen atom to be sp^3 hybridised.

Table 30. Tankyrase-1 IC_{50} values obtained for **99a, 100b, 101a, 106** (n = 1).

Compound	IC_{50}, nM	$logIC_{50}$ ± SD
99a	10600	1.03 ± 0.84
100b	350	-0.46 ± 0.85
101a	2200	0.34 ± 0.77
106a	189	-0.72 ± 2.89
106c	2	-2.77 ± 2.92
106d	8	-2.12 ± 2.72
106e	134	-0.87 ± 1.44
106f	423	-0.37 ± 0.59

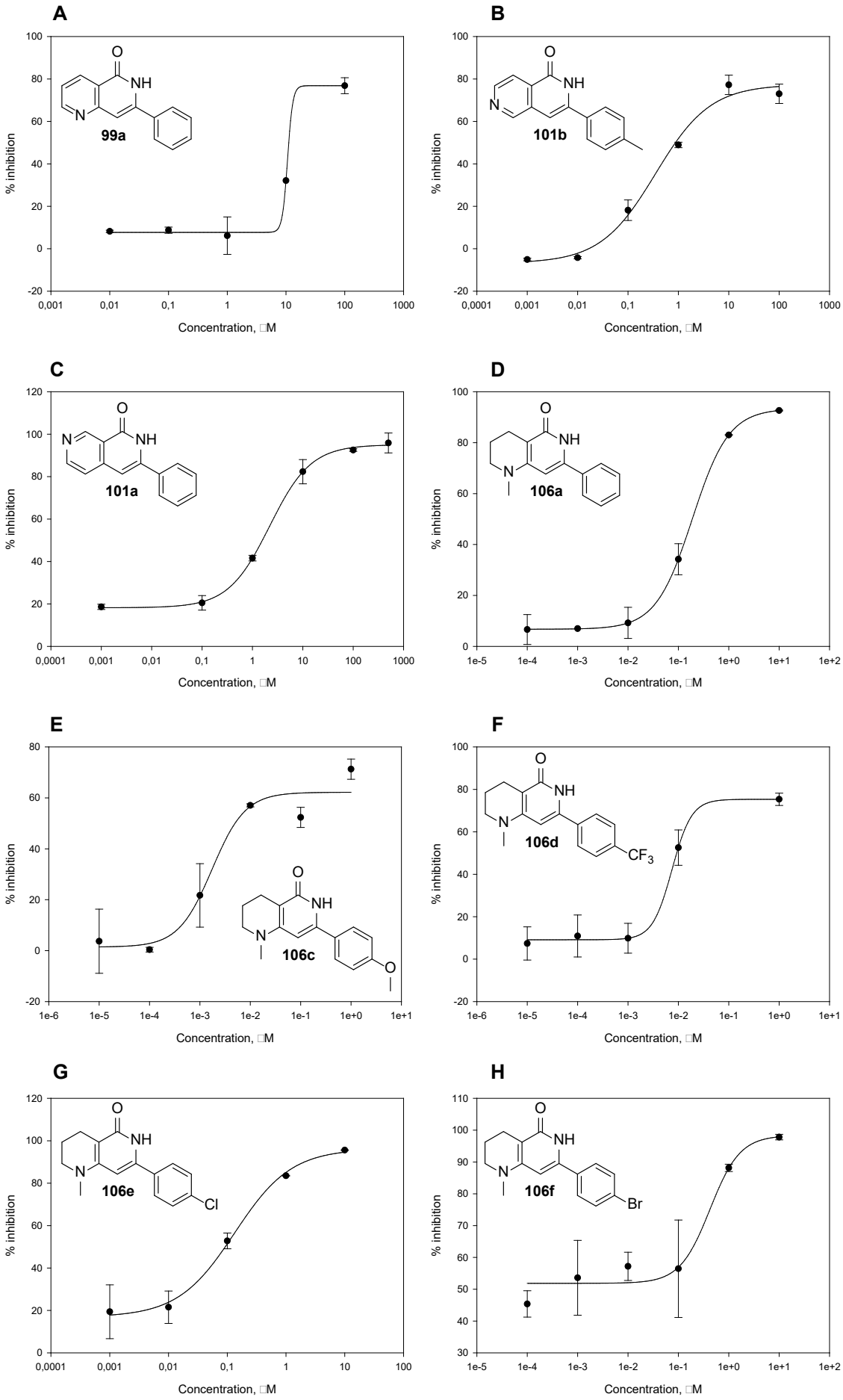

Figure 54. Tankyrase-1 IC_{50} curves obtained for compounds **99a** (**A**), **100b** (**B**), **101a** (**C**), **106a** (**D**), **106c** (**E**), **106d** (**F**), **106e** (**G**), **106f** (**H**). Error bars indicate ±1SD.

However, the performed modelling did not reveal any interactions of the halogen atoms, apart from the neat fitting of them into the hydrophobic nook formed by Phe[1035] and Ile[1075]. Further investigations should be performed in order to explain this interesting finding.

Nevertheless, the slight selectivity towards isoform-2 was expected, as it was described before.[60,166] In the light of this fact, the data obtained for the compound **100b** were rather surprising. It was 4-fold selective towards tankyrase-1, which was not observed before. Despite the moderate potency, this selectivity was unusual and therefore interesting. Molecular modelling of the compound **100b** into the nicotinamide-binding sites of tankyrase-1 and tankyrase-2 showed (Figure 57):

1. Three hydrogen bonds between the lactam moiety and Gly[1032] and Ser[1068];
2. π-π Stacking interactions between the phenyl ring and Tyr[1071] and between the lactam ring and Tyr[1050];
3. The pyridyl nitrogen and Lys[1121] were revealed to be within the interaction distance in the models of both isoforms. However, as it was observed before for compounds **106**, such interaction would require the nitrogen atom to be sp^3 hybridised.

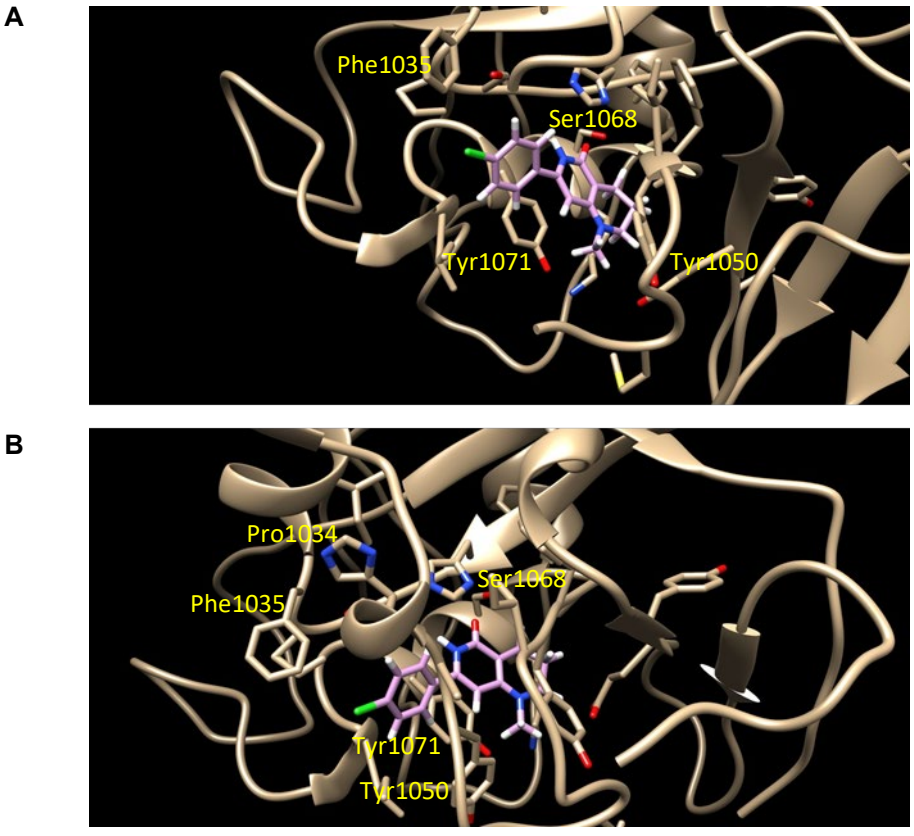

Figure 55. A: Molecular modelling of compound **106e** into the nicotinamide-binding site of tankyrase-1. **B**: Molecular modelling of compound **106e** into the nicotinamide-binding site of tankyrase-2.

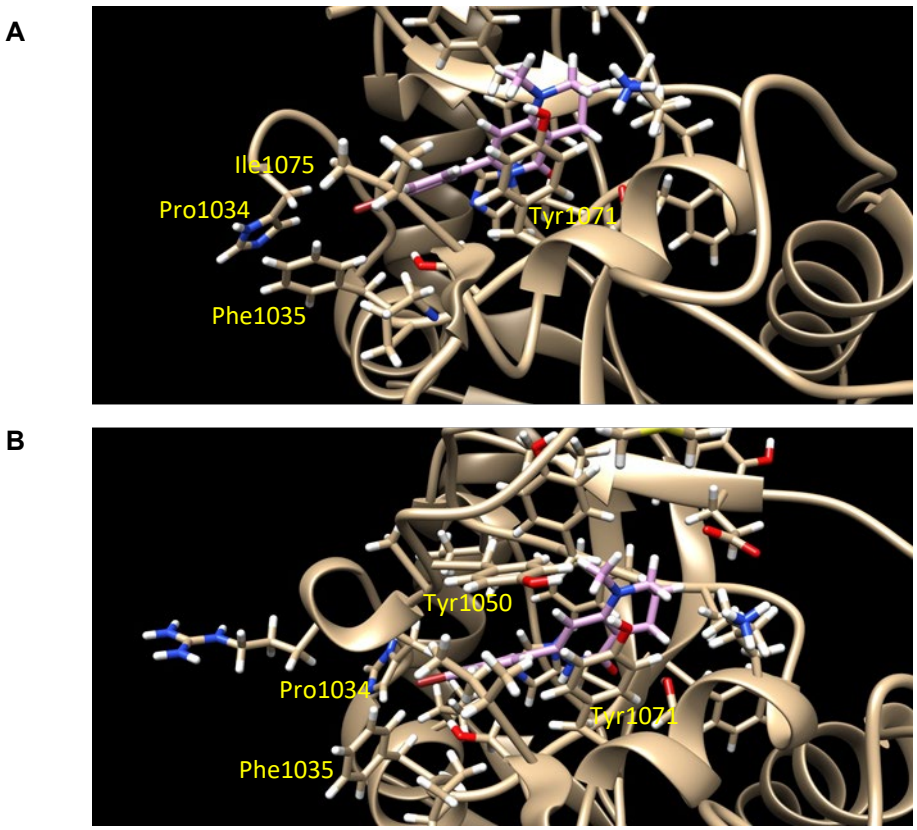

Figure 56. A: Molecular modelling of compound **106f** into the nicotinamide-binding site of tankyrase-1. **B**: Molecular modelling of **106f** into the nicotinamide-binding site of tankyrase-2.

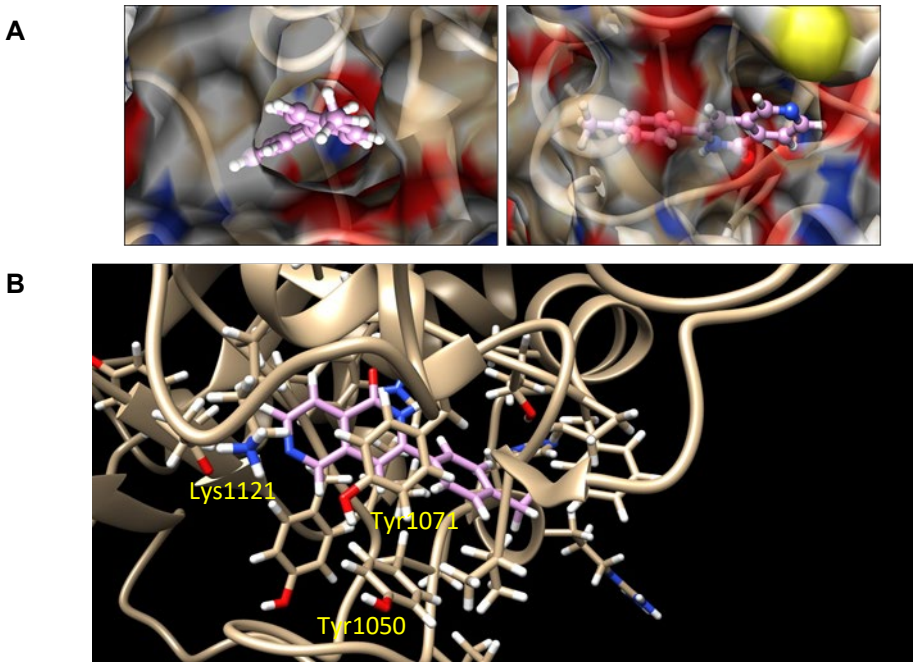

Figure 57. A: Molecular modelling of compound **100b** into the nicotinamide-binding site of tankyrase-1. **B**: Molecular modelling of compound **100b** into the nicotinamide-binding site of tankyrase-2.

As for compounds **106e** and **106f**, no obvious reasons for the cross-isoform selectivity were found after molecular modelling of **100b** (Figure 57). No possible explanation could be observed for such selectivity without further investigation.

3.5 Determination of IC_{50} values against PARP-1.

Aiming to examine further the selectivity of the target compounds towards tankyrase-1/2, counter-screening against PARP-1 was performed. A commercially available assay kit was used for the determination of the IC_{50} values. The assay measured the colorimetric signal, which correlated with the amount of biotinylated poly(ADP-ribose) bound to histone proteins. Therefore, this assay employed the ability of PARP-1 to poly(ADP-ribosyl)ate histones. The pre-hydrated histone-coated full volume 96-well plate was loaded with the solution of the enzyme, the "PARP cocktail" (a substrate) and the inhibitor solution in the assay buffer to make a total reaction volume 50 μL. The inhibitors were initially dissolved in DMSO to give stock solutions of appropriate concentrations and then diluted with assay buffer to obtain the final concentration of DMSO of 1% (v/v). The plate was incubated at 25 °C for one hour. After washing with PBS-T and PBS, a streptavidin / HRP solution was added to all wells and the plate was incubated at 25 °C for one hour. After another washing with PBS-T and PBS the plate was loaded with pre-warmed (30 ºC) TACS-Sapphire™ in order to generate the colour. After fifteen minutes, the reaction was stopped by addition of aq. hydrochloric acid (0.2 M) and the absorbance at 450 nm was read immediately. The IC_{50} values were calculated using SigmaPlot® 12 software basing on the four-parameter logistic sigmoidal curve.

Table 31. PARP-1 IC_{50} values obtained for **100b, 106a,c-f** (n = 1).

Compound	IC_{50}, μM	$logIC_{50}$ ± SD
101b	43	1.63 ± 2.70
106a	1	-0.02 ± 0.66
106c	3	0.53 ± 0.68
106d	5	0.68 ± 0.20
106e	2	0.18 ± 0.53
106f	2	0.31 ± 0.40

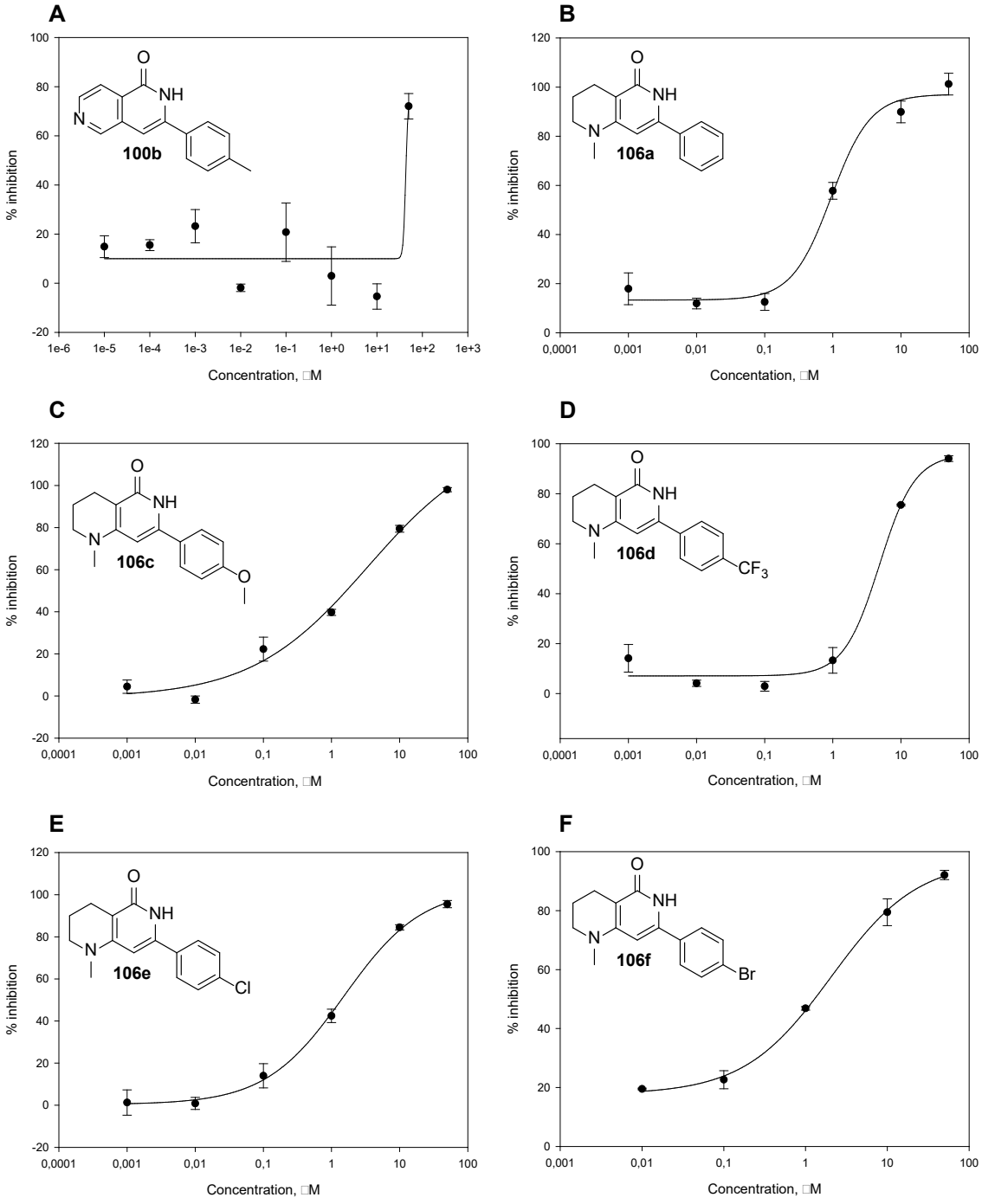

Figure 58. A graphical representation of the inhibition of the catalytic activity of PARP-1 by the compounds **100b** (**A**), **106a** (**B**), **106c** (**C**), **106d** (**D**), **106e** (**E**), **106f** (**F**). Error bars indicate ±1SD.

Only the tankyrase-active compounds were screened for their activity towards PARP-1. Thus the IC_{50} values were calculated for compounds **100b** and **106a,c-f** only (Figure 58, Table 31). All compounds showed good selectivity, inhibiting the catalytic activity of PARP-1 at moderate to high micromolar range only.

3.6 Determination of cytotoxicity.

3.6.1 Cytotoxicity against cancer cells.

In order to determine the cytotoxic effect of the tankyrase-1/2 inhibitors, an MTS anti-proliferative assay with HT29 human Caucasian colon adenocarcinoma cell line was performed. It is a colorimetric assay, which uses the 96-well plate format. The key reagent is MTS (Owen's reagent, a tetrazolium compound [3-(4,5-dimethylthiazol-2-yl)-5-(3-carboxymethoxyphenyl)-2-(4-sulfophenyl)-2*H*-tetrazolium inner salt **268**) and an electron-coupling reagent (phenazine ethosulfate, PES). The general mechanism involves MTS being reduced by NADPH or NADH, catalysed by the cells' mitochondrial electron-transport chain dehydrogenases, into a coloured water-soluble formazan product **269** (Scheme 46).[270] The quantity of the formazan product **269** is correlated to the viability of the cells and can be measured using colorimetry.

Table 32. IC_{50} values for cytotoxicity against HT29 cells, obtained for compounds **99a, 100b, 101a, 106a,c-f** (n = 1).

Compound	IC_{50}, μM	$logIC_{50} \pm SD$
99a	>500	
100b	157	2.19 ± 1.95
101a	>500	
106a	>500	
106c	>200	
106d	>200	
106e	26	1.41 ± 0.68
106f	26	1.42 ± 0.74

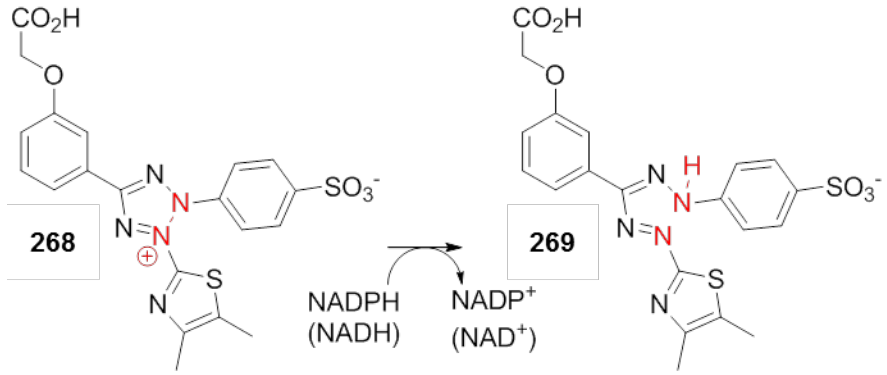

Scheme 46. Conversion of the MTS inner salt **268** into a formazan product **269** performed by NADPH/NADH in living cells.

However, the majority of selected compounds did not show any cytotoxicity against HT29 cells, even at 500 μM (Table 32). The halogen-substituted compounds **106e** and **106f** were cytotoxic against cancer cells (Figure 59). In light of their tankyrase-2 selectivity, this feature is of particular interest for further research.

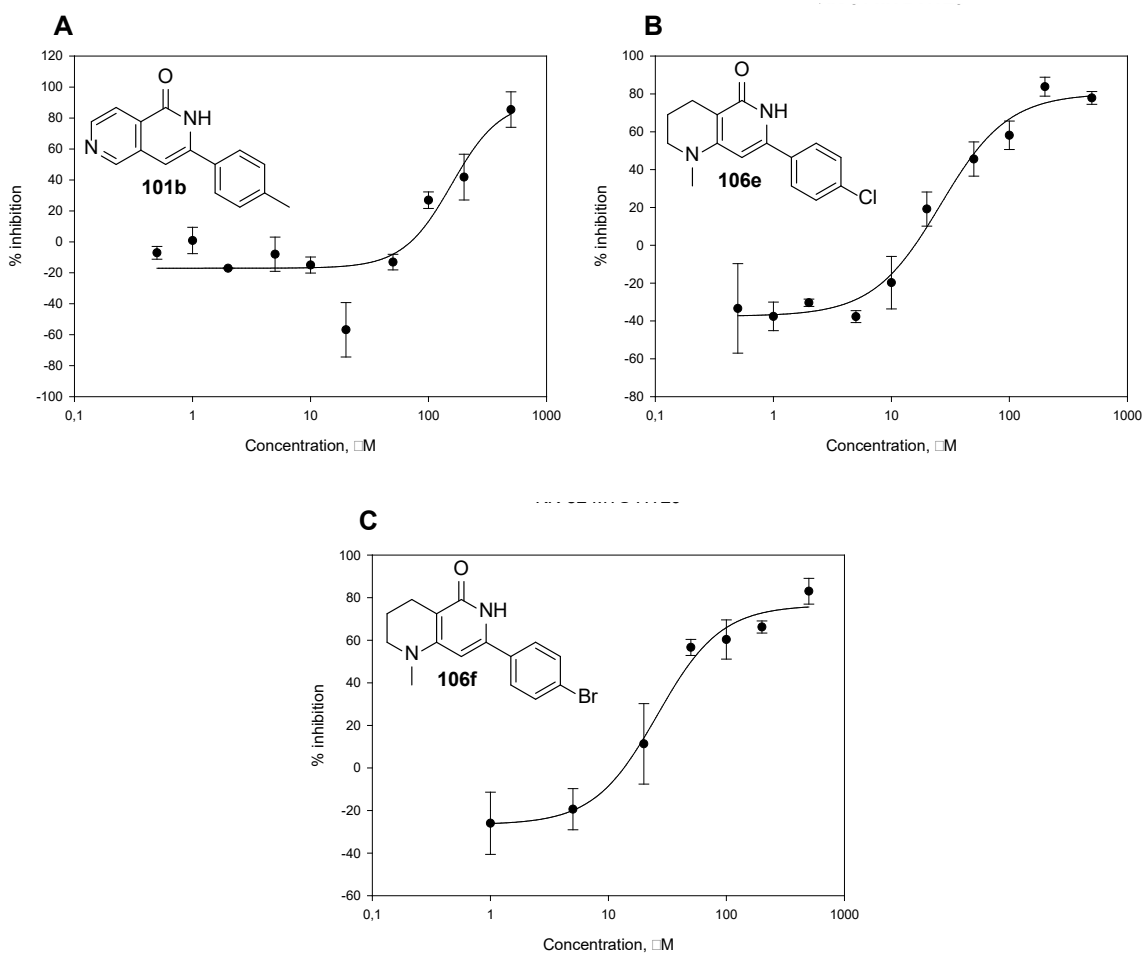

Figure 59. A graphical representation of the viability of HT29 colon cancer cells after treatment with the compounds **100b** (**A**), **106e** (**B**), **106f** (**C**). Error bars indicate ±1SD.

3.6.2 Cytotoxicity against "normal" cells.

To determine the viability of normal cells after the treatment with the selected tankyrase-1/2 inhibitors, the same assay was chosen as for the cancerous HT29 cells. FEK4 human skin fibroblasts were used as a "normal" cell line. These cells were obtained from human newborn foreskin explants in the laboratory of Dr. C. Pourzand.[271,272] During primary derivatisation, the cells were irradiated (35 Gy),[271] which should be kept in mind, since their properties as normal cells might have been altered. Commercially available MTS reagent was used as a colour-producing detector.

Table 33. IC_{50} values for cytotoxicity against FEK4 cells, obtained for compounds **99a, 100b, 101a, 106a,c-f** (n = 1).

Compound	IC_{50}, μM
99a	>500
100b	>500
101a	>500
106a	>500
106c	>200
106d	>200
106e	>500
106f	>500

Since the selected compounds, except three of them, were not cytotoxic against HT29 cells, it was not expected that they would be toxic against normal cells. Indeed, none of them killed the cells, even at 500 μM (Table 33). The main concern was those compounds which showed some cytotoxicity towards cancer cells. However, compounds **100b**, **106e** and **106f** did not show any cytotoxic effect on FEK4 cells, even at 500 μM, which was an encouraging sign of their safety.

3.7 Conclusion.

The biological evaluation of the synthesised target compounds provided interesting data for the structure-activity relationship of the inhibitors of tankyrase-1/2. The three-point screening against tankyrase-2 proved the previously established point that the size of the substituent at position-4 of the phenyl ring was important for inhibition of tankyrases-1/2.[162] The screening against tankyrase-2 also showed that the partly saturated ring was beneficial for the inhibitory activity but that the addition of the nitrogen in the lactam ring dramatically decreased the inhibition. The movement of the nitrogen around the ring and change of electron-density in the molecule of the inhibitor led to slightly increased activity of the compounds. The change of the position of nitrogen also led to unusual cross-isoform selectivity. A change of the hydrophobic sulfur atom in the structure of XAV939 **47** into the basic secondary amine completely abolished the activity of the compound. The halogen atom at the position-4 of the phenyl ring of 1-methyl-7-aryl-1,2,3,4-tetrahydro-1,6-naphthyridinones **106** provided the cross-isoform selectivity towards tankyrase-2 and, at the same time, toxicity against cancer cells. The designed compounds did not affect PARP-1. The cytotoxic effect of the compounds **100b, 106e** and **106f** was therefore not related to the inhibition of other enzymes (although the inhibition of PARP-1 is not, in itself, a cytotoxic event, except in *BRCA*-deficient cells)[97,98] but might be connected to the cross-isoform selectivity. The synthesised compounds were not toxic to the normal human skin fibroblasts, even at high concentrations, providing a good safety profile.

Chapter 4. Conclusions

Soon after its discovery in 1998,[38] the tankyrases have been promising targets for anti-cancer drug design. In this work, a set of diverse azaheterocyclic tankyrase-1/2 inhibitors was synthesised and evaluated biochemically in order to broaden the existing knowledge of the structure-activity relationships. The influence of the heterocyclic nitrogen atom on the potency and selectivity of the tankyrase-1/2 inhibitors was investigated.

Initially, the known structure of PARP inhibitor 5-AIQ **48a** was modified by replacing the basic 5-amino group with heterocyclic nitrogen and adding a 3-(4-substituted)aryl moiety. In order to make these compounds, two synthetic strategies were explored, both based on metallic catalysis. The first approach involved a Sonogashira coupling of 2-bromo-3-cyanopyridine **115** with a variety of arylethynes **145**; the coupled products, 2-arylethynyl-3-cyanopyridines **116**, were introduced into acid-catalysed electrophilic cyclisation, providing a mixture of 6-*endo*-dig products: 7-arylphenylpyrano[4,3-*b*]pyridin-5-ones **117a-e,g-i** and the desired 7-aryl-1,6-naphthyridin-5-ones **99a-e,g-i**. The cyclisation of 2-(pyridylethynyl)-3-cyanopyridine **116h** was investigated. Since this molecule contained two pyridine rings, which were equally electron-deficient, both 5-*exo*-dig and 6-*endo*-dig cyclisation patterns were feasible. However, the cyclisation of **116h** failed after multiple attempts with various electrophiles, giving an unidentifiable mixture of compounds. It was possible that, in the highly acidic conditions of the cyclisation, both heterocyclic nitrogen atoms in the molecule of **116h** were protonated, thus depleting the electron-density of the triple bond and preventing it from participating in the cyclisation. Compounds **117** were converted into the desired naphthyridinones **99** improving a method previously developed in our laboratory:[12] gaseous ammonia was passed through a solution of **117** in 2-methoxyethanol and then heated under pressure. *N*-Alkylation of compounds **99** was investigated. Under neutral conditions, 1-N is more nucleophilic than 6-N and, therefore, is more prone to alkylation. Bearing this in mind, compounds **99** were treated with iodomethane in DMF and the desired products of 1-N methylation were obtained in good yields. N^1-alkylated compounds **103** were reduced to 1-methyl-7-aryl-1,2,3,4-tetrahydro-1,6-naphthyridin-5-ones **106** using borane.pyridine complex. Extending the developed synthetic pathway, 3-aryl-2,6-naphthyridin-1-ones **100** and 3-aryl-2,7-naphthyridin-1-ones **101** were prepared similarly. However, some dissimilarities in the reactivity patterns were

observed, which are due to different distributions of electron-density resulting from the position of the heterocyclic nitrogen. Thus, the scope of synthesis of 3-aryl-2,7-naphthyridin-1-ones **101** was limited to compounds bearing electron-donating substituents at position-4' on the aryl ring. It is probable that the electron-withdrawing substituent on the aryl ring depletes the electron-density of the triple bond, not allowing it to bind a proton and thus arresting electrophilic cyclisation. At the same time, electron-donating substituents of the aryl ring should increase the basicity of the triple bond, favouring the ring closure. Several attempts to cyclise 3-arylethynyl-4-cyanopyridines **120** using previously established conditions (hot aq. sulfuric acid) failed, providing an unidentifiable mixture of compounds. However, the electrophilic cyclisation of **120** with hot polyphosphoric acid gave the desired naphthyridinones **100**. Polyphosphoric acid, being as strong as sulfuric acid, but having less oxidising effect, should have created milder cyclisation conditions, preserving the products from degradation. Two examples of naphthyridinones **100** and **101** were N^1-alkylated; however, the reduction of the alkylated compounds **104c** and **105a** failed, possibly due to different distribution of electron-density in the molecule.

The second approach to make naphthyridinones **99**, **100**, **101** involved Hurtley coupling - intramolecular cyclisation of bromopyridinecarboxylic acids with a variety of symmetrical β-diketones. Copper-free conditions proved to be more efficient than the canonical Hurtley coupling conditions, resulting in a set of pyranopyridinones **117**, **121**, **125**. Compounds **117**, **121**, **125** were converted into the corresponding naphthyridinones **99**, **100**, **101** using the method described previously. Importantly, the bromo-analogue **99f** was obtained by this pathway, providing an opportunity to investigate metal-catalysed couplings on position-4' of the aryl ring. Unfortunately, several attempts to perform Sonogashira coupling of **99f** with phenylethyne failed, most likely due to insolubility of the former, caused by H-bond interactions of the lactam group. A two-step strategy of conversion of the lactam group into an imino ester was proposed; however, the first step of obtaining a halonaphthyridinone failed, providing an unidentifiable mixture of compounds only and forcing abandonment of this route to extended substitution in 4'-aryl region.

To examine the influence of additional nitrogen atoms on the inhibitory activity of the compounds towards the tankyrases, one of the carbons in the lactam ring was replaced with a heterocyclic nitrogen, providing a series of pyridopyrimidinones **109-111**. Compounds **109-111** were synthesised *via* Ullmann-type copper-catalysed coupling of

bromopyridinecarboxylic acids with a variety of benzamidines **241** under basic conditions. The best yields of pyridopyrimidinones **109-111** were obtained when the corresponding benzamidine had an electron-neutral or electron-withdrawing *para*-substituent. Chloro-, bromo- and pyridine-containing benzamidines failed to couple with any of the bromopyridinecarboxylic acids, most likely due to inappropriate ligation or reaction of the nitrogen or halogen atoms, respectively, with the copper catalyst. 2-Aryl-5,6,7,8-tetrahydropyrido[4,3-*d*]pyrimidinones **113** were synthesised to evaluate the effect of polar cationic species on the inhibition of the tankyrases, substituting the non-polar sulfur of XAV939 isosterically with a cationic protonated secondary amine. In order to make compounds **113**, methyl 1-benzyl-4-oxopiperidine-3-carboxylate **262** was condensed with a variety of benzamidines under basic conditions. Notably, 4-halo-substituted benzamidines coupled to compound **262** in these copper-free conditions, consistent with the unfavourable effect of copper on the halogen atoms observed earlier. The resulting N^6-benzylated tetrahydropyridopyrimidinones **112** were introduced into palladium-mediated reductive removal of the benzyl group, resulting in the desired compounds **113**. Interestingly, when ammonium formate was used as a source of hydrogen, it did not lead to the debenzylation; however, when it was substituted by formic acid, the reaction went to completion. This outcome might be due to protonation of the benzylamine facilitating reductive cleavage as the leaving group is improved.

All compounds were fully characterised using ^{1}H NMR, ^{13}C NMR, ^{19}F NMR and ^{15}N NMR (where applicable), 2D NMR, such as COSY, HMBC and HSQC and HRMS. IR spectra were obtained for the selected compounds. Solid compounds were re-crystallised and the melting points were measured. However, the facilities used did not allow performing HPLC and elemental analysis. This should be kept in mind, since no proof of the purity of the compounds can be provided at the moment.

Preliminary biological evaluation against the catalytic activity of tankyrase-2 revealed the outstanding inhibitory activity of 1-methyl-7-aryl-1,2,3,4-tetrahydro-1,6-naphthyridin-5-ones **106**. For example, the 4'-methoxy derivative **106c** and the 4'-trifluoromethyl analogue **106d** inhibited 50% of the catalytic activity of tankyrase-2 at 1.1 nM and 1.5 nM, respectively, making them more potent than XAV939 **47** (TNKS-1 IC_{50} = 0.011 μM; TNKS-2 IC_{50} = 0.004 μM).[60] These compounds showed similar values of inhibition of the catalytic activity of another isoform, tankyrase-1 (2 nM for **106c**; 8 nM for **106d**). Molecular modelling and crystallisation of the compounds with the enzymes showed that they fitted neatly into the nicotinamide-binding site pocket,

forming several important interactions with the amino-acids: the lactam moiety formed three hydrogen bonds with Gly^{1032} and Ser^{1068}; the phenyl ring and the lactam ring formed π-π stacking interactions with Tyr^{1050} and Tyr^{1071}, respectively. Interestingly, the biological evaluation of halo-substituted compounds **106e** and **106f** showed remarkable cross-isoform selectivity: the 4'-chloro analogue **106e** appeared to be 6-fold less active against tankyrase-1 than against tankyrase-2 and the 4'-bromo analogue **106f** was 69-fold less active against tankyrase-1 than against tankyrase-2. The modelling did not reveal any possible interactions of the halogen atoms with the enzyme, apart from the snug fitting of them into the hydrophobic nook formed by Phe^{1035} and Ile^{1075}. Rather unusual cross-isoform selectivity was also observed for the 4'-methyl compound **100b**: it was 4-fold selective towards tankyrase-1. Counter-screening of the target compounds against the catalytic activity of PARP-1 showed good selectivity of the inhibitors towards the tankyrases: the compounds inhibited PARP-1 in the micromolar range only. The viability assay against HT29 colon cancer cells revealed the cytotoxic properties of compounds **106e** and **106f**. Together with their cross-isoform selectivity, this observation was rather intriguing. The viability assay against "normal" FEK-4 fibroblasts showed that none of the compounds were cytotoxic against them, which was a promising sign of their toxicity profile.

Overall, a synthesis of novel naphthyridinones, tetrahydronaphthyridines, pyrido-pyrimidinones and tetrahydropyridopyrimidinones was developed. The completed synthesis, biological evaluation and molecular modelling helped to broaden the understanding of SAR of inhibitors of the tankyrases. Encouraged by the promising results, we now aim to transfer the lead compounds into the next stages of drug development. Further biological evaluation is planned to be performed on the synthesised compounds: a functional assay for *Wnt* signalling activity; counter-screening against the catalytic activity of IMPDH2; cell viability assay on diverse cancerous cell lines. Future work would also involve further synthesis of diverse tetrahydronaphthyridinones *via* our newly established synthetic route and subsequent biological evaluation.

Chapter 5. Experimental

5.1 General procedures.

Melting points were obtained using a Reichert-Jung heated-stage microscope and are uncorrected. NMR spectra were recorded on Varian Mercury VX 400 MHz spectrometer. Me_4Si was used as an internal standard for samples dissolved in $CDCl_3$, $(CD_3)_2SO$ or $(CD_3)_2CO$. Multiplicities are indicated by s (singlet), d (doublet), t (triplet), q (quartet), quin (quintet), m (multiplet) and br (broad). Chemical shifts for deuterated NMR solvents were as follows: ^1H NMR $CDCl_3$ δ 7.26, ^{13}C NMR $CDCl_3$ δ 77.1; ^1H NMR $(CD_3)_2SO$ δ 2.50, ^{13}C NMR $(CD_3)_2SO$ 39.5; ^1H NMR $(CD_3)_2CO$ 2.04, ^{13}C NMR $(CD_3)_2CO$ δ 29.8. Mass spectra were obtained using ESI-TOF at the University of Bath Mass Spectrometry Service. Thin layer chromatography was performed on Merck aluminium-backed TLC plates silica gel 60 F_{254} and viewed using UV light (λ = 254 nm). Column chromatography was carried out on silica gel 60 (35 – 70 micron).

All reagents for chemical synthesis were purchased from Acros Organics, Sigma-Aldrich Chemical Co., Alfa Aesar and Lancaster Chemical Company and were used without further purification. All solvents were of HPLC grade and were used without prior distillation, unless otherwise specified. Experiments were conducted at ambient temperature, unless otherwise stated. Where experiments were repeated, only one description is provided. Organic solvents were evaporated under reduced pressure. Solutions in organic solvents were dried with magnesium sulfate.

2-(4-(Trifluoromethyl)phenyl)-7,8-dihydro-3*H*-thiopyrano[4,3-*d*]pyrimidin-4(5*H*)-one (47).

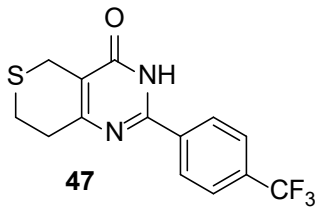

47

A mixture of **131** (205 mg, 1.1 mmol), **241d** (212 mg, 1.1 mmol) and Cs_2CO_3 (844 mg, 2.6 mmol) in MeOH (25 mL) was stirred at reflux overnight. The mixture was cooled and poured into water (20 mL). The mixture was extracted with EtOAc (3 × 30 mL). The precipitate formed in the organic layer was collected by filtration; the organic filtrate was dried and filtered and the solvent was evaporated. The combined solids were recrystallised from $CHCl_3$ to give **47** (191 mg, 61%) as a white powder: R_f 0.40 (petroleum ether / EtOAc 3:1); mp 253-254 ºC; ^1H NMR ($CDCl_3$) δ 2.89 (4 H, m, 7,8-H_4), 3.54 (2H, s, 5-H_2), 7.87 (2H, d, *J* = 8.5

Hz, Ph 2,6-H_2), 8.28 (2H, d, *J* = 8.5 Hz, Ph 3,5-H_2), 12.92 (1H, br s, NH); ^{13}C ($CDCl_3$) (HSQC / HMBC) δ 22.8 (5-C_2), 34.49 (7-C_2), 32.7 (8-C_2), 118.5 (4a-C), 123.0 (q, *J* = 312.5 Hz, CF_3), 125.4 (q, *J* = 3.5 Hz, Ph 2,6-H_2), 128.4 (Ph 3,5-C_2), 132.0 (Ph 1-C), 137.8 (q, *J* = 62.5 Hz, Ph 4-C), 152.5 (8a-C), 159.8 (4-C), 163.0 (2-C); ^{19}F NMR ($CDCl_3$) δ -61.29 (CF_3); MS (ESI) *m/z* 335.0430 $(M + Na)^+$ ($C_{14}H_{11}N_2F_3OSNa$ requires 335.0436).[260]

General procedure for 5,6-dihydro-1,6-naphthyridin-5-ones (99a-e,g).

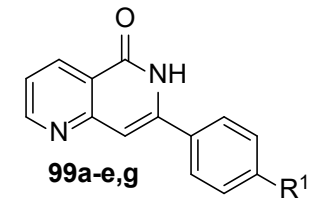

99a-e,g

a: R^1 = H; **b**: R^1 = Me; **c**: R^1 = OMe; **d**: R^1 = CF_3; **e**: R^1 = Cl; **g**: R^1 = NH_2

The 3-cyano-2-(phenylethynyl)pyridine **116a-e,g** (300 mg) was stirred under reflux in aq. H_2SO_4 (9 M, 20 mL) for 1 h. After cooling, aq. NaOH (5 M) was added to pH 9. The mixture was extracted with EtOAc (5 × 25 mL). The combined organic layers were dried and the solvent was evaporated. The residue was transferred into a pressure tube equipped with magnetic stirrer and dissolved in $MeO(CH_2)_2OH$ (10 mL). NH_3 was bubbled through the solution, the vessel was closed and the mixture was heated at 100 °C for 30 min. The reaction mixture was cooled in ice and NH_3 was bubbled again, followed by closure and heating (30 min). The cycle was repeated until the reaction was complete (TLC). Evaporation gave **99a-e,g**, which were recrystallised from $MeO(CH_2)_2OH$.

7-Phenyl-5,6-dihydro-1,6-naphthyridin-5-one (99a): Yield: 75%; white solid, mp 226-230 °C (lit.[273] mp 228-229 °C); R_f = 0.35 (petroleum ether / EtOAc 1:3); ^{1}H NMR ($(CD_3)_2SO$) δ 6.98 (1 H, s, 8-H), 7.54 (1 H, dd, *J* = 8.0, 4.5 Hz, 3-H), 7.57-7.60 (3 H, m, Ph 3,4,5-H_3), 7.89 (2 H, d, *J* = 7.9 Hz, Ph 2,6-H_2), 8.57 (1 H, dd, *J* = 8.0, 1.8 Hz, 4-H), 8.98 (1 H, dd, *J* = 4.5, 1.8 Hz, 2-H), 11.74 (br s, NH); ^{13}C NMR ($(CD_3)_2SO$) (HSQC / HMBC) δ 104.6 (8-C), 120.4 (3-C), 121.6 (4a-C), 127.0 (2C, Ph 3,5-C_2), 128.8 (2C, Ph 2,6-C_2), 129.8 (Ph 4-C), 133.4 (Ph 1-C), 135.0 (4-C), 144.0 (7-C), 154.2 (2-C), 155.0 (8a-C), 162.9 (5-C); ^{15}N NMR ($(CD_3)_2SO$) δ 124.9 (6-N), 278.9 (1-N), MS (ESI) *m/z* 245.0676 $(M + Na)^+$ ($C_{14}H_{10}N_2NaO$ requires 245.0691).

7-(4-Methylphenyl)-5,6-dihydro-1,6-naphthyridin-5-one (99b): Yield: 48%; ivory solid; mp 255-258 °C; R_f = 0.35 (petroleum ether / EtOAc 1:3); ^{1}H NMR ($(CD_3)_2SO$) δ 2.43 (3 H, s, Me), 6.95 (1 H, s, 8-H), 7.38 (2 H, d, *J* = 8.1 Hz, Ph 3,5-H_2), 7.54 (1 H, dd, *J* = 8.0, 4.5 Hz, 3-H), 7.79 (2 H, d, *J* = 8.2 Hz, Ph 2,6-H_2), 8.55 (1 H, dd, *J* = 8.0, 1.7

Hz, 4-H), 8.97 (1 H, dd, *J* = 4.5, 1.8 Hz, 2-H), 11.74 (1 H, br s, NH); ^{13}C NMR ($(CD_3)_2SO$) δ (HSQC / HMBC) 20.8 (Me), 104.0 (8-C), 120.3 (4a-C), 121.4 (3-C), 126.8 (Ph 2,6-C_2), 129.4 (2C, Ph 3,5-C_2), 130.5 (Ph 1-C), 135.0 (4-C), 139.6 (Ph 4-C), 144.0 (7-C), 154.3 (8a-C), 154.9 (2-C), 162.9 (5-C); MS (ESI) *m/z* 259.0826 $(M + Na)^+$ ($C_{15}H_{12}N_2NaO$ requires 259.0847).

7-(4-Methoxyphenyl)-5,6-dihydro-1,6-naphthyridin-5-one (99c): Yield: 70%; ivory solid; mp 276-280 °C; R_f = 0.35 (petroleum ether / EtOAc 1:3); ^{1}H NMR ($(CD_3)_2SO$) δ 3.89 (3 H, s, Me), 6.92 (1 H, s, 8-H), 7.12 (2 H, d, *J* = 9.9 Hz, Ph 3,5-H_2), 7.50 (1 H, dd, *J* = 8.0, 4.6 Hz, 3-H), 7.86 (2 H, d, *J* = 9.9 Hz, Ph 2,6-H_2), 8.54 (1 H, dd, *J* = 8.0, 1.8 Hz, 4-H), 8.95 (1 H, dd, *J* = 4.5, 1.8 Hz, 2-H), 11.65 (1 H, br s, NH); ^{13}C NMR ($(CD_3)_2SO$) (HSQC / HMBC) δ 55.4 (OMe), 114.2 (Ph 3,5-C_2), 120.0 (8-C), 122.4 (4a-C), 123.7 (Ph 1-C), 125.6 (3-C), 128.4 (Ph 2,6-C_2), 134.9 (7-C), 136.9 (4-C), 143.8 (2-C), 154.9 (8a-C), 157.0 (5-C), 158.8 (Ph 4-C); MS (ESI) *m/z* 275.0767 $(M + Na)^+$ ($C_{15}H_{12}N_2NaO_2$ requires 275.0796), 253.0978 $(M + H)^+$ ($C_{15}H_{13}N_2O_2$ requires 253.0977).

7-(4-Trifluoromethylphenyl)-5,6-dihydro-1,6-naphthyridin-5-one (99d): Yield: 55%; white solid; mp >325 °C; R_f = 0.45 (petroleum ether / EtOAc 1:3); ^{1}H NMR ($(CD_3)_2SO$) δ 7.03 (1 H, s, 8-H), 7.53 (1 H, dd, *J* = 8.0, 4.6 Hz, 3-H), 7.92 (2 H, d, *J* = 8.4 Hz, Ph 3,5-H_2), 8.10 (2 H, d, *J* = 8.4 Hz, Ph 2,6-H_2), 8.53 (1 H, dd, *J* = 8.0, 1.7 Hz, 4-H), 9.00 (1 H, dd, *J* = 4.5, 1.8 Hz, 2-H), 11.25 (1 H, br s, NH); ^{13}C NMR ($(CD_3)_2SO$) (HSQC / HMBC) δ 105.9 (8-C), 120.9 (4a-C), 122.1 (3-C), 124.1 (q, *J* = 264 Hz, CF_3), 125.6 (q, *J* = 3.6 Hz, Ph 3,5-C_2), 128.0 (Ph 2,6-C_2), 129.8 (q, *J* = 32 Hz, Ph 4-C), 135.1 (4-C), 137.3 (Ph 1-C), 142.5 (7-C), 153.9 (2-C), 155.1 (8a-C), 162.9 (5-C); ^{15}N NMR ($(CD_3)_2SO$) δ 123.4 (6-N), 279.7 (1-N); ^{19}F NMR ($(CD_3)_2SO$) δ -61.2 (s, CF_3); MS (ESI) *m/z* 291.0727 $(M + H)^+$ ($C_{15}H_{10}F_3N_2O$ requires 291.0745).

7-(4-Chlorophenyl)-1,6-naphthyridin-5-one (99e) Yield: 33%; grey powder; mp 296-298 °C; IR ν_{max} 3163 (NH), 1669 (C=O), 1627 (C=C_{Ar}), 1588, 720 (C-Cl) cm^{-1}; ^{1}H NMR ($(CD_3)_2SO$) δ 6.95 (1 H, s, 8-H), 7.50 (1 H, dd, *J* = 8.0, 4.5 Hz, 3-H), 7.58 (2 H, d, *J* = 9.0 Hz, Ph 3,5-H_2), 7.91 (2 H, d, *J* = 9.0 Hz, Ph 2,6-H_2), 8.51 (1 H, d, *J* = 8.0 Hz, 4-H), 8.98 (1 H, d, *J* = 4.5 Hz, 2-H), 11.74 (1 H, br s, NH); ^{13}C ($(CD_3)_2SO$) (HSQC / HMBC) δ 104.9 (8-C), 120.6 (4a-C), 121.8 (3-C), 128.8 (Ph 3,5-C_2), 128.9 (Ph 2,6-C_2), 134.6 (4-C), 135.0 (Ph 1-C), 155.1 (C=O), 162.9 (8a-C); ^{15}N NMR ($(CD_3)_2SO$)

(HMBC) δ 124.2 (s, 6-N); MS *m/z* 279.0303 $(M + H)^+$ ($C_{14}H_9N_2O^{35}ClNa$ requires 279.0296).

7-(4-Aminophenyl)-5,6-dihydro-1,6-naphthyridin-5-one (99g): Yield: 66%; yellow powder; mp >300 ºC; R_f = 0.2 (petroleum ether / EtOAc 1:3); ^1H NMR ($(CD_3)_2SO$) δ 5.65 (2 H, br s, NH_2), 6.80 (1 H, s, 8-H), 7.43 (1 H, dd, *J* = 8.0, 4.8 Hz, 3-H), 7.60 (2 H, d, *J* = 8.6 Hz, Ph 3,5-H_2), 7.71 (2 H, d, *J* = 8.7 Hz, Ph 2,6-H_2), 8.49 (1 H, dd, *J* = 8.0, 1.8 Hz, 4-H), 8.90 (1 H, dd, *J* = 4.8, 1.8 Hz, 2-H), 11.50 (1 H, br s, NH); ^{13}C NMR ($(CD_3)_2SO$) (HSQC / HMBC) δ 99.1 (8-C), 113.6 (Ph 2,6-C_2), 117.6 (3-C), 122.2 (4a-C), 124.9 (Ph 1-C), 127.8 (4-C), 130.5 (Ph 3,5-C_2), 136.9 (7-C), 150.6 (2-C), 153.6 (Ph 4-C), 156.6 (8a-C), 161.65 (5-C).

7-(4-Bromophenyl)-1,6-naphthyridin-5(6*H*)-one (99f).

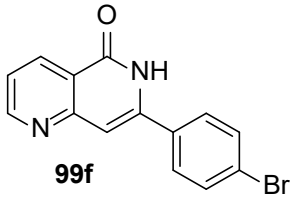

99f

NH_3 was bubbled through a suspension of **117f** (140 mg, 0.47 mmol) in $MeO(CH_2)_2OH$ (10 mL) for 10 min in a pressure vessel. The vessel was closed and the mixture was heated at 120ºC for 30 min. The reaction mixture was cooled in ice and NH_3 was bubbled again, followed by closure and heating (30 min). The cycle was repeated until the reaction was complete (TLC). Evaporation and recrystallisation from EtOH gave **99f** (100 mg, 75%) as a buff powder: R_f 0.25 (petroleum ether / EtOAc 3:1); mp 304-305 ºC; ^1H NMR ($(CD_3)_2SO$) δ 7.05 (1 H, s, 8-H), 7.50 (1 H, dd, *J* = 7.7, 4.8 Hz, 3-H), 7.39 (2 H, d, *J* = 8 Hz, Ph 3,5-H_2), 7.84 (2 H, d, *J* = 8 Hz, Ph 2,6-H_2), 8.30 (1 H, d, *J* = 7.7 Hz, 4-H), 8.69 (1 H, d, *J* = 4.8 Hz, 2-H), 9.15 (1 H, br s, NH); ^{13}C NMR ($(CD_3)_2SO$) (HSQC / HMBC) δ 105.8 (8-C), 122.5 (4a-C), 123.0 (Ph 4-C), 123.6 (3-C), 127.4 (Ph 1-C), 130.2 (Ph 2,6-C_2), 130.8 (Ph 3,5-C_2), 131.9 (7-C), 134.6 (4-C), 156.7 (8a-C), 168.1 (5-C); MS (ESI) *m/z* 324.9771 $(M + Na)^+$ ($C_{14}H_9{}^{81}BrN_2NaO$ requires 324.9774), 322.9790 $(M + Na)^+$ ($C_{14}H_9{}^{79}BrN_2NaO$ requires 322.9805).

7-(4-Hydroxyphenyl)-1,6-naphthyridin-5-one (99i).

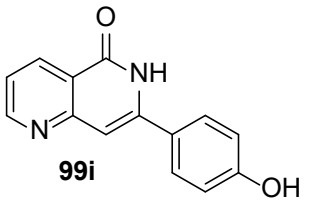

99i

3-Cyano-2-(4-phenylmethoxyphenylethynyl)pyridine **116j** (270 mg, 0.87 mmol) was stirred under reflux in aq. H_2SO_4 (9 M, 20 mL) for 1 h. After cooling, aq. NaOH (5 M) was added to pH 9. The mixture was extracted with EtOAc (3 × 30 mL). The combined organic layers were dried and the

solvent was evaporated. The residue was transferred into a pressure tube equipped with magnetic stirrer and dissolved in $MeO(CH_2)_2OH$ (10 mL). NH_3 was bubbled through the solution, the vessel was closed and the mixture was heated at 100°C for 30 min. The reaction mixture was cooled in ice and NH_3 was bubbled again, followed by closure and heating (30 min). The cycle was repeated until the reaction was complete (TLC). Evaporation and recrystallisation ($MeO(CH_2)_2OH$) gave **99i** (20 mg, 10%): mp 258-260 °C; IR ν_{max} 3423, 1660, 1617, 1589 cm^{-1}; ^1H NMR ($(CD_3)_2SO$) δ 6.87 (1 H, s, 8-H), 6.93 (2H, d, *J* = 8.6 Hz, Ph 2,6-H_2), 7.37 (1 H, d, *J* = 7.4 Hz, 3-H), 7.73 (2 H, d, *J* = 8.6 Hz, Ph 3,5-H_2), 8.52 (1 H, d, *J* = 2.5 Hz, 4-H), 8.94 (1 H, d, *J* = 2.5 Hz, 2-H), 9.99 (1 H, br s, OH), 11.67 (1 H, br s, NH); ^{13}C NMR ($(CD_3)_2SO$) (HSQC / HMBC) δ 115.6 (8-C), 119.0 (3-C), 121.0 (Ph 1-C), 126.0 (4a-C), 128.1 (Ph 2,6-C_2), 128.4 (Ph 3,5-C_2), 135.0 (4-C), 147.0 (2-C), 153.0 (Ph 4-C), 154.9 (8a-C), 163.0 (5-C); MS *m/z* 239.0815 $(M + H)^+$ ($C_{14}H_{11}N_2O_2$ requires 239.0816).

General procedure for 2,6-naphthyridin-1(2*H*)-ones (100a-c,e).

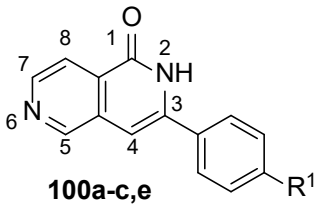

100a-c,e

a: R^1 = H; **b**: R^1 = Me; **c**: R^1 = OMe; **e**: R^1 = Cl

The corresponding 3-(phenylethynyl)isonicotinonitrile **120** (100 mg) was stirred under reflux in PPA (10 mL) for 1 h. After cooling, aq. NaOH (5 M) was added to pH 8. The mixture was extracted with EtOAc (3 × 30 mL). The combined organic layers were dried and the solvent was evaporated. The residue was transferred into a pressure tube equipped with magnetic stirrer and dissolved in $MeO(CH_2)_2OH$ (5 mL). NH_3 was bubbled through the solution, the vessel was closed and the mixture was heated at 130 °C for 30 min. The reaction mixture was cooled in ice and NH_3 was bubbled again, followed by closure and heating (30 min). The cycle was repeated until the reaction was complete (TLC). Evaporation gave **100**, which were recrystallised from EtOH.

An inseparable mixture of 3-phenyl-2,6-naphthyridin-1(2*H*)-one (100a) and 3-phenyl-1*H*-pyrano[4,3-*c*]pyridin-1-one (121a).

100a: Yield: 56%; ^1H NMR ($(CD_3)_2SO$) δ 7.11 (1 H, s, 4-H), 7.39 (1 H, m, Ph 4-H), 7.42 (2 H, m, Ph 3,5-H_2), 7.67 (2 H, d, *J* = 7.0 Hz, Ph 2,6-H_2), 8.64 (1 H, s, 8-H), 8.70 (1 H, s, 7-H), 8.99 (1 H, s, 5-H), 11.68 (1 H, br s, NH); ^{13}C NMR ($(CD_3)_2SO$) (HSQC / HMBC) δ 101.5 (4-C), 121.2 (8-C), 125.5 (m, Ph 3,4,5-C_3), 128.5 (Ph 2,6-C_2), 131.0

(Ph 1-C), 132.9 (8a-C), 146.5 (7-C), 151.5 (5-C); MS (ESI) *m/z* 223.0875 $(M + H)^+$ ($C_{14}H_{11}N_2O$ requires 223.0866).

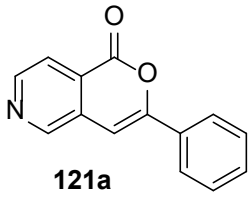

121a

121a: Yield: 22%; ^{1}H NMR ($(CD_3)_2SO$) δ 7.10 (1 H, s, 4-H), 7.86 (2 H, d, *J* = 8.2 Hz, Ph 2,6-H_2), 7.98-8.00 (3 H, m, Ph 3,4,5-H_3), 8.08 (1 H, d, *J* = 5.2 Hz, 8-H), 8.67 (1 H, d, *J* = 5.3 Hz, 7-H), 9.17 (1 H, s, 5-H); ^{13}C NMR ($(CD_3)_2SO$) (HSQC / HMBC) δ 98.5 (4-C), 118.0 (8-C), 125.4 (Ph 2,6-C_2), 127.0 (8^a-C), 129.01 (Ph 3,5-C_2), 130.6 (Ph 4-C), 131.2 (Ph 1-C), 132.0 (3-C), 148.4 (7-C), 149.0 (5-C), 151.0 (1-C); MS (ESI) *m/z* 224.0708 $(M + H)^+$ ($C_{14}H_{10}N_1O_2$ requires 224.0712).

3-(4-Methylphenyl)-2,6-naphthyridin-1(2*H*)-one (100b).

Yield: 6%; ivory-coloured solid; mp 188-189 °C; R_f = 0.25 (petroleum ether / EtOAc 1:3); ^{1}H NMR ($(CD_3)_2SO$) δ 7.07 (1 H, s, 4-H), 7.38 (2 H, d, *J* = 8.1 Hz, Ph 3,5-H_2), 7.76 (2 H, d, *J* = 8.2 Hz, Ph 2,6-H_2), 8.04 (1 H, d, *J* = 5.3 Hz, 8-H), 8.66 (1 H, d, *J* = 5.3 Hz, 7-H), 9.15 (1 H, d, *J* = 0.8 Hz, 5-H), 11.90 (1 H, br s, NH); ^{13}C NMR ($(CD_3)_2SO$) (HSQC / HMBC) δ 20.7 (Me), 100.1 (4-C), 119.8 (8-C), 127.1 (Ph 2,6-C_2), 129.5 (Ph 3,5-C_2), 146.2 (7-C), 148.9 (5-C); MS (ESI) *m/z* 259.0834 ($C_{15}H_{12}N_2NaO$ requires 259.0847), 237.1022 $(M + H)^+$ ($C_{15}H_{13}N_2O$ requires 237.1028).

3-(4-Methoxyphenyl)-2,6-naphthyridin-1(2*H*)-one (100c).

Yield: 37%; ivory-coloured solid; mp 244-245 °C; R_f = 0.15 (petroleum ether / EtOAc 1:3); ^{1}H NMR ($(CD_3)_2SO$) δ 3.90 (3 H, s, Me), 7.11 (1 H, s, 4-H), 7.12 (2 H, d, *J* = 8.9 Hz, Ph 3,5-H_2), 7.63 (2 H, d, *J* = 8.9 Hz, Ph 2,6-H_2), 7.80 (1 H, d, *J* = 5.1 Hz, 8-H), 8.83 (1 H, d, *J* = 5.1 Hz, 7-H), 9.04 (1 H, s, 5-H); ^{13}C NMR ($(CD_3)_2SO$) (HSQC / HMBC) δ 55.5 (Me), 113.8 (Ph 3,5-C_2), 114.7 (4-C), 121.1 (4a-C), 124.9 (8-C), 130.3 (Ph 2,6-C_2), 131.8 (Ph 1-C), 134.2 (8a-C), 135.1 (3-C), 149.0 (7-C), 152.1 (5-C), 160.4 (1-C), 161.00 (Ph 4-C); MS (ESI) *m/z* 275.0772 ($C_{15}H_{12}N_2NaO_2$ requires 275.0796), 253.0960 $(M + H)^+$ ($C_{15}H_{13}N_2O_2$ requires 253.0977).

3-(4-Chlorophenyl)-2,6-naphthyridin-1(2*H*)-one (100e).

Yield: 27%; ivory-coloured solid; mp 257-259 °C; R_f = 0.35 (petroleum ether / EtOAc 1:3); ^{1}H NMR ($(CD_3)_2SO$) δ 7.12 (1 H, s, 4-H), 7.64 (2 H, d, *J* = 8.7 Hz, Ph 3,5-H_2),7.88 (2 H, d, *J* = 8.6 Hz, Ph 2,6-H_2), 8.05 (1 H, d, *J* = 5.3 Hz, 8-H), 8.69 (1 H, d, *J* = 5.3 Hz, 7-H), 9.17 (1 H, s, 5-H), 11.75 (1 H, br s, NH); ^{13}C NMR ($(CD_3)_2SO$) (HSQC / HMBC)

δ 101.9 (4-C), 119.1 (8-C), 128.7 (Ph 2,6-C_2), 128.8 (Ph 3,5-C_2), 130.0 (4a-C), 132.1 (Ph 1-C), 134.1 (Ph 4-C),137.1 (8a-C), 142.0 (3-C), 146.5 (7-C), 150.2 (5-C), 156.3 (1-C); MS (ESI) *m/z* 257.0475 $(M + H)^+$ ($C_{14}H_{10}{}^{35}ClN_2O$ requires 257.0482).

General procedure for 3-aryl-2,7-naphthyridin-1(2*H*)-ones (101a,c).

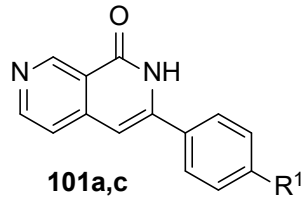

101a,c

a: R^1 = H; **c**: R^1 = OMe

The 4-(arylethynyl)pyridine-3-nitrile **124a,c** (100 mg) were stirred under reflux in aq. H_2SO_4 (9 M, 20 mL) for 1 h. After cooling, aq. NaOH (5 M) was added to pH 9. The mixture was extracted with EtOAc (5 × 25 mL). The combined organic layers were dried and the solvent was evaporated. The residue was transferred into a pressure tube equipped with magnetic stirrer and dissolved in $MeO(CH_2)_2OH$ (10 mL). NH_3 was bubbled through the solution, the vessel was closed and the mixture was heated at 100 °C for 30 min. The reaction mixture was cooled in ice and NH_3 was bubbled again, followed by closure and heating (30 min). The cycle was repeated until the reaction was complete (TLC). Evaporation gave **101a,c,** which were recrystallised from $MeO(CH_2)_2OH$.

3-Phenyl-2,7-naphthyridin-1(2*H*)-one (101a).

Yield: 40%; off-white solid; mp 236-237 °C (lit.[274] 239-239.5 °C); R_f = 0.2 (petroleum ether / EtOAc 1:3); IR ν_{max} 3447 (NH_2), 1669 (C=O), 1631 (C=C_{Ar}), 1595, 1461 (C=N) cm^{-1}; ^1H NMR ($(CD_3)_2SO$) δ 6.97 (1 H, s, 4-H), 7.58 (3 H, m, Ph 3,4,5-H_3), 7.66 (1 H, d, *J* = 5.4 Hz, 5-H), 7.86 (2 H, dd, *J* = 7.6 Hz, Ph 2,6-H_2), 8.76 (1 H, d, *J* = 5.4 Hz, 6-H), 9.38 (1 H, s, 8-H), 11.91 (1 H, br s, NH); ^{13}C NMR ($(CD_3)_2SO$) (HSQC / HMBC) δ 101.4 (4-C), 119.7 (5-C), 127.1 (Ph 2,6-C_2), 128.9 (Ph 3,5-C_2), 130.1 (Ph 4-C), 133.2 (Ph 1-C), 143.1 (4a-C), 145.3 (8a-C), 149.8 (8-C), 151.0 (6-C), 162.4 (1-C); MS *m/z* 223.0866 $(M + H)^+$ ($C_{14}H_{11}N_2O$ requires 223.0935).

3-(4-Methoxyphenyl)-2,7-naphthyridin-1(2*H*)-one (101c).

Yield: 32%; orange solid, mp >300 °C (decomposition) - R_f = 0.15 (petroleum ether / EtOAc 1:3); ^1H NMR ($(CD_3)_2SO$) δ 3.89 (3 H, s, Me), 6.90 (1 H, s, 4-H), 7.13 (2 H, d, *J* = 8.5 Hz, Ph 3,5-H_2), 7.62 (1 H, d, *J* = 8.9 Hz, 5-H), 7.84 (2 H, d, *J* = 8.5 Hz, Ph 2,6-H_2), 8.72 (1 H, d, *J* = 5.4, 1.3 Hz, 6-H), 9.35 (1 H, s, 8-H), 11.82 (1 H, br s, NH); ^{13}C NMR ($(CD_3)_2SO$) (HSQC / HMBC) δ 55.4 (Me), 100.2 (4-C), 114.3 (Ph 3,5-C_2), 119.3 (4a-C), 119.4 (5-C), 125.4 (Ph 1-C), 128.5 (Ph 2,6-C_2), 143.3 (8a-C), 145.0 (3-C), 149.8

(8-C), 150.8 (6-C), 160.8 (Ph 4-C), 162.4 (1-C); MS (ESI) *m/z* 253.0972 $(M + Na)^+$ ($C_{15}H_{13}N_2O_2$ requires 253.0985).

3-(4-Methylphenyl)-2,7-naphthyridin-1(2*H*)-one (101b).

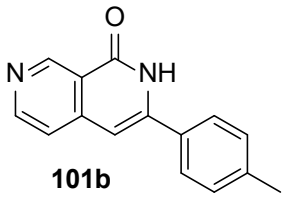

101b

NH_3 was bubbled through a suspension of **125** (35 mg, 0.15 mmol) in $MeO(CH_2)_2OH$ (10 mL) for 10 min in a pressure vessel. The vessel was closed and the mixture was heated at 120ºC for 30 min. The reaction mixture was cooled in ice and NH_3 was bubbled again, followed by closure and heating (30 min). The cycle was repeated until the reaction was complete (TLC). Evaporation and recrystallisation (EtOH) gave **101b** (12 mg, 31%) as an ivory-coloured powder: R_f 0.3 (petroleum ether / EtOAc 3:1); mp > 300 ºC; ^{1}H NMR ($(CD_3)_2SO$) δ 2.43 (3 H, s, Me), 6.94 (1 H, s, 4-H), 7.38 (2 H, d, *J* = 8.1 Hz, Ph 3,5-H_2), 7.63 (1 H, d, *J* = 5.6 Hz, 5-H), 7.77 (2 H, d, *J* = 8.2 Hz, Ph 2,6-H_2), 8.73 (1 H, d, *J* = 5.5 Hz, 6-H), 9.36 (1 H, s, 8-H), 11.70 (1 H, br s, NH); ^{13}C NMR ($(CD_3)_2SO$) (HSQC / HMBC) δ 21.2 (Me), 100.8 (4-C), 119.6 (8a-C), 127.4 (Ph 2,6-C_2,), 128.7 (5-C), 129.4 (Ph 3,5-C_2), 129.4 (Ph 1-C), 144.1 (Ph 4-C), 145.2 (4a-C), 146.0 (3-C), 150.9 (8-C), 153.0 (6-C), 162.4 (1-C); MS (ESI) *m/z* 259.0841 $(M + Na)^+$ ($C_{15}H_{12}N_2NaO$ requires 259.0842).

3-(4-Aminophenyl)-2,7-naphthyridin-1(2*H*)-one (101g).

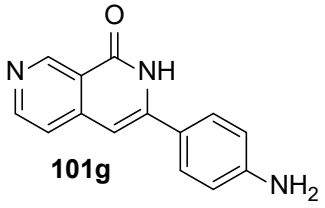

101g

Compound **124g** (40 mg, 0.18 mmol) was stirred under reflux in aq. H_2SO_4 (9 M, 20 mL) for 1 h. After cooling, aq. NaOH (5 M) was added to pH 9. The mixture was extracted with EtOAc (5 × 25 mL). Concentrated HCl was added to the aqueous layer to pH 1. The latter was extracted with EtOAc (3 × 10 mL). The organic layer was discarded. The aqueous layer was basified with aq. NaOH (5M) to pH 9 and extracted with EOAc (5 × 25 mL). Combined organic layers were dried and the solvent was evaporated. The residue was recrystallised from EtOAc to give **101g** (15 mg, 36%) as a white solid: R_f = 0.25 (petroleum ether / EtOAc 1:3); mp 235-236 °C; IR υ_{max} 3172 (NH_2), 1669 (C=O), 1617 (C=C_{Ar}), 1594, cm^{-1}; ^{1}H NMR ($(CD_3)_2SO$) δ 5.71 (2 H, br s, NH_2), 6.69 (2 H, dd, *J* = 8.8 Hz, Ph 3,5-H_2), 6.77 (1 H, s, 4-H), 7.54 (1 H, d, *J* = 5.7 Hz, 5-H), 7.59 (2 H, d, *J* = 8.8 Hz, Ph 2,6-H_2), 8.65 (1 H, d, *J* = 5.7 Hz, 6-H), 9.28 (1 H, s, 8-H), 11.74 (1 H, br s, NH); ^{13}C NMR (HSQC / HMBC) 98.0 (4-C), 112.4 (Ph 1-C), 113.5 (3,5-C_2), 199.1 (5-C), 128.0 (2,6-C_2), 130.4

(3-C), 143.6 (4a-C), 146.0 (8a-C), 150.6 (8-C), 150.9 (6-C), 152.0 (Ph 4-C), 162.5 (1-C); MS (ESI) *m/z* 238.0975 $(M + H)^+$ ($C_{14}H_{12}N_3O$ requires 238.0950).

7-Phenyl-5,6-dihydro-1,6-naphthyridin-5-one 1-oxide (102a).

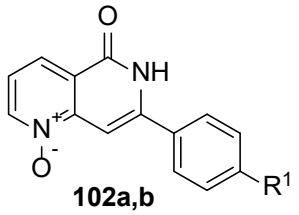

102a,b

a: R^1 = H; **b**: R^1 = Me

Urea.H_2O_2 complex (78 mg, 0.80 mmol) was added to **99a** (100 mg, 0.45 mmol) in DMF (15 mL). The mixture was cooled to 0 °C. $(F_3CCO)_2O$ (189 mg, 0.90 mmol) was added dropwise. The mixture was stirred at 0 °C for 12 h. The precipitate was collected and washed with water and $CHCl_3$. The solvent was evaporated from the filtrate. The solid fractions were combined and purified by flash chromatography (petroleum ether / EtOAc 1:7 → AcOH / petroleum ether / EtOAc 1:3:21) to give **102a** (51 mg, 50%) as a white solid; mp 293-295 °C; R_f = 0.2 (petroleum ether / EtOAc 1:3); ^{1}H NMR ($(CD_3)_2SO$) δ 7.31 (s, 8-H), 7.41 (1 H, dd, *J* = 8.0, 3-H), 7.53 (2 H, d, *J* = 6.0, Ph 3,5-H_2), 7.83 (2 H, d, *J* = 6.0 Hz, Ph 2,6-H_2), 7.99 (1 H, dd, *J* = 8.0 Hz, 4-H), 8.62 (1 H, dd, *J* = 6.5, 1.0 Hz, 2-H); ^{13}C NMR ($(CD_3)_2SO$) (HSQC / HMBC) δ 93.8 (8-C), 121.9 (4a-C), 123.2 (3-C), 123.3 (Ph 4-C), 127.2 (Ph 2,6-C_2), 128.9 (Ph 3,5-C_2), 130.3 (4-C), 137.3 (Ph 1-C), 140.8 (7-C), signals for 2-C and 5-C were not observed, 162.11 (8a-C); ^{15}N NMR ($(CD_3)_2SO$) δ 252.8 (s, 1-N), 129.6 (s, 6-N); IR ν_{max} 3434 (N-H), 3105 (C_{Ar}-H), 1678 (C=O), 1620, 1585, 1505 (C=C_{Ar}), 1244 (N^+-O^-) cm^{-1}.

7-(4-Methylphenyl)-5,6-dihydro-1,6-naphthyridin-5-one 1-oxide (102b).

Urea.H_2O_2 complex (60 mg, 0.60 mmol) was added to **99b** (75 mg, 0.30 mmol) in DMF (10 mL). The mixture was cooled to 0 °C. $(F_3CCO)_2O$ (123 mg, 0.60 mmol) was added dropwise. The mixture was stirred at 0 °C for 12 h. The precipitate was collected and washed with water and Me_2CO. The solvent was evaporated from the filtrate. Combined solids were recrystallised from petroleum ether / EtOAc to give **102b** (20 mg, 29%) as a white solid; mp 258-260 °C, R_f = 0.2 (petroleum ether / EtOAc 1:3); ^{1}H NMR ($(CD_3)_2SO$) δ 2.38 (3 H, s, Me), 6.90 (1 H, s, 8-H), 7.32 (2 H, d, *J* = 8.5 Hz, Ph 3,5-H_2), 7.47 (1 H, dd, *J* = 8.0, 4.5, 3-H), 7.73 (2 H, d, *J* = 8.5 Hz, Ph 2,6-H_2), 8.50 (1 H, dd, *J* = 8.0, 1.0 Hz, 4-H), 8.62 (1 H, dd, *J* = 4.5, 1.5 Hz, 2-H), 11.78 (1 H, s, 6-H); ^{13}C NMR ($(CD_3)_2SO$) (HSQC / HMBC) δ 20.8 (Me), 104.0 (8-C), 121.5 (3-C), 126.9 (Ph 2,6-C_2), 129.4 (Ph 3,5-C_2), 135.0 (4-C), 155.0 (2-C), signals for quaternary carbons were not observed; MS (ESI) *m/z* 253.0996 $(M + H)^+$ ($C_{15}H_{13}N_2O_2$ requires 253.0972); IR ν_{max}

3450 (N-H), 3169 (C_{Ar}-H), 3037 (C_{Me}-H), 1654 (C=O), 1581 (C=C_{Ar}), 1284 (N^+-O^-) cm^{-1}.

1-Methyl-5-oxo-7-phenyl-5,6-dihydro-1,6-naphthyridinium iodide (103a).

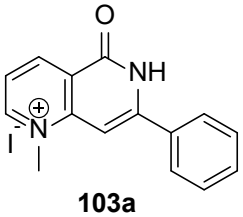

103a

MeI (410 mg, 2.90 mmol) was stirred with **99a** (120 mg, 0.54 mmol) in dry DMF (5 mL) for 36 h. The mixture was poured into Me_2CO (3 mL). The solid was collected, washed with Me_2CO and dried to give **103a** (142 mg, 72%) as a yellow solid. mp 280-284 °C, R_f = 0.2 (petroleum ether / EtOAc 1:3); ^{1}H NMR ($(CD_3)_2SO$) δ 4.40 (3 H, s, Me), 7.18 (1 H, s, 8-H), 7.63 (3 H, m, Ph 3,4,5-H_3), 7.88 (1 H, dd, *J* = 8.0, 6.0 Hz, 3-H), 7.98 (2 H, d, *J* = 7.5 Hz, Ph 2,6-H_2), 9.09 (1 H, dd, *J* = 8.0 Hz, 4-H), 9.20 (1 H, dd, *J* = 6.0 Hz, 2-H), 12.87 (1 H, s, 6-H); ^{13}C NMR ($(CD_3)_2SO$) (HSQC / HMBC) δ 45.0 (Me), 93.61 (8-C), 121.2 (3-C), 123.0 (4a-C), 128.0 (Ph 2,6-C_2), 129.0 (Ph 3,5-C_2), 131.6 (Ph 4-C), 132.0 (Ph 1-C), 144.1 (4-C), 148.0 (8a-C), 150.9 (2-C), 153.0 (7-C), 161.0 (5-C); MS (ESI) *m/z* 237.1012 (M^+) ($C_{15}H_{13}N_2O$ requires 237.1022).

1-Methyl-7-(4-methylphenyl)-5-oxo-5,6-dihydro-1,6-naphthyridin-1-ium iodide (103b).

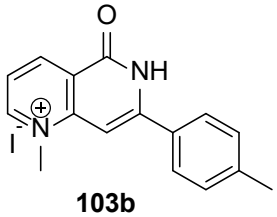

103b

MeI (228 mg, 1.60 mmol) was stirred with **99b** (75 mg, 0.32 mmol) in dry DMF (5 mL) for 36 h. The mixture was poured into Me_2CO (3.0 mL). The solid was collected, washed with Me_2CO and dried to give **103b** (77 mg, 64%) as a yellow solid: mp 273-276 °C, R_f = 0.2 (petroleum ether / EtOAc 1:3); IR ν_{max} 3431 (N-H), 3250 (C_{Ar}-H), 3050 (C_{Me}-H), 1665 (C=O), 1606, 1507 (C=C_{Ar}) cm^{-1}; ^{1}H NMR ($(CD_3)_2SO$) δ 2.41 (3 H, s, PhMe), 4.38 (3 H, s, NMe), 7.13 (1 H, s, 8-H), 7.40 (2 H, d, *J* = 8.0 Hz, Ph 3,5-H_2), 7.82 (1 H, m, 3-H), 7.92 (2 H, d, *J* = 8.0 Hz, Ph 2,6-H_2), 9.04 (1 H, d, *J* = 8.0 Hz, 4-H), 9.16 (1 H, br d, 2-H); ^{13}C NMR ($(CD_3)_2SO$) (HSQC / HMBC) δ 21.0 (PhMe), 44.8 (NMe), 92.6 (8-C), 120.6 (3-C), 122.8 (4a-C), 127.9 (Ph 2,6-C_2), 129.4 (Ph 1-C), 129.5 (Ph 3,5-C_2), 141.7 (Ph 4-C), 144.0 (4-C), 148.0 (8a-C), 150.6 (2-C), 153.5 (br s, 7-C); ^{15}N NMR ($(CD_3)_2SO$) (HMBC) δ 155.0 (1-N); MS (ESI) *m/z* 251.1170 (M^+) ($C_{16}H_{15}N_2O$ requires 251.1179).

7-(4-Methoxyphenyl)-1-methyl-5-oxo-1,6-naphthyridin-1-ium iodide (103c).

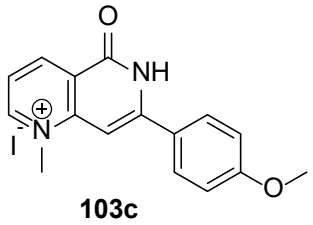

103c

MeI (144 mg, 1.02 mmol) was stirred with **99c** (76 mg, 0.3 mmol) in dry DMF (5 mL) for 72 h. The mixture was poured into the mixture of EtOAc and petroleum ether (1:1). The solid was collected, washed with petroleum ether and dried to give **103c** (5 mg, 4%) as a yellow solid: mp >300°C (extensive decomposition); ^{1}H NMR ($(CD_3)_2SO$) δ 3.94 (3 H, s, OMe), 4.46 (3 H, s, NMe), 7.19 (1 H, s, 8-H), 7.22 (2 H, d, *J* = 8.9 Hz, Ph 3,5-H_2), 7.93 (1 H, dd, *J* = 8.0, 1.8 Hz, 3-H), 8.04 (2 H, d, *J* = 8.9 Hz, Ph 2,6-H_2), 9.13 (1 H, d, *J* = 7.5 Hz, 4-H), 9.25 (1 H, d, *J* = 6.3 Hz, 2-H), 12.77 (1 H, br s, NH); ^{13}C NMR ($(CD_3)_2SO$) (HSQC / HMBC) δ 44.0 (NMe), 57.0 (OMe), 127.0 (Ph 2,6-C_2), 132.0 (Ph 3,5-C_2), 148.0 (4-C); MS (ESI) *m/z* 267.1128 (M^+) ($C_{16}H_{15}N_2O_2$ requires 267.1128).

1-Methyl-5-oxo-7-(4-trifluoromethylphenyl)-5,6-dihydro-1,6-naphthyridin-1-ium iodide (103d).

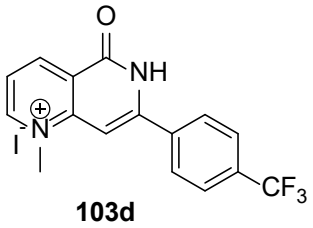

103d

MeI (90 mg, 0.63 mmol) was stirred with **99d** (30 mg, 0.10 mmol) in dry DMF (5.0 mL) for 72 h. The mixture was poured into EtOAc (3.0 mL). The solid was collected, washed with EtOAc and dried to give **103d** (40 mg, 93%) as a yellow solid. mp 298-299°C, R_f = 0.1 (petroleum ether / EtOAc 1:3); ^{1}H NMR ($(CD_3)_2SO$) δ 4.45 (3 H, s, NMe), 7.31 (1 H, s, 8-H), 7.59 (1 H, m, 3-H), 7.99 (2 H, d, *J* = 8.8 Hz, Ph 2,6-H_2), 8.17 (2 H, d, *J* = 6.4 Hz, Ph 3,5-H_2), 9.15 (1 H, d, *J* = 6.4 Hz, 4-H), 9.30 (1 H, d, *J* = 4.4 Hz, 2-H), 13.00 (1 H, br s, NH); ^{13}C NMR ($(CD_3)_2SO$) (HSQC / HMBC) δ 45.34 (N-Me), 95.52 (8-C), 122.44 (3-C), 123.64 (4a-C), 124.94 (q, *J* = 271.0 Hz, CF_3), 125.81 (q, *J* = 3.6 Hz, Ph 3,5-C_2), 129.21 (Ph 2,6-C_2), 131.16 (q, *J* = 34.0 Hz, Ph 4-C), 136.15 (7-C), 144.30 (3-C), 147.81 (8a-C), 149.89 (Ph 1-C), 151.41 (2-C), 160.46 (1-C); ^{19}F NMR ($(CD_3)_2SO$) δ -61.35 (CF_3); MS (ESI) *m/z* 305.0895 (M^+) ($C_{16}H_{12}N_2OF_3$ requires 305.0896).

7-(4-Chlorophenyl)-1-methyl-5-oxo-1,6-naphthyridin-1-ium iodide (103e).

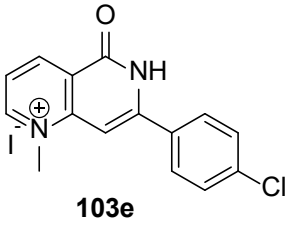

103e

MeI (226 mg, 1.6 mmol) was stirred with **99e** (78 mg, 0.30 mmol) in dry DMF (5.0 mL) for 96 h. The solvent was evaporated. The residue was washed with EtOAc and

petroleum ether and dried to give **103e** (20 mg, 16%) as a yellow solid: mp > 300 °C (extensive decomposition); ^{1}H NMR ((CD$_3$)$_2$SO) δ 4.42 (3 H, s, Me), 7.26 (1 H, s, 8-H), 7.84 (1 H, dd, *J* = 6.5, 5.8 Hz, 3-H); 7.99 (2 H, d, *J* = 8.3 Hz, Ph 2,6-H$_2$), 8.31 (2 H, d, *J* = 8.2 Hz, Ph 3,5-H$_2$), 9.07 (1 H, d, *J* = 6.5 Hz, 4-H), 9.18 (1 H, d, *J* = 5.8 Hz, 2-H), 12.53 (1 H, br s, NH); ^{13}C NMR ((CD$_3$)$_2$SO) (HSQC / HMBC) δ 48.56 (Me), 90.0 (8-C), 118.0 (3-C), 127.0 (Ph 2,6-C$_2$), 130.0 (Ph 3,5-C$_2$), 151.0 (2-C); MS *m/z* 273.0626 (M + H)$^+$ (C$_{15}$H$_{12}$^{37}ClN$_2$O requires 273.0608); 271.0634 (M + H)$^+$ (C$_{15}$H$_{12}$^{35}ClN$_2$O requires 271.0638); MS (ESI) *m/z* 271.0634 (M) (C$_{15}$H$_{12}$N$_2$O^{35}Cl requires 271.0633), 273.0626 (M$^+$) (C$_{15}$H$_{12}$N$_2$O^{37}Cl requires 273.0608).

7-(4-Bromophenyl)-1-methyl-5-oxo-5,6-dihydro-1,6-naphthyridin-1-ium iodide (103f).

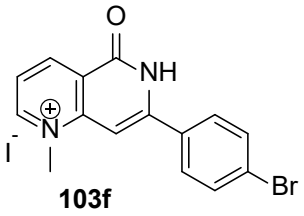

103f

MeI (179 mg, 1.26 mmol) was stirred with **99f** (64 mg, 0.21 mmol) in dry DMF (5 mL) for 72 h. The mixture was poured into EtOAc (3 mL). The solid was collected, washed with Me$_2$CO and dried to give **103f** (50 mg, 52%) as a yellow solid: R$_f$ = 0.1 (petroleum ether / EtOAc 1:3); mp 292-294 °C, ^{1}H NMR ((CD$_3$)$_2$SO) δ 4.48 (3 H, s, Me), 7.29 (1 H, s, 8-H), 7.89 (2 H, d, *J* = 8.7 Hz, Ph 2,6-H$_2$), 7.97 (1 H, m, 3-H), 7.98 (2 H, d, *J* = 8.7 Hz, Ph 3,5-H$_2$), 9.18 (1 H, d, *J* = 7.9 Hz, 4-H), 9.30 (1 H, d, *J* = 5.8 Hz, 2-H), 12.94 (1 H, s, NH); ^{13}C NMR ((CD$_3$)$_2$SO) (HSQC / HMBC) δ 45.98 (Me), 95.00 (8-C), 122.40 (3-C), 123.00 (4a-C), 126.00 (Ph 4-C), 130.12 (Ph 2,6-C$_2$), 130.50 (Ph 1-C), 131.98 (Ph 3,5-C$_2$), 132.55 (3-C), 144.50 (4-C), 148.50 (8a-C), 152.50 (2-C), 155.5 (1-C); MS (ESI) *m/z* 317.0108 (M + Na)$^+$ (C$_{15}$H$_{12}$^{81}BrN$_2$NaO requires 317.0221), 315.0128 (M + Na)$^+$ (C$_{15}$H$_{12}$^{79}BrN$_2$NaO requires 315.0110).

7-(4-Aminophenyl)-1-methyl-5-oxo-1,6-naphthyridin-1-ium iodide (103g).

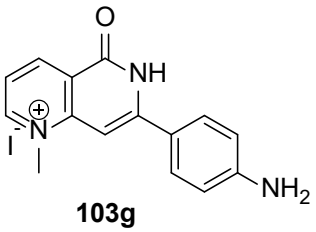

103g

MeI (144 mg, 1.02 mmol) was stirred with **99g** (42 mg, 0.19 mmol) in dry DMF (5.0 mL) for 96 h at room temperature, then at 80°C for 2 h. The mixture was poured into the mixture of EtOAc and petroleum ether (1:1). The solid was collected, washed with petroleum ether and dried to give **103g** (28 mg, 41%) as a yellow solid: mp > 300 °C (decomposition); ^{1}H NMR ((CD$_3$)$_2$SO) δ 4.40 (3 H, s, NMe), 6.89 (2 H, d, *J* = 9.0 Hz,

Ph 3,5-H_2), 7.08 (1 H, s, 8-H), 7.78 (1 H, dd, *J* = 7.8, 5.2 Hz, 3-H), 7.98 (2 H, d, *J* = 9.1 Hz, Ph 2,6-H_2), 9.03 (1 H, d, *J* = 7.8 Hz, 4-H), 9.14 (1 H, d, *J* = 5.2 Hz, 2-H), 12.53 (1H, br s, NH); ^{13}C NMR ($(CD_3)_2SO$) (HSQC / HMBC) δ 44.7 (Me), 90.5 (8-C), 111.6 (Ph 3,5-C_2), 117.3 (Ph 1-C), 119.3 (3-C), 122.2 (4a-C), 129.3 (Ph 2,6-C_2), 143.6 (7-C), 148.2 (2-C), 150.7 (Ph 4-C), 151.7 (4-C), 152.6 (8a-C), 160.6 (5-C); IR ν_{max} 3431 (N-H), 3212 (NH_2), 2912 (N-Me), 1666 (C=O), 1593, 1565 (C=C_{Ar}), 1244 (N^+-O^-) cm^{-1}.

7-(4-Methoxyphenyl)-2-methyl-5-oxo-5,6-dihydro-2,6-naphthyridin-2-ium iodide (104c).

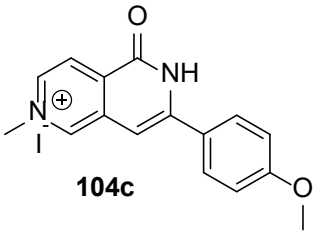

104c

MeI (228 mg, 1.6 mmol) was stirred with **100c** (35 mg, 0.13 mmol) in dry DMF (5.0 mL) for 36 h. The mixture was poured into EtOAc (3.0 mL). The solid was collected, washed with Me_2CO and dried to give **104c** (26 mg, 52%) as a yellow solid: mp 263-265 °C, R_f = 0.1 (petroleum ether / EtOAc 1:3); ^{1}H NMR ($(CD_3)_2SO$) δ 3.91 (3 H, s, OMe), 4.51 (3 H, br s, NMe), 7.15 (1 H, s, 8-H), 7.18 (2 H, d, *J* = 8.9 Hz, Ph 3,5-H_2), 7.85 (2 H, d, *J* = 8.9 Hz, Ph 2,6-H_2), 8.63 (1 H, d, *J* = 6.1 Hz, 4-H), 8.80 (1 H, d, *J* = 6.1 Hz, 3-H), 9.59 (1 H, br s, NH); ^{13}C NMR ($(CD_3)_2SO$) (HSQC / HMBC) δ 48.7 (NMe), 55.5 (OMe), 98.5 (8-C), 114.5 (Ph 3,5-C_2), 124.6 (4-C), 124.7 (Ph 1-C), 128.9 (Ph 2,6-C_2), 131.9 (8a-C), 138.9 (3-C), 146.2 (7-C), 147.2 (1-C), 160.1 (4a-C), 161.2 (Ph 4-C), 162.3 (5-C); MS (ESI) *m/z* 267.1127 (M^+) ($C_{16}H_{15}N_2O_2$ requires 267.1128).

2-Methyl-8-oxo-6-phenyl-7,8-dihydro-2,7-naphthyridin-2-ium iodide (105a).

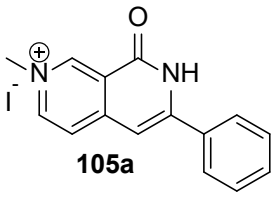

105a

MeI (228 mg, 1.6 mmol) was stirred with **101a** (55 mg, 0.23 mmol) in dry DMF (5.0 mL) for 72 h. The mixture was poured into EtOAc (2.0 mL), followed by petroleum ether (20 mL). The solid was collected, washed with petroleum ether and dried to give **105a** (10 mg, 12%) as a yellow solid: R_f = 0.1 (petroleum ether / EtOAc 1:3); mp 280-283 °C (decomposition); ^{1}H NMR ($(CD_3)_2SO$) δ 4.41 (3 H, s, Me), 7.28 (1 H, s, 4-H), 7.64-7.69 (3 H, m, Ph 3,4,5-H_3), 7.95 (2 H, d, *J* = 8.2 Hz, Ph 2,6-H_2), 8.20 (1 H, d, *J* = 6.4 Hz, 5-H), 8.82 (1 H, d, *J* = 6.4 Hz, 6-H), 9.71 (1 H, s, 8-H), 12.75 (1 H, br s, NH); ^{13}C NMR ($(CD_3)_2SO$) (HSQC / HMBC) δ 35.8 (Me), 101.2 (4-C), 120.7 (8a-C), 123.3 (5-C), 127.8 (Ph 2,6-C_2), 129.1 (Ph 3,5-C_2), 131.6 (Ph 4-C), 132.1 (Ph 1-C), 143.8 (3-C), 147.3 (6-C), 147.5 (8-C),

152.1 (1-C), 160.8 (4a-C); MS (ESI) *m/z* 237.1038 (M^+) ($C_{15}H_{13}N_2O$ requires 237.1022).

1-Methyl-7-phenyl-1,2,3,4-tetrahydro-1,6-naphthyridin-5(6*H*)-one (106a).

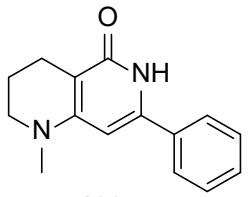
106a

To **103a** (80 mg, 0.22 mmol) in HCOOH (5 mL) at 0 °C was added dropwise BH_3.Py complex (~8 M BH_3, 0.06 mL). The mixture was stirred for 5 d. Each day, additional amount BH_3.Py complex (0.01 mL) was added. The mixture was then concentrated *in vacuo*. The residue was triturated with MeOH (10 mL) and was recrystallised from ^{i}PrOH to give **106a** (21 mg, 20%) as a pale grey solid: mp 315-317 °C; R_f = 0.3 (petroleum ether / EtOAc 1:3); IR ν_{max} 1655 (C=O), 1620 (C=C_{Ph}) cm^{-1}; ^{1}H NMR ($CDCl_3$) δ 1.89 (2 H, m, 3-H_2), 2.51 (2 H, m, 4-H_2), 3.11 (3 H, s, N-CH_3), 3.36 (2 H, m, 2-H_2), 6.30 (1 H, s, 8-H), 7.43 (3 H, m, Ph 3,4,5-H_3), 7.68 (2 H, m, Ph 2,6-H_2); ^{13}C NMR ($CDCl_3$) (HSQC / HMBC) δ 19.6 (4-C), 20.1 (N-Me), 50.8 (2-C), 96.8 (8-C), 100.2 (4a-C), 126.6 (Ph 2,6-C_2), 129.3 (Ph 3,5-C_2), 130.5 (4-C), 132.8 (Ph 1-C), 144.3 (7-C), 155.0 (8a-C), 159.0 (5-C); MS *m/z* 263.1177 $(M + Na)^+$ ($C_{15}H_{16}N_2NaO$ requires 263.1160).

7-(4-Methoxyphenyl)-1-methyl-1,2,3,4-tetrahydro-1,6-naphthyridin-5(6*H*)-one (106c).

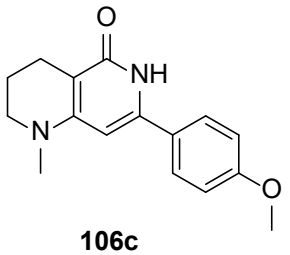
106c

To **103c** (50 mg, 0.127 mmol) in HCOOH (5.0 mL) at 0 °C was added dropwise BH_3.Py complex (~8 M BH_3, 0.10 mL). The mixture was stirred for 5 d. Each day, additional BH_3.Py complex (0.01 mL) was added. The solvent was evaporated. The residue was dissolved in AcOH (2.0 mL) and the solution was diluted with water (10 mL). The mixture was extracted with EtOAc (3 × 15 mL). The solvent was evaporated from the combined organic layers. The residue was recrystallised from water (5.0 mL) to give **106c** (1.0 mg, 3%) as a white powder: mp 221-223 ºC; R_f = 0.3 (petroleum ether / EtOAc 1:3); ^{1}H NMR ($CDCl_3$) δ 1.93 (2 H, qn, *J* = 6.2 Hz, 3-H_2), 2.61 (2 H, t, *J* = 6.3 Hz, 4-H_2), 3.02 (3 H, s, NMe), 3.28 (2 H, t, *J* = 5.4 Hz, 2-H_2), 3.85 (3 H, s, OMe), 5.98 (1 H, s, 8-H), 6.96 (2 H, d, *J* = 8.9 Hz, Ph 3,5-H_2), 7.47 (2 H, d, *J* = 8.9 Hz, Ph 2,6-H_2); ^{13}C NMR ($CDCl_3$) (HSQC / HMBC) δ 20.6 (4-C), 20.8 (3-C), 38.8 (NMe), 50.8 (2-C), 55.4 (OMe), 94.0 (8-C), 100.5 (4a-C), 114.6 (Ph 3,5-C_2), 126.9 (Ph 1-C), 127.2 (Ph 2,6-C_2), 142.5 (Ph 4-

C), 153.3 (8a-C), 160.7 (7-C), 162.3 (5-C); MS (ESI) *m/z* 293.1259 $(M + Na)^+$ ($C_{16}H_{18}N_2NaO_2$ requires 293.1266), 271.1452 $(M + H)^+$ ($C_{16}H_{19}N_2O_2$ requires 271.1447).

1-Methyl-7-(4-trifluoromethylphenyl)-1,2,3,4-tetrahydro-1,6-naphthyridin-5(6*H*)-one (106d).

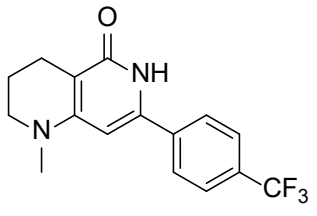

106d

To **103d** (30 mg, 0.069 mmol) in HCOOH (5.0 mL) at 0 °C was added dropwise BH_3.Py complex (~8 M BH_3, 0.10 mL). The mixture was stirred for 10 d. Each day, additional BH_3.Py complex (0.01 mL) was added. The solvent was evaporated. The residue was dissolved in water (5.0 mL) and the mixture was sonicated. The precipitate was collected and recrystallised from water to give **106d** (5.0 mg, 24%) as a white powder: mp 287-288 ºC; R_f = 0.35 (petroleum ether / EtOAc 1:3); ^{1}H NMR ($CDCl_3$) δ 1.94 (2 H, qn, *J* = 5.5 Hz, 3-H_2), 2.63 (2 H, t, *J* = 6.0 Hz, 4-H_2), 3.31 (2 H, t, *J* = 5.5 Hz, 2-H_2), 6.09 (1 H, s, 8-H), 7.67 (2 H, d, *J* = 8.5 Hz, Ph 2,6-H_2), 7.72 (2 H, d, *J* = 8.5 Hz, Ph 3,5-H_2); ^{13}C NMR ($CDCl_3$) (HSQC / HMBC) δ 20.6 (4-C), 20.9 (3-C), 50.0 (2-C), 96.1 (8-C), 101.8 (4a-C), 125.1 (q, *J* = 275 Hz, CF_3), 126.4 (m, Ph 2,3,5,6-C_4), 131.9 (q, *J* = 37.5 Hz, Ph 4-C), 140.0 (Ph 1-C), 141.8 (7-C), 149.1 (5-C), 157.2 (8a-C); ^{19}F NMR ($CDCl_3$) δ -62.8 (CF_3); MS (ESI) *m/z* 331.1061 $(M + Na)^+$ ($C_{16}H_{15}F_3N_2NaO$ requires 331.1034), 309.1239 $(M + H)^+$ ($C_{16}H_{16}F_3N_2O$ requires 309.1215).

7-(4-Chlorophenyl)-1-methyl-1,2,3,4-tetrahydro-1,6-naphthyridin-5(6*H*)-one (106e).

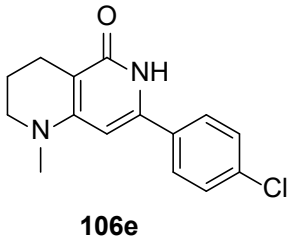

106e

To **103e** (91 mg, 0.23 mmol) in HCOOH (5.0 mL) at 0 °C was added dropwise BH_3.Py complex (~8 M BH_3, 0.10 mL). The mixture was stirred for 10 d. Each day, additional BH_3.Py complex (0.01 mL) was added. The solvent was evaporated. The residue was dissolved in water (5.0 mL) and the mixture was sonicated. The precipitate was collected and recrystallised from water to give **106e** (27 mg, 44%) as a white powder: mp 195-197 ºC; R_f = 0.3 (petroleum ether / EtOAc 1:3); ^{1}H NMR ($CDCl_3$) δ 1.95 (2 H, qn, *J* = 6.4 Hz, 3-H_2), 2.60 (2 H, t, *J* = 6.4 Hz, 4-H_2), 3.04 (3 H, s, NMe), 3.30 (2 H, t, *J* = 5.6 Hz, 2-H_2), 6.06 (1 H, s, 8-H), 7.43 (2 H, d, *J* = 8.6 Hz, Ph 3,5-H_2), 7.54 (2 H, d, *J* = 8.7 Hz, Ph 2,6-

H_2); ^{13}C NMR ($CDCl_3$) (HSQC / HMBC) δ 20.6 (4-C), 20.8 (3-C), 38.8 (NMe), 50.4 (2-C), 95.3 (8-C), 102.0 (4a-C), 127.5 (Ph 2,6-C_2), 129.3 (Ph 3,5-C_2), 134.3 (Ph 1-C), 137.7 (Ph 4-C), 142.3 (7-C), 154.0 (8a-C), 157.5 (5-C); MS (ESI) *m/z* 275.0941 $(M + H)^+$ ($C_{15}H_{16}{}^{35}ClN_2O$ requires 275.0946), 549.1819 $(2M + H)^+$ ($C_{30}H_{31}{}^{35}ClN_2O$ requires 549.1824).

7-(4-Bromophenyl)-1-methyl-1,2,3,4-tetrahydro-1,6-naphthyridin-5(6*H*)-one (106f).

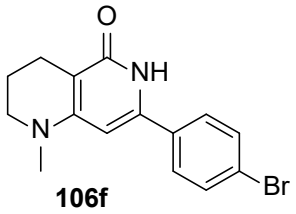

106f

To **103f** (12 mg, 0.027 mmol) in HCOOH (2.0 mL) at 0 °C was added dropwise BH_3.Py complex (0.02 mL). The mixture was stirred for 10 d. Each day, additional BH_3.Py complex (~8 M BH_3, 0.01 mL) was added. The solvent was evaporated. The residue was dissolved in water (5.0 mL) and the mixture was sonicated. The precipitate was collected by filtration and recrystallised from water (1.0 mL) to give **106f** (4.0 mg, 47%) as a white powder: R_f = 0.35 (petroleum ether / EtOAc 1:3); mp 205-207 ºC; ^1H NMR ($CDCl_3$) δ 1.95 (2 H, quin, *J* = 6.4 Hz, 3-H_2), 2.61 (2 H, t, *J* = 6.3 Hz, 4-H_2), 3.29 (3 H, s, Me), 3.29 (2 H, t, *J* = 5.5 Hz, 2-H_2), 6.02 (1 H, s, 8-H), 7.42 (2 H, d, *J* = 8.7 Hz, Ph 2,6-H_2), 7.59 (2 H, d, *J* = 8.7 Hz, Ph 3,5-H_2); ^{13}C NMR ($CDCl_3$) (HSQC / HMBC) δ 20.8 (4-C), 21.6 (3-C), 38.7 (NMe), 50.8 (2-C), 94.4 (8-C), 101.5 (4a-C), 123.9 (Ph 4-C), 127.4 (Ph 2,6-C_2), 132.3 (Ph 3,5-C_2), 133.4 (Ph 1-C), 141.8 (7-C), 153.2 (8a-C), 162.4 (5-C); MS (ESI) *m/z* 343.0249 $(M + Na)^+$ ($C_{15}H_{15}{}^{81}BrN_2NaO$ requires 343.0245), 341.0264 $(M + Na)^+$ ($C_{15}H_{15}{}^{79}BrN_2NaO$ requires 341.0265), 321.0426 $(M + H)^+$ ($C_{15}H_{16}{}^{81}BrN_2O$ requires 321.0426), 319.0448 $(M + H)^+$ ($C_{15}H_{16}{}^{79}BrN_2O$ requires 319.0446).

2-Phenylpyrido[2,3-*d*]pyrimidin-4(3*H*)-one (109a).

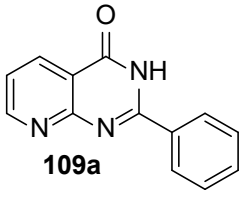

109a

2-Bromopyridine-3-carboxylic acid **126** (101.50 mg, 0.50 mmol), benzamidine **241a** (60 mg, 0.50 mmol), CuI (19.2 mg, 0.10 mmol) and Cs_2CO_3 (325 mg, 1.0 mmol) were stirred in DMF (5.0 mL) at room temperature under Ar for 10 h, then at 80 °C for 3 h. The mixture was cooled and filtered. The solvent was evaporated from the filtrate. The residue was dissolved in MeOH (20 mL), filtered and evaporated. The residue was dissolved in EtOAc / CH_2Cl_2 (1:1, 20 mL) and filtered. The filtrate was washed with sat. aq. solution of EDTA (50 mL) and the organic layer was separated and evaporated. The aqueous layer was extracted with CH_2Cl_2 (6 × 20 mL) and EtOAc (6 ×

20 mL). The combined organic layers were evaporated to give **109a** (58 mg, 53%) as an off-white solid: mp 225-227 °C (lit.[275] mp 284-285 °C); ^{1}H NMR ($CDCl_3$) δ 7.45 (1 H, dd, 7-H), 7.60 (5 H, m, Ph-H_5), 8.41 (1 H, dd, *J* = 7.5, 2.0 Hz, 8-H), 8.91 (1 H, dd, *J* = 4.5, 2.0 Hz, 6-H), 11.10 (1 H, br s, NH); ^{13}C NMR ($CDCl_3$) δ 116.1 (8a-C), 121.5 (7C), 128.5 (Ph 3,5-C_2), 129.0 (3C), 129.1 (Ph 2,6-C_2), 132.5 (Ph 4-C), 134.1 (Ph 1-C), 140.2 (8-C), 155.5 (6-C), 159.3 (4a-C), 166.5 (1-C); MS *m/z* 224.0818 $(M + H)^+$ ($C_{13}H_{10}N_3O$ requires 224.0835).

2-(4-Methylphenyl)pyrido[2,3-*d*]pyrimidin-4(3*H*)-one (109b).

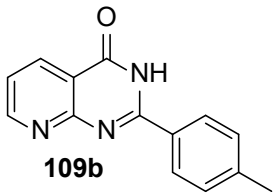

109b

2-Bromopyridine-3-carboxylic acid **126** (101.5 mg, 0.50 mmol) was stirred with 4-methylbenzamidine **241b** (67 mg, 0.50 mmol), CuI (19.2 mg, 0.10 mmol) and Cs_2CO_3 (325 mg, 1.0 mmol) in DMF (5.0 mL) at 80 °C for 3 h, then at room temperature for 10 h under Ar. The mixture was filtered and the solvent was evaporated. The residue was dissolved in MeOH (20 mL), the precipitate was filtered and the filtrate was evaporated. The evaporation residue was dissolved in sat. aq. EDTA (20 mL). The solution was kept at 2-8 °C for 30 min and the solid was collected by filtration. The solid was washed with petroleum ether and with water and was dried to give **109b** (41 mg, 35%) as a white powder: mp 249-251 °C, ^{1}H NMR ($(CD_3)SO$) δ 2.47 (3 H, s, Me), 7.28 (1 H, dd, *J* = 7.4, 4.7 Hz, 6-H), 7.48 (2 H, d, *J* = 8.1 Hz, Ph 3,5-H_2), 7.94 (2 H, d, *J* = 8.1 Hz, Ph 2,6-H_2), 8.44 (1 H, d, *J* = 7.5 Hz, 5-H), 8.48 (1 H, d, *J* = 4.7 Hz, 7-H), 11.09 (1 H, br s, NH); ^{13}C NMR ($(CD_3)_2SO$) δ 21.0 (Me), 119.1 (4a-C), 119.8 (6-C), 127.3 (Ph 3,5-C_2), 129.5 (Ph 1-C), 129.6 (Ph 2,6-C_2), 140.2 (5-C), 142.8 (Ph 4-C), 148.3 (7-C), 155.6 (8a-C), 159.7 (2-C), 166.8 (4-C); MS *m/z* 236.0836 $(M - H)^-$ ($C_{14}H_{10}N_3O$ requires 236.0824).

2-(4-Trifluoromethylphenyl)pyrido[2,3-*d*]pyrimidin-4(3*H*)-one (109d).

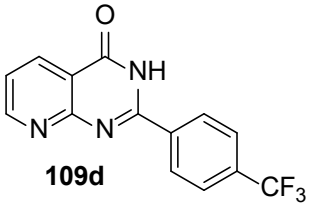

109d

2-Bromopyridine-3-carboxylic acid **126** (101.5 mg, 0.50 mmol) was stirred with 4-trifluoromethylbenzamidine **241d** (94 mg, 0.50 mmol), CuI (19.2 mg, 0.10 mmol) and Cs_2CO_3 (325 mg, 1.0 mmol) in DMF (5.0 mL) at 80 °C for 3 h, then at room temperature for 10 h under Ar. The mixture was filtered and the solvent was evaporated. The residue was dissolved in MeOH (20 mL), the precipitate was filtered and the filtrate was evaporated. The evaporation residue was

dissolved in sat. aq. EDTA (20 mL). The solution was kept at 2-8 °C for 30 min and the solid was collected by filtration. The solid was washed with petroleum ether and with water and was dried to give **109d** (64 mg, 45%) as a white powder: mp 254-256 °C; ^{1}H NMR ($(CD_3)_2SO$) δ 7.29 (1 H, dd, *J* = 6.8, 4.0 Hz, 6-H), 8.04 (2 H, m, Ph 2,6-H_2), 8.22 (2 H, m, Ph 3,5-H_2), 8.46 (1 H, d, *J* = 6.8 Hz, 5-H), 8.54 (1 H, d, *J* = 4.0 Hz, 7-H), 11.01 (1 H, br s, NH); ^{1}H NMR ($(CD_3)_2SO$) (HSQC / HMBC) δ 119.0 (6-C), 126.10 (Ph 2,6-C_2), 128.22 (q *J* = 2.7 Hz, Ph 3,5-C_2), 140.10 (5-C), 149.5 (7-C); ^{19}F NMR ($(CD_3)_2SO$) δ -61.35 (CF_3); MS 292.0699 $(M + H)^+$ ($C_{14}H_9F_3N_3O$ requires 292.0692).

2-(4-Chlorophenyl)pyrido[2,3-*d*]pyrimidin-4(3*H*)-one (109e).

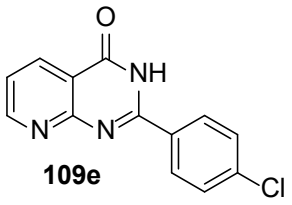

109e

2-Bromopyridine-3-carboxylic acid **126** (101.5 mg, 0.50 mmol) was stirred with 4-chlorobenzamidine **241e** (77 mg, 0.50 mmol), CuI (19.2 mg, 0.10 mmol) and Cs_2CO_3 (325 mg, 1.0 mmol) in DMF (5.0 mL) at 80 °C for 3 h, then at room temperature for 10 h under Ar. The mixture was filtered and the solvent was evaporated. The residue was dissolved in MeOH (20 mL), the precipitate was filtered and the filtrate was evaporated. The evaporation residue was dissolved in sat. aq. EDTA (20 mL). The solution was kept at 2-8 °C for 30 min. The solid was collected by filtration and recrystallised (EtOAc / CH_2Cl_2) to give **109e** (10 mg, 8%) as a pale grey powder: mp 266-268 °C (lit.[276] mp 300.5 °C); ^{1}H NMR ($(CD_3)_2SO$) δ 7.25 (1 H, m, 6-H), 7.73 (2 H, d, *J* = 8.9 Hz, Ph 2,6-H_2), 8.06 (2 H, d, *J* = 8.9 Hz, Ph 3,5-H_2), 8.42 (1 H, m, 5-H), 8.45 (1 H, m, 7-H), 11.10 (1 H, br s, NH); ^{1}H NMR ($(CD_3)_2SO$) δ 119.3 (4a-C), 119.8 (6-C), 129.3 (Ph 3,5-C_2), 129.5 (Ph 2,6-C_2), 132.0 (Ph 1-C), 137.0 (Ph 4-C), 140.3 (5-C), 149.3 (7-C), 151.0 (8a-C), 157.0 (2-C), 160.2 (1-C); MS 282.0225 $(M + Na)^+$ ($C_{13}H_8{}^{37}ClN_3NaO$ requires 282.0224), 280.0257 $(M + Na)^+$ ($C_{13}H_8{}^{35}ClN_3NaO$ requires 280.0254).

2-Phenylpyrido[3,4-*d*]pyrimidin-4(3*H*)-one (110a).

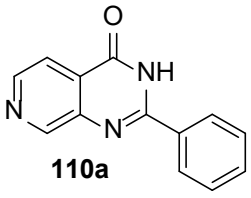

110a

3-Bromopyridine-4-carboxylic acid **127**[277] (101.5 mg, 0.50 mmol) was stirred with benzamidine **241a** (60 mg, 0.50 mmol), CuI (19 mg, 0.10 mmol) and Cs_2CO_3 (325 mg, 1.0 mmol) in DMF (5.0 mL) at 80 °C for 3 h, then at room temperature for 12 h under Ar. The mixture was cooled and filtered and the solvent was evaporated. The residue was dissolved in MeOH (20 mL), the precipitate was filtered

and the solvent was evaporated from the filtrate. The residue was dissolved in sat. aq. EDTA (20 mL) and sonicated for 5 min. The solution was kept at 2-8 °C for 1 h. The solid was collected by filtration. The filtrate was extracted with EtOAc (4 × 25 mL). The combined extracts were dried and the solvent was evaporated. The combined solids were washed (water, then petroleum ether) and were dried to give **110a** (14 mg, 13%) as a white powder: mp 228-230 °C (lit.[273] mp 266-267 °C); ^{1}H NMR ((CD$_3$)$_2$SO) δ 7.62 (3 H, m, Ph 3,4,5-H$_3$), 8.02 (1 H, d, *J* = 5.0 Hz, 5-H), 8.26 (2 H, d, *J* = 6.9 Hz, Ph 2,6-H$_2$), 8.68 (1 H, d, *J* = 5.0 Hz, 6-H), 9.16 (1 H, s, 8-H), 10.40 (1 H, br s, NH); ^{13}C NMR ((CD$_3$)$_2$SO) (HSQC / HMBC) δ 118.1 (5-C), 127.4 (Ph 1-C), 127.9 (Ph 2,6-C$_2$), 129.0 (Ph 3,5-C$_2$), 129.0 (4a-C), 131.6 (8a-C), 133.0 (Ph 4-C), 145.4 (6-C), 150.7 (8-C), 155.1 (2-C), 162.1 (4-C); MS *m/z* 246.0448 (M + Na)$^+$ (C$_{13}$H$_9$N$_3$NaO requires 246.0641).

2-(4-Methylphenyl)pyrido[3,4-*d*]pyrimidin-4(3*H*)-one (110b).

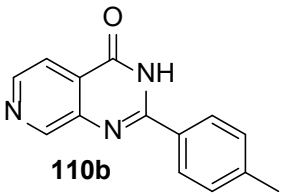

110b

3-Bromopyridine-3-carboxylic acid **127**[277] (101.5 mg, 0.50 mmol) was stirred with 4-methylbenzamidine **241b** (67 mg, 0.50 mmol), CuI (19 mg, 0.10 mmol) and Cs$_2$CO$_3$ (325 mg, 1.0 mmol) in DMF (5.0 mL) at 80 °C for 3 h, then at room temperature for 10 h under Ar. The mixture was cooled and filtered and the solvent was evaporated. The residue was dissolved in MeOH (20 mL), the precipitate was filtered and the solvent was evaporated from the filtrate. The residue was dissolved in sat. aq. EDTA (20 mL) and this solution was extracted with CH$_2$Cl$_2$ (3 × 25 mL). The combined extracts were dried and the solvent was evaporated to give **110b** (10 mg, 9%) as a white powder: mp 214-216 °C, ^{1}H NMR ((CD$_3$)$_2$SO) δ 2.44 (3 H, s, Me), 7.36 (2 H, d, *J* = 8.1 Hz, Ph 3,5-H$_2$), 7.91 (1 H, d, *J* = 5.2 Hz, 5-H), 8.24 (2 H, d, *J* = 8.2 Hz, Ph 2,6-H$_2$), 8.52 (1 H, d, *J* = 5.2 Hz, 6-H), 9.03 (1 H, s, 7-H), 10.20 (1 H, br s, NH); ^{13}C NMR ((CD$_3$)$_2$SO) (HSQC / HMBC) δ 21.0 (Me), 118.2 (5-C), 126.0 (4a-C), 127.5 (Ph 1-C), 127.5 (Ph 2,6-C$_2$), 128.9 (Ph 3,5-C$_2$), 129.5 (Ph 4-C), 144.0 (6-C), 149.0 (8a-C), 150.4 (8-C), 168.9 (2-C); MS *m/z* 236.0836 (M - H)$^-$ (C$_{14}$H$_{10}$N$_3$O requires 236.0824).

2-(4-Trifluoromethylphenyl)pyrido[3,4-*d*]pyrimidin-4(3*H*)-one (110d).

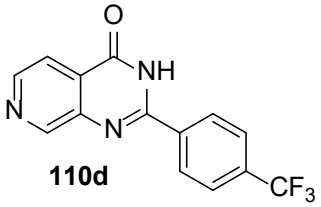

110d

3-Bromopyridine-4-carboxylic acid **127** (101.5 mg, 0.50 mmol) was stirred with 4-trifluoromethylbenzamidine **241d** (94 mg, 0.50 mmol), CuI (19.2 mmol, 0.10 mmol) and

Cs_2CO_3 (325 mg, 1.0 mmol) in DMF (5.0 mL) at 80 °C for 3 h, then at room temperature for 10 h under Ar. The mixture was filtered and the solvent was evaporated. The residue was suspended in MeOH (10 mL), the suspension was filtered and the solvent was evaporated from the filtrate. The residue was dissolved in aq. EDTA (saturated, 20 mL). The solution was kept at 2-8 °C for 1 h and the solid was collected by filtration. The filtrate was extracted with EtOAc (6 × 25 mL). The combined organic layers were dried and the solvent was evaporated. The combined solids were washed with petroleum ether and water and were dried to give **110d** (34 mg, 24%) as a pale green powder: ^{1}H NMR ($(CD_3)_2SO$) δ 7.87 (2 H, d, *J* = 8.3 Hz, Ph 2,6-H_2), 8.12 (1 H, m, 5-H), 8.43 (2 H, d, *J* = 8.2 Hz, Ph 3,5-H_2), 8.71 (1 H, br d, 6-H), 9.23 (1 H, br s, 8-H), 13.10 (1 H, br s, NH); ^{13}C NMR ($(CD_3)_2SO$) (HSQC / HMBC) δ 125.2 (q, *J* = 289.3 Hz, CF_3), 125.6 (q, *J* = 2.3 Hz, Ph 3,5-C_2), 128.9 (Ph 2,6-C_2), 131.5 (4a-C), 136.3 (q, *J* = 31.7 Hz, Ph 4-C), 138.0 (Ph 1-C), 147.0 (5-C), 149.0 (8-C), 154.0 (2-C), 155.5 (6-C), 158.0 (8a-C), 161.3 (4-C); MS *m/z* 292.0705 $(M + H)^+$ ($C_{14}H_9F_3N_3O$ requires 292.0692).

2-Phenylpyrido[4,3-*d*]pyrimidin-4(3*H*)-one (111a).

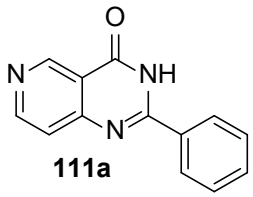

111a

4-Bromopyridine-3-carboxylic acid **128** (101.5 mg, 0.50 mmol) was stirred with benzamidine **241a** (60 mg, 0.50 mmol), CuI (19.2 mg, 0.10 mmol) and Cs_2CO_3 (325 mg, 1.0 mmol) in DMF (5.0 mL) at 80 °C for 3 h, then at 50 °C for 10 h under Ar. The mixture was filtered and the solvent was evaporated. The residue was suspended in MeOH (10 mL), the precipitate was filtered and the filtrate was evaporated. The evaporation residue was dissolved in aq. EDTA (saturated, 20 mL) and the suspension was sonicated for 5 min. This mixture was extracted with EtOAc (6 × 25 mL). The combined organic layers were dried. The solvent was evaporated to give **111a** (50 mg, 44%) as an ivory-coloured powder: mp 273-275 °C (lit.[250] 284-286 °C), ^{1}H NMR ($(CD_3)_2SO$) δ 7.61 (1 H, m, 8-H), 7.63 (3 H, m, Ph 3,4,5-H_3), 8.28 (2 H, d, *J* = 7.2 Hz, Ph 2,6-H_2), 8.83 (1 H, br d, 7-H), 9.33 (1 H, br s, 5-H), 12.80 (1 H, br s, NH); ^{13}C NMR ($(CD_3)_2SO$) (HSQC / HMBC) δ 117.5 (4a-C), 120.0 (8-C), 124.0 (Ph 1-C), 128.3 (Ph 3,5-C_2), 128.6 (Ph 2,6-C_2), 132.0 (Ph 4-C), 135.0 (3-C), 149.0 (5-C), 152.0 (7-C), 156.0 (8a-C), 162.0 (4-C); MS *m/z* 224.0818 $(M + H)^+$ ($C_{13}H_{10}N_3O$ requires 224.0813).

2-(4-Methylphenyl)pyrido[4,3-*d*]pyrimidin-4(3*H*)-one (111b).

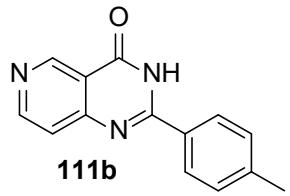

111b

4-Bromopyridine-3-carboxylic acid **128** (101.5 mg, 0.50 mmol) was stirred with 4-methylbenzamidine **241b** (67 mg, 0.50 mmol), CuI (19.2 mmol, 0.10 mmol) and Cs_2CO_3 (325 mg, 1.0 mmol) in DMF (5.0 mL) at 80 °C for 12 h under Ar. The mixture was filtered and the solvent was evaporated. The residue was suspended in MeOH (10 mL). The mixture was filtered and the solvent was evaporated from the filtrate. The evaporation residue was dissolved in aq. EDTA (saturated, 20 mL). The solution was extracted with EtOAc (6 × 25 mL). The combined organic extracts were dried and the solvent was evaporated to give **111b (**46 mg, 42%) as an ivory-coloured powder: mp 276-278 °C (lit.[250] 296-299 °C); ^{1}H NMR ($(CD_3)_2SO$) δ 2.45 (3 H, s, Me), 7.29 (2 H, d, *J* = 8.2 Hz, Ph 3,5-H_2), 7.64 (1 H, d, *J* = 5.4 Hz, 5-H), 8.18 (2 H, d, *J* = 8.2 Hz, Ph 2,6-H_2), 8.85 (1 H, br s, 7-H), 9.33 (1 H, br d, 8-H); ^{13}C NMR ($(CD_3)_2SO$) (HSQC / HMBC) δ 21.0 (Me), 120.1 (8a-C), 120.4 (5-C), 128.2 (Ph 2,6-C_2), 129.2 (Ph 3,5-C_2), 129.3 (Ph 1-C), 131.5 (Ph 4-C), 142.3 (3-C), 149.5 (8-C), 157.4 (4a-C), 162.4 (1-C); MS *m/z* 238.0975 $(M + H)^+$ ($C_{14}H_{12}N_3O$ requires 238.0984).

2-(4-Trifluoromethylphenyl)pyrido[4,3-*d*]pyrimidin-4(3*H*)-one (111d).

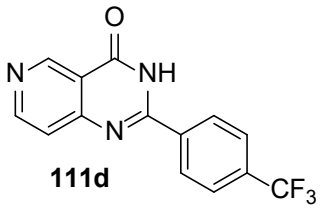

111d

4-Bromopyridine-3-carboxylic acid **128** (101.5 mg, 0.50 mmol) was stirred with 4-trifluoromethylbenzamidine **241d** (94 mg, 0.50 mmol), CuI (19.2 mmol, 0.10 mmol) and Cs_2CO_3 (325 mg, 1.0 mmol) in DMF (5.0 mL) at 80 °C for 3 h, then at room temperature for 10 h under Ar. The mixture was filtered and the solvent was evaporated. The residue was suspended in MeOH (10 mL). The suspension was filtered. The solvent was evaporated from the filtrate. The residue was dissolved in aq. EDTA (saturated, 20 mL). The solution was kept at 2-8 °C for 1 h and the precipitated solid was collected by filtration. The filtrate was extracted with EtOAc (6 × 25 mL). The combined organic extracts were dried and the solvent was evaporated. The combined solids were washed with petroleum ether and water and were dried to give **111d (**70 mg, 50%) as a pale green powder: mp 267-268 °C; ^{1}H NMR ($(CD_3)_2SO$) δ 7.71 (1 H, d, *J* = 4.4 Hz, 8-H), 8.00 (2 H, d, *J* = 8.3 Hz, Ph 2,6-H_2), 8.44 (2 H, d, *J* = 8.2 Hz, Ph 3,5-H_2), 9.08 (1 H, br d, 7-H), 9.38 (1 H, br s, 5-H), 13.10 (1 H, br s, NH); ^{13}C NMR ($(CD_3)_2SO$) (HSQC / HMBC) δ 122.0 (8a-C), 125.2 (8-C), 125.2 (Ph 2,6-C_2), 125.5 (q, *J* = 3.5 Hz, Ph 3,5-C_2), 129.2 (6-C), 131.8 (q, *J* =

340.6 Hz, CF_3), 134.0 (q, J = 27.5 Hz, Ph 4-C), 138.0 (Ph 1-C), 149.5 (5-C), 153.5 (4a-C), 156.3 (3-C), 162.0 (1-C); ^{19}F NMR ($(CD_3)_2SO$) δ -61.3 (s, CF_3); MS *m/z* 292.0702 $(M + H)^+$ ($C_{14}H_9F_3N_3O$ requires 292.0692).

2-(4-Chlorophenyl)pyrido[4,3-*d*]pyrimidin-4(3*H*)-one (111e).

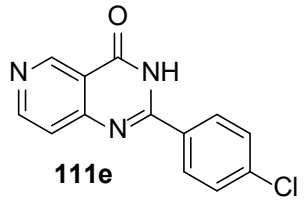

111e

4-Bromopyridine-3-carboxylic acid **128** (101.5 mg, 0.50 mmol) was stirred with 4-chlorobenzamidine **241e** (77.3 mg, 0.50 mmol), CuI (19.2 mmol, 0.10 mmol) and Cs_2CO_3 (325 mg, 1.0 mmol) in DMF (5.0 mL) at 80 °C for 12 h under Ar. The mixture was filtered. The solvent was evaporated from the filtrate. The residue was dissolved in MeOH (20 mL) and filtered. The solvent was evaporated from the filtrate. The residue was dissolved in aq. EDTA (saturated, 20 mL). The solution was extracted with EtOAc (6 × 25 mL). The combined organic extracts were dried. The solvent was evaporated and the residue was washed with petroleum ether and water and dried to give **111e (**17 mg, 13%) as a white powder: ^{1}H NMR ($(CD_3)_2SO$) δ 7.66 (1 H, d, J = 5.6 Hz, 5-H), 7.69 (2 H, d, J = 8.6 Hz, Ph 2,6-H_2), 8.29 (2 H, d, J = 8.6 Hz, Ph 3,5-H_2), 8.86 (1 H, d, J = 5.5 Hz, 6-H), 9.34 (1 H, br d, 8-H), 13.05 (1 H, br s, NH); ^{13}C NMR ($(CD_3)_2SO$) (HSQC / HMBC) δ 120.0 (5-C), 126.5 (8a-C), 128.8 (Ph 3,5-C_2), 130.1 (Ph 2,6-C_2), 131.0 (Ph 4-C), 137.2 (Ph 1-C), 146.0 (4-C), 153.5 (8-C), 156.0 (3-C), 162.0 (1-C); MS *m/z* 282.0269 $(M + Na)^+$ (requires 282.0222), 280.0248 $(M + Na)^+$ ($C_{13}H_8{}^{35}ClN_3NaO$ requires 280.0260).

General procedure for 6-benzyl-2-aryl-5,6,7,8-tetrahydropyrido[4,3-*d*]pyrimidin-4(3*H*)-ones 112a,b,d-f,h.

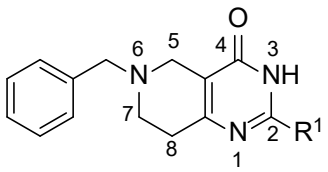

112a,b,d-f,h

a: R^1 = Ph; **b**: R^1 = 4-ArMe; **d**: R^1 = 4-ArCF$_3$; **e**: R^1 = 4-ArCl; **f**: R^1 = 4-ArBr; **h**: R^1 = 4-Py

To **262** (1420 mg, 5.0 mmol) in dry MeOH (10 mL) were added the corresponding benzamidine **241** (5.0 mmol) in dry MeOH (10 mL) and NaOMe (from Na (690 mg, 30 mmol) and dry MeOH (10 mL)). The mixture was stirred under reflux for 10 h, then cooled. The solvent was evaporated. The residue was suspended in water. The mixture was sonicated for 5 min. The suspension was kept at 2-8 °C for 1 h, then the solid was collected by filtration. The material was washed with water (50 mL) and EtOAc (50 mL) and dried to give a corresponding product **112a,b,d-f,h**.

6-Benzyl-2-phenyl-5,6,7,8-tetrahydropyrido[4,3-*d*]pyrimidin-4(3*H*)-one (112a).

Yield: 53%, off-white powder: R_f 0.65 (petroleum ether / EtOAc 1:3); mp 233-235 °C; ^{1}H NMR ($(CD_3)_2SO$) δ 2.70-2.74 (4 H, m, 7,8-H_4), 3.24 (2 H, s, 5-H_2), 3.69 (2 H, s, $PhCH_2N$), 7.28-7.37 (5 H, m, Ph(Bn) 2,3,4,5,6-H_5), 7.47-7.53 (3 H, m, Ph 3,4,5-H_3), 8.08 (2 H, d, *J* = 7.0 Hz, Ph 2,6-H_2); 12.50 (1 H, br s, NH); ^{13}C NMR ($(CD_3)_2SO$) (HSQC / HMBC) δ 31.4 (8-C), 49.12 (7-C), 49.5 (5-C), 61.7 (Ph-CH_2-N), 117.0 (4a-C), 127.0 (Ph(Bn) 4-C), 127.5 (Ph 2,6-C_2), 128.2 (Ph 2,6-C_2), 128.4 (Ph(Bn) 3,5-H_2), 128.8 (Ph(Bn) 2,6-H_2), 138.3 (Ph 1-C), 139.0 (Ph(Bn) Ph 1-C), 145.0 (8a-C), 153.5 (4-C), 159.0 (2-C); MS (ESI) *m/z* 318.1586 $(M + H)^+$ ($C_{20}H_{20}N_3O$ requires 318.1586).

6-Benzyl-2-(4-methylphenyl)-5,6,7,8-tetrahydropyrido[4,3-*d*]pyrimidin-4(3*H*)-one (112b).

Yield: 56%, off-white powder: R_f 0.65 (petroleum ether / EtOAc 1:3); mp 234-235 °C; ^{1}H NMR ($(CD_3)_2SO$) δ 2.37 (3 H, s, Me), 2.69-2.73 (4 H, m, 7,8-H_4), 3.24 (2 H, s, 5-H_2), 3.69 (2 H, s, $PhCH_2N$), 7.29-7.31 (3 H, m, Ph(Bn) 4-H, Ph 3,5-H_2), 7.34-7.37 (4 H, m, Ph(Bn) 2,3,5,6-H_4), 7.98 (2 H, d, *J* = 8.0 Hz, Ph 2,6-H_2); 12.50 (1 H, br s, NH); ^{13}C NMR ($(CD_3)_2SO$) (HSQC / HMBC) δ 21.0 (Me), 32.0 (8-C), 49.5 (7-C), 49.8 (5-C), 62.0 (Ph-CH_2-N), 125.8 (4a-C), 126.0 (Ph(Bn) 4-C), 127.4 (Ph 2,6-C_2), 128.2 (Ph 3,5-C_2), 128.8 (Ph(Bn) 2,6-C_2), 129.1 (Ph(Bn) 3,5-C_2), 132.0 (Ph 1-C), 140.0 (Ph(Bn) 1-C), 142.0 (Ph 4-C), 158.0 (8a-C), 161.5 (4-C), 175.0 (2-C); MS (ESI) *m/z* 332.1747 $(M + H)^+$ ($C_{21}H_{22}N_3O$ requires 332.1757).

6-Benzyl-2-(4-trifluoromethylphenyl)-5,6,7,8-tetrahydropyrido[4,3-*d*]pyrimidin-4(3*H*)-one (112d).

Yield: 60%, off-white powder: R_f 0.7 (petroleum ether / EtOAc 1:3); mp 234-235 °C; ^{1}H NMR ($(CD_3)_2SO$) δ 2.66-2.73 (4 H, m, 7,8-H_4), 3.24 (2 H, s, 5-H_2), 3.70 (2 H, s, $PhCH_2N$), 7.39-7.41 (5 H, m, Ph(Bn) 2,3,4,5,6-H_5), 7.77 (2 H, d, *J* = 7.8 Hz, Ph 3,5-H_2), 8.44 (2 H, d, *J* = 7.7 Hz, Ph 2,6-H_2), 12.50 (1 H, br s, NH); ^{13}C NMR ($(CD_3)_2SO$) (HSQC / HMBC) δ 31.5 (8-C), 50.1 (7-C), 50.6 (5-C), 62.2 ($PhCH_2N$), 115.4 (4a-C), 123.4 (q, *J* = 265.0 Hz, CF_3), 124.6 (q, *J* = 3.6 Hz, Ph 3,5-C_2), 126.9 (Ph-(Bn) 4-C), 127.9 (Ph-(Bn) 3,5-C_2), 128.2 (Ph 2,6-C_2), 128.6 (q, *J* = 32 Hz, Ph 4-C), 128.7 (Ph-(Bn) 2,6-C_2), 138.7 (Ph-(Bn) 1-C), 142.8 (Ph 1-C), 156.7 (8a-C), 157.8 (2-C), 169.1 (4-C); ^{19}F NMR ($(CD_3)_2SO$) -60.8 (CF_3); MS (ESI) *m/z* 386.1493 $(M + H)^+$ ($C_{21}H_{19}F_3N_3O$ requires 386.1475).

6-Benzyl-2-(4-chlorophenyl)-5,6,7,8-tetrahydropyrido[4,3-*d*]pyrimidin-4(3*H*)-one (112e).

Yield: 58%, off-white powder: R_f 0.6 (petroleum ether / EtOAc 1:3); mp 211-213 °C; ^{1}H NMR ($(CD_3)_2SO$) δ 2.75-2.78 (4 H, m, 7,8-H_4), 3.29 (2 H, s, 5-H_2), 3.74 (2 H, s, $PhCH_2N$), 7.34-7.42 (5 H, m, Ph(Bn) 2,3,4,5,6-H_5), 7.61 (2 H, d, J = 8.2 Hz, Ph 3,5-H_2), 8.15 (2 H, d, J = 8.2 Hz, Ph 2,6-H_2); 12.65 (1 H, br s, NH); ^{13}C NMR ($(CD_3)_2SO$) (HSQC / HMBC) δ 32.0 (8-C), 49.8 (7-C), 49.9 (5-C), 62.0 ($PhCH_2N$), 128.5 (Ph 3,5-C_2), 128.8 (m, Ph(Bn) 2,3,4,5,6-C_5), 129.5 (8a-C), 129.8 (Ph 2,6-C_2), 139.0 (4a-C), 154.0 (1-C); MS (ESI) *m/z* 350.1066 $(M + H)^+$ ($C_{20}H_{17}{}^{35}ClN_3O$ requires 350.1066).

6-Benzyl-2-(4-bromophenyl)-5,6,7,8-tetrahydropyrido[4,3-*d*]pyrimidin-4(3*H*)-one (112f).

Yield: 43%, off-white powder: R_f 0.7 (petroleum ether / EtOAc 1:3); mp 253-255 °C; ^{1}H NMR ($(CD_3)_2SO$) δ 2.70-2.74 (4 H, m, 7,8-H_4), 3.24 (2 H, s, 5-H_2), 3.69 (2 H, s, $PhCH_2N$), 7.28-7.37 (5 H, m, Ph(Bn) 2,3,4,5,6-H_5), 7.71 (2 H, d, J = 8.5 Hz, Ph 3,5-H_2), 8.05 (2 H, d, J = 8.5 Hz, Ph 2,6-H_2); 12.60 (1 H, br s, NH); ^{13}C NMR ($(CD_3)_2SO$) (HSQC / HMBC) δ 32.0 (8-C), 49.5 (7-C), 49.8 (5-C), 62.0 ($PhCH_2N$), 118.7 (4a-C), 127.0 (Ph(Bn) 4-C), 128.2 (Ph(Bn) 2,3,5,6-C_4), 128.8 (Ph 2,6-C_2), 129.5 (Ph 3,5-C_2), 131.5 (Ph 1-C), 139.0 (Ph(Bn) 1-C), 156.0 (8a-C), 163.0 (4-C); MS (ESI) *m/z* 398.0726 $(M + H)^+$ ($C_{20}H_{19}{}^{81}BrN_3O$ requires 398.0688), 396.0699 $(M + H)^+$ ($C_{20}H_{19}{}^{79}BrN_3O$ requires 396.0706).

6-Benzyl-2-(pyrid-4-yl)-5,6,7,8-tetrahydropyrido[4,3-*d*]pyrimidin-4(3*H*)-one (112h).

Yield: 86%, off-white powder: R_f 0.1 (petroleum ether / EtOAc 1:3); mp 298-300 °C; ^{1}H NMR ($(CD_3)_2SO$) δ 2.63 (2 H, m, 8-H_2), 2.71 (2 H, m, 7-H_2), 3.23 (2 H, s, 5-H_2), 3.69 (2 H, s, $PhCH_2N$), 7.31-7.42 (5 H, m, Ph(Bn) 2,3,4,5,6-H_5), 8.16 (2 H, d, J = 4.5 Hz, Py 3,5-H_2), 8.58 (2 H, d, J = 4.5 Hz, Py 2,6-H_2), 12.50 (1 H, br s, NH); ^{13}C NMR ($(CD_3)_2SO$) (HSQC / HMBC) δ 31.2 (8-C), 50.5 (7-C), 53.7 (5-C), 62.5 (Ph-CH_2-N), 117.6 (8a-C), 121.6 (Py 3,5-C_2), 128.1 (Ph-(Bn) 4-C), 128.7 (Ph-(Bn) 2,3,5,6-C_4), 139.5 (Ph-(Bn) 1-C), 148.1 (Py 1-C), 149.8 (Py 2,6-C_2), 157.0 (4a-C), 160.1 (3-C); 182.6 (1-C); MS (ESI) *m/z* 319.1532 $(M + H)^+$ ($C_{19}H_{19}N_4O$ requires 319.1553).

6-Benzyl-2-(4-phenylethynylphenyl)-5,6,7,8-tetrahydropyrido[4,3-*d*]pyrimidin-4(3*H*)-one (112k).

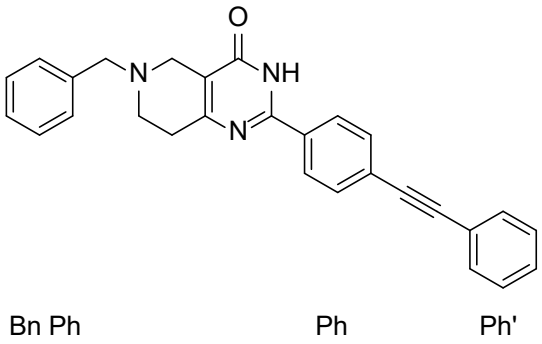

112k

NaOMe (259 mg, 4.8 mmol) in dry MeOH (5.0 mL) was added to **262** (216 mg, 0.8 mmol) in dry MeOH (5 mL), followed by **241k** (177.5 mg, 0.80 mmol) in dry MeOH (5.0 mL). The mixture was stirred at reflux for 16 h. The solvent was evaporated. The residue was extracted with EtOAc (3 × 30 mL). The precipitate was collected by filtration. The solvent was evaporated from the combined organic layers. The combined solids were recrystallised from water (20 mL) to give **112k** (190 mg, 57%) as an off-white powder: R_f = 0.55 (petroleum ether / EtOAc 1:3); mp 66-67 ºC; ^{1}H NMR ($(CD_3)_2SO$) δ 2.36-2.66 (2 H, m, 8-H_2), 2.86-3.25 (2 H, m, 7-H_2), 3.46-3.63 (2 H, m, 5-H_2), 3.68 (2 H, s, $PhCH_2N$), 7.24-7.38 (4 H, m, Ph'-2,3,5,6-H_4), 7.45-7.52 (4 H, m, Ph(Bn)-2,3,5,6-H_4), 7.60-7.69 (2 H, m, Ph'-4H, Ph(Bn) 4-H), 7.80 (2 H, d, *J* = 8.1 Hz, Ph 3,5-H_2), 7.96 (2 H, d, *J* = 8.0 Hz, Ph 2,6-H_2); ^{13}C NMR ($(CD_3)_2SO$) (HSQC / HMBC) δ 29.7 (8-C), 50.2 (7-C), 51.8 (5-C), 59.9 (Bn-CH_2-N), 87.9 (ethynyl 1-C), 93.3 (ethynyl 2-C), 111.0 (Ph 4-C), 118.4 (Ph' 1-C), 121.4 (Bn Ph 1-C), 127.0 (Ph 1-C), 128.8 (Ph' 2,3,5,6-H_4), 128.9 (Bn Ph 2,3,5,6-H_4), 129.5 (Ph' 4-C), 131.6 (Bn Ph 4-C), 132.1 (Ph 3,5-C_2), 132.6 (Ph 2,6-C_2), 138.3 (8a-C), 165.5 (4-C), 169.1 (2-C); MS (ESI) *m/z* 418.1983 $(M + H)^+$ ($C_{28}H_{24}N_3O$ requires 418.1919).

General procedure for 2-aryl-5,6,7,8-tetrahydropyrido[4,3-*d*]pyrimidin-4(3*H*)-ones 113a,b,d,h.

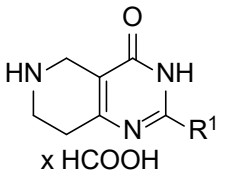

113a,b,d,h

a: R^1 = Ph; **b**: R^1 = 4-ArMe; **d**: R^1 = 4-ArCF_3; **h**: R^1 = 4-Py

A mixture of the 6-benzyl-2-aryl-5,6,7,8-tetrahydropyrido-[4,3-*d*]pyrimidin-4(3*H*)-one **112** (50 mg) and Pd/C (10%, 50 mg) in dry MeOH (10 mL) and HCOOH (1.0 mL) was stirred for 10 h under Ar. The mixture was filtered through Celite® and the solvent was evaporated from the filtrate to give compounds **113a,b,d,h.**

2-Phenyl-5,6,7,8-tetrahydropyrido[4,3-*d*]pyrimidin-4(3*H*)-onium formate (113a).

Yield: 89%, off-white powder: mp 244-245 °C (decomposition) (lit.[261] 214-216 °C); R_f 0.15 (petroleum ether / EtOAc 1:3); ^{1}H NMR ($(CD_3)_2SO$) δ 2.46 (2 H, m, 8-H_2), 3.20 (2 H, m, 7-H_2), 3.79 (2 H, s, 5-H_2), 7.59 (3 H, m, Ph 3,4,5-H_3), 8.14 (2 H, d, *J* = 7.2 Hz, Ph 2,6-H_2), 9.25 (2 H, br s, 3-NH, 7-NH); ^{13}C NMR ($(CD_3)_2SO$) (HSQC / HMBC) δ 29.5 (8-C), 40.1 (5-C), 41.0 (7-C), 127.6 (Ph 3,5-C_2), 128.6 (Ph 2,6-C_2), 131.4 (Ph 4-C), 132.6 (Ph 1-C), 154.8 (4a-C), 158.0 (8a-C), 161.9 (2-C), 164.6 (4-C); MS (ESI) *m/z* 250.0947 $(M + Na)^+$ ($C_{13}H_{13}N_3NaO$ requires 250.0956).

2-(4-Methylphenyl)-5,6,7,8-tetrahydropyrido[4,3-*d*]pyrimidin-4(3*H*)-onium formate (113b).

Yield: 86%, off-white powder: mp 279-280 °C; R_f 0.15 (petroleum ether / EtOAc 1:3); ^{1}H NMR ($(CD_3)_2SO$) δ 2.42 (3 H, s, Me), 2.45 (2 H, m, 8-H_2), 2.73 (2 H, m, 7-H_2), 3.33 (2 H, s, 5-H_2), 7.36 (2 H, d, *J* = 7.9 Hz, Ph 3,5-H_2), 8.03 (2 H, d, *J* = 8.0 Hz, Ph 2,6-H_2), 8.31 (2 H, br s, 3-NH, 7-NH); ^{13}C NMR ($(CD_3)_2SO$) (HSQC / HMBC) δ 20.9 (Me), 31.0 (7-C), 45.1 (8-C), 46.0 (5-C), 116.9 (4a-C), 127.5 (Ph 2,6-C_2), 129.2 (Ph 3,5-C_2), 129.5 (Ph 1-C), 141.4 (Ph 4-C), 154.1 (2-C), 158.1 (8a-C), 161.5 (4-C); MS (ESI) *m/z* 242.1294 $(M + H)^+$ ($C_{14}H_{16}N_3O$ requires 242.1288).

2-(4-Trifluoromethylphenyl)-5,6,7,8-tetrahydropyrido[4,3-*d*]pyrimidin-4(3*H*)-onium formate (113d).

Yield: 68%, off-white powder: mp 280-281 °C (decomposition); R_f 0.15 (petroleum ether / EtOAc 1:3); ^{1}H NMR ($(CD_3)_2SO$) δ 2.32 (2 H, m, 8-H_2), 2.55 (2 H, m, 7-H_2), 3.13 (2 H, s, 5-H_2), 7.66 (2 H, d, *J* = 8.1 Hz, Ph 3,5-H_2), 8.43 (2 H, d, *J* = 8.0 Hz, Ph 2,6-H_2); ^{13}C NMR ($(CD_3)_2SO$) (HSQC / HMBC) δ 31.5 (7-C), 46.1 (8-C), 53.4 (5-C), 114.4 (4a-C), 123.6 (q, *J* = 270.1 Hz, CF_3), 124.4 (q, *J* = 3.6 Hz, Ph 3,5-C_2), 127.8 (Ph 2,6-C_2), 128.4 (q, *J* = 31.1 Hz, Ph 4-C), 144.8 (Ph 1-C), 156.0 (8a-C), 157.0 (4-C), 159.3 (2-C); ^{19}F NMR ($(CD_3)_2SO$) δ -60.7 (CF_3); MS (ESI) *m/z* 296.1016 $(M + H)^+$ ($C_{14}H_{13}F_3N_3O$ requires 296.1005).

2-(Pyridin-4-yl)-5,6,7,8-tetrahydropyrido[4,3-*d*]pyrimidin-4(3*H*)-onium formate (113h).

Yield: 80%, off-white powder: mp 222-224 °C (lit.[261] 244-246 ºC); R_f 0.1 (petroleum ether / EtOAc 1:3); ^{1}H NMR ($(CD_3)_2SO$) (HSQC / HMBC) δ 3.02 (2 H, m, 8-H_2), 3.27

(2 H, m, 7-H_2), 3.44 (2 H, s, 5-H_2), 7.16 (2 H, d, *J* = 8.2 Hz, Py 2,6-H_2), 7.53 (2 H, d, *J* = 8.1 Hz, Py 3,5-H_2); ^{13}C NMR ($(CD_3)_2SO$) (HSQC / HMBC) δ 31.1 (7-C), 45.3 (8-C), 50.6 (5-C), 116.9 (4a-C), 117.2 (Py 1-C), 125.5 (Py 2,6-C_2), 128.1 (Py 3,5-C_2), 156.9 (8a-C), 160.4 (4-C), 161.2 (2-C).

2-(4-Phenylethynylphenyl)-5,6,7,8-tetrahydropyrido[4,3-*d*]pyrimidin-4(3*H*)-one hydrochloride (113k).

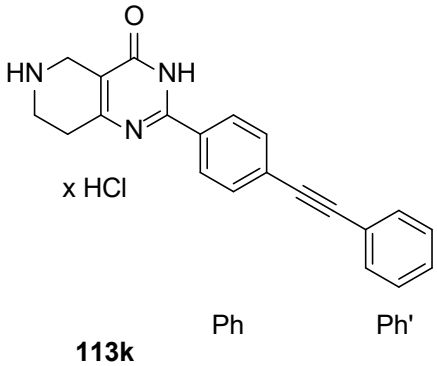

113k

Compound **112k** (170 mg) and Pd/C (10%, 200 mg) in dry MeOH (10 mL) and HCOOH (1.0 mL) were stirred for 10 h under Ar. The mixture was filtered through Celite® and the solvent was evaporated from the filtrate. The residue was recrystallised from EtOH (10 mL). The buff gummy formate salt was treated with HCl in dioxane (3.0 mL, 4.0 M) and Et_2O (5.0 mL). The precipitate was collected by filtration and washed with petroleum ether to give **113k** (44 mg, 34%) as a white crystalline powder: mp 177-180 °C; R_f = 0.05 (petroleum ether / EtOAc 1:3); ^{1}H NMR ($(CD_3)_2SO$) δ 2.92-2.95 (4 H, m, 7,8-H_4), 4.02-4.04 (2 H, m, 5-H_2), 7.24 (1 H, m, Ph' 4-H), 7.28 (2 H, d, *J* = 7.3 Hz, Ph 3,5-H_2), 7.30-7.35 (4 H, m, Ph' 2,3,5,6-H_4), 7.41 (2 H, d, *J* = 7.3 Hz, Ph 2,6-H_2), 8.26 (2 H, br s, NH_2); ^{13}C NMR ($(CD_3)_2SO$) (HSQC / HMBC) δ 36.5 (8-C), 36.9 (7-C), 41.9 (5-C), 66.3 (ethynyl 1-C), 92.2 (ethynyl 2-C), 128.2 (Ph' 3,5-C_2), 128.3 (Ph 3,5-C_2), 128.4 (Ph 4-C), 128.5 (Ph' 2,6-C_2), 128.7 (Ph' 1-C), 128.8 (Ph 1-C), 128.9 (Ph 2,6-C_2), 131.5 (4a-C), 141.3 (8a-C), 141.8 (2-C), 167.3 (4-C); MS (ESI) *m/z* 350.1963 $(M + Na)^+$ ($C_{21}H_{17}N_3NaO$ requires 350.1264).

2-Bromo-3-cyanopyridine (115). Method A.

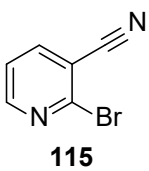

115

Bu_4NBr (8.55 g, 26 mmol) and P_2O_5 (3.67 g, 26 mmol) were heated in toluene (250 mL) at 80 °C for 30 min. 3-Cyanopyridine-2-one **140** (1.59 g, 13 mmol) was added and the mixture was boiled under reflux for 12 h. The reaction mixture was cooled, poured into cold water and extracted with EtOAc (2 × 50 mL). Drying and evaporation gave **115** (2.24 g, 94%) as ivory crystals: R_f = 0.4 (petroleum ether / EtOAc 3:1); mp 114-118 °C (lit.[278] mp 105 °C); IR ν_{max} 2236 (C≡N), 1668 (C=O), 1574, 1550, 1472 cm^{-1}; ^{1}H NMR ($CDCl_3$) δ 7.42 (1 H,

dd, J = 7.7, 4.8 Hz, 5-H), 8.01 (1 H, dd, J = 7.8, 2.0 Hz, 4-H), 8.57 (1 H, dd, J = 4.9, 2.0 Hz, 6-H); ^{13}C NMR ($(CD_3)_2$)SO) δ 114.3 (3-C), 115.6 (≡C), 122.4 (5-C), 142.5 (4-C), 143.8 (2-C), 152.9 (6-C).

2-Bromo-3-cyanopyridine (115). Method B.

To an ice-cold $POCl_3$ (5 mL) was added **141** (500 mg, 2.49 mmol) and the mixture was stirred at reflux for 2 h. The reaction mixture was cooled, poured into ice (100 g) with stirring and neutralised with 5 M NaOH (60 mL). The mixture was extracted with Et_2O (2 × 50 mL). Combined organic layers were washed with saturated aq. $NaHCO_3$, treated with charcoal, filtered and concentrated. The solid was recrystallised from petroleum ether (5 mL) to give **115** as an off-white powder (255 mg, 55%) with properties as above.

3-Cyano-2-(phenylethynyl)pyridine (116a). Method A.

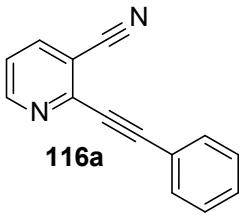

116a

CuI (27 mg, 0.14 mmol) and $(Ph_3P)_2PdCl_2$ **270** (49 mg, 70 μmol) were placed in a flask, which was degassed and filled with Ar. Pr^i_2NH (3.0 mL) was injected, followed by 2-chloro-3-cyanopyridine **114** (200 mg, 1.4 mmol) in THF (8.0 mL). The mixture was stirred at 45°C for 30 min. PhC≡CH **145a** (204 mg, 2.0 mmol) was added and the mixture was stirred at 45 °C for 16 h. Evaporation and chromatography (petroleum ether / EtOAc 7:1) gave **116a** (150 mg, 52%) as a buff powder: R_f = 0.8 (petroleum ether / EtOAc 3:1), mp 83-85 °C (lit.[279] mp 85-87 °C); ^{1}H NMR ($CDCl_3$) δ 7.33 (1H, dd, J = 8.0, 4.8 Hz, 5-H), 7.40 (m, Ph 3,4,5-H_3), 7.68 (d, J = 5.6 Hz, Ph 2,6-H_2), 7.95 (1 H, dd, J = 8.0, 2.0 Hz, 4-H), 8.77 (1 H, dd, J = 4.8, 1.8 Hz, 6-H); ^{13}C NMR ($CDCl_3$) (HSQC / HMBC) δ 85.6 (ethyne 2-C), 96.2 (ethyne 1-C), 112.8 (3-C), 115.9 (C≡N), 121.0 (5-C), 121.9 (Ph 1-C), 128.5 (Ph 3,5-C_2), 130.0 (Ph 4-C), 132.5 (Ph 2,6-C_2), 139.8 (4-C), 146.0 (2-C), 152.8 (6-C); MS (ESI) *m/z* 227.0575 $(M + Na)^+$ ($C_{14}H_8N_2Na$ requires 227.0586), 205.0755 $(M + H)^+$ ($C_{14}H_9N_2$ requires 205.0766).

3-Cyano-2-(phenylethynyl)pyridine (116a). Method B.

2-Chloro-3-cyanopyridine **114** (97 mg, 0.70 mmol) in THF (5.0 mL) was added to CuI (13.3 mg, 70 μmol) and $(Ph_3P)_4Pd$ (40.5 mg, 35 μmol) in Pr^i_2NH (5.0 mL) under Ar. The mixture was stirred for 30 min. PhC≡CH **145a** (143 mg, 1.4 mmol) was injected

and the mixture was stirred at 40 °C for 5 d. Evaporation and chromatography (petroleum ether / EtOAc 3:1) gave **116a** (140 mg, 98%), with properties as above.

3-Cyano-2-(phenylethynyl)pyridine (116a). Method C.

2-Bromo-3-cyanopyridine **115** (150 mg, 0.80 mmol) in THF (5.0 mL) was added to CuI (15.2 mg, 80 μmol) and $(Ph_3P)_2PdCl_2$ (28 mg, 40 μmol) in Pr^i_2NH (5.0 mL) under Ar. The mixture was stirred at 45°C for 30 min. PhC≡CH (163 mg, 1.6 mmol) was injected and the mixture was stirred at 40 °C for 5 d. Evaporation and chromatography (petroleum ether / EtOAc 3:1) gave **116a** (80 mg, 50%), with properties as above.

3-Cyano-2-((4-methylphenyl)ethynyl)pyridine (116b). Method A.

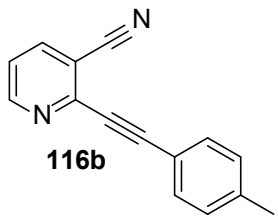

116b

2-Bromo-3-cyanopyridine **115** (184 mg, 1.0 mmol) in THF (5.0 mL) was added to CuI (19.2 mg, 0.1 mmol) and $(Ph_3P)_2PdCl_2$ **270** (35 mg, 50 μmol) in Pr^i_2NH (5 mL) under Ar. The mixture was stirred at 40 °C for 30 min. 1-Ethynyl-4-methylbenzene **145b** (174 mg, 1.5 mmol) was injected and the mixture was stirred at 40 °C for 12 h. Evaporation and chromatography (petroleum ether / EtOAc 3:1) gave **116b** (150 mg, 69%) as a pale buff powder: R_f = 0.4 (petroleum ether / EtOAc 3:1) mp 175-178 °C; ^{1}H NMR ($CDCl_3$) δ 2.38 (3 H, s, Me), , 7.32 (1 H, dd, *J* = 8.0, 4.9 Hz, 5-H), 7.40 (2 H, *J* = 8.1 Hz, Ph 3,5-H_2), 7.58 (2 H, d, *J* = 8.1 Hz, Ph 2,6-H_2), 7.95 (1 H, dd, *J* = 8.0, 1.8 Hz, 4-H), 8.77 (1 H, dd, *J* = 4.9, 1.7 Hz, 6-H); ^{13}C NMR (HSQC) ($CDCl_3$) δ 21.7 (Me), 112.7 (2-C), 121.7 (5-C), 129.3 (Ph 3,5-C_2), 132.5 (Ph 2,6-C_2), 139.8 (4-C), 140.6 (Ph 4-C), 152.8 (6-C), other signals are to weak to be assessed; MS (ESI) *m/z* 219.0905 $(M + H)^+$ ($C_{15}H_{11}N_2$ requires 219.0922).

3-Cyano-2-((4-methylphenyl)ethynyl)pyridine (116b). Method B.

Pr^i_2NH (5.0 mL) and THF (5.0 mL) were added to 2-bromo-3-cyanopyridine **115** (184 mg, 1.0 mmol), CuI (19.2 g, 0.1 mmol), sodium ascorbate (20 mg, 0.10 mmol) and $(Ph_3P)_2PdCl_2$ **270** (35 mg, 50 μmol) under Ar. The mixture was stirred at 40 °C for 30 min. 1-Ethynyl-4-methylbenzene **145b** (116 mg, 1.0 mmol) was injected and the mixture was stirred at 40 °C for 36 h. Evaporation and chromatography (petroleum ether / EtOAc 5:1 → 3:1) gave **116b** (170 mg, 80%), with properties as above.

General procedure for 2-(arylethynyl)-3-cyanopyridines (116c-e,g). Method A.

Pr^{i}_2NH (10 mL) was added to CuI (36 mg, 19 μmol) and $(Ph_3P)_2PdCl_2$ (66.5 mg, 9.5 μmol) under Ar and the mixture was stirred until a green suspension formed. 2-Bromo-3-cyanopyridine **115** (350 mg, 1.9 mmol) in THF (10 mL) was added and the mixture was stirred for 30 min. The corresponding ethynylbenzene **145c-e,g** (3.8 mmol) was added and the mixture was stirred at 40°C for 12 h. Evaporation and chromatography (petroleum ether / EtOAc 5:1 → 1:3) gave **116c-e,g**.

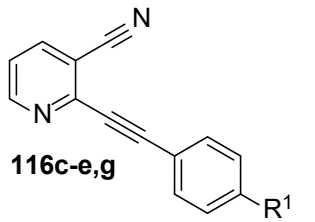

116c-e,g

c: R^1 = OMe; **d**: R^1 = CF_3; **e**: R^1 = Cl; **g**: R^1 = NH_2

General procedure for 2-(arylethynyl)-3-cyanopyridines (116c-e,g). Method B.

Pr^{i}_2NH (10 mL) and THF (10 mL) were added to 2-bromo-3-cyanopyridine **115** (0.4 g, 2.2 mmol), $(Ph_3P)_2PdCl_2$ **270** (76 mg, 0.11 mmol), CuI (40 mg, 0.22 mmol) and sodium ascorbate (25 mg, 0.12 mmol) under Ar. The mixture was stirred at 40 °C for 30 min. The corresponding ethynylbenzene **145c-e,g** (2.2 mmol) was added and the mixture was stirred at 40 °C for 12 h. Evaporation and chromatography (petroleum ether / EtOAc 5:1 → 1:3) gave **116c-e,g**.

3-Cyano-2-(4-methoxyphenylethynyl)pyridine (116c). Yield: 43% (method A), 81% (method B); pale buff powder; mp 118-120 °C; R_f = 0.55 (petroleum ether / EtOAc 3:1); ^{1}H NMR ($CDCl_3$) δ 3.83 (3 H, s, Me), 6.90 (2 H, d, *J* = 9.5 Hz, Ph 3,5-H_2), 7.30 (1 H, dd, *J* = 8.0, 4.9 Hz, 5-H), 7.62 (2 H, d, *J* = 9.5 Hz, Ph 2,6-H_2), 7.93 (1 H, dd, *J* = 6.2, 3.1 Hz, 4-H), 8.75 (1 H, dd, *J* = 4.9, 1.7 Hz, 6-H); ^{13}C NMR ($CDCl_3$) (HMBC) δ 55.3 (OMe), 85.0 (ethyne 2-C), 96.9 (ethyne 1-C), 112.9 (5-C), 114.2 (Ph 3,5-C_2), 116.1 (C≡N), 121.5 (3-C), 134.2 (Ph 2,6-C_2), 139.7 (4-C), 146.4 (6-C), 152.7 (2-C), 161.1 (Ph 4-C); MS (ESI) *m/z* 257.0670 $(M + Na)^+$ ($C_{15}H_{10}N_2NaO$ requires 257.0691).

3-Cyano-2-(4-trifluoromethylphenylethynyl)pyridine (116d): Yield: 52% (method A); pale buff powder; mp 129-132 °C; R_f = 0.4 (petroleum ether / EtOAc 3:1); ^{1}H NMR ($CDCl_3$) δ 7.40 (1 H, dd, *J* = 7.9, 4.9 Hz, 6-H), 7.66 (2 H, d, *J* = 8.0 Hz, Ph 3,5-H_2), 7.79 (2 H, d, *J* = 8.0 Hz, Ph 2,6-H_2), 8.00 (1 H, dd, *J* = 8.0, 1.8 Hz, 4-H), 8.81 (1 H, dd, *J* = 4.9, 1.8 Hz, 6-H); ^{13}C NMR ($CDCl_3$) (HSQC / HMBC) δ 87.3 (ethyne 2-C), 94.0 (ethyne 1-C), 113.2 (3-C), 115.8 (C≡N), 122.5 (5-C), 124.7 (Ph 1-C), 125.5 (q, *J* = 3.6 Hz, Ph 3,5-C_2), 131.8 (q, *J* = *ca.* 30 Hz, Ph 4-C), 132.8 (Ph 2,6-C_2), 139.9 (4-C), 145.5

(2-C), 153.0 (6-C); ^{19}F NMR ($CDCl_3$) δ -63.0 (s, CF_3); MS (ESI) *m/z* 295.0428 $(M + Na)^+$ ($C_{15}H_7F_3N_2Na$ requires 295.0459), 273.0622 $(M + H)^+$ ($C_{15}H_8N_2F_3$ requires 273.0640).

2-(4-Chlorophenylethynyl)-3-cyanopyridine (116e): Yield: 25% (method B); R_f = 0.35 (petroleum ether / EtOAc 3:1); shiny amber powder; mp 84-86 °C; ^{1}H NMR ($CDCl_3$) δ 7.36 (1 H, dd, *J* = 4.8, 2.4 Hz, 5-H), 7.37 (2 H, d, *J* = 8.7 Hz, Ph 3,5-H_2), 7.61 (2 H, d, *J* = 8.7 Hz, Ph 2,6-H_2), 7.98 (1 H, dd, *J* = 7.9, 1.7 Hz, 4-H), 8.79 (1 H, dd, *J* = 5.0, 1.7 Hz, 6-H); ^{13}C NMR ($CDCl_3$) (HSQC / HMBC) δ 86.4 (ethyne 2-C), 94.8 (ethyne 1-C), 112.9 (3-C), 115.8 (C≡N), 119.4 (Ph 1-C), 122.3 (5-C), 128.9 (Ph 3,5-C_2), 133.6 (Ph 2,6-C_2), 136.3 (Ph 4-C), 139.8 (4-C), 145.8 (2-C), 152.9 (6-C); MS (ESI) *m/z* 239.0353 $(M + H)^+$ ($C_{14}H_8{}^{35}ClN_2H$ requires 239.0376).

2-(4-Aminophenylethynyl)-3-cyanopyridine (116g): Yield: 87% (method A), 39% (method B); R_f = 0.2 (petroleum ether / EtOAc 1:3); dark green powder; mp 128-130 °C; ^{1}H NMR ($CDCl_3$) δ 3.96 (2 H, br s, NH_2), 6.64 (2 H, d, *J* = 9.1 Hz, Ph 3,5-H_2), 7.30 (1 H, dd, *J* = 8.5, 1.8 Hz, 5-H), 7.49 (2 H, d, *J* = 9.1 Hz, Ph 2,6-H_2), 7.92 (1 H, dd, *J* = 7.9, 1.7 Hz, 4-H), 8.73 (1 H, dd, *J* = 4.9, 1.7 Hz, 6-H); ^{13}C NMR ($CDCl_3$) (HSQC / HMBC) δ 82.9 (ethyne 2-C), 98.1 (ethyne 1-C), 106.45 (Ph 1-C), 113.7 (Ph 3,5-C_2), 116.5 (5-C), 121.9 (C≡N), 133.6 (Ph 2,6-C_2), 140.7 (3-C), 145.4 (4-C), 150.1 (6-C), 151.2 (Ph 4-C), 153.3 (2-C); MS (ESI) *m/z* 242.0693 $(M + Na)^+$ ($C_{14}H_9N_3Na$ requires 242.0694), 220.0876 $(M + H)^+$ ($C_{14}H_{10}N_3$ requires 220.0875).

3-Cyano-2-(pyridin-4-ylethynyl)pyridine (116h).

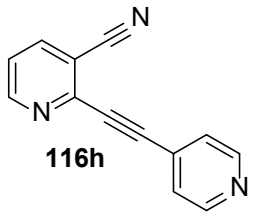

116h

CuI (19.2 mg, 0.10 mmol), $(Ph_3P)_4Pd$ (57.8 mg, 0.05 mmol), 2-bromo-3-cyanopyridine **115** (184 mg, 1.0 mmol), 4-ethynylpyridine **145h** (103 mg, 1.0 mmol) and sodium ascorbate (19.8 mg, 0.10 mmol) were placed in a flask, which was degassed and filled with Ar. Pr^i_2NH (10 mL) was injected, followed by DMF (10 mL). The mixture was stirred at 40 °C for 10 h. Evaporation and chromatography (petroleum ether / EtOAc 3:1 → 1:1 → 1:3) gave **116h** (58.1 mg, 28%) as an ivory-coloured powder: R_f = 0.2 (petroleum ether / EtOAc 3:1), mp 110-113 °C; ^{1}H NMR ($CDCl_3$) δ 7.42 (1 H, d, *J* = 4.8 Hz, 5-H), 7.52 (2 H, d, *J* = 4.4 Hz, Py 3,5-H_2), 8.01 (1 H, d, *J* = 1.8 Hz, 4-H), 8.65 (2 H, d, *J* = 4.7 Hz, Py 2,6-H_2), 8.82 (1 H, dd, *J* = 4.9, 1.8 Hz, 6-H); ^{13}C NMR ($CDCl_3$) (HSQC / HMBC) δ 88.7 (ethyne 2-C), 92.2

(ethyne 1-C), 113.5 (5-C), 115.5 (C≡N), 123.0 (3-C), 125.8 (Py 2,6-C_2), 129.0 (Py 1-C), 139.9 (4-C), 150.0 (Py 3,5-C_2), 150.6 (6-C), 153.9 (2-C); MS (ESI) *m/z* 206.0713 $(M + H)^+$ ($C_{13}H_8N_3$ requires 206.0699).

2-((4-(benzyloxy)phenyl)ethynyl)nicotinonitrile (116j).

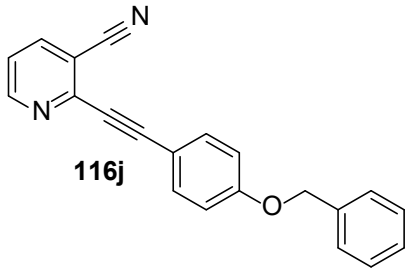

116j

CuI (19.2 mg, 0.10 mmol), $(Ph_3P)_2PdCl_2$ **270** (35 mg, 0.05 mmol), 2-bromo-3-cyanopyridine **115** (184 mg, 1.0 mmol), 1-(benzyloxy)-4-ethynylbenzene **145j** (206 mg, 1.0 mmol) and sodium ascorbate (19.8 mg, 0.1 mmol) were placed in a flask, which was degassed and filled with Ar. Pr^i_2NH (5.0 mL) was injected, followed by THF (5.0 mL). The mixture was stirred at 40 °C for 16 h. Evaporation and chromatography (petroleum ether / EtOAc 3:1) gave **116j** (89 mg, 29%) as an ivory powder: R_f = 0.2 (petroleum ether / EtOAc 3:1), mp 129-132 °C; IR ν_{max} 3073 (C-H), 2233 (C≡N) 2189 (C≡C), 1599 (C=C_{Ar}), 1506, 1464 (C=N) cm^{-1}; ^1H NMR ($CDCl_3$) δ 5.08 (2H, s, CH_2), 6.98 (2H, dd, *J* = 4.8 Hz, 9.5 Hz, 2',6'-H_2) 7.29 (1H, dd, *J* = 4.9 Hz, 7.9 Hz, 5-H), 7.31-7.44 (5H, m, 2",3",4",5",6"-H_5), 7.62 (2H, dd, *J* = 4.8 Hz, 9.5 Hz, 3,5-H_2), 7.93 (1 H, dd, *J* = 1.7 Hz, 7.9 Hz, 4-H), 8.74 (1 H, dd, *J* = 1.7 Hz, 4.9 Hz, 6-H); ^{13}C NMR ($CDCl_3$) (HSQC / HMBC) δ 70.1 (CH_2), 85.1 (C≡N), 96.9 (ethyne 2-C), 112.4 (ethyne 1-C), 113.2 (3-C), 115.1 (2C, 2',6'-C_2), 116.1 (1'-C), 121.5 (5-C), 127.4 (2C, 3",5"-C_2), 128.1 (4"-C), 128.6 (2C, 2",6"-C_2), 134.2 (2C, 3',5'-C_2), 136.3 (1"-C), 139.7 (4-C), 146.3 (2-C), 152.7 (6-C), 160.2 (4'-C); MS (ESI) *m/z* 311.1179 $(M + H)^+$ ($C_{21}H_{15}N_2O$ requires 311.1181).

7-(4-Methylphenyl)-5*H*-pyrano[4,3-*b*]pyridin-5-one (117b).

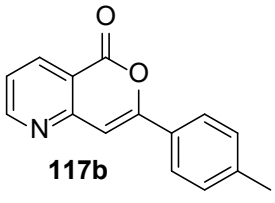

117b

A mixture of 2-bromopyridine-3-carboxylic acid **126** (101.5 mg, 0.50 mmol), 1,3-di-(4–methylphenyl)propane-1,3-dione **200** (252 mg, 1.0 mmol) and Cs_2CO_3 (163 mg, 0.50 mmol) in MeCN (15 mL) was stirred under reflux for 10 h. The mixture was cooled and poured into water (10 mL) and the mixture was extracted with CH_2Cl_2 (3 × 25 mL). The combined organic layers were dried and the solvent was evaporated. The residue was suspended in petroleum ether (50 mL), the mixture was sonicated and was filtered. The collected solid was washed with water and petroleum ether to give **117b** (110 mg, 93%) as an off-white powder: R_f 0.5 (petroleum

ether / EtOAc 3:1); mp 135-136 ºC; ^{1}H NMR ($CDCl_3$) δ 2.42 (3 H, s, Me), 7.18 (1 H, s, 8-H), 7.29 (2 H, d, *J* = 8.0 Hz, Ph 3,5-H_2), 7.41 (1 H, dd, *J* = 7.9, 4.7 Hz, 3-H), 7.81 (2 H, d, *J* = 8.1 Hz, Ph 2,6-H_2), 8.5 (1 H, dd, *J* = 7.9, 1.2 Hz, 4-H), 8.9 (1 H, dd, *J* = 4.7, 1.8 Hz, 2-H); ^{13}C NMR ($CDCl_3$) (HSQC / HMBC) δ 21.0 (Me), 102.9 (8-C), 117.0 (4a-C), 123.0 (3-C), 125.6 (Ph 2,6-C_2), 126.0 (Ph 1-C), 129.7 (Ph 3,5-C_2), 137.5 (4-C), 141.0 (4-C), 150.0 (7-C), 156.3 (5-C), 158.0 (2-C), 162.0 (8a-C); MS (ESI) *m/z* 238.0850 $(M + Na)^+$ ($C_{15}H_{12}NNaO_2$ requires 238.0863).

7-(4-Methoxyphenyl)-5*H*-pyrano[4,3-*b*]pyridin-5-one (117c).

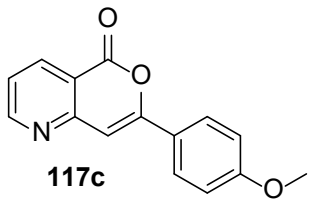

117c

A mixture of 2-bromopyridine-3-carboxylic acid **126** (101.5 mg, 0.50 mmol), **201** (142 mg, 0.50 mmol) and Cs_2CO_3 (163 mg, 0.50 mmol) in MeCN (15 mL) was stirred under reflux for 48 h. The reaction mixture was cooled and poured into water (10 mL) and the mixture was extracted with CH_2Cl_2 (3 × 25 mL). The combined organic layers were washed with brine and dried. The solvent was evaporated. The residue was washed with petroleum ether to give **117c** (28.3 mg, 22%) as an off-white powder: R_f 0.35 (petroleum ether / EtOAc 3:1); mp 169-171 ºC (lit.[280] 178-180 ºC); ^{1}H NMR ($CDCl_3$) δ 3.78 (3 H, s, Me), 6.63 (1 H, s, 8-H), 6.88 (2 H, d, *J* = 8.5 Hz, Ph 3,5-H_2), 7.28 (1 H, dd, *J* = 7.5, 4.0 Hz, 3-H), 7.76 (2 H, d, *J* = 8.5 Hz, Ph 2,6-H_2), 8.41 (1 H, d, *J* = 8.0 Hz, 4-H), 8.81 (1 H, m, 2-H); ^{13}C NMR ($CDCl_3$) (HSQC / HMBC) δ 50.4 (Me), 91.5 (Ph 1-C), 101.9 (8-C), 113.8 (4a-C), 116.5 (Ph 3,5-C_2), 122.4 (3-C), 129.5 (Ph 2,6-C_2), 137.7 (4-C), 156.1 (2-C), 157.5 (7-C), 161.8 (8a-C), 163.7 (5-C); MS (ESI of solution in MeOH, which converts **117c** to methyl 2-(2-(4-methoxyphenyl)-2-oxoethyl)pyridine-3-carboxylate) *m/z* 286.1075 $(M + H)^+$ ($C_{16}H_{16}NO_4$ requires 286.1082).

7-(4-Chlorophenyl)-5*H*-pyrano[4,3-*b*]pyridin-5-one (117e).

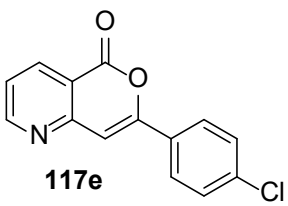

117e

A mixture of 2-bromopyridine-3-carboxylic acid **126** (101.5 mg, 0.50 mmol), **197** (146.5 mg, 0.50 mmol) and Cs_2CO_3 (163 mg, 0.50 mmol) in MeCN (15 mL) was stirred under reflux for 12 h. The mixture was cooled and poured into water (10 mL) and then the mixture was extracted with EtOAc (3 × 25 mL). The combined organic layers were washed with brine and dried. The solvent was evaporated. The residue was washed with petroleum ether to give **117e** (80 mg, 63%) as an off-white powder: R_f 0.35 (petroleum ether / EtOAc 3:1); mp 188-190 ºC; ^{1}H NMR

($CDCl_3$) δ 7.13 (1 H, s, 8-H), 7.36 (1 H, dd, *J* = 8.0, 4.5 Hz, 3-H), 7.40 (2 H, d, *J* = 8.5 Hz, Ph 3,5-H_2), 7.78 (2 H, d, *J* = 8.5 Hz, Ph 2,6-H_2), 8.47 (1 H, d, *J* = 8.0 Hz, 4-H), 8.87 (1 H, d, *J* = 4.5 Hz, 2-H); ^{13}C NMR ($CDCl_3$) (HSQC / HMBC) δ 117.02 (8a-C), 123.0 (3-C), 126.9 (Ph 3,5-C_2), 129.3 (Ph 2,6-C_2), 129.8 (8-C), 137.0 (Ph 4-C), 137.6 (4-C), 154.9 (7-C), 156.2 (4a-C), 156.5 (2-C), 161.8 (5-C); MS (ESI of solution in MeOH, which converts **117e** to methyl 2-(2-(4-chlorophenyl)-2-oxoethyl)pyridine-3-carboxylate) *m/z* 292.0582 $(M + H)^+$ ($C_{15}H_{13}{}^{37}ClNO_3$ requires 292.0554), 290.0590 $(M + H)^+$ ($C_{15}H_{13}{}^{35}ClNO_3$ requires 290.0578).

7-(4-Bromophenyl)-5*H*-pyrano[4,3-*b*]pyridin-5-one (117f).

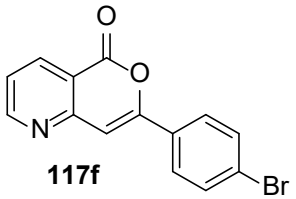

117f

A mixture of 2-bromo-3-carboxylic acid **126** (101.5 mg, 0.50 mmol), **199** (382 mg, 1.0 mmol) and Cs_2CO_3 (163 mg, 0.50 mmol) in MeCN (15 mL) was stirred under reflux for 16 h. The mixture was cooled and poured into water (10 mL) and the mixture was extracted with EtOAc (3 × 25 mL). The combined organic layers were washed with brine and dried and the solvent was evaporated. The residue was washed with petroleum ether to give **117f** (140 mg, 93%) as an off-white powder: R_f 0.45 (petroleum ether / EtOAc 3:1); mp 170-171 ºC; ^{1}H NMR ($CDCl_3$) δ 7.25 (1 H, s, 8-H), 7.47 (1 H, dd, *J* = 8.0, 4.5 Hz, 3-H), 7.66 (2 H, d, *J* = 8.5 Hz, Ph 3,5-H_2), 7.81 (2 H, d, *J* = 8.5 Hz, Ph 2,6-H_2), 8.57 (1 H, d, *J* = 8.0 Hz, 4-H), 8.97 (1 H, d, *J* = 4.5 Hz, 2-H); ^{13}C NMR ($CDCl_3$) (HSQC / HMBC) δ 104.0 (8-C), 117.0 (4a-C), 123.1 (3-C), 125.4 (Ph 4-C), 127.1 (Ph 2,6-C_2), 130.3 (Ph 1-C), 132.3 (Ph 3,5-C_2), 137.6 (4-C), 154.9 (8a-C), 156.3 (3-C), 156.5 (2-C), 161.8 (5-C); MS (ESI of solution in MeOH, which converts **117f** to methyl 2-(2-(4-bromophenyl)-2-oxoethyl)pyridine-3-carboxylate) *m/z* 336.0074 $(M + H)^+$ ($C_{15}H_{13}{}^{81}BrNO_3$ requires 336.0054), 334.0063 $(M + H)^+$ ($C_{15}H_{13}{}^{79}BrNO_3$ requires 334.0073).

3-Bromopyridine-4-nitrile (119). Method A.

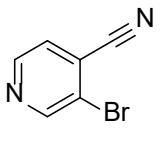

119

To ice-cold $POCl_3$ (5.0 mL) was added **162** (687 mg, 3.4 mmol) and the mixture was stirred at reflux for 2 h. The mixture was cooled, poured onto ice (100 g) with stirring and neutralised with aq. NaOH (5 M, 60 mL). The mixture was extracted with Et_2O (2 × 50 mL). The combined organic layers were washed with sat. aq. $NaHCO_3$, treated with charcoal and filtered. The solvent was evaporated. The solid was recrystallised from petroleum ether (5.0 mL) to give **119** as an off-white powder (292 mg, 42%): R_f 0.80 (petroleum

ether / EtOAc 3:1); mp 79-81 ºC (lit.[281] mp 92-93 ºC); ^{1}H NMR ($CDCl_3$) δ 7.53 (1 H, d, *J* = 4.9 Hz, 5-H), 8.69 (1 H, d, *J* = 4.9 Hz, 6-H), 8.92 (1 H, s, 2-H); ^{13}C NMR ($CDCl_3$) (HSQC / HMBC) δ 114.8 (C≡N), 122.1 (4-C), 124.2 (3-C), 126.8 (5-C), 148.8 (6-C), 152.7 (2-C); MS (ESI) *m/z* 182.9552 $(M + H)^+$ ($C_6H_4N_2{}^{79}Br$ requires 182.9541).

3-Bromoisonicotinonitrile (119). Method B.

BuLi in THF (1.6 M, 2.5 mL, 4.0 mmol) was added to a stirring stirred solution of 2,2,6,6-tetramethylpiperidine (577 mg, 4.0 mmol) in dry THF (5.0 mL) at -45 °C under Ar in one portion. The LTMP solution was stirred at -45 °C for 15 min and then cooled to -95 °C and stirred for 30 min. 4-Cyanopyridine **163** (212 mg, 2.0 mmol) in dry THF (1.0 mL) was then added dropwise during 5 min. CBr_4 (250 mg, 2.4 mmol) in dry THF (1.0 mL) was added in one portion and the mixture was stirred for 10 s, then quenched with sat. aq. NH_4Cl (5 mL). The aqueous layer was separated and extracted with EtOAc (3 × 20 mL). The organic layer was combined with the extract and dried. The solvent was evaporated. The residue was purified by chromatography (petroleum ether / EtOAc, 7:1 → 5:1 → 3:1) to give **119** (20 mg, 5%) with properties as above.

3-(Phenylethynyl)pyridine-4-nitrile (120a).

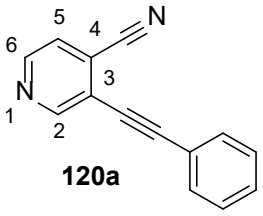

120a

A mixture of **119** (91.5 mg, 0.50 mmol), $(PPh_3)_4Pd$ (30 mg, 0.025 mmol), CuI (9.6 mg, 0.05 mmol) and sodium ascorbate (9.9 mg, 0.05 mmol) in THF (5.0 mL) and $^iPr_2NH$ (5.0 mL) was stirred at 40 ºC under Ar for 30 min. PhC≡CH **145a** (102 mg, 1.0 mmol) was added and the mixture was stirred at 40 ºC under Ar for 16 h. The mixture was cooled and the solvents were evaporated. The residue was purified by chromatography (petroleum ether / EtOAc 4:1 → 3:1 → 3:2 → 1:1 → 2:3 → 1:3) to give **120a** (55 mg, 50%) as a buff powder: R_f 0.5 (petroleum ether / EtOAc 3:1); mp 46-48 ºC (lit.[279] 49-53ºC); ^{1}H NMR ($CDCl_3$) δ 7.40 (3 H, m, Ph 3,4,5-H_3), 7.53 (1 H, d, *J* = 4.9 Hz, 5-H), 7.62 (2 H, d, *J* = 9.6 Hz, Ph 2,6-H_2), 8.68 (1 H, d, *J* = 4.9 Hz, 6-H), 8.92 (1 H, s, 2-H); ^{13}C NMR ($CDCl_3$) (HSQC / HMBC) δ 82.5 (1-C), 99.5 (2-C), 115.6 (C≡N), 121.3 (Ph 1-C), 122.4 (3-C), 125.0 (5-C), 128.4 (4-C), 128.5 (Ph 3,5-C_2), 129.8 (Ph 4-C), 132.1 (Ph 2,6-C_2), 148.4 (6-C), 152.8 (2-C); MS (ESI) *m/z* 227.0590 $(M + Na)^+$ ($C_{14}H_8N_2Na$ requires 227.0580).

3-((4-Methylphenyl)ethynyl)pyridine-4-nitrile (120b).

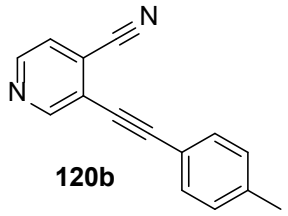

120b

A mixture of **119** (91.5 mg, 0.50 mmol), $(PPh_3)_4Pd$ (30 mg, 0.025 mmol), CuI (9.6 mg, 0.05 mmol) and sodium ascorbate (9.9 mg, 0.05 mmol) in THF (5.0 mL) and Pr^i_2NH (5.0 mL) was stirred at 40 ºC under Ar for 30 min. Ethynylbenzene **145b** (120 mg, 1.0 mmol) was added and the mixture was stirred at 40 ºC under Ar for 16 h. The mixture was cooled and the solvent was evaporated. The residue was purified by chromatography (petroleum ether / EtOAc 4:1 → 3:1 → 3:2) to give **120b** (65.8 mg, 62%) as a buff powder: R_f 0.45 (petroleum ether / EtOAc 3:1); mp 94-96 ºC; ^{1}H NMR ($CDCl_3$) δ 2.39 (3 H, s, Me), 7.20 (2 H, d, *J* = 8.4 Hz, Ph 3,5-H_2), 7.51 (3 H, m, 5-H, Ph 2,6-H_2), 8.65 (1 H, d, *J* = 5.0 Hz, 6-H), 8.90 (1 H, s, 2-H); ^{13}C NMR ($CDCl_3$) (HSQC / HMBC) δ 21.6 (Me), 100.0 (ethynyl 1-C), 113.2 (C≡N), 114.9 (ethynyl 2-C), 119.5 (Ph 1-C), 123.5 (4-C), 124.9 (5-C), 129.2 (Ph 4-C), 129.3 (Ph 3,5-C_2), 132.0 (Ph 2,6-C_2), 140.5 (3-C), 148.2 (6-C), 152.0 (2-C); MS (ESI) *m/z* 219.0910 $(M + H)^+$ ($C_{15}H_{11}N_2$ requires 219.0922).

3-((4-Methoxyphenyl)ethynyl)pyridine-4-nitrile (120c).

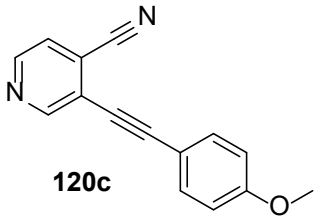

120c

A mixture of **119** (91.5 mg, 0.50 mmol), $(PPh_3)_4Pd$ (30 mg, 0.025 mmol), CuI (9.6 mg, 0.05 mmol) and sodium ascorbate (9.9 mg, 0.05 mmol) in THF (5.0 mL) and Pr^i_2NH (5.0 mL) was stirred at 40 ºC under Ar for 30 min. 1-Ethynyl-4-methoxybenzene **145c** (132 mg, 1.0 mmol) was added and the mixture was stirred at 40 ºC under Ar for 16 h. The mixture was cooled and the solvent was evaporated. The residue was purified by chromatography (petroleum ether / EtOAc 4:1 → 3:1 → 3:2) to give **120c** (84 mg, 72%) as a buff powder: R_f 0.45 (petroleum ether / EtOAc 3:1); mp 96-97 ºC; ^{1}H NMR ($CDCl_3$) δ 3.85 (3 H, s, Me), 6.91 (2 H, d, *J* = 8.9 Hz, Ph 3,5-H_2), 7.55 (1 H, d, *J* = 5.0 Hz, 5-H), 7.56 (2H, d, *J* = 8.9 Hz, Ph 2,6-H_2), 8.64 (1 H, d, *J* = 5.0 Hz, 6-H), 8.88 (1 H, s, 2-H); ^{13}C NMR ($CDCl_3$) (HSQC / HMBC) δ 55.4 (Me), 81.7 (ethynyl 1-C), 100.0 (ethynyl 2-C), 113.3 (Ph 1-C), 114.2 (Ph 3,5-C_2), 115.4 (C≡N), 121.9 (4-C), 122.9 (3-C), 124.9 (5-C), 133.8 (Ph 2,6-C_2), 147.9 (6-C), 152.6 (2-C), 160.8 (Ph 4-C); MS (ESI) *m/z* 235.0854 (M) ($C_{15}H_{10}N_2O$ requires 235.0827).

3-((4-Trifluoromethylphenyl)ethynyl)isonicotinonitrile (120d).

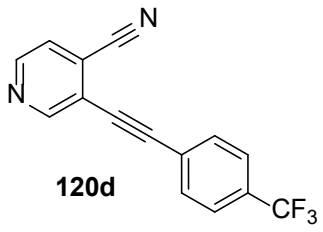

120d

A mixture of **119** (91.5 mg, 0.50 mmol), $(PPh_3)_4Pd$ (30 mg, 0.025 mmol), CuI (9.6 mg, 0.05 mmol) and sodium ascorbate (9.9 mg, 0.05 mmol) in THF (5 mL) and Pr^i_2NH (5.0 mL) was stirred at 40 ºC under Ar for 30 min. 1-Ethynyl-4-trifluoromethylbenzene **145d** (179 mg, 1.0 mmol) was added and the mixture was stirred at 40 ºC under Ar for 16 h. The mixture was cooled and the solvent was evaporated. The residue was purified by chromatography (petroleum ether / EtOAc 4:1 → 3:1 → 3:2) to give **120d** (64.7 mg, 48%) as an orange powder: R_f 0.35 (petroleum ether / EtOAc 3:1); mp 39-40 ºC; ^{1}H NMR ($CDCl_3$) δ 7.57 (1 H, d, *J* = 5.0 Hz, 5-H), 7.67 (2 H, d, *J* = 8.0 Hz, Ph 3,5-H_2), 7.74 (2 H, d, *J* = 8.0 Hz, Ph 2,6-H_2), 8.73 (1 H, d, *J* = 5.0 Hz, 6-H), 8.95 (1 H, s, 2-H); ^{13}C NMR ($CDCl_3$) (HSQC / HMBC) δ 84.5 (ethynyl 2-C), 97.5 (ethynyl 1-C), 115.2 (C≡N), 121.8 (3-C), 122.2 (4-C), , 123.3 (q, *J* = 298.3 HzCF_3), 125.1 (5-C), 125.6 (q, *J* = 3.6 Hz, Ph 3,5-C_2), 131.5 (q, *J* = 32.8 Hz, Ph 4-C), 132.4 (Ph 2,6-C_2), 149.1 (6-C), 152.9 (2-C); ^{19}F NMR ($CDCl_3$) δ -63.0 (s, CF_3); MS (ESI) *m/z* 295.0451 $(M + Na)^+$ ($C_{15}H_7F_3N_2Na$ requires 295.0454).

3-(4-Chlorophenylethynyl)pyridine-4-nitrile (120e).

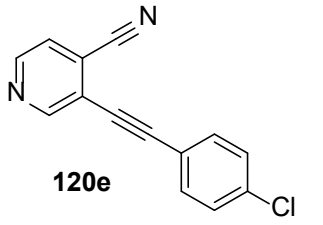

120e

A mixture of **119** (91.5 mg, 0.50 mmol), $(PPh_3)_4Pd$ (30 mg, 0.025 mmol), CuI (9.6 mg, 0.05 mmol) and sodium ascorbate (9.9 mg, 0.05 mmol) in THF (5.0 mL) and Pr^i_2NH (5.0 mL) was stirred at 40 ºC under Ar for 30 min. 4-Chloro-1-ethynylbenzene **145e** (137.5 mg, 1.0 mmol) was added and the mixture was stirred at 40 ºC under Ar for 16 h. The mixture was cooled and the solvent was evaporated. The residue was purified by chromatography (petroleum ether / EtOAc 4:1 → 3:1 → 3:2) to give **120e** (49.5 mg, 41%) as a buff powder: R_f 0.3 (petroleum ether / EtOAc 3:1); mp 200-201 ºC; ^{1}H ($CDCl_3$) δ 7.38 (2 H, d, *J* = 6.7 Hz, Ph 2,6-H_2), 7.53 (1 H, m, 5-H), 7.56 (2 H, d, *J* = 6.7 Hz, Ph 3,5-H_2), 8.69 (1 H, d, *J* = 5.5 Hz, 6-H), 8.91 (1 H, s, 2-H); ^{13}C NMR ($CDCl_3$) (HSQC / HMBC) δ 92.0 (ethynyl 2-C), 98.7 (ethynyl 1-C), 113.9 (C≡N), 118.9 (Ph 4-C), 119.2 (3-C), 123.9 (4-C),124.6 (5-C), 133.3 (Ph 3,5-C_2), 133.65 (Ph 2,6-C_2), 135.7 (Ph 1-C), 148.7 (6-C), 152.7 (2-C); MS (ESI) *m/z* 239.0391 $(M + H)^+$ ($C_{14}H_8{}^{35}ClN_2$ requires 239.0371).

3-Phenyl-1*H*-pyrano[4,3-*c*]pyridin-1-one (121a).

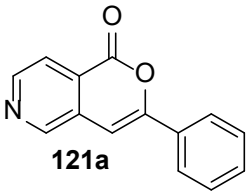

121a

A mixture of **127** (101.5 mg, 0.50 mmol), 1,3-diphenylpropane-1,3-dione **214** (114 mg, 0.50 mmol), K_3PO_4 (212 mg, 1.0 mmol) and CuI (10 mg, 0.05 mmol) was stirred in dry DMF (7 mL) at 100 °C under Ar for 6 d. The reaction mixture was cooled to 20 °C and water (7 mL) was added. The mixture was extracted with EtOAc (3 × 10 mL). The combined organic layers were dried and the solvent was evaporated. The residue was purified by chromatography (petroleum ether : EtOAc 5:1 → 3:1) to give **121a** (7.6 mg, 7%) as a yellow powder: R_f 0.3 (petroleum ether / EtOAc 3:1), mp 171-173 ºC (lit.[279] 166-168 ºC); ^{1}H NMR ($CDCl_3$) δ 7.02 (1 H, s, 4-H), 7.48 (3 H, m, Ph 3,4,5-H_3), 7.89 (2 H, m, Ph 2,6-H_2), 8.06 (1 H, d, *J* = 5.2 Hz, 8-H), 8.76 (1 H, d, *J* = 5.1 Hz, 7-H), 8.97 (1 H, s, 5-H); ^{13}C NMR ($(CD_3)_2SO$) (HSQC / HMBC) δ 98.5 (4-C), 118.0 (8-C), 125.4 (Ph 2,6-C_2), 127.0 (8a-C), 129.0 (Ph 3,5-C_2), 130.6 (Ph 4-C), 131.0 (Ph 1-C), 132.0 (3-C), 148.4 (7-C), 149.0 (5-C), 151.0 (1-C); MS (ESI) *m/z* 224.0708 $(M + H)^+$ ($C_{14}H_{10}NO_2$ requires 224.0712).

3-Cyano-4-(phenylethynyl)pyridine (124a). Method A.

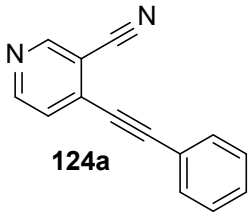

124a

CuI (9.6 mg, 0.05 mmol), $Pd(PPh_3)_2Cl_2$ **270** (29 mg, 0.025 mmol) and sodium ascorbate (9.9 mg, 0.05 mmol) were placed in a flask, which was degassed and filled with Ar. Et_3N (5.0 mL) was added, followed by 4-bromo-3-cyanopyridine **123** (92 mg, 0.5 mmol) in THF (5.0 mL). The mixture was stirred at 40 °C for 30 min. PhC≡CH **145a** (76.5 mg, 0.75 mmol) was added and the mixture was stirred at 40 °C for 10 h. Evaporation and chromatography (petroleum ether / EtOAc 3:1) gave **124a** (10 mg, 9.8%) as an off-white powder: mp 74-75 °C (lit.[279] 85-87 °C); IR ν_{max} 2222 (C≡N), 2150 (C≡C), 1582 (C=C_{Ar}), 1495 (C=N) cm^{-1}; ^{1}H NMR ($CDCl_3$) δ 7.39-7.43 (3 H, m, Ph 3,4,5-H_3), 7.45 (1 H, d, *J* = 5.2 Hz, 5-H), 7.63 (2 H, d, *J* = 8.2 Hz, Ph 2,6-H_2), 8.75 (1 H, d, *J* = 5.2 Hz, 6-H), 8.87 (1 H, s, 2-H); ^{13}C NMR ($CDCl_3$) (HSQC / HMBC) δ 83.5 (ethyne 2-C), 101.3 (ethyne 1-C), 111.7 (4-C), 115.5 (C≡N), 120.8 (Ph 1-C), 125.1 (5-C), 128.6 (Ph 3,5-C_2), 130.3 (Ph 4-C), 132.4 (Ph 2,6-C_2), 134.9 (3-C), 152.4 (2-C), 152.7 (6-C); MS *m/z* 227.0569 $(M + Na)^+$ ($C_{14}H_8N_2Na$ requires 227.0585).

3-Cyano-4-(phenylethynyl)pyridine (124a). Method B.

CuI (9.6 mg, 0.05 mmol), $(Ph_3P)_4Pd$ (28.9 mg, 25 μmol) and sodium ascorbate (9.9 mg, 0.05 mmol) were placed in a flask, which was degassed and filled with Ar. Et_3N (5.0 mL) was injected, followed by 4-bromo-3-cyanopyridine **122** (92 mg, 0.50 mmol) in THF (5.0 mL). The mixture was stirred at 40 °C for 30 min. PhC≡CH (76.5 mg, 0.75 mmol) was added and the mixture was stirred at 40 °C for 10 h. Evaporation and chromatography (petroleum ether / EtOAc 3:1) gave **124a** (80 mg, 78%) with properties as above.

General procedure for 3-cyano-4-(arylethynyl)pyridines 124c-e,g.

CuI (9.6 mg, 0.05 mmol), $(Ph_3P)_4Pd$ (28.9 mg, 25 μmol) and sodium ascorbate (9.9 mg, 0.05 mmol) were placed in a flask, which was degassed and filled with Ar. Et_3N (5.0 mL) was injected, followed by 4-bromo-3-cyanopyridine **123** (92 mg, 0.50 mmol) in THF (5.0 mL). The mixture was stirred at 40 °C for 30 min. The corresponding ethynylbenzene **145** (0.50 mmol) was added and the mixture was stirred at 40 °C for 10 h. Evaporation and chromatography (petroleum ether / EtOAc 3:1 → 2:1) gave **124c-e,g**.

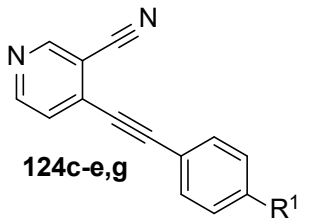

124c-e,g

c: R^1 = OMe; **d**: R^1 = CF_3; **e**: R^1 = Cl; **g**: R^1 = NH_2

4-(4-Methoxyphenylethynyl)pyridine-3-nitrile (124c).

Yield: 68%; yellow powder; R_f = 0.3 (petroleum ether / EtOAc 3:1), mp = 101-102 °C; IR υ_{max} 2218 (C≡N), 2184 (C≡C), 1608 (C=C_{Ar}), 1581, 1515, 1 cm^{-1}; ^1H NMR ($CDCl_3$) δ 3.84 (3 H, s, CH_3), 6.90 (2 H, d, *J* = 9.0 Hz, Ph 3,5-H_2), 7.43 (1 H, d, *J* = 5.3 Hz, 5-H), 7.57 (2 H, d, *J* = 9.0 Hz, Ph 2,6-H_2), 8,71 (1 H, d, *J* = 8.0, 6-H), 8.84 (1 H, s, 2-H); ^{13}C NMR ($CDCl_3$) (HSQC / HMBC) δ 55.3 (CH_3), 83.0 (ethyne 1-C), 102.1 (ethyne 2-C), 112.8 (3-C), 114.1 (C≡N), 114.3 (Ph 3,5-C_2), 115.7 (Ph 1-C), 124.7 (5-C), 134.2 (Ph 2,6-C_2), 135.3 (4-C), 152.2 (6-C), 152.6 (2-C), 161.3 (Ph 4-C); MS (ESI) *m/z* 257.0695 $(M + Na)^+$ ($C_{15}H_{10}N_2NaO$ requires 257.0691).

4-((4-Trifluoromethylphenyl)ethynyl)pyridine-3-nicotinonitrile (124d).

Yield: 44%; yellow powder; R_f = 0.35 (petroleum ether / EtOAc 3:1), mp = 66-68 °C; IR υ_{max} 2232 (C≡N), 1612 (C=C_{Ar}), 1568, 1064 (C-F) cm^{-1}; ^1H NMR ($CDCl_3$) δ 7.49 (1 H, d, *J* = 5.2 Hz, 5-H), 7.74 (2 H, d, *J* = 8.1 Hz, Ph 2,6-H_2), 8.58 (1 H, d, *J* = 5.2 Hz, 6-

H), 8.80 (2 H, d, *J* = 8.0 Hz, Ph 3,5-H_2), 8.91 (1 H, s, 2-H); ^{13}C NMR ($CDCl_3$) (HSQC / HMBC) δ 85.1 (ethyne 2-C), 101.2 (ethyne 1-C), 116.2 (3-C), 125.2 (5-C), 125.6 (Ph 2,6-C_2), 132.6 (Ph 3,5-C_2), 133.0 (4-C), 152.6 (6-C); ^{19}F NMR ($CDCl_3$) -63.1 (CF_3); MS (ESI) *m/z* 273.0634 $(M + H)^+$ ($C_{15}H_8F_3N_2$ requires 273.0636).

4-(4-Chlorophenylethynyl)pyridine-3-nitrile (124e).

Yield: 59%; yellow powder; R_f = 0.35 (petroleum ether / EtOAc 3:1), mp = 79-81 °C; IR υ_{max} 2232 (C≡N), 1569 (C=C_{Ar}), 1491, 724 (C-Cl) cm^{-1}; ^{1}H NMR ($CDCl_3$) δ 7.37 (2 H, d, *J* = 8.4 Hz, Ph 2,6-H_2), 7.47 (1 H, d, *J* = 5.2 Hz, 5-H), 7.55 (2 H, d, *J* = 8.4 Hz, Ph 3,5-H_2), 8.75 (1 H, d, *J* = 5.2 Hz, 6-H), 8.87 (1 H, s, 2-H); ^{13}C NMR ($CDCl_3$) (HSQC / HMBC) δ 99.6 (1-ethyne), 111.7 (3-C), 115.0 (C≡N), 119.3 (Ph 1-C), 125.0 (2-C), 129.1 (Ph 2,6-C_2), 133.6 (Ph 3,5-C_2), 137.8 (Ph 4-C), 152.5 (5-C), 152.7 (6-C); MS (ESI) *m/z* 261.0183 $(M + Na)^+$ ($C_{14}H_7{}^{35}ClN_2Na$ requires 261.0196), 263.0156 $(M + Na)^+$ ($C_{14}H_7{}^{37}ClN_2Na$ requires 263.0166).

4-(4-Aminophenylethynyl)pyridine-3-nitrile (124g).

Yield: 35%; orange powder; R_f = 0.15 (petroleum ether / EtOAc 3:1), mp = 155-159 °C; IR υ_{max} 3447 (NH_2), 2218 (C≡N), 2184 (C≡C), 1631 (C=C_{Ar}), 1603, 1579, cm^{-1}; ^{1}H NMR ($CDCl_3$) δ 4.01 (2 H, br, NH_2), 6.63 (2 H, d, *J* = 8.7 Hz, Ph 3,5-H_2), 7.40 (1H , d, *J* = 4.5 Hz, 5-H), 7.44 (2 H, d, *J* = 8.7 Hz, Ph 2,6-H_2), 8.67 (1 H, d, *J* = 4.5 Hz, 6-H), 8.81 (1 H, s, 2-H); ^{13}C NMR ($CDCl_3$) (HSQC / HMBC) δ 82.7 (ethyne 1-C), 103.5 (ethyne 2-C), 109.7 (Ph 1-C), 111.2 (3-C), 114.6 (Ph 3,5-C_2), 124.5 (5-C), 134.2 (Ph 2,6-C_2), 136.1 (4-C), 148.6 (Ph 4-C), 152.1 (Ph 4-C), 152.6 (2-C); MS (ESI) *m/z* 242.0681 $(M + Na)^+$ ($C_{14}H_9N_3Na$ requires 242.0694).

3-(4-Methylphenyl)-1*H*-pyrano[3,4-*c*]pyridin-1-one (125b).

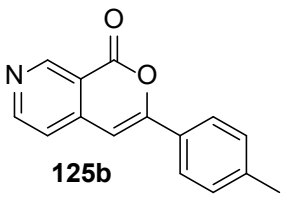

125b

A mixture of 4-bromopyridine-3-carboxylic acid **128** (101.5 mg, 0.50 mmol), **200** (252 mg, 1.0 mmol) and Cs_2CO_3 (163 mg, 0.50 mmol) in MeCN (15 mL) was stirred under reflux for 48 h. The reaction mixture was cooled and poured into water (10 mL) and the mixture was extracted with CH_2Cl_2 (3 × 25 mL). The solvent was evaporated from the combined organic layers. The residue was suspended in petroleum ether (50 mL), the mixture was sonicated and was filtered. The collected solid was washed with water and petroleum ether to give **125b** (38 mg, 32%)

as an off-white powder: R_f 0.45 (petroleum ether / EtOAc 3:1); mp 120-123 ºC; ^{1}H NMR ($CDCl_3$) δ 2.45 (3 H, s, Me), 6.90 (1 H, s, 4-H), 7.31 (2 H, d, *J* = 8.0 Hz, Ph 3,5-H_2), 7.33 (1 H, d, *J* = 5.5 Hz, 5-H), 7.83 (2 H, d, *J* = 8.0 Hz, Ph 2,6-H_2), 8.83 (1 H, d, *J* = 5.5 Hz, 6-H), 9.49 (1 H, s, 8-H); ^{13}C NMR ($CDCl_3$) (HSQC / HMBC) δ 20.5 (Me), 100.0 (4-C), 118.0 (4a-C), 118.5 (5-C), 121.5 (Ph 1-C), 125.8 (Ph 2,6-C_2), 128.9 (Ph 4-C), 129.8 (Ph 3,5-C_2), 130.0 (3-C), 139.5 (8-C), 141.0 (8a-C), 154.0 (6-C), 159.5 (1-C); MS (ESI) *m/z* 238.0851 $(M + H)^+$ ($C_{15}H_{12}NO_2$ requires 238.0863).

3-(4-Methoxyphenyl)-1*H*-pyrano[3,4-*c*]pyridin-1-one (125c).

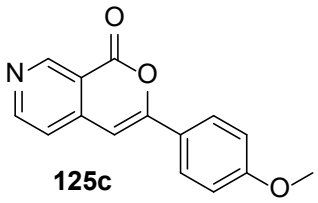

125c

A mixture of 4-bromopyridine-3-carboxylic acid **128** (101.5 mg, 0.50 mmol), **201** (142 mg, 0.5 mmol) and Cs_2CO_3 (163 mg, 0.50 mmol) in MeCN (15 mL) was stirred under reflux for 48 h. The mixture was cooled, poured into water (10 mL) and extracted with CH_2Cl_2 (3 × 25 mL). The combined organic layers were washed with brine and dried. The solvent was evaporated. The residue was washed with petroleum ether to give **125c** (16.3 mg, 13%) as an off-white powder: (petroleum ether / EtOAc 3:1); mp 185-186 ºC; R_f 0.35 ^{1}H NMR ($CDCl_3$) δ 3.91 (H, s, Me), 6.76 (1 H, s, 4-H), 6.96 (2 H, d, *J* = 8.5 Hz, Ph 3,5-H_2), 7.33 (1 H, d, *J* = 5.5 Hz, 5-H), 7.88 (2 H, d, *J* = 8.5 Hz, Ph 2,6-H_2), 8.81 (1 H, d, *J* = 5.5 Hz, 6-H), 9.47 (1 H, s, 8-H); ^{13}C NMR ($CDCl_3$) (HSQC / HMBC) δ 55.5 (Me), 91.5 (4-C), 109.0 (Ph 1-C), 114.5 (Ph 3,5-C_2), 119.0 (5-C), 127.6 (Ph 4-C), 128.2 (Ph 2,6-C_2), 131.4 (3-C), 141.0 (8a-C), 143.0 (6-C), 152.8 (8-C), 163.0 (1-C); MS (ESI of solution in MeOH, which converts **125c** to methyl 4-(2-(4-methoxyphenyl)-2-oxoethyl)pyridine-3-carboxylate) *m/z* 286.1074 $(M + H + MeOH)^+$ ($C_{16}H_{16}NO_4$ requires 286.1082).

3-(4-Bromophenyl)-1*H*-pyrano[3,4-*c*]pyridin-1-one (125f).

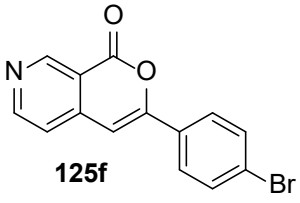

125f

A mixture of 4-bromo-3-carboxylic acid **128** (101.5 mg, 0.50 mmol), **199** (382 mg, 1.0 mmol) and Cs_2CO_3 (163 mg, 0.50 mmol) in MeCN (15 mL) was stirred under reflux for 72 h. The mixture was cooled and poured into water (10 mL) and the mixture was extracted with EtOAc (3 × 25 mL). The combined organic layers were washed with brine and dried. The solvent was evaporated. The residue was washed with petroleum ether to give **125f** (10 mg, 7%) as a buff sticky oil: R_f 0.45 (petroleum ether / EtOAc 3:1); ^{1}H NMR ($CDCl_3$) δ 6.83 (1 H, s, 4-H), 7.36 (2 H, d, *J* = 8.5 Hz, Ph 3,5-H_2), 7.69 (2 H, d, *J* = 8.5 Hz, Ph 2,6-H_2), 7.90 (1

H, dd, J = 8.5, 4.5 Hz, 5-H), 8.73 (1 H, d, J = 4.5 Hz, 6-H), 9.37 (1 H, s, 8-H); ^{13}C NMR ($CDCl_3$) (HSQC / HMBC) δ 92.5 (4-C), 118.5 (3-C), 119.0 (4a-C), 127.4 (Ph 3,5-C_2), 129.9 (Ph 1-C), 132.01 (Ph 2,6-C_2), 134.5 (Ph 4-C), 143.5 (8a-C), 152.2 (8-C), 153.9 (6-C), 165.0 (1-C); MS (ESI of solution in MeOH, which converts **125f** to methyl 4-(2-(4-bromophenyl)-2-oxoethyl)pyridine-3-carboxylate) *m/z* 336.0011 $(M + H)^+$ ($C_{15}H_{13}{}^{81}BrNO_3$ requires 336.0054), 334.0066 $(M + H)^+$ ($C_{15}H_{13}{}^{79}BrNO_3$ requires 334.0073).

Methyl 4-hydroxy-5,6-dihydro-2H-thiopyran-3-carboxylate (131).

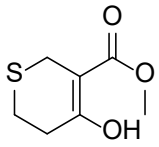

131

To a suspension of NaOMe (2565 mg, 47.5 mmol) in dry THF (30 mL) was added dimethyl 3,3'-thiodipropanoate **130** (750 mg, 3.6 mmol) in dry THF (5 mL) at 0 ºC under Ar. The mixture was stirred at reflux for 2 h. The mixture was cooled and transferred to a beaker with a stirrer bar, then acidified to pH 3 with aq. H_2SO_4 (9 M) at 0 ºC. The mixture was extracted with EtOAc (3 × 25 mL). The combined organic layers were dried and filtered and the solvent was evaporated to give **131** (600 mg, 95%) as a yellow liquid: R_f 0.50 (petroleum ether / EtOAc 3:1); ^{1}H NMR ($CDCl_3$) δ 2.58 (2 H, t, J = 5.8 Hz, 5-H_2), 2.76 (2 H, t, J = 5.8 Hz, 6-H_2), 3.34 (2 H, s, 2-H_2), 3.77 (3 H, s, Me), 12.48 (1 H, s, OH); ^{13}C NMR ($CDCl_3$) (HSQC / HMBC) δ 23.4 (2-C), 24.6 (6-C), 30.8 (5-C), 51.7 (Me), 97.2 (3-C), 171.8 (C=O), 172.4 (4-C); MS (ESI) *m/z* 197.0240 $(M + Na)^+$ ($C_7H_{10}NaO_3S$ requires 197.0243).

2-Chloropyridine-3-carboxamide (132).

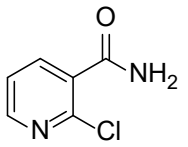

132

Aq. H_2O_2 (35%, 50 mL, 0.47 mol) was added slowly to 2-chloro-3-cyanopyridine **114** (3.0 g, 22 mmol) and KOH (1.2 g, 22 mmol) in EtOH (50 mL). The mixture then was heated at 60-70 °C for 30 min. Further aq. H_2O_2 (35%, 11.4 mL, 12 mmol) was added and heating continued for 30 min more. Evaporation and chromatography (Me_2CO / CH_2Cl_2 1:1) gave **132** (1.49 g, 50%) as a white powder: R_f = 0.5 (Me_2CO / CH_2Cl_2 1:1); mp 161-165 °C (lit.[282] mp 163-165 °C); ^{1}H NMR ($(CD_3)_2$)SO) δ 7.47 (1 H, dd, J = 7.6, 4.8 Hz, 5-H), 7.72 (1 H, br s, NH), 7.87 (1 H, dd, J = 7.6, 2.0 Hz, 4-H), 8.03 (1 H, br, NH), 8.43 (1 H, dd, J = 4.8, 2.0 Hz, 6-H); ^{13}C NMR ($(CD_3)_2$)SO) δ 123.0 (2-C), 133.2 (3-C), 137.8 (4-C), 146.2 (2-C), 150.0 (6-C), 167.0 (C=O); MS (ESI) *m/z*

178.9975 $(M + Na)^+$ ($C_6H_6{}^{35}ClN_2NaO$ requires 178.9988), 157.0160 $(M + H)^+$ ($C_6H_7{}^{35}ClN_2O$ requires 157.0169).

3-Cyano-2-(trimethylsilylethynyl)pyridine (136). Method A.

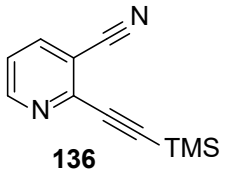

136

CuI (42 mg, 0.22 mmol) and $(Ph_3P)_4Pd$ (127 mg, 0.11 mmol) were placed in a flask, which was degassed and filled with Ar. $Pr^i{}_2NH$ (10 mL) was injected, followed by 2-chloro-3-cyanopyridine **114** (279 mg, 2.2 mmol) in THF (10 mL). The mixture was stirred at 40 °C for 30 min. $Me_3SiC{\equiv}CH$ (436 mg, 4.4 mmol) was added and the mixture was stirred at 40 °C for 24 h. Evaporation and chromatography (petroleum ether / EtOAc 3:1) gave **136** (270 mg, 62%) as a pale grey solid: R_f = 0.4 (petroleum ether / EtOAc 5:1); mp 56-60 °C (lit.[283] mp 55 °C); ^1H NMR ($CDCl_3$) δ 0.31 (9 H, s, $SiMe_3$), 7.38 (1 H, dd, *J* = 8.0, 4.8 Hz, 5-H), 8.00 (1 H, dd, *J* = 8.0, 2.0 Hz, 4-H), 8.60 (1 H, dd, *J* = 4.8, 2.0 Hz, 6-H); ^{13}C ($CDCl_3$) δ 0.0 (Si-C), 100.5 (≡C-Si), 111.6 (≡C), 113.9 (3-C), 116.3 (-C≡N), 122.7 (5-C), 122.9 (4-C), 146.2 (2-C), 153.4 (6-C), MS (ESI) *m/z* 223.0669 $(M + Na)^+$ ($C_{11}H_{12}N_2NaSi$ requires 223.0666), 201.0832 $(M + H)^+$ ($C_{11}H_{13}N_2Si$ requires 201.0846).

3-Cyano-2-(trimethylsilylethynyl)pyridine (136). Method B.

2-Bromo-3-cyanopyridine **115** (184 mg, 1.0 mmol) was stirred with sodium ascorbate (11.9 mg, 60 μmol), CuI (19.2 g, 0.1 mmol) and $(Ph_3P)_2PdCl_2$ (35 mg, 50 μmol) in THF (5.0 mL) and $Pr^i{}_2NH$ (5.0 mL) under Ar for 30 min. $Me_3SiC{\equiv}CH$ (200 mg, 2.0 mmol) was added and mixture was stirred at 40-50 °C for 24 h. Work-up as for method A gave **136** (60 mg, 30%), with properties as above.

3-Cyano-2-ethynylpyridine (137).

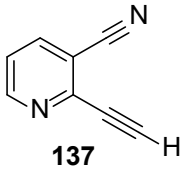

137

CuI (15.2 mg, 0.08 mmol) and $(Ph_3P)_2PdCl_2$ (28 mg, 0.04 mmol) were placed in a flask, which was degassed and filled with Ar. $Pr^i{}_2NH$ (5.0 mL) was injected, followed by **115** (150 mg, 0.8 mmol) in THF (5.0 mL). The mixture was stirred at 40 °C for 30 min. $Me_3SiC{\equiv}CH$ (230 ml, 1.6 mmol) was added and the mixture was stirred at 40 °C for 2 h. Evaporation and chromatography (petroleum ether / EtOAc 3:1) gave **137** (81 mg, 78%) as a pale grey solid: R_f = 0.35 (petroleum ether / EtOAc 3:1); mp 123-126 °C (lit.[287] mp 125 °C); IR ν_{max} 2250 (C≡N), 1617 ($C{=}C_{Ar}$), 1261 (C-Si) cm^{-1}; ^1H NMR ($CDCl_3$) δ

3.57 (1 H, s, C≡CH), 7.39 (1 H, dd, *J* = 8.0, 4.9 Hz, 5-H), 7.96 (1 H, dd, *J* = 8.0, 1.7 Hz, 4-H), 8.78 (1 H, dd, *J* = 4.9, 1.7 Hz, 6-H) ^{13}C ($CDCl_3$) δ 77.5 (ethyne 2-C), 81.8 (ethyne 1-C), 113.6 (3-C), 120.2 (C≡N), 121.0 (5-C), 138.0 (4-C), 143.0 (2-C), 151.0 (6-C).

2-Hydroxy-3-cyanopyridine (139).

3-Cyanopyridin-2-one (140).

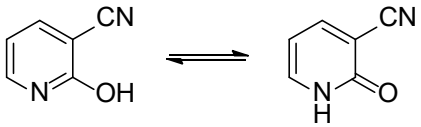

139 **140**

2-Chloro-3-cyanopyridine **114** (3680 mg, 26 mmol) was boiled under reflux with AcOH (100 mL) for 12 h. The evaporation residue, in THF (80 mL) and water (20 mL), was boiled under reflux for 4 h. Evaporation gave **140** (3.12 g, quant.) as white crystals: R_f = 0.25 (petroleum ether / EtOAc 1:3); mp 110-114 °C (lit.[284] 233 °C); ^{1}H NMR ($(CD_3)_2CO$) δ 6.47 (1 H, t, *J* = 6.6 Hz, 5-H), 7.91 (1 H, dd, *J* = 6.5, 2.1 Hz, 4-H), 8.14 (1 H, dd, *J* = 7.0, 2.1 Hz, 6-H), 11.48 (1 H, s, 1-H); ^{13}C NMR ($(CD_3)_2SO$) δ 105.8 (3-C), 124.1 (5-C), 141.9 (≡C), 144.5 (6-H), 150.0 (4-C), 154.2 (2-C); MS (ESI) *m/z* 143.0214 $(M + Na)^+$ ($C_6H_4N_2NaO$ requires 143.0222).

2-Bromonicotinamide (141).

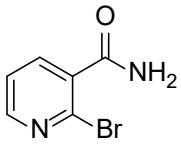

141

Ethyl chloroformate (1160 mg, 10.8 mmol) was added dropwise to an ice-cold mixture of 2-bromopyridine-3-carboxylic acid **126** (2.00 g, 9.2 mmol), dry THF (20 mL) and dry Et_3N (2.0 mL). The mixture was stirred for 1 h at 0 ºC and NH_3 was bubbled through the suspension for 15 min. The mixture was filtered. The solids were washed with hot Me_2CO. The solvent was evaporated from the combined filtrate and washings. The residue was recrystallised from $CHCl_3$ (20 mL) to give **141** as an off-white powder (1.65 g, 89%): R_f 0.25 (petroleum ether / EtOAc 3:1); mp 161-163 ºC (lit.[285] mp 171-172 ºC); ^{1}H NMR ($CDCl_3$) (HSQC / HMBC) δ 7.54 (1 H, dd, *J* = 4.8, 7.5 Hz, 5-H), 7.77 (1 H, br s, NH), 7.86 (1 H, d, *J* = 7.5 Hz, 4-H), 8.07 (1 H, br s, NH), 8.46 (1 H, d, *J* = 4.8 Hz, 6-H); ^{13}C ($CDCl_3$) δ 123.2 (5-C), 136.3 (3-C), 137.1 (2-C), 137.8 (2-C), 150.3 (6-C), 167.6 (C=O); MS (ESI) *m/z* 224.9456 $(M + Na)^+$ ($C_6H_5N_2NNa^{81}Br$ requires 224.9457), 222.9487 $(M + Na)^+$ ($C_6H_5N_2ONa^{79}Br$ requires 222.9477).

3-Cyano-2-(3-hydroxy-3-methylbut-1-yn-1-yl)pyridine (142).

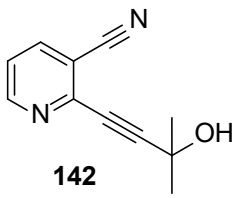

142

2-Bromo-3-cyanopyridine **115** (100 mg, 0.54 mmol), CuI (4.1 mg, 22 μmol), PPh_3 (11.5 mg, 43 μmol) and Pd/C 10% (11.4 mg, 11 μmol Pd) were stirred in a mixture of $MeOCH_2CH_2OMe$ / water (1:1) for 30 min. 2-Methylbut-3-yn-2-ol (113 mg, 1.3 mmol) was added and the mixture was boiled under reflux for 4 h, then cooled, filtered and concentrated. The residue was acidified with aq. HCl (2 M) to pH 2.5 and extracted with toluene. The aqueous layer was basified with solid K_2CO_3 and extracted with EtOAc. The combined organic layers were washed with brine. Drying and chromatography (petroleum ether / EtOAc 1:1) gave **142** (6 mg, 6%) as an orange solid: mp > 210 °C, R_f = 0.2 (petroleum ether / EtOAc 1:3); IR (cm^{-1}): 3434 (OH), 2232 (C≡N), 1672 ($C=C_{Ar}$) cm^{-1}; ^1H NMR ($(CD_3)_2SO$) δ 1.69 (6 H, s, Me_2), 2.19 (1 H, s, OH), 7.67 (1 H, dd, *J* = 7.5, 1.5 Hz, 5-H), 7.95 (1 H, dd, *J* = 7.5, 1.5 Hz, 4-H), 8.75 (1 H, dd, *J* = 5.0, 1.5 Hz, 6-H).

General procedure A for ethynyl(trimethylsilyl)benzenes (144c-e,g).

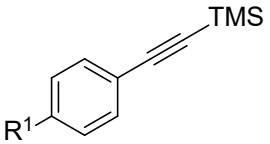

144c-e,g

c: R^1 = OMe; **d**: R^1 = CF_3; **e**: R^1 = Cl; **g**: R^1 = NH_2

The 4-substituted iodobenzene **143** (5.25 mmol) in THF (10 mL) was added to CuI (10 mg, 52.5 μmol) and $(Ph_3P)_2PdCl_2$ **270** (37 mg, 52.5 μmol) in Et_3N (15 mL) under Ar. The mixture was stirred for 10 min at 40 °C. $Me_3SiC{\equiv}CH$ (1.03 g, 10.5 mmol) was injected. The reaction mixture was stirred at 40 °C until completion (defined by TLC). The evaporation residue, in CH_2Cl_2, was washed with water (twice) and dried. Chromatography (petroleum ether / EtOAc 99:1) gave **144c-e,g**.

General procedure B for ethynyl(trimethylsilyl)benzenes (144c-e,g).

Et_3N (10 mL) and THF (10 mL) were added to the 4-substituted iodobenzene (4.5 mmol), CuI (86.4 mg, 450 μmol) and $(Ph_3P)_2PdCl_2$ (157.5 mg, 225 μmol) and sodium ascorbate (89 mg, 450 μmol) under Ar. The mixture was stirred at 40 °C for 30 minutes. $Me_3SiC{\equiv}CH$ (1.03 g, 10.5 mmol) was injected. The mixture was stirred at 40 °C until completion (defined by TLC). The evaporation residue, in CH_2Cl_2, was washed with water (twice) and dried. Chromatography (petroleum ether / EtOAc 99:1) gave **144c-e,g**.

4-Methoxy-1-trimethylsilylethynylbenzene (144c). Yield: 77% (method A), 99% (method B); dark-yellow oil (lit.[286] colourless oil); R_f = 0.9 (petroleum ether / EtOAc 99:1); ^{1}H NMR ($CDCl_3$) δ 0.23 (9 H, s, $SiMe_3$), 3.79 (3 H, s, OMe), 6.80 (2 H, d, *J* = 6.8 Hz, 3,5-H_2), 7.40 (2 H, d, *J* = 6.7 Hz, 2,6-H_2); ^{13}C NMR ($CDCl_3$) δ 0.0 ($SiMe_3$), 55.2 (OMe_3), 92.3 (ethyne C_1), 105.2 (ethyne C_2), 113.8 (2,6-C_2), 115.3 (4-C), 133.4 (3,5-C_2), 159.7 (1-C); MS (ESI) *m/z* 205.1037 $(M + H)^+$ ($C_{12}H_{17}OSi$ requires 205.1049).

4-Trifluoromethyl-1-trimethylsilylethynylbenzene (144d). Yield: 92% (method A); yellow oil (lit.[287] yellowish-buff oil); R_f = 0.9 (petroleum ether / EtOAc 99:1); IR ν_{max} 1323 (C-F), 1511, 1614 (C=C_{Ar}), 2063, 2161 (C≡C) cm^{-1}; ^{1}H NMR ($CDCl_3$) δ 0.27 (9 H, s, $SiMe_3$), 7.54 (4 H, s, 2,3,5,6- H_4); ^{13}C NMR ($CDCl_3$) (HSQC / HMBC) δ 0.0 ($SiMe_3$), 88.1 (ethyne 2-C), 97.1 (ethyne 1-C), 123.9 (q, *J* = 272 Hz, CF_3), 125.1 (q, *J* = 3.9 Hz, 3,5-C_2), 127.0 (1-C), 130.2 (q, *J* = 32.7 Hz, 4-C), 132.2 (2,6-C_2); ^{19}F NMR ($CDCl_3$) δ -62.9 (s, CF_3).

4-Chloro-1-trimethylsilylethynylbenzene (144e): Yield: 96% (method B); buff powder, mp 42-45 °C (lit.[288] colourless prisms, mp 43-45 °C); R_f = 0.95 (CH_2Cl_2); IR ν_{max} 2157 (C≡C), 1643 (C=C_{Ar}), 1588, 825 (Si-Me), 756 (C-Cl) cm^{-1}; ^{1}H NMR ($CDCl_3$) δ 0.24 (9 H, s, $SiMe_3$), 7.26 (2 H, d, *J* = 8.8 Hz, 2,6-C_2), 7.37 (2 H, d, *J* = 8.9 Hz, 3,5-C_2); ^{13}C NMR ($CDCl_3$) δ 0.0 ($SiMe_3$), 95.5 (ethyne 2-C), 121.8 (ethyne 1-C), 115.1 (4-C), 128.7 (2,6-C_2), 133.3 (3,5-C_2), 134.6 (1-C).

4-Trimethylsilylethynylbenzeneamine (144g). Yield: 74% (method A), 37% (method B); R_f = 0.3 (petroleum ether / EtOAc 5:1) pale green solid (lit.[1] solid); mp 94-98 °C (lit.[289] mp 95-96 °C); IR ν_{max} 3467 (NH_2), 2158 (C≡C), 1622 (C=C_{Ar}), 1510 cm^{-1}; ^{1}H NMR ($CDCl_3$) δ 0.22 (9 H, s, $SiMe_3$), 3.77 (2 H, br s, NH_2), 6.56 (2 H, d, *J* = 8.6 Hz, 2,6-H_2), 7.27 (2 H, d, *J* = 8.5 Hz, 3,5-H_2); ^{13}C NMR ($CDCl_3$) δ 0.0 ($SiMe_3$), 91.2 (ethyne 2-C), 105.9 (ethyne 1-C), 112.5 (4-C), 114.4 (2,6-C_2), 133.2 (3,5-C_2), 146.6 (1-C).

4-(Trimethylsilylethynyl)pyridine (144h). Method A.

CuI (9.6 mg, 0.05 mmol), $(Ph_3P)_4Pd$ (28.9 mg, 0.025 mmol), sodium ascorbate (9.9 mg, 0.05 mmol) and 4-iodopyridine (102.5 mg, 0.50 mmol) were placed in a flask, which was degassed and filled with Ar. Pr^i_2NH (5.0 mL) was injected, followed by THF

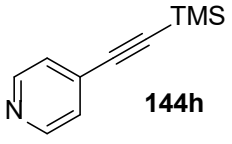

144h

(5.0 mL). The mixture was stirred at 40 °C for 30 min. $Me_3SiC{\equiv}CH$ (48.7 mg, 0.50 mmol) was added and the mixture was stirred at 40 °C for 16 h. Evaporation and chromatography (petroleum ether / EtOAc 3:1) gave **144h** (51 mg, 58%) as a buff oil (lit.[290] colourless oil); R_f = 0.5 (petroleum ether / EtOAc 3:1); ^{1}H NMR ($CDCl_3$) δ 0.27 (9 H, s, $SiMe_3$), 7.29 (2 H, d, *J* = 4.4 Hz, 3,5-H_2) 8.55 (2 H, d, *J* = 4.4 Hz, 2,6-H_2); ^{13}C NMR ($CDCl_3$) (HSQC / HMBC) δ 0.0 ($SiMe_3$), 100.2 (ethyne 2-C), 102.3 (ethyne 1-C), 126.2 (3,5-C_2), 131.5 (4-C), 150.0 (2,6-C_2).

4-(Trimethylsilylethynyl)pyridine (144h). Method B.

CuI (95 mg, 0.50 mmol), $(Ph_3P)_2PdCl_2$ **270** (174.3 mg, 0.25 mmol), sodium ascorbate (98 mg, 0.50 mmol) and 4-bromopyridine hydrochloride (97 mg, 5.0 mmol) were placed in a flask, which was degassed and filled with Ar. Pr^i_2NH (10 mL) was injected, followed by THF (10 mL). The mixture was stirred at 40 °C for 30 min. $Me_3SiC{\equiv}CH$ (531.7 mg, 0.50 mmol) was added and the mixture was stirred at 40 °C for 10 h. Evaporation and chromatography (petroleum ether / EtOAc 5:1 → 3:1) gave **144h** (767 mg, 89%) with properties as above.

((4-Benzyloxyphenyl)ethynyl)trimethylsilane (144j).

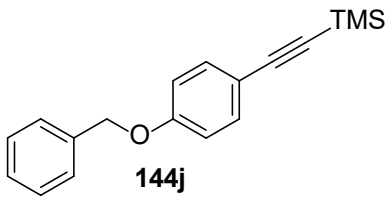

144j

Pr^i_2NH (10 mL) and THF (10 mL) were added to **146** (1.08 g, 3.48 mmol), CuI (67 mg, 0.35 mmol), $(Ph_3P)_2PdCl_2$ **270** (122 mg, 0.174 mmol) and sodium ascorbate (69 mg, 0.348 mmol) under Ar. The mixture was stirred at 40°C for 30 min. $Me_3SiC{\equiv}CH$ (336 mg, 3.5 mmol) was injected. The mixture was stirred at 40 °C until completion (defined by TLC). The evaporation residue, in CH_2Cl_2, was washed with water (twice) and dried. Chromatography (petroleum ether / EtOAc 99:1) gave **144j** (1.76 g, 92%); mp 45-47 °C (lit.[291] mp 50 °C); R_f = 0.4 (petroleum ether / EtOAc 99:1); IR ν_{max} 2157 (C≡C), 1602 (C=C_{Ar}), cm^{-1}; ^{1}H NMR ($CDCl_3$) δ 0.25 (9 H, s, $SiMe_3$), 5.06 (2 H, s, CH_2), 6.89 (2 H, d, *J* = 6.8 Hz, 3,5-H_2), 7.25-7.40 (7 H, m, 2,6-H_2, Ph 2,3,4,5,6-H_5); ^{13}C NMR ($CDCl_3$) (HSQC / HMBC) δ 0.0 ($SiMe_3$), 70.0 (CH_2), 92.5 (ethyne 2-C), 105.1 (ethyne 1-C), 114.7 (3,5-C_2), 115.3 (1-C), 127.4 (Ph 2,6-C_2), 128.0 (Ph 4-C), 128.6 (Ph 3,5-C_2), 133.4 (2,6-C_2), 136.5 (Ph 1-C), 158.87 (4-C).

General procedure for ethynylbenzenes (145c-e,g).

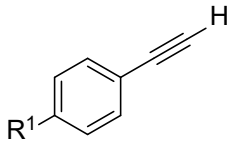

145c-e,g

c: R^1 = OMe; **d**: R^1 = CF_3; **e**: R^1 = Cl; **g**: R^1 = NH_2

Compounds **144c-e,g** (4.9 mmol) in THF (100 mL) were stirred with Bu_4NF in THF (1.0 M, 10 mL) for 16 h. Saturated aq. $NaHCO_3$ was added and the mixture was extracted with Et_2O (3 × 30 mL). The aqueous layer was further extracted twice with Et_2O (3 × 30 mL). The combined organic layers were dried. Chromatography (petroleum ether / EtOAc 19:1) gave **145c-e,g**.

1-Ethynyl-4-methoxybenzene (145c). Yield: 92%; pale yellow oil (lit.[292] colourless oil); R_f = 0.9 (petroleum ether / EtOAc 19:1); IR ν_{max} 2158 (C≡C), 1607 (C=C_{Ar}), 1570, 1507 cm^{-1}; ^1H NMR ($CDCl_3$) δ 2.98 (1 H, s, C≡CH), 3.80 (3 H, s, Me), 6.83 (2 H, d, *J* = 9.5 Hz, 3,5-H_2), 7.42 (2 H, d, *J* = 9.4 Hz, 2,6-H_2); ^{13}C NMR ($CDCl_3$) δ 55.2 (OMe), 67.9 (ethyne 2-C), 83.6 (ethyne 1-C), 113.9 (2,6-C_2), 114.1 (4-C), 133.5 (3,5-C_2), 159.9 (1-C).

1-Ethynyl-4-trifluoromethylbenzene (145d). Yield: 57%; colourless oil (lit.[293] oil); R_f = 0.85 (petroleum ether / EtOAc 19:1); IR ν_{max} 1519 (C=C_{Ar}), 1323 (C-F) cm^{-1}; ^1H NMR ($CDCl_3$) δ 3.18 (1 H, s, C≡CH), 7.58 (4 H, s, 2,3,5,6-H_4), ^{13}C NMR ($CDCl_3$) (HSQC) δ 79.5 (ethyne 2-C), 82.1 (ethyne 1-C), 123.8 (q, *J* = 288 Hz, CF_3), 125.2 (2,6-C_2), 125.9 (4-C), 130.6 (q, *J* = 33 Hz, 4-C), 132.3 (3,5-C_2), 1-C not observed; ^{19}F NMR ($CDCl_3$) δ -63.0 (s, CF_3).

4-Chloro-1-ethynylbenzene (145e). Yield: 57%; shiny amber powder, mp 41-44 °C (lit.[294] mp 45-46 °C); R_f = 0.65 (petroleum ether / EtOAc 1:3); IR ν_{max} 2154 (C≡C), 1645 (C=C_{Ar}), 1589, 1488, 756 (C-Cl); ^1H NMR ($CDCl_3$) δ 3.09 (1 H, s, C≡CH), 7.29 (2 H, d, *J* = 8.8 Hz, 3,5-H_2), 7.41 (2 H, d, *J* = 8.9 Hz, 2,6-H_2); ^{13}C NMR ($CDCl_3$) δ 78.1 (ethyne 2-C), 85.5 (ethyne 1-C), 120.6 (4-C), 128.6 (3,5-C_2), 133.3 (2,6-C_2), 134.9 (1-C).

4-Ethynylbenzeneamine (145g). Yield: 77%; pale green solid; mp 81-85 °C (lit.[295] mp 88-90 °C); R_f = 0.35 (petroleum ether / EtOAc 3:1); IR 3486 (NH), 3388 (NH), 2095 (C≡C), 1619 (C=C_{Ar}), 1513 cm^{-1}; ^1H NMR ($CDCl_3$) δ 2.95 (1 H, s, C≡CH), 3.79 (2 H, s, NH_2), 6.58 (2 H, d, *J* = 7.6 Hz, 2,6-H_2), 7.28 (2 H, d, *J* = 7.7 Hz, 3,5-H_2); ^{13}C NMR

($CDCl_3$) (HSQC) δ 74.8 (ethyne 2-C), 84.3 (ethyne 1-C), 111.3 (4-C), 114.5 (2,6-C_2), 133.4 (3,5-C_2), 146.9 (1-C).

4-(Trimethylsilylethynyl)pyridine (145h).

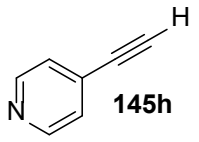

145h

Compound **144h** (2300 mg, 13.1 mmol) in THF (30 mL) was stirred at 40 °C with Bu_4NF in THF (1.0 M, 30 mL) for 10 h. Saturated aq. $NaHCO_3$ was added and the mixture was extracted with EtOAc (3 × 30 mL). The aqueous layer was further extracted twice with EtOAc (3 × 30 mL). The combined organic layers were dried. Chromatography (petroleum ether / EtOAc 3:1) gave **145h** (550 mg, 42%) as an ivory-coloured powder with a strong unpleasant smell: R_f = 0.3 (petroleum ether / EtOAc 3:1); mp 51-54 °C (lit.[296] 63-65 °C); IR ν_{max} 3378 (C-H), 2925 (C≡C), 1641 (C=C_{Ar}), 1594, cm^{-1}; ^1H NMR ($CDCl_3$) δ 3.28 (1 H, s, C≡CH), 7.33 (2 H, d, *J* = 5.8 Hz, 3,5-H_2) 8.59 (2 H, m, 2,6-H_2); ^{13}C NMR ($CDCl_3$) (HSQC / HMBC) δ 60.3 (ethyne 1-C), 80.9 (ethyne 2-C), 126.2 (3,5-C_2), 130.3 (4-C), 149.7 (2,6-C_2).

1-(Benzyloxy)-4-ethynylbenzene (145j).

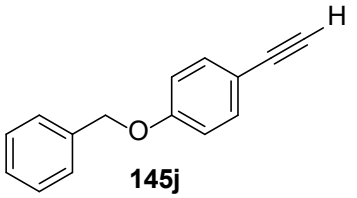

145j

Compound **144j** (1760 mg, 6.33 mmol) in THF (100 mL) was stirred with Bu_4NF in THF (1.0 M, 20 mL) for 16 h. Saturated aq. $NaHCO_3$ was added and the mixture was extracted with Et_2O (3 × 30 mL). The aqueous layer was further extracted twice with Et_2O (3 × 30 mL). The combined organic layers were dried. Chromatography (petroleum ether / Et_2O 95:5) gave **145j** (947 mg, 72%) as an ivory-coloured powder: mp = 64-65 °C (lit.[297] mp 65 °C); R_f = 0.8 (petroleum ether / Et_2O 19:1); IR ν_{max} 3272 (C-H), 2104 (C≡C), 1600 (C=C_{Ar}), cm^{-1}; ^1H NMR ($CDCl_3$) δ 3.00 (1 H, s, C≡CH), 5.07 (2 H, s, CH_2), 6.92 (2 H, d, *J* = 8.8 Hz, 2,6-H_2), 7.25-7.57 (7 H, m, 3,5-H_2, Ph 2,3,4,5,6-H_5); ^{13}C NMR ($CDCl_3$) (HSQC / HMBC) δ 70.0 (CH_2), 75.8 (ethyne 2-C), 83.6 (ethyne 1-C), 114.8 (1-C), 115.0 (3,5-C_2), 127.4 (Ph 2,6-C_2), 128.0 (Ph 4-C), 128.6 (Ph 3,5-C_2), 133.6 (2,6-C_2), 136.5 (Ph 1-C), 159.1 (4-C).

1-Benzyloxy-4-iodobenzene (146). Method A.

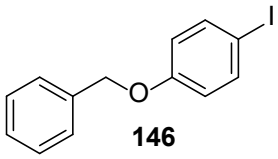

146

Dry DMF (10 mL) was added to 4-iodophenol **143i** (2000 mg, 9.1 mmol) and K_2CO_3 (1570 mg, 11.4 mmol), to which was

added BnBr (2.16 g, 12.5 mmol). The mixture was stirred at 20 °C for 2 h and at 60 °C for 1 h. The mixture was cooled, diluted with water (10 mL) and extracted with EtOAc (6 × 10 mL). The organic extract was washed with water and brine and dried. The evaporation residue was purified by chromatography (petroleum ether / EtOAc, 99:1), which gave **146** (1560 mg, 55%) as white crystalline powder: mp 59-61 °C (lit.[298] mp 60-62 °C); R_f = 0.8 (petroleum ether / EtOAc 99:1); IR ν_{max} 1582 (C=C_{Ar}) cm^{-1}; ^1H NMR ($CDCl_3$) (HSQC / HMBC) δ 4.99 (2 H, s, CH_2), 6.76 (2 H, d, *J* = 9.0 Hz, 5.3 Hz, 3,5-H_2), 7.31-7.43 (5 H, m, Ph 2,3,4,5,6-H_5), 7.56 (2 H, d, *J* = 9.0 Hz, 5.3 Hz, 2,6-H_2); ^{13}C NMR ($CDCl_3$) δ 70.1 (CH_2), 83.0 (4-C), 117.3 (2,6-C_2), 127.4 (Ph 3,5-C_2), 128.1 (Ph 4-C), 128.6 (Ph 2,6-C_2), 136.5 (Ph 1-C), 138.2 (3,5-C_2), 158.6 (1-C).

1-(Benzyloxy)-4-iodobenzene (146). Method B.

Dry DMF (10 mL) was added to 4-iodophenol (1000 mg, 4.6 mmol) and Cs_2CO_3 (1500 mg, 4.6 mmol). To the suspension was added BnBr (389 mg, 4.7 mmol). The mixture was stirred at r.t. for 1.5 h. Then the mixture was cooled, diluted by water (10 mL) and extracted with EtOAc (3 × 20 ml). The organic extract was washed with water and brine, dried over $MgSO_4$ and purified by flash chromatography (petroleum ether / EtOAc, 99:1) to give **146** (1200 mg, 82%) with properties as above.

1-(Benzyloxy)-4-iodobenzene (146). Method C.

To 4-iodophenol (1000 mg, 4.6 mmol) in dry DMF (10 mL) was added NaH (60% in mineral oil, 155 mg, 4.6 mmol). To that mixture was added BnBr (389 mg, 4.7 mmol). The mixture was stirred for 2 h. Then the mixture was diluted with water (10 mL) and extracted with EtOAc (3 × 20 mL). The organic extract was washed with water and brine and dried. Chromatography (petroleum ether / EtOAc, 99:1) gave **146** (1080 mg, 76%) with properties as above.

3-Bromopyridine-4-carboxaldehyde (159).

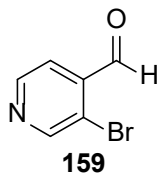

159

To a THF solution (50 mL) of LDA, prepared from $^iPr_2NH$ (1130 mg, 12 mmol) and *n*-BuLi (6.25 mL, 1.6 M in hexane, 10 mmol), 3-bromopyridine **158** (1570 mg, 10 mmol) in THF (5.0 mL) was added dropwise at -78°C under Ar. The solution was stirred for 10 min at -78 °C. DMF (2190 mg, 30 mmol) in THF solution (10 mL) was then added. The mixture was stirred for 1 h at -78 °C, warming to 20 °C during 1 h. The

mixture was poured into cold stirred 5% $NaHCO_3$ (50 mL) and diluted with Et_2O (100 mL). The organic layer was separated. The aqueous layer was extracted with Et_2O (3 × 50 ml). The combined organic solution was washed with brine (2 × 100 mL) and dried. Evaporation and chromatography (petroleum ether : EtOAc, 3:1) gave **159** (750 mg, 40%) as a white needles: mp = 65-69 °C (lit.[111] 80-82 °C); R_f 0.4 (petroleum ether : EtOAc, 3:1); ^{1}H NMR ($CDCl_3$) δ 7.68 (1 H, d, *J* = 4.8 Hz, 5-H), 8.71 (1 H, d, *J* = 4.8 Hz, 6-H), 8.99 (1 H, s, 2-H), 10.36 (1 H, s, CHO); ^{13}C NMR ($CDCl_3$) (HSQC / HMBC) δ 122.0 (5-C), 124.7 (3-C), 138.7 (4-C), 147.8 (2-C), 149.3 (6-C), 190.5 (C=O).

3-Bromopyridine-4-carboxaldehyde oxime (160).

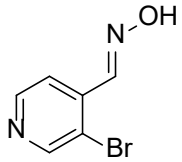

160

Compound **159** (210 mg, 1.1 mmol) and NaOAc (112 mg, 1.38 mmol) were suspended in water (200 mL) and heated to 100 °C. $H_2NOH{\cdot}HCl$ (114 mg, 1.65 mmol) was added to the mixture. The mixture was removed from heat and stirred for 5 min while cooling to 0 °C. The precipitate was collected by filtration and washed with ice-cold water to give **160** (224 mg, 99%) as a white fibrous crystalline material: mp = 95-97 °C IR υ_{max} 3437 (br, OH), 1587, 649 (C-Br) cm^{-1}; ^{1}H NMR ($CDCl_3$) δ 7.70 (1 H, d, *J* = 5.0 Hz, 5-H), 7.94 (1 H, s, OH), 8.44 (1 H, s, oxime CH), 8.50 (1 H, d, *J* = 4.9 Hz, 6-H), 8.76 (1 H, s, 2-H) ^{13}C NMR ($CDCl_3$) (HSQC / HMBC) δ 120.8 (3,5-C_2), 139.5 (4-C), 148.0 (C=N), 148.2 (6-C), 153.2 (2-C). This material was used directly in the next step without further purification.

3-Bromopyridine-4-carboxylic acid (161).

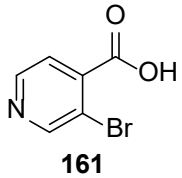

161

To a dry ice-cold solution of LDA (5360 mg, 1.5 mmol) was added 3-bromopyridine **158** (164 mg, 1 mmol) and the mixture was stirred at -78 °C for 30 min under Ar. Crushed dry ice was added under Ar, and then the cooling was removed. The mixture was stirred until reaching room temperature. Water (10 mL) was added. The organic solvents were evaporated. The residue was washed with Et_2O (3 × 20 mL) and the aqueous layer was collected. To the aqueous layer, conc. aq. HCl was added to pH 3. The mixture was stirred for 1 h and extracted with EtOAc (3 × 20 mL). The organic layers were combined and washed with brine and dried. Evaporation gave **161** (20 mg, 10%) as white needles: mp 175-176 ºC (decomposition); ^{1}H NMR ($(CD_3)_2SO$) δ 7.71 (1 H, d, *J* = 4.8 Hz, 6-H), 8.70 (1 H, d, *J* = 4.9 Hz, 5-H), 8.91 (1 H, s, 2-H) 12.56 (1 H, br s, OH); ^{13}C NMR ($CDCl_3$) (HSQC / HMBC) δ 117.3 (4-C), 123.8 (6-C), 148.9 (5-C), 152.6 (2-

C), 165.0 (C=O), 166.1 (3-C); MS (ESI) *m/z* 201.9335 $(M + H)^+$ ($C_6H_5{}^{79}BrNO_2$ requires 201.9504), 201.9458 $(M + H)^+$ ($C_6H_5{}^{81}BrNO_2$ requires 203.948396).

3-Bromopyridine-4-carboxamide (162) and ethyl 3-bromoisonicotinate (165).

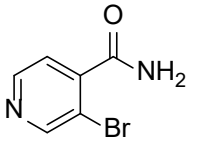

162

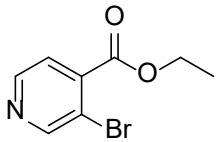

165

Ethyl chloroformate (580 mg, 5.4 mmol) was added dropwise to an ice-cold mixture of **161** (1000 mg, 4.6 mmol), dry THF (15 mL) and dry Et_3N (1.0 mL). The mixture was stirred for 1 h at 0 ºC, then NH_3 was bubbled through the suspension for 15 min. The mixture was filtered. The solids were washed with hot Me_2CO and discarded. The solvent was evaporated from the combined filtrate and washings. The residue was recrystallised from EtOH to give **162** as an off-white powder (777 mg, 78%): R_f 0.25 (petroleum ether / EtOAc 3:1); mp 149-150 ºC; ^1H NMR ($CDCl_3$) δ 7.48 (1 H, d, *J* = 4.8 Hz, 5-H), 7.88 (1 H, br s, NH), 8.11 (1 H, br s, NH), 8.65 (1 H, d, *J* = 4.8 Hz, 6-H), 8.84 (1 H, s, 2-H); ^{13}C NMR ($CDCl_3$) (HSQC / HMBC) δ 116.8 (3-C), 122.7 (5-C), 146.0 (4-C), 148.6 (6-C), 151.7 (2-C), 167.0 (C=O); MS (ESI) *m/z* 224.9469 (M + Na) ($C_6H_5{}^{81}BrN_2NaO$ requires 224.9457), 222.9485 (M + Na) ($C_6H_5{}^{79}BrN_2NaO$ requires 222.9477). Evaporation of the solvent from the mother liquor gave **165** (0.06 g, 4.8%) as a yellow liquid: R_f 0.85 (petroleum ether / EtOAc 3:1); ^1H NMR ($CDCl_3$) δ 1.41 (3 H, t, *J* = 7.2 Hz, Me), 4.43 (2 H, q, *J* = 7.3 Hz, CH_2), 7.59 (1 H, d, *J* = 4.9 Hz, 5-H), 8.59 (1 H, d, *J* = 4.9 Hz, 6-H), 8.83 (1 H, s, 2-H); ^{13}C NMR ($CDCl_3$) (HSQC / HMBC) δ 14.0 (Me), 62.3 (CH_2), 118.7 (3-C), 124.2 (5-C), 139.3 (4-C), 148.4 (6-C), 153.6 (2-C), 164.5 (C=O); MS (ESI) *m/z* 253.9623 $(M + Na)^+$ ($C_8H_8{}^{81}BrNNaO_2$ requires 253.9611), 251.9638 $(M + Na)^+$ ($C_8H_8{}^{79}BrNNaO_2$ requires 251.9631).

1,3-Di(pyridin-4-yl)propane-1,3-dione (166).
3-Hydroxy-1,3-di(pyridin-4-yl)prop-2-en-1-one (167).

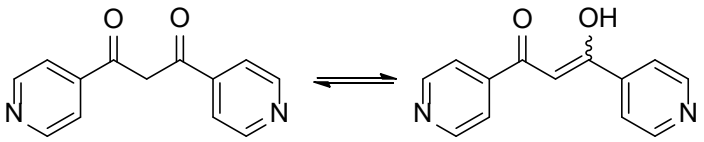

166

167

To an oven-dried 50 mL round-bottom flask was added NaH (1000 mg, 25 mmol, 60% in oil); this material was washed free from oil with dry hexane (10 mL) at 0 ºC under Ar. Dry THF (30 mL) was added to give a suspension. To this suspension were added **169** (1510 mg, 11 mmol) in dry THF (10 mL) and 4-

acetylpyridine **168** (1210 mg, 10 mmol) in dry THF (10 mL) at 0 ºC under Ar. The suspension was stirred under reflux for 16 h. After cooling to 20 °C, the mixture was filtered through Celite®, which was washed with EtOH (20 mL). The filtrate was poured into a mixture of Et_2O, water and aq. HCl (45.2 mL) to pH 4.5. The precipitate was collected by filtration and was washed with petroleum ether to give enol form **167** (960 mg, 42%) as buff needles: R_f 0.15 (petroleum ether / EtOAc 1:3); mp 158-159 ºC (lit.[236] 156-157 ºC); ^{1}H NMR ($(CD_3)_2SO$) (enol form) δ 7.77 (1 H, s, CH), 8.34 (4 H, d, *J* = 5.0 Hz, 2 × pyridine 3,5-H_2), 9.01 (4 H, d, *J* = 5.1 Hz, 2 × pyridine 2,6-H_2); ^{13}C NMR ($(CD_3)_2SO$) (HSQC / HMBC) δ 97.5 (CH), 121.8 (2 × pyridine 3,5-C_2), 144.0 (2 × pyridine 4-C), 148.7 (2 × pyridine 2,6-C_2), 184.0 (C=O, C-OH); MS (ESI) *m/z* 227.0826 $(M + H)^+$ ($C_{13}H_{11}N_2O_2$ requires 227.0815).

1-(Pyridin-4-yl)butane-1,3-dione (170).

3-Hydroxy-1-(pyridin-4-yl)but-2-en-1-one (176). Method A.

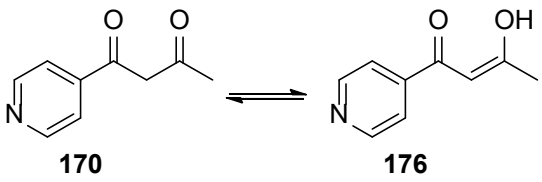

170 **176**

To a stirred solution of methyl pyridine-4-carboxylate **175** (2000 mg, 14.6 mmol) in dry Me_2CO (3.5 mL, 48 mmol) and dry THF (10 mL) at 40 °C was added MeONa (810 mg, 15 mmol) during 15 min. The mixture was stirred at 20 °C for 30 min, then heated under reflux for 2.5 h. Five additional portions of THF (5 mL) were added. The reaction mixture was cooled. The precipitate was collected, washed with Et_2O (50 mL) and dissolved in water (10 mL). The aqueous solution was acidified with AcOH (0.9 mL) to pH 5 and extracted with $CHCl_3$ (4 × 25 ml). The solvent was evaporated from the combined organic layers to give **176** (enol form) (620 mg, 27%) as a colourless oil, which solidified on standing: R_f 0.3 (petroleum ether / EtOAc 3:1), mp = 72-74 °C (lit.[238] 71-73 ºC); ^{1}H NMR ($CDCl_3$) δ 2.23 (3 H, s, Me), 6.20 (1 H, s, 2-H), 7.67 (2 H, d, *J* = 4.5 Hz, pyridine 3,5-H_2), 8.73 (2 H, dd, *J* 4.5 Hz, pyridine 2,6-H_2), 15.70 (1 H, br s, OH); ^{13}C NMR ($CDCl_3$) (HSQC / HMBC) δ 26.6 (Me), 97.8 (2-C), 120.4 (pyridine 3,5-C_2), 142.1 (pyridine 4-C), 150.0 (pyridine 2,6-C_2), 178.4 (3-C), 196.8 (C=O); MS (ESI) *m/z* 164.0704 $(M + H)^+$ ($C_9H_9NO_2$ requires 164.0712).

3-Hydroxy-1-(pyridin-4-yl)but-2-en-1-one (176). Method B.

To a mixture of NaH (60% wt in oil, 584 mg, 14.6 mmol) and methyl pyridine-4-carboxylate **175** (2000 mg, 14.6 mmol) in dry THF (10 mL) at 0 °C was added dropwise a mixture of Me_2CO (2770 mg, 48 mmol) and dry THF (1.0 mL). The mixture was stirred under reflux for 2.5 h, cooled and acidified to pH 5 with aq. HCl (1 M, 10 mL). The solution was extracted with Et_2O (2 × 25 mL). The combined organic layers were washed with sat. aq. $NaHCO_3$ and dried. The solvent was evaporated and the the residue was washed with petroleum ether and water to give **176** (1480 mg, 62%) with properties as above.

1-(4-Chlorophenyl)butane-1,3-dione (183a).
1-(4-Chlorophenyl)-3-hydroxybut-2-en-1-one (183b).

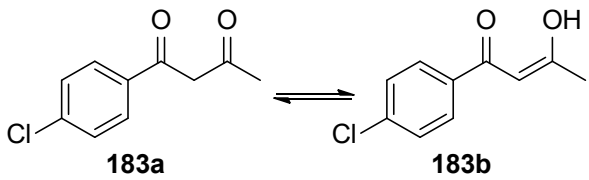

183a **183b**

To an ice-cold suspension of NaH (60% in oil, 100 mg, 2.5 mmol) in dry THF (2.5 mL) were added dropwise methyl 4-chlorobenzoate **177** (425 mg, 2.5 mmol) in dry THF (1.0 mL) and Me_2CO (197.8 mg, 3.4 mmol) in dry THF (1.0 ml).The mixture was stirred under reflux for 3 h, then was cooled and acidified to pH 4 with aq. HCl (2 M, 5.0 mL). The solution was extracted with Et_2O (2 × 25 mL). The combined organic layers were dried and the solvent was evaporated. The residue was washed with petroleum ether and water to give enol form **183b** (250 mg, 51%) as a yellow powder: R_f = 0.9 (petroleum ether / EtOAc 1:3); mp 208-210 °C (lit.[299] 112-116 °C); ^{1}H NMR ($CDCl_3$) δ 2.19 (3 H, s, Me), 6.13 (1 H, s, 2-H), 7.40 (2 H, d, *J* = 8.8 Hz, Ph 3,5-H_2), 7.80 (2 H, d, *J* = 8.8 Hz, Ph 3,5-H_2), 16.05 (1 H, br s, OH); ^{13}C NMR ($CDCl_3$) (HSQC / HMBC) δ 25.7 (Me), 96.6 (2-C), 128.3 (Ph 2,6-C_2), 129.1 (Ph 3,5-C_2), 133.3 (Ph 1-C), 138.5 (Ph 4-C), 182.2 (COH), 193.7 (C=O); MS (ESI) *m/z* 221.0155 $(M + Na)^+$ ($C_{10}H_9{}^{37}ClNaO_2$ requires 221.0153), 219.0176 $(M + Na)^+$ ($C_{10}H_9{}^{35}ClNaO_2$ requires 219.0183).

1-(4-(Trifluoromethyl)phenyl)butane-1,3-dione (184a).
3-Hydroxy-1-(4-trifluoromethylphenyl)but-2-en-1-one (184b).

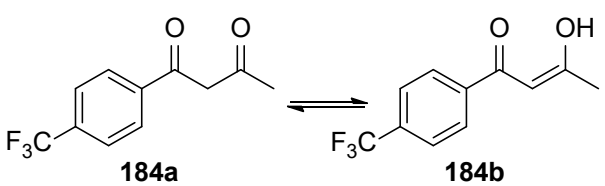

184a **184b**

To an ice-cold suspension of NaH (60% in oil, 116 mg, 2.9 mmol) in dry THF (2.5 mL) were added

dropwise methyl 4-trifluoromethylbenzoate **178** (596 mg, 2.9 mmol) in dry THF (1.0 mL) and Me_2CO (229 mg, 3.9 mmol) in dry THF (1.0 mL).The mixture was stirred under reflux for 2.5 h, then was cooled and acidified to pH 4 with aq. HCl (2 M, 5.0 mL). The solution was extracted with Et_2O (2 × 25 ml). The combined organic layers were dried. The solvent was evaporated to give enol form **184b** (303 mg, 45%) as a waxy yellow solid: R_f = 0.9 (petroleum ether / EtOAc 1:3); mp 36-38 °C; ^{1}H NMR ($CDCl_3$) δ 2.23 (3 H, s, Me), 6.19 (1 H, s, 2-H), 7.70 (2 H, d, *J* = 8.3 Hz, Ph 2,6-H_2), 7.96 (2 H, d, *J* = 8.2 Hz, Ph 3,5-H_2), 15.97 (1 H, br s, OH); ^{13}C NMR ($CDCl_3$) (HSQC / HMBC) δ 26.1 (Me), 97.3 (2-C), 101.0 (q, *J* = 269.7 Hz, CF_3), 125.5 (q, *J* = 3.7 Hz, Ph 3,5-C_2), 127.2 (Ph 2,6-C_2), 132.0 (Ph 1-C), 139.0 (Ph q, *J* = 30 Hz, 4-C), 181.0 (COH), 196.0 (C=O); ^{19}F NMR ($CDCl_3$) δ -61.5 (CF_3); MS (ESI) *m/z* 253.0453 $(M + Na)^+$ ($C_{11}H_9F_3NaO_2$ requires 253.0447).[300]

1-(4-Bromophenyl)butane-1,3-dione (185a).

1-(4-Bromophenyl)-3-hydroxybut-2-en-1-one (185b).

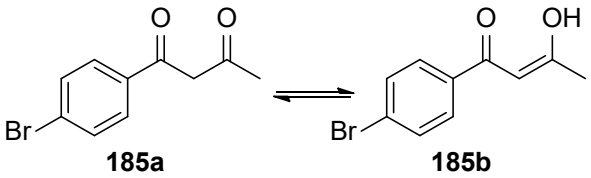

185a **185b**

To an ice-cold suspension of NaH (60% wt in oil, 40 mg, 1.0 mmol) in dry THF (2.5 mL) were added dropwise methyl 4-bromobenzoate **179** (215 mg, 1.0 mmol) in dry THF (1.0 mL) and Me_2CO (79.1 mg, 1.4 mmol) in dry THF (1.0 mL).The mixture was stirred under reflux for 3 h, then was cooled and acidified to pH 4 with aq. HCl (2 M, 5.0 mL). The solution was extracted with Et_2O (2 × 25 mL). The combined organic layers were dried and the solvent was evaporated. The residue was washed with petroleum ether and water to give enol form **185b** as a yellow solid (80 mg, 33%): R_f = 0.8 (petroleum ether / EtOAc 1:3); mp 71-73 °C (lit.[301] 92-93 °C); ^{1}H NMR ($CDCl_3$) δ 2.20 (3 H, s, Me), 6.13 (1 H, s, 2-H), 7.57 (2 H, d, *J* = 8.6 Hz, Ph 3,5-H_2), 7.94 (2 H, d, *J* = 8.5 Hz, Ph 2,6-H_2), 16.00 (1 H, br s, OH); ^{13}C NMR ($CDCl_3$) (HSQC / HMBC) δ 31.0 (Me), 96.6 (CH), 127.0 (Ph 4-C), 128.4 (Ph 2,6-C_2), 131.8 (Ph 3,5-C_2), 133.5 (Ph 1-C), 195.0 (COH), 211.0 (C=O); MS (ESI) *m/z* 264.9658 $(M + Na)^+$ ($C_{10}H_9{}^{81}BrNaO_2$ requires 264.9687), 262.9678 $(M + Na)^+$ ($C_{10}H_9{}^{79}BrNaO_2$ requires 262.9684).

1,3-bis(4-Chlorophenyl)propane-1,3-dione (197a).

1,3-bis(4-Chlorophenyl)-3-hydroxyprop-2-en-1-one (197b).

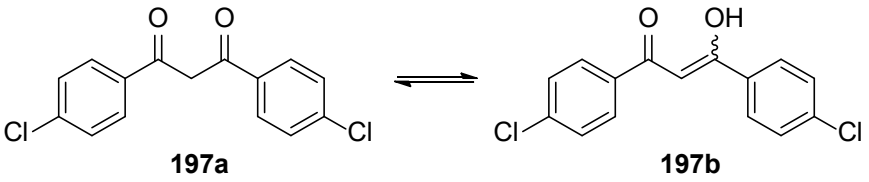

197a **197b**

To an oven-dried 100 mL round-bottom flask was added NaH (100 mg, 2.5 mmol, 60% in oil); this material was washed free from oil with dry hexane (5.0 mL) at 0 ºC under Ar. Dry THF (10 mL) was added to give a suspension. To this suspension were added methyl 4-chlorobenzoate **177** (187.5 mg, 1.1 mmol) in dry THF (5.0 mL) and 4-chloroacetophenone **192** (154.5 mg, 1.0 mmol), dried over activated 4 Å-molecular sieves, in dry THF (5.0 mL) at 0 ºC under Ar. The suspension was stirred under reflux for 16 h. After cooling to 20 ºC, the mixture was filtered through Celite®, which was washed with EtOH (10 mL). The filtrate was poured into a mixture of Et_2O (5.0 mL) and aq. HCl (1 M, 5.0 mL). The ethereal layer was separated. The aqueous layer was extracted with Et_2O (2 × 20 mL). The combined organic layers were washed with brine (3 × 20 mL) and dried. The solvent was evaporated. The residue was recrystallised from EtOH to give **197b** as a shiny dark-pink plates (200 mg, 68%): R_f 0.85 (petroleum ether / EtOAc 3:1); mp 130-131 ºC (lit.[302] 157.5-159.5 ºC); ^{1}H NMR ($CDCl_3$) (enol form) δ 6.70 (1 H, s, CH), 7.40 (4 H, d, J = 8.5 Hz, 2 × Ph 3,5-H_2), 7.85 (4 H, d, J = 8.5 Hz, 2 × Ph 2,6-H_2); ^{13}C NMR ($CDCl_3$) (HSQC / HMBC) δ 92.8 (CH), 128.5 (2 × Ph 2,6-C_2), 129.0 (2 × Ph 3,5-C_2), 133.7 (2 × Ph 1-C), 138.9 (2 × Ph 4-C), 184.7 (C=O, C-OH); MS (ESI) *m/z* 316.9863 $(M + Na)^+$ ($C_{15}H_{10}{}^{35}Cl^{37}ClNaO_2$ requires 316.9923), 314.9948 $(M + Na)^+$ ($C_{15}H_{10}{}^{35}Cl_2NaO_2$ requires 314.9950).

1,3-bis(4-Trifluoromethylphenyl)propane-1,3-dione (198a).

1,3-bis(4-Trifluoromethylphenyl)-3-hydroxyprop-2-en-1-one (198b).

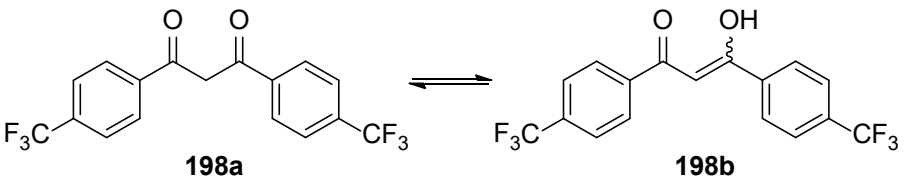

198a **198b**

To an oven-dried 50 mL round-bottom flask was added NaH (1000 mg, 25 mmol, 60% in oil); this material was washed free from oil with dry hexane (10 mL) at 0

ºC under Ar. Dry THF (10 mL) was added to give a suspension. To that suspension were added methyl 4-(trifluoromethyl)benzoate **178** (2240 mg, 11 mmol) in dry THF (10 mL) and 1-(4-(trifluoromethyl)phenyl)ethanone **193** (1885 mg, 10 mmol) in dry THF (10 mL) at 0 ºC under Ar. The suspension was stirred under reflux for 16 h. After cooling to 20 °C, the mixture was filtered through Celite®, which was washed with EtOH (20 mL). The filtrate was poured into a mixture of Et_2O (20 mL) and aq. HCl (1 M, 20 mL). The ethereal layer was separated. The aqueous layer was extracted with Et_2O (2 × 40 mL). The combined organic layers were washed with brine (3 × 40 mL) and dried. The solvent was evaporated. The residue was recrystallised from EtOH to give enol form **198b** as an ivory-coloured powder (2035 mg, 57%): R_f 0.85 (petroleum ether / EtOAc 3:1); mp 116-117 ºC (lit.[303] 130 ºC); ^{1}H NMR ($CDCl_3$) (enol form) δ 6.91 (1 H, s, CH), 7.80 (4 H, s, 2 × Ph 3,5-H_2), 8.12 (4 H, s, 2 × Ph 2,6-H_2); ^{13}C NMR ($CDCl_3$) (HSQC / HMBC) δ 94.2 (CH), 122.5 (2 × Ph 1-C), 124.7 (q, J = 270.8 Hz, 2× CF_3,), 125.8 (q, J = 3.5 Hz, 2 × Ph 3,5-C_2), 127.6 (2 × Ph 2,6-C_2), 134.3 (q, J = 32.8 Hz, 2 × Ph 4-C,), 184.7 (C=O, C-OH); MS (ESI) *m/z* 383.0466 $(M + Na)^+$ ($C_{17}H_{10}F_6NaO_2$ requires 383.0477).

1,3-bis(4-Bromophenyl)propane-1,3-dione (199a).
1,3-bis(4-Bromophenyl)-3-hydroxyprop-2-en-1-one (199b).

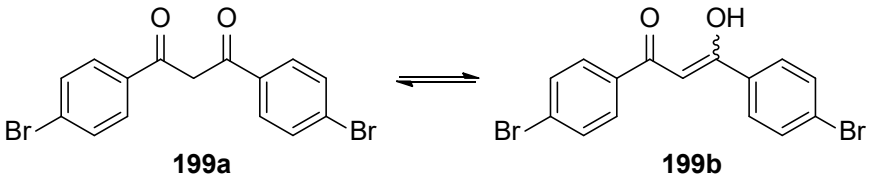

To an oven-dried 100 mL round-bottom flask was added NaH (2000 mg, 50 mmol, 60% in oil); this material was washed free from oil with dry hexane (10 mL) at 0 ºC under Ar. Dry THF (30 mL) was added to give a suspension. To this suspension were added methyl 4-bromobenzoate **179** (4730 mg, 22 mmol) in dry THF (10 mL) and 4-bromoacetophenone **194** (3980 mg, 20 mmol) in dry THF (10 mL) at 0 ºC under Ar. The suspension was stirred under reflux for 16 h. After cooling to 20 °C, the mixture was filtered through Celite® and the solid was washed with EtOH (20 mL). The filtrate was poured into a mixture of Et_2O (20 mL) and aq. HCl (1 M, 20 mL). The ethereal layer was separated. The aqueous layer was extracted with Et_2O (2 × 40 mL). The combined organic layers were washed with brine (3 × 40 mL) and dried. The solvent was evaporated and the residue was recrystallised from EtOH to give enol form **199b** (2300 mg, 30%) as a shiny ivory-coloured powder: R_f 0.85 (petroleum ether / EtOAc

3:1); mp 198-200 ºC (lit.[304] 191.5-194.5 ºC); ^{1}H NMR ($CDCl_3$) (enol form) δ 6.70 (1 H, s, CH), 7.55 (4 H, d, *J* = 8.5 Hz, 2 × Ph 3,5-H_2), 7.77 (4 H, d, *J* = 8.5 Hz, 2 × Ph 2,6-H_2); ^{13}C NMR ($CDCl_3$) (HSQC / HMBC) δ 92.5 (CH), 126.8 (2 × Ph 4-C), 128.6 (2 × Ph 2,6-C_2), 132.0 (2 × Ph 3,5-C_2), 134.0 (2 × Ph 1-C), , 184.7 (C=O, C-OH); MS (ESI) *m/z* 402.8960 $(M + Na)^+$ ($C_{15}H_{10}{}^{79}Br_2NaO_2$), 404.8966 $(M + Na)^+$ ($C_{15}H_{10}{}^{79}Br^{81}BrNaO_2$ requires 404.8920), 406.8946 $(M + Na)^+$ ($C_{15}H_{10}{}^{81}Br_2NaO_2$ requires 406.8901).

1,3-bis-(4-Methylphenyl)propane-1,3-dione (200a).
3-Hydroxy-1,3-di-(4-methylphenyl)prop-2-en-1-one (200b).

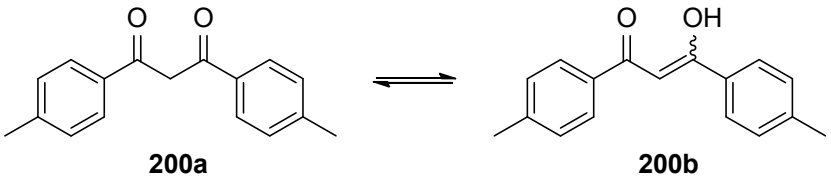

200a **200b**

To an oven-dried 100 mL round-bottom flask was added NaH (2000 mg, 50 mmol, 60% in oil); this material was washed free from oil with dry hexane (10 mL) at 0 ºC under Ar. Dry THF (30 mL) was added to give a suspension. To this suspension were added methyl 4-methylbenzoate **180** (3300 mg, 22 mmol) in dry THF (10 mL) and 4-methylacetophenone **195** (2660 mg, 20 mmol) in dry THF (10 mL) at 0 ºC under Ar. The suspension was stirred under reflux for 16 h. After cooling to 20 °C, the mixture was filtered through Celite® and the solid was washed with EtOH (20 mL). The filtrate was poured into a mixture of Et_2O (20 mL) and aq. HCl (1 M, 20 mL). The ethereal layer was separated. The aqueous layer was extracted with Et_2O (2 × 40 mL). The combined organic layers were washed with brine (3 × 40 mL) and dried. The solvent was evaporated and the residue was recrystallised from EtOH to give enol form **200b** (2500 mg, 50%) as shiny bright-yellow needles: R_f 0.85 (petroleum ether / EtOAc 3:1); mp 112-113 ºC (lit.[305] 117-118 ºC); ^{1}H NMR ($CDCl_3$) (enol form) δ 2.46 (6 H, s, 2 × Me), 6.84 (1 H, s, CH), 7.31 (4 H, d, *J* = 8.5 Hz, 2 × Ph 3,5-H_2), 7.91 (4 H, d, *J* = 8.5 Hz, 2 × Ph 2,6-H_2); ^{13}C NMR ($CDCl_3$) (HSQC / HMBC) δ 21.7 (2 × Me), 92.5 (CH), 127.2 (2 × Ph 2,6-C_2), 129.4 (2 × Ph 3,5-C_2), 132.9 (2 × Ph 1-C), 143.1 (2 × Ph 4-C), 185.5 (C=O, C-OH); MS (ESI) *m/z* 275.1055 $(M + Na)^+$ ($C_{17}H_{16}NaO_2$ requires 275.1043).

1,3-bis(4-Methoxyphenyl)propane-1,3-dione (201a).

3-Hydroxy-1,3-bis(4-methoxyphenyl)prop-2-en-1-one (201b).

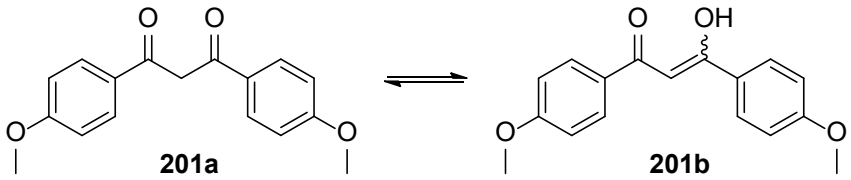

To an oven-dried 50 mL round-bottom flask was added NaH (1000 mg, 25 mmol, 60% in oil); this material was washed free from oil with dry hexane (10 mL) at 0 ºC under Ar. Dry THF (10 mL) was added to give a suspension. To this suspension were added methyl 4-methoxybenzoate **191** (1830 mg, 11 mmol) in dry THF (10 mL) and 4-methoxyacetophenone **196** (1510 mg, 10 mmol) in dry THF (10 mL) at 0 ºC under Ar. The suspension was stirred under reflux for 16 h. After cooling to 20 °C, the mixture was filtered through Celite® and the solid was washed with EtOH (20 mL). The filtrate was poured into a mixture of Et_2O (20 mL) and aq. HCl (1 M, 20 mL). The ethereal layer was separated. The aqueous layer was extracted with Et_2O (2 × 40 mL). The combined organic layers were washed with brine (3 × 40 mL) and dried. The solvent was evaporated and the residue was recrystallised from EtOH to give enol form **201b** (1320 mg, 46%) as an ivory-coloured powder: R_f 0.8 (petroleum ether / EtOAc 3:1); mp 110-111 ºC (lit.[304] 111.5-113.5 ºC); ^{1}H NMR ($CDCl_3$) (enol form) δ 3.90 (3 H, s, Me), 6.76 (1 H, s, CH), 6.99 (4 H, d, J = 9.0 Hz, 2 × Ph 3,5-H_2), 8.01 (4 H, d, J = 9.0 Hz, 2 × Ph 2,6-H_2); ^{13}C NMR ($CDCl_3$) (HSQC / HMBC) δ 55.5 (2 × Me), 91.5 (CH), 114.0 (2 × Ph 3,5-C_2), 128.2 (2 × Ph 1-C), 128.1 (2 × Ph 2,6-C_2), 163.0 (2 × Ph 4-C), 184.6 (C=O, C-OH); MS (ESI) *m/z* 307.0933 $(M + Na)^+$ ($C_{17}H_{16}NaO_4$ requires 307.0941).

4-Phenylethynylbenzonitrile (239k).

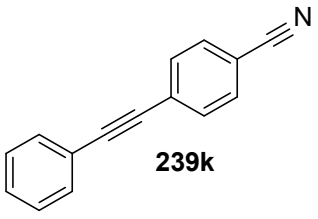

CuI (52 mg, 0.3 mmol), $(Ph_3P)_4Pd$ (162 mg, 0.14 mmol), sodium ascorbate (33 mg, 0.16 mmol) and 4-bromobenzonitrile **239f** (500 mg, 2.75 mmol) were placed in a flask, which was degassed and filled with Ar. Pr^i_2NH (5.0 mL) was injected, followed by THF (10 mL). The mixture was stirred at 40 °C for 30 min. PhC≡CH (281 mg, 2.75 mmol) was added and the mixture was stirred at 40 °C for 16 h. Evaporation and chromatography (petroleum ether / EtOAc 199:1 → 99:1) gave **239k** (480 mg, 87%) as an off-white powder: R_f = 0.5 (petroleum ether); mp 84-86 ºC (lit.[306] 109-110 ºC); ^{1}H NMR ($CDCl_3$) δ 7.33-7.41

(3 H, m, Ph 3,4,5-H_3), 7.50-7.56 (2 H, m, Ph 2,6-H_2), 7.59-7.65 (NCPh 2,3,5,6-H_4); ^{13}C NMR ($CDCl_3$) (HSQC / HMBC) 87.7 (ethyne 1-C), 93.7 (ethyne 2-C), 111.4 (C≡N), 118.5 (NCPh 1-C), 122.2 (Ph 1-C), 128.2 (NCPh 4-C), 128.5 (Ph 3,5-C_2), 129.1 (Ph 4-C), 131.8 (Ph 2,6-C_2), 132.0 (NCPh 2,6-C_2), 132.0 (NCPh 3,5-C_2).

***N*-Hydroxy-4-methylbenzamidine (240b).**

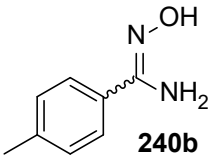

240b

4-Methylbenzonitrile **239b** (940 mg, 8.0 mmol) in EtOH (30 mL) was added to $NH_2OH.HCl$ (3340 mg, 48 mmol) and $NaHCO_3$ (2540 mg, 24 mmol) in water (30 mL) and the mixture was stirred at 100 °C for 3 h. The EtOH was evaporated from the cooled mixture and the residue was poured into ice-cold water. The precipitate was collected by filtration, washed (water) and dried to give **240b** (940 mg, 78%) as a white powder: mp 138-139 °C (lit.[307] 136-137 °C); ^{1}H NMR ($(CD_3)_2SO$) δ 2.37 (3H, s, Me), 5.77 (2H, br s, NH_2), 7.22 (2H, d, *J* = 8.0 Hz, Ph 3,5-H_2), 7.61 (2H, d, *J* = 8.0 Hz, Ph 2,6-H_2), 9.55 (1H, s, OH); ^{13}C NMR ($(CD_3)_2SO$) δ 20.8 (Me), 125.2 (2,6-C_2), 128.6 (3,5-C_2), 130.6 (1-C), 138.2 (4-C), 150.7 (C=N); MS *m/z* 151.0888 $(M + H)^+$ ($C_8H_{11}N_2O_1$ requires 151.0871).

***N*-Hydroxy-4-trifluoromethylbenzamidine (240d).**

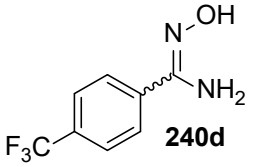

240d

4-Trifluoromethylbenzonitrile **239d** (1370 mg, 8.0 mmol) in EtOH (30 mL) was added to $NH_2OH.HCl$ (3340 mg, 48 mmol) and $NaHCO_3$ (2540 mg, 24 mmol) in water (30 mL) and the mixture was stirred at 100 °C for 3 h. The EtOH was evaporated from the cooled mixture and the residue was poured into ice-cold water. The precipitate was collected by filtration, washed (water) and dried to give **240d** (1600 mg, 98%) as a white powder: 118-120 °C (lit.[308] 128-129 °C); ^{1}H NMR ($(CD_3)_2SO$) δ 6.01 (2 H, br s, NH_2), 7.79 (2 H, d, *J* = 8.4 Hz, Ph 2,6-H_2), 7.94 (2 H, d, *J* = 8.4 Hz, Ph 3,5-H_2), 9.96 (1 H, s, OH); ^{13}C NMR ($(CD_3)_2SO$) δ 125.0 (q, *J* = 3.1 Hz, 3,5-C_2), 125.5 (q, *J* = 331 Hz, CF_3), 126.1 (2,6-C_2), 129.2 (1-C), 137.3 (q, *J* = 28 Hz, 4-C), 149.8 (C=N); ^{19}F NMR ($CDCl_3$) δ -62.8 (CF_3); MS *m/z* 205.0610 $(M + H)^+$ ($C_8H_8N_2OF_3$ requires 205.0589).

***N*-Hydroxy-4-chlorobenzamidine (240e).**

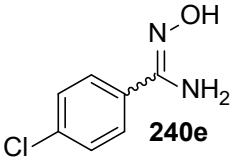

240e

4-Chlorobenzonitrile **239e** (550 mg, 4.0 mmol) in EtOH (15 mL) was added to $NH_2OH.HCl$ (1670 mg, 24 mmol) and $NaHCO_3$ (1270 mg, 12 mmol) in water (15 mL) and the mixture was stirred

at 100 °C for 2 h. The EtOH was evaporated from the cooled mixture and the residue was poured into ice-cold water. The precipitate was collected by filtration, washed (water) and dried to give **240e** (650 mg, 95%) as a white powder: mp 126-128 °C (lit.[309] 128-129 °C); ^{1}H NMR ($(CD_3)_2SO$) δ 5.90 (2 H, br s, NH_2), 7.48 (2 H, d, *J* = 9.2 Hz, Ph 2,6-H_2), 7.74 (2 H, d, *J* = 9.2 Hz, Ph 3,5-H_2), 9.76 (1 H, s, OH); ^{13}C NMR ($(CD_3)_2SO$) δ 127.1 (3,5-C_2), 128.1 (2,6-C_2), 132.2 (1-C), 133.4 (4-C), 149.9 (C=N); MS *m/z* 171.0320 $(M + H)^+$ ($C_7H_8N_2O^{35}Cl$ requires 171.0325).

_N_-Hydroxy-4-bromobenzamidine (240f).

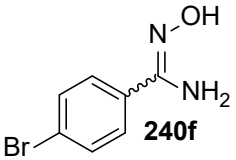

240f

4-Bromobenzonitrile **239f** (1456 mg, 8.0 mmol) in EtOH (30 mL) was added to $NH_2OH.HCl$ (3336 mg, 48 mmol) and $NaHCO_3$ (2544 mg, 24 mmol) in water (30 mL). The mixture was stirred at 100 °C for 2.5 hours and was cooled. The EtOH was evaporated. The residue was poured into ice-cold water. The precipitate was collected by filtration and washed (water) to give **240f** (1550 mg, 90%) as a white powder: R_f 0.35 (petroleum ether / EtOAc 3:1); mp 140-141 °C (lit.[310] 139-141 °C); ^{1}H NMR ($(CD_3)_2SO$) δ 5.90 (2 H, br s, NH_2), 7.60 (2 H, d, *J* = 8.8 Hz, Ph 3,5-H_2), 7.67 (2 H, d, *J* = 8.8 Hz, Ph 2,6-H_2), 9.77 (1 H, s, OH); ^{13}C NMR ($(CD_3)_2SO$) (HSQC / HMBC) δ 122.1 (4-C), 127.4 (3,5-C_2), 131.0 (2,6-C_2), 132.6 (1-C), 150.0 (C=N); MS (ESI) *m/z* 214.9814 $(M + H)^+$ ($C_7H_8BrN_2O$ requires 214.9820).

N-Hydroxy-4-aminobenzamidine (240g).

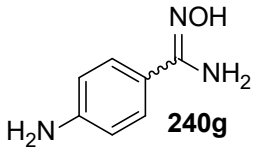

240g

To an aq. solution (15 mL) of $NH_2OH.HCl$ (1668 mg, 24 mmol) and $NaHCO_3$ (1272 mg, 12 mmol) was added 4-aminobenzonitrile **239g** (472 mg, 4.0 mmol) in EtOH (15 mL). The mixture was stirred for 8 h at 100 °C and cooled. The EtOH was evaporated. The residue was poured into ice-cold water and extracted with EtOAc (3 × 25 ml). The combined organic layers were dried and the solvent was evaporated to give **240g** (90 mg, 15%) as a white powder: R_f 0.7 (petroleum ether / EtOAc 1:3); mp 157-158 °C (lit.[311] 169.5 °C); ^{1}H NMR ($(CD_3)_2SO$) δ 5.30 (2 H, br s, NH_2), 5.62 (2 H, br s, NH_2), 6.57 (2 H, d, *J* = 8.6 Hz, Ph 3,5-H_2), 7.38 (2 H, d, *J* = 8.6 Hz, Ph 2,6-H_2), 9.25 (1 H, s, OH); ^{13}C NMR ($CDCl_3$) (HSQC / HMBC) δ 113.0 (3,5-C_2), 120.4 (1-C), 126.3 (2,6-C_2), 149.6 (4-C), 151.5 (C=N); MS (ESI) *m/z* 152.0853 $(M + H)^+$ ($C_7H_{10}N_3O$ requires 152.0824).

Pyridine-4-carboximidamide (240h).

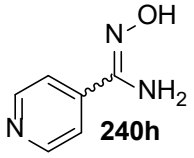

240h

Pyridine-4-nitrile **239h** (832 mg, 8.0 mmol) in EtOH (30 mL) was added to $NH_2OH.HCl$ (3336 mg, 48 mmol) and $NaHCO_3$ (2544 mg, 24 mmol) in water (30 mL). The mixture was stirred at 100 °C for 3 h and cooled. The EtOH was evaporated. The residue was poured into ice-cold water. The precipitate was collected and washed (water) to give **240h** (910 mg, 83%) as a white powder: R_f 0.45 (petroleum ether / EtOAc 1:3); mp 181-184 °C (lit.[312] 178-179 °C); ^{1}H NMR ($CDCl_3$) δ 6.04 (2 H, br s, NH_2), 7.69 (2 H, d, J = 4.6 Hz, 3,5-H_2), 8.62 (2H, d, J = 4.7 Hz, 2,6-H_2), 10.08 (1 H, s, OH); ^{13}C NMR ($CDCl_3$) (HSQC / HMBC) δ 121.9 (2,6-C_2), 143.1 (1-C), 150.4 (3,5-C_2), 152.2 (C=N); MS (ESI) *m/z* 138.0683 $(M + H)^+$ ($C_6H_8N_3O$ requires 138.0667).

N-Hydroxy-4-nitrobenzamidine (240i).

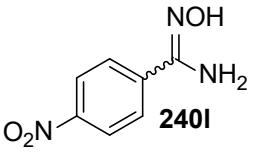

240l

To an aq. solution (30 mL) of $NH_2OH.HCl$ (3336 mg, 48 mmol) and $NaHCO_3$ (2544 mg, 24 mmol) was added 4-nitrobenzonitrile **239i** (1180 mg, 8.0 mmol) in EtOH (30 mL). The mixture was stirred for 4 h at 100 °C and cooled. The EtOH was evaporated. The residue was poured into ice-cold water. The precipitate was collected and washed with petroleum ether to give **240i** (1400 mg, 97%) as a white powder: R_f 0.60 (petroleum ether : EtOAc 1:3); mp 174-176 °C (lit.[313] 176 °C); ^{1}H NMR ($(CD_3)_2SO$) δ 4.62 (2 H, br s, NH_2), 7.95 (2 H, d, J = 8.7 Hz, Ph 2,6-H_2), 8.32 (2 H, d, J = 8.7 Hz, Ph 3,5-H_2); ^{13}C NMR ($(CD_3)_2SO$) (HSQC / HMBC) δ 124.5 (3,5-C_2), 128.2 (2,6-C_2), 137. 0 (1-C), 149.0 (4-C), 163.0 (C=N); MS (ESI) *m/z* 182.0562 $(M + H)^+$ ($C_7H_8N_3O_3$ requires 182.0566).

4-Methylbenzamidine (241b).

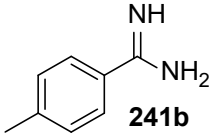

241b

$HCOONH_4$ (403 mg, 6.3 mmol) was boiled with **240b** (150 mg, 1.0 mmol) and Pd/C (10%, 150 mg) in AcOH (5.0 mL) under reflux for 4 d under Ar. The cooled mixture was filtered through Celite®. The solvent was evaporated from the filtrate. Aq. NaOH (1.0 M, 20 mL) was added and the mixture was extracted with EtOAc (3 × 25 mL). The combined organic layers were dried and the solvent was evaporated evaporated *in vacuo* to give **241b** (82 mg, 61%) as a white powder: mp 53-55 °C (lit.[314] 68 °C); ^{1}H NMR ($(CD)_3SO$) δ 2.42 (3H, s, CH_3), 6.72 (3H, br s, NH and NH_2), 7.25 (2H, d, J = 8.4 Hz, Ph 3,5-H_2),

7.72 (2H, d, J = 8.3 Hz, Ph 2,6-H_2); ^{13}C NMR ($(CD)_3SO$) δ 20.1 (CH_3), 126.5 (2,6-C_2), 128.6 (3,5-C_2), 133.2 (1-C), 139.4 (4-C), 162.6 (C=N); MS *m/z* 135.1018 $(M + H)^+$ ($C_8H_{11}N_2$ requires 135.0922).

4-(Trifluoromethyl)benzamidine (241d).

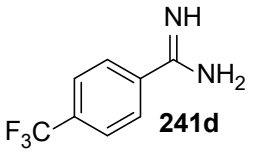

241d

$HCOONH_4$ (806 mg, 12.6 mmol) was boiled with **240d** (267 mg, 1.3 mmol) and Pd/C (10%, 267 mg) in AcOH (5.0 mL) under reflux for 10 h under Ar. The cooled mixture was filtered through Celite®. The solvent was evaporated from the filtrate. Aq. NaOH (1.0 M, 20 mL) was added and the mixture was extracted with EtOAc (3 × 25 mL). The combined organic layers were dried and the solvent was evaporated evaporated *in vacuo* to give **241d** (220 mg, 92%) as a white powder: mp 78-80 °C; ^{1}H NMR ($(CD)_3SO$) δ 6.72 (2 H, br s, NH_2), 7.30 (1 H, br s, NH), 7.81 (2 H, d, J = 8.1 Hz, Ph 2,6-H_2), 8.03 (2 H, d, J = 8.0 Hz, Ph 3,5-H_2); ^{13}C NMR ($(CD)_3SO$) δ 124.1 (q, J = 278 Hz, CF_3), 126.4 (2,6-C_2), 128.7 (q, J = 4.5 Hz, 3,5-C_2), 133.2 (1-C), 140.9 (q, J = 35.4 Hz, 4-C), 166.5 (C=N); ^{19}F NMR ($CDCl_3$) δ -61.2 (CF_3); MS *m/z* 189.0661 $(M + H)^+$ ($C_8H_8N_2F_3$ requires 189.0640).

4-Chlorobenzamidine (241e).

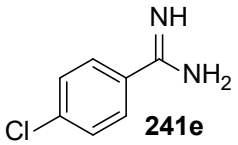

241e

$HCOONH_4$ (1.03 g, 16.1 mmol) was boiled with **240e** (279 mg, 1.6 mmol) and Pt/C (5%, 300 mg) in AcOH (5.0 mL) under reflux for 36 h under Ar. The cooled mixture was filtered through Celite®. The solvent was evaporated from the filtrate. Aq. NaOH (1.0 M, 20 mL) was added and the mixture was extracted with EtOAc (3 × 25 mL). The combined organic layers were dried and the solvent was evaporated evaporated *in vacuo* to give **241e** (173 mg, 70%) as a white powder: mp 89-92 °C; ^{1}H NMR ($(CD)_3SO$) δ 7.39 (2 H, br s, NH_2), 7.50 (2 H, d, J = 8.1 Hz, Ph 2,6-H_2), 7.93 (2 H, d, J = 8.1 Hz, Ph 3,5-H_2), 8.01 (1 H, br s, NH); ^{13}C NMR ($(CD)_3SO$) δ 126.8 (1-C), 127.4 (3,5-C_2), 128.2 (2,6-C_2), 167.9 (4-C), 171.4 (C=N); MS *m/z* 155.0430 $(M + H)^+$ ($C_7H_8N_2Cl$ requires 155.0430).

4-Bromobenzamidine (241f).

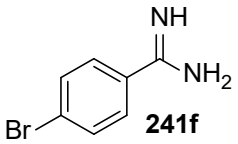

241f

To **240f** (150 mg, 0.70 mmol) in AcOH (5.0 mL) were added $HCOONH_4$ (400 mg, 6.3 mmol) and Pt/C (150 mg, 5%). The

mixture was stirred under reflux for 72 h under Ar and was filtered through Celite®. The solvent was evaporated from the filtrate and the residue was basified with aq. NaOH (1 M), then extracted with EtOAc (3 × 25 mL). The combined organic layers were dried and the solvent was evaporated to give **241f** (94 mg, 68%) as a white powder: R_f 0.85 (petroleum ether / EtOAc 3:1); mp 257-259 °C (lit.[315] 250°C); ^{1}H NMR ((CD)$_3$SO) δ 7.51 (2 H, br s, NH_2), 7.53 (2 H, d, *J* = 7.6 Hz, 3,5-H_2), 7.79 (2 H, d, *J* = 7.6 Hz, 2,6-H_2), 7.93 (1 H, br s, NH); ^{13}C NMR ((CD)$_3$SO) (HSQC / HMBC) δ 126.7 (3,5-C_2), 128.2 (2,6-C_2), 129.6 (4-C), 131.2 (1-C), 166.9 (C=N); MS (ESI) *m/z* 198.9877 (M + H)$^+$ ($C_7H_8{}^{79}BrN_2$ requires 198.9871), 200.9851 (M + H)$^+$ ($C_7H_8{}^{81}BrN_2$ requires 200.9851).

4-Aminobenzamidine (241g).

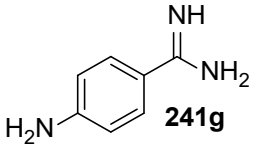

241g

To **240l** (181 mg, 1.0 mmol) in AcOH (5.0 mL) were added Pd/C (1%, 362 mg) and $HCOONH_4$ (800 mg, 12.6 mmol). The mixture was stirred under reflux for 4 d, cooled and filtered through Celite®. The solvent was evaporated from the filtrate. The residue was basified with aq. NaOH (5 M, 20 mL) and extracted with EtOAc (3 × 25 ml). The combined organic layers were dired and the solvent was evaporated to give **241g** (80 mg, 59%) as a white powder: R_f 0.25 (petroleum ether / EtOAc 1:3); mp 200-201 °C (lit.[316] 171 °C); ^{1}H NMR ((CD)$_3$SO) δ 6.70 (3 H, br s, NH and NH_2), 7.35 (2 H, br s, NH_2), 7.66 (2 H, d, *J* = 8.6 Hz, Ph 3,5-H_2), 7.73 (2 H, d, *J* = 8.6 Hz, Ph 2,6-H_2); ^{13}C NMR ((CD)$_3$SO) (HSQC / HMBC) δ 117.8 (3,5-C_2), 127.2 (2,6-C_2), 133.0 (1-C), 140.0 (4-C), 152.0 (C=N); MS (ESI) *m/z* 136.0898 (M + H)$^+$ ($C_7H_{10}N_3$ requires 136.0875).

Pyridine-4-carboximidamide (241h). Method A.

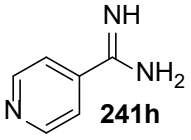

241h

To **240h** (150 mg, 1.0 mmol) in AcOH (5 mL) were added Pd/C (1%, 150 mg) and $HCOONH_4$ (400 mg, 6.3 mmol). The mixture was stirred under reflux for 4 d, cooled and filtered through Celite®. The solvent was evaporated from the filtrate and the residue was basified with aq. NaOH (5 M, 20 mL) and extracted with EtOAc (3 × 25 ml). The combined organic layers were dried and the solvent was evaporated to give **241h** (30.5 mg, 25%) as a white powder: R_f 0.25 (petroleum ether / EtOAc 1:3); mp > 200 °C (lit.[317] 250-252 °C); ^{1}H NMR ((CD)$_3$SO) δ 7.78 (2 H, d, *J* = 5.5 Hz, Py 3,5-H_2), 8.87 (2 H, d, *J* = 5.5 Hz, Py 2,6-H_2), 9.52 (3 H, br s, NH and NH_2); ^{13}C NMR ((CD)$_3$SO) (HSQC / HMBC) δ 121.4

(3,5-C_2), 141.2 (4-C), 150.2 (2,6-C_2), 166.4 (C=N); MS (ESI) *m/z* 122.0734 $(M + H)^+$ ($C_6H_8N_3$ requires 122.0718).

Pyridine-4-carboximidamide (241h). Method B.

NaOMe (1.08 g, 20 mmol) was added to 4-pyridinecarbonitrile **239h** (2.00 g, 19.2 mmol) in dry MeOH (10 mL) and the mixture was stirred under reflux for 2 h. NH_4Cl (2.20 g, 42.2 mmol) was added and the stirring under reflux was continued for 2 h. The solvent was evaporated and the residue was recrystallised from water (12 mL) to give **241h** (0.67 g, 22%) of with properties as above.

4-Phenylethynylbenzamidine (241k).

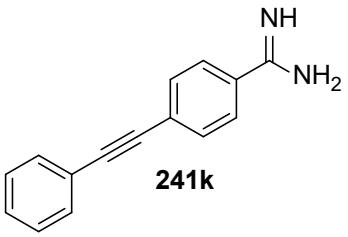

241k

NaOMe (133.9 mg, 2.48 mmol) was added to a stirred solution of **239k** (480 mg, 2.36 mmol) in dry MeOH (15 mL) and the mixture was stirred under reflux for 2 h. NH_4Cl (278.2 mg, 5.2 mmol) was added to the mixture and the stirring under reflux was continued for 2 h. The solvent was evaporated and the residue was recrystallised from water (25 mL) to give **241k** (355 mg, 68%) as an off-white powder: R_f = 0.15 (petroleum ether / EtOAc 1:3); mp 90-91 ºC; ^{1}H NMR ($(CD_3)_2SO$) δ 7.51-7.54 (3 H, m, Ph 3,4,5-H_3), 7.67 (2 H, m, Ph 2,6-H_2), 7.81 (2 H, m, amidine Ph 2,6-H_2), 7.89 (1 H, br s, NH), 7.97 (2 H, m, amidine-Ph 3,5-H_2), 9.06 (1 H, br s, NH), 9.45 (1 H, br s, NH); ^{13}C NMR ($(CD_3)_2SO$) (HSQC / HMBC) δ 88.3 (ethyne 1-C), 93.6 (ethyne 2-C), 111.1 (amidine Ph 1-C), 118.4 (amidine Ph 4-C), 121.4 (Ph 1-C), 128.9 (Ph 3,4,5-C_3), 129.6 (Ph 4-C), 131.6 (Ph 2,6-C_2), 132.2 (amidine Ph 3,5-C_2), 132.6 (amidine Ph 2,6-C_2); MS (ESI) $(M + H)^+$ *m/z* 221.1090 ($C_{15}H_{13}N_2$ requires 221.1073).

***N*-Methoxy-4-methylbenzamidine (248b).**

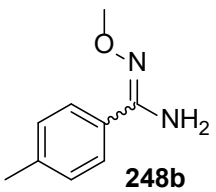

248b

4-Methylbenzonitrile **239b** (234 mg, 2.0 mmol) in MeOH (10 mL) was added to methoxylamine hydrochloride (167 mg, 2.0 mmol) and Na_2CO_3 (212 mg, 2.0 mmol) in water (5.0 mL) and the mixture was stirred for 1 d. Additional methoxylamine hydrochloride (83.5 mg, 1.0 mmol) was added and the mixture was stirred at 25 °C for 48 h. The mixture was filtered. The solvent was evaporated. The residue, in CH_2Cl_2, was dried and the solvent was evaporated. The residue was recrystallised from $CHCl_3$ /

petroleum ether (5:1) to give **248b** (10 mg, 3%) of as a white powder: R_f 0.65 (petroleum ether : EtOAc 3:1); mp 89-91 °C (lit.[318] 85 °C); ^{1}H NMR (CD_3OD) δ 2.43 (3 H, s, PhMe), 3.89 (3 H, s, OMe), 7.27 (2 H, d, *J* = 8.2 Hz, Ph 3,5-H_2), 7.59 (2 H, d, *J* = 8.2 Hz, Ph 2,6-H_2); ^{13}C NMR ($CDCl_3$) (HSQC / HMBC) δ 21.8 (PhMe), 61.4 (OMe), 125.7 (2,6-C_2), 129.3 (3,5-C_2); MS (ESI) *m/z* 165.1036 $(M + H)^+$ ($C_9H_{13}N_2O$ requires 165.1028).

***N*-Methoxy-4-(trifluoromethyl)benzamidine (248d).**

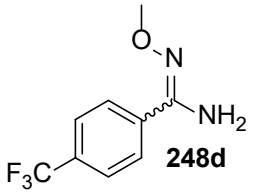

248d

4-Trifluoromethylbenzonitrile **239d** (342 mg, 2.0 mmol) in MeOH (5.0 mL) was added to methoxylamine hydrochloride (167 mg, 2.0 mmol) and Na_2CO_3 (212 mg, 2.0 mmol) in water (5 mL). The mixture was sonicated at 55 °C for 30 min, then the stirring was continued at 20 °C for 20 h. Additional methoxylamine hydrochloride (83.5 mg, 1.0 mmol) was added and the mixture was stirred at 25 °C for 24 h. The mixture was filtered. The solvent was evaporated. The residue, in CH_2Cl_2, was dried and the solvent was evaporated. The residue was recrystallised from $CHCl_3$ / petroleum ether (5:1) to give **248d** (85 mg, 20%) as a white powder: R_f 0.7 (petroleum ether / EtOAc 3:1); mp 92-94 °C; ^{1}H NMR (CD_3OD) δ 3.95 (3 H, s, Me), 7.76 (2 H, d, *J* = 8.7 Hz, Ph 3,5-H_2), 7.90 (2 H, d, *J* = 8.8 Hz, Ph 2,6-H_2), 13.99 (2 H, br s, NH_2); ^{13}C NMR ($CDCl_3$) (HSQC / HMBC) δ 125.6 (3,5-C_2), 127.3 (1-C), 129.2 (2,6-C_2), 140.0 (4-C), 152.7 (C=N); MS (ESI) *m/z* 219.0730 $(M + H)^+$ ($C_9H_{10}FN_2O$ requires 219.0745).

Dimethyl 3,3'-thiodipropanoate (263).

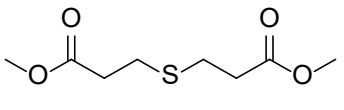

263

A mixture of 3,3'-thiodipropanoic acid **130** (5000 mg, 21 mmol) and conc. H_2SO_4 (5 drops) in MeOH (50 mL) was stirred under reflux for 10 h. The mixture was cooled and poured into water (50 mL). The mixture was extracted with $CHCl_3$ (3 × 50 mL). The combined organic layers were dried and filtered and the solvent was evaporated to give **263** (5740 mg, 99%) as a colourless liquid (lit.[319] liquid): R_f 0.65 (petroleum ether / EtOAc 3:1); ^{1}H NMR ($CDCl_3$) δ 2.55 (4 H, t, *J* = 7.5 Hz, 2 × CH_2CO_2), 2.73 (2 H, t, *J* = 7.5 Hz, 2 × SCH_2), 3.62 (6 H, s, 2 ×Me); ^{13}C NMR ($CDCl_3$) (HSQC / HMBC) δ 27.0 (2 × SCH_2), 34.6 (2 × *C*H_2CO_2), 51.8 (2 × Mr), 172.1 (2 × C=O); MS (ESI) *m/z* 229.0514 $(M + Na)^+$ ($C_8H_{14}NaO_4S$ requires 229.0505).

Diethyl 3,3'-thiodipropanoate (264).

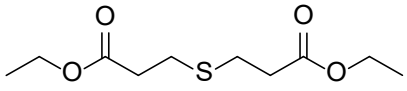

264

A mixture of 3,3'-thiodipropanoic acid **130** (5000 mg, 21 mmol) and conc. H_2SO_4 (11040 mg, 110 mmol) in EtOH (500 mL) was stirred at room temperature for 72 h. The reaction mixture was cooled and the solvent was evaporated until *ca.* 100 mL remained. This solution was basified with sat. aq. $NaHCO_3$ (25 mL) to pH 8. The mixture was filtered and extracted with CH_2Cl_2 (3 × 50 mL). The combined organic layers were dried and filtered and the solvent was evaporated to give **264** (1290 mg, 26%) as a colourless liquid (lit.[320] - liquid): R_f 0.65 (petroleum ether / EtOAc 3:1); ^{1}H NMR ($CDCl_3$) δ 1.19 (6 H, t, *J* = 7.0 Hz, 2 × Me), 2.53 (2 H, t, *J* = 7.0 Hz, 2 × CH_2CO_2), 2.72 (2 H, t, *J* = 7.5 Hz, 2 × SCH_2), 4.08 (4H, q, *J* = 7.0 Hz, 2 × OCH_2); ^{13}C NMR ($CDCl_3$) (HSQC / HMBC) δ 14.0 (2 × Me), 26.9 (2 × SCH_2), 34.7 (2 ×$CO\mathit{C}H_2$), 60.7 (2 × OCH_2), 172.1 (2 × C=O); MS (ESI) *m/z* 235.1002 $(M + H)^+$ ($C_{10}H_{19}O_4S$ requires 235.1004).

Bis(triphenylphosphine)palladium(II) dichloride (270).

$PdCl_2$ (124 mg, 0.70 mmol) was heated at 80 °C with PPh_3 (365 mg, 1.4 mmol) in DMF (20 mL) for 24 h. The precipitate was collected by filtration and dried to give **270** (490 mg, 100%) as a yellow solid. IR ν_{max} (KBr) 1479, 1432 ($C=C_{Ar}$) cm^{-1}.

5.2 Sources of materials for biological evaluation.

All chemicals were obtained from the Sigma-Aldrich Chemical Co. (Gillingham, U.K.) or Fisher Scientific Ltd. (Loughborough, U.K.) and were used without further purification, unless otherwise noted. Human recombinant TNKS-2 enzyme (849-end; Catalogue # 80515BPS) was purchased from AMSbio Europe Ltd. (Abingdon, U.K.). Biotinylated NAD^+ (Catalogue # 4670-500-01) was from AMSBio Europe Ltd. (Abingdon, U.K.). Non-radioactive NAD^+ (Catalogue # BML-KI282-0500) was purchased from Axxora (Nottingham, U.K.). Streptavidin / HRP solution (Catalogue # DY998) and substrate solutions A and B (Catalogue # DY999) were purchased from R & D systems (Minneapolis, MN, U.S.A.). TNKS-1 colorimetric activity assay kit (Catalogue # 4700-096-K) was purchased from AMSbio Europe Ltd. (Abingdon, U.K.). TNKS-1 assay kit components: 5x Antibody diluent, anti-PAR monoclonal antibody, goat anti-mouse IgG-HR, 20x I-PAR assay buffer, histone-coated natural strip well plate, I-PAR, Tankyrase-1 (10 mUnits/µL), assay substrate, XAV939 1 mM (known

tankyrase-1/2 inhibitor), TACS-Sapphire™. Universal PARP-1 colorimetric kit (Catalogue # 4676-096-K) was purchased from AMSbio Europe Ltd. (Abingdon, U.K.). PARP-1 assay kit components: PARP-1 enzyme, histone-coated strip wells, PARP buffer and cocktail, colorimetric detection reagents, activated DNA, streptavidin / HRP with diluent, 3-aminobenzamide (known PARP inhibitor). "CellTiter 96® AQ_{ueous} One Solution Cell Proliferation Assay" reagent was purchased from Promega (Southampton, U.K.). DMEM (glucose 25 mM, with L-glutamine) tissue culture medium (Catalogue # 41966), penicillin / streptomycin 100x concentrate (Catalogue # 15140), heat inactivated foetal bovine serum (Catalogue # 10500), trypsin / EDTA 0.05% (w/v) (Catalogue # 25300) and Dulbecco's PBS (without Ca^{2+} / Mg^{2+}) (Catalogue # 14190) were purchased from Invitrogen (Glasgow, U.K.). MEM tissue culture medium (Catalogue # 21430), trypsin 0.25% (w/v) (Catalogue # 25200), sodium bicarbonate 0.9 M solution (Catalogue # 25080) and L-glutamine 100x concentrate (Catalogue # 25030) were purchased from Invitrogen (Glasgow, U.K.).

5.3 Preparation of buffers.

Aqueous solutions were made in 18.2 Mega-Ω cm^{-1} Milli-Q water and pH adjusted with HCl or NaOH solutions as appropriate. pH values were measured using pH210 microprocessor pH meter (HANNA Instrumental, Leighton Buzzard, U.K.) with HI 1332 electrode (HANNA Instrumental, Leighton Buzzard, U.K.); following pH standards were used for calibration: pH 4.01 (Catalogue # FB67160, Fisher Scientific, Loughborough, U.K.), pH 7.00 (Catalogue # FB67161, Fisher Scientific, Loughborough, U.K.), pH 10.01 (Catalogue # FB67162, Fisher Scientific, Loughborough, U.K.).

Sterile TNKS-2 assay buffer was made at 25°C from 50 mM Tris-HCl (adjusted to pH 8.0), 5 mM $MgCl_2$ and 20 μM $ZnCl_2$; the resulting solution was filter-sterilised using Minisart® NY25 syringe filters (Catalogue # 17846 ACK; Sartorius UK Ltd., Epsom, U.K.).

Phosphate buffered saline (PBS) was purchased in tablets (Catalogue # P4417) and reconstituted with water (one tablet was dissolved in 200 mL of water, yielding 0.01 M phosphate buffer, 2.7 mM potassium chloride and 0.137 M sodium chloride, pH 7.4) at 25°C. Phosphate buffered saline – Tween (PBS-T) [0.1% (v/v)] was made from PBS by adding Tween® 20 at 25°C.

5.4 Cells storage and handling.

All reagents for cell work were purchased sterile. All tissue culture experiments were carried out in Class 2 safety cabinet (M.D.H, InterMed) with the usage of sterile technique. The centrifugation was performed using a desk-top Jouan B3.11centrifuge (25°C, 1300 r.p.m., 378 *g*, 7.0 min).

HT29 cells was purchased from Cancer Research UK, stored under liquid nitrogen and handled using aseptic technique. Cells were cultured in DMEM with high glucose (25 mM), supplemented with penicillin (100 U mL^{-1}), streptomycin (0.17 mM) and foetal bovine serum at 10% (v/v) and were used within passages 7-11.

FEK4 cell culture was kindly provided by Dr. C. Pourzand (University of Bath, U.K.), stored under liquid nitrogen and handled using aseptic technique. Cells were cultured in MEM with L-glutamine, supplemented with penicillin 100 U mL^{-1}, streptomycin 100 μg mL^{-1} and foetal bovine serum at 15% (v/v) and were used within passages 11-12.

5.5 Three-point ranging study against tankyrase-2.

TNKS-2 Auto(PAR)sylation assay. The ELISA quality half-volume 96-wells plate was pre-hydrated with TNKS-2 assay buffer (defined in Section 5.2.2.) (50 μL $well^{-1}$). The calculated amount of TNKS-2 enzyme in 25 μL TNKS-2 assay buffer was loaded per each well apart from negative controls, in which enzyme was replaced by buffer. The plate was kept at 2-8ºC for 15 h, then washed with PBS-T (4 x 200 μL) and drained well. The blocking agent [skimmed milk (Marvel) [5% (w/v)] in TNKS-2 assay buffer

Table 34. Amount of reagents according to the reaction conditions in TNKS-2 auto(PAR)sylation assay.

Reagent / Condition	Buffer, μL	5% (v/v) DMSO solution in buffer, μL	5% (v/v) DMSO stock solution of inhibitor in buffer, μL	b-NAD^+ / u-NAD^+, μL
Background	20	-	-	5
Enzyme only	20	-	-	5
1% (v/v) DMSO	15	5	-	5
Inhibitor	15	-	5	5

(100 μL) was added to all wells and the plate was allowed to stay at room temperature for 1 h. The plate was washed with PBS-T (100 μL well^{-1}) and drained. The wells were loaded with TNKS-2 buffer, inhibitor solutions and biotinylated NAD^+ / unlabelled NAD^+ (Table 34) to make the total reaction volume 25 μL and to give total reaction concentration of 5 μM. The plate was incubated at 30ºC for 2 h. After incubating, the plate was washed with PBS-T (100 μL well^{-1}) four times, drained well and loaded with streptavidin / HRP solution (100 μL well^{-1}). The plate was left at room temperature for 2 h, then it was washed with PBS-T (100 μL well^{-1}) four times. Finally, a substrate solution was added to each well (100 μL). The plate was covered, protected from light and left at room temperature for 30 minutes. ELISA stop solution (1 M aq. H_2SO_4, 25 μL well^{-1}) was added into each well and the absorbance at 450 nm was read immediately using the VersaMax microplate reader (Molecular devices, Sunnyvale, U.S.A.). The assay was performed in triplicates (dependent repeats).

5.6 IC_{50} values determination against TNKS-2.

Auto-poly(ADP-ribosyl)ation assay. As above.

5.7 IC_{50} values determination against TNKS-1.

ELISA colorimetric TNKS-1 catalytic activity assay. The histone-coated full volume 96-wells plate was pre-hydrated with the assay buffer (50 μL well^{-1}). After removing the buffer, the plate was loaded according to a template (Table 35) to make a total reaction volume 50 μL. The plate was kept at room temperature for 30 minutes and then washed twice with PBS-T and twice with PBS. After draining the plate, 50 μL of the first

Table 35. Amount of reagents according to the reaction conditions in ELISA colorimetric TNKS-1 catalytic activity assay.

Reagent / Condition	Buffer, μL	5% (v/v) DMSO solution in buffer, μL	5% (v/v) DMSO stock solution of inhibitor in buffer, μL	Substrate, μL	Enzyme, μL
Background	30	5	-	15	-
1% (v/v) DMSO	5	5	-	15	25
Inhibitor in 1% DMSO	5	-	5	15	25

antibody solution were added to each well. The plate was left at room temperature for 30 minutes and then washed twice with PBS-T and twice with PBS. After washing and draining, 50 μL of the second antibody solution were loaded to each well and the plate was left at room temperature for 30 minutes. The last washing with PBS-T and PBS was performed and the plate was loaded with pre-warmed (30ºC) TACS-sapphire™ (50 μL well^{-1}). The plate was kept in the dark for 15 minutes at room temperature. The reaction was stopped with 0.2 M aq. HCl solution (50 μL well^{-1}). The absorbance was immediately read at 450 nm using the VersaMax microplate reader (Molecular devices, Sunnyvale, U.S.A.). The assay was performed in triplicates (dependent repeats).

5.8 IC_{50} values determination against PARP-1.

Colorimetric PARP-1 catalytic activity assay. The histone-coated full volume 96-wells plate was pre-hydrated with the assay buffer (50 μL well^{-1}). After removing the buffer, the plate was loaded according to a template (Table 36) to make the total reaction volume 50 μL. The plate was incubated at room temperature for 1 h and then it was washed twice with PBS-T (100 μL well^{-1}) and twice with PBS (100 μL well^{-1}). After washing and draining, streptavidin / HRP solution (50 μL) was added to all wells and the plate was kept at room temperature for 1 h. All wells were washed twice with PBS-T (100 μL) and twice with PBS (100 μL) and drained well. The plate was loaded with pre-warmed (30ºC) TACS-sapphire™ (50 μL well^{-1}). The plate was kept in the dark for 15 minutes at room temperature. The reaction was stopped with 0.2 M aq. HCl solution (50 μL well^{-1}). The absorbance was immediately read at 450 nm using the VersaMax

Table 36. Amount of reagents according to the reaction conditions in colorimetric PARP-1 catalytic activity assay.

Reagent / Condition	Buffer, mL	Enzyme, μL	5% (v/v) DMSO solution in buffer, μL	5% (v/v) DMSO stock solution of inhibitor in buffer, μL	Cocktail, μL
Background	25	-	5	-	20
1% (v/v) DMSO	-	25	5	-	20
Inhibitor in 1% DMSO	-	25	-	5	20

microplate reader (Molecular devices, Sunnyvale, U.S.A.). The assay was performed in triplicates (dependent repeats).

5.9 IC_{50} values determination on anti-proliferative assays.

HT29 anti-proliferative assay and FEK4 anti-proliferative assay. As it is a cell-based assay, all equipment and reagents were sterile and an aseptic technique was used. The medium from a cell culture maintained in a 75 cm^2 tissue culture flask (Nunc) was poured off and the cells were rinsed with Dulbecco's PBS (5 mL). Trypsin / EDTA [0.05% (w/v), 2 mL] was loaded and the flask was incubated at 37ºC, 5% (v/v) CO_2, until the cells were completely detached from the plastic. The medium (8 mL) was added to the flask, the cells were suspended in the resulted mixture and the suspension was transferred into a 30 mL tube. The suspension was centrifuged using a desk-top Jouan B3.11 centrifuge (25°C, 1300 r.p.m., 378 *g*, 7 min). The supernatant liquid was poured off and the cell pellet was re-suspended in the medium (5 mL; DMEM for HT29 cells; MEM for FEK4 cells). The resulting suspension was ten times diluted with the same medium. The cells count was performed using haemocytometer and the cell dilution for the experiment was calculated and performed. The seed density used was of 500 cells per well in a 50 μL final volume. The wells were loaded according to a template (Table 37) to give a total reaction volume 100 μL. The plate was incubated at 37ºC, 5% (v/v) CO_2 for 3 to 4 h. After incubating, the inhibitor solutions (50 μL) were loaded into appropriate wells apart from negative controls in which cells was replaced by buffer. The plate was incubated at the same conditions for 3 days. After 4 days, MTS

Table 37. Amount of reagents according to the reaction conditions in colorimetric MTS HT29 / FEK4 anti-proliferative assay.

Reagent / Condition	Medium, μL	Cell culture dilution, μL	5% (v/v) DMSO solution in buffer, μL	5% (v/v) DMSO stock solution of inhibitor in buffer, μL
Background	100	-	-	-
Cells only	50	50	-	-
1% (v/v) DMSO	-	50	50	-
Inhibitor in 1% DMSO	-	50	-	50

reagent (20 μL) was added into each well and the plate was returned to the incubator for 2 to 3 h. The absorbance was immediately read at 490 nm using the VersaMax microplate reader (Molecular devices, Sunnyvale, U.S.A.). The assay was performed in quadruplicates (dependent repeats).

5.10 Molecular modelling.

Molecular modelling was performed using SYBYL™ software and Chimera™ for visualisation. Ligands were constructed, minimised and charged (*Gasteiger-Huckel*) using SYBYL™. Ring twist (where appropriate) was initially set to the same orientation as the XAV939 **47** or the lowest energy conformation for the ME0328 / PARP-1 models.[321] The structures were docked into the nicotinamide-binding site of the enzymes generated by removing the inhibitor (XAV939 **47** for TNKS-1 and TNKS-2; ME0328 for PARP-1) from the published structures.[148,155,321] After docking, ligands were subjected to molecular dynamics (2000fs, 300K using *Boltzman* initial velocities and the *Tripos* force-field); the resulting structures were then minimised. Throughout the initial molecular dynamics and mechanics calculations the hydrogen bonds (between the amide carbonyl and Ser^{1068} and Gly^{1032} and between NH and Gly^{1032}) were maintained with distance and angle constraints. The conformation of the receptor pocket and the enzyme was also fixed. The receptor / ligand complexes generated above with established binding conformation of the ligands were then minimised and refined without constraints through molecular dynamics and molecular mechanics to give the final structures.

References

1. http://www.who.int/gho/ncd/mortality_morbidity/cancer_text/en/ (visited on 12/09/2013).
2. http://epp.eurostat.ec.europa.eu/statistics_explained/index.php/Causes_of_death_statistics (visited on 12/09/2013).
3. http://www.cdc.gov/nchs/pressroom/states/CANCER_STATE_2010.pdf (visited on 12/09/2013).
4. http://globocan.iarc.fr/factsheets/populations/factsheet.asp?uno=900 (visited on 12/09/2013).
5. http://www.ons.gov.uk/ons/dcp171778_239518.pdf (visited 12/09/2013).
6. Shall, S.; de Murcia, G. Poly (ADP-ribose) polymerase-1: what have we learned from the deficient mouse model? *Mutat. Res.-DNA Repair* **2000,** *460*, 1-15.
7. Szabó, C.; Dawson, V. L. Role of poly(ADP-ribose) synthetase in inflammation and ischaemia-reperfusion. *Trends Pharmacol. Sci.* **1998,** *19*, 287-298.
8. Genovese, T.; Mazzon, E.; Di Paola, R.; Muià, C.; Threadgill, M. D.; Caputi, A. P.; Thiemermann, C.; Cuzzocrea, S. Inhibitors of poly (ADP-ribose) polymerase modulate signal transduction pathways and the development of bleomycin-induced lung injury. *J. Pharmacol. Exp. Ther.* **2005**, *313*, 529-538.
9. Rajesh, M.; Mukhopadhyay, P.; Godlewski, G.; Bátkai, S.; Haskó, G.; Liaudet, L.; Pacher, P. Poly(ADP-ribose)polymerase inhibition decreases angiogenesis. *Biochem. Biophys. Res. Commun.* **2006,** *350*, 1056-1062.
10. Jagtap, P.; Szabó, C. Poly (ADP-ribose) polymerase and the therapeutic effects of its inhibitors. *Nature Rev. Drug Discov.* **2005,** *4*, 421-440.
11. Li, M.; Cai, L.; Wang, Y.-L. Effect of poly(ADP-ribose) polymerase inhibitor 5-AIQ on invasion and metastasis of CT26 cells. *J. 3rd Military Med. Univ.* **2008**, *30*, 237-240.
12. McDonald, M. C.; Mota-Filipe, H.; Wright, J. A.; Abdelrahman, M.; Threadgill, M. D.; Thompson, A. S.; Thiemermann, C. Effects of 5-aminoisoquinolinone, a water soluble, potent inhibitor of the activity of poly (ADP ribose) polymerase on the organ injury and dysfunction caused by haemorrhagic shock. *Br. J. Pharmacol.* **2000,** *130*, 843-850.
13. Ratnam, K.; Low, J. A. Current development of clinical inhibitors of poly(ADP-ribose) polymerase in oncology. *Clin. Cancer Res.* **2007,** *13*, 1383-1388.

14. Curtin, N. J.; Wang, L.-Z.; Yiakouvaki, A.; Kyle, S.; Arris, C. A.; Canan-Koch, S.; Webber, S. E.; Durkacz, B. W.; Calvert, H. A.; Hostomsky, Z.; Newell D. R. Novel poly(ADP-ribose) polymerase-1 inhibitor, AG14361, restores sensitivity to temozolomide in mismatch repair-deficient cells. *Clin. Cancer Res.* **2004,** *10*, 881-889.
15. Miknyoczki, S. J.; Jones-Bolin, S.; Pritchard, S.; Hunter, K.; Zhao, H.; Wan, W.; Ator, M.; Bihovsky, R.; Hudkins, R.; Chatterjee, S. Klein-Szanto, A.; Dionne, C.; Ruggeri, B. Chemopotentiation of temozolomide, irinotecan, and cisplatin activity by CEP-6800, a poly(ADP-ribose) polymerase inhibitor. *Mol. Cancer Ther.* **2003,** *2*, 371-382.
16. Nguewa, P. A.; Fuertes, M. A.; Cepeda, V.; Alonso, C.; Quevedo, C.; Soto, M.; Perez, J. M. Poly(ADP-ribose) polymerase-1 inhibitor 3-aminobenzamide enhances apoptosis induction by platinum complexes in cisplatin-resistant tumor cells. *Med. Chem.* **2006,** *2*, 47-53.
17. Tentori, L.; Portarena, I.; Barbarino, M.; Balduzzi, A.; Levati, L.; Vergati, M.; Biroccio, A.; Gold, B.; Lombardi, M. L.; Graziani, G. Inhibition of telomerase increases resistance of melanoma cells to temozolomide, but not to temozolomide combined with poly (ADP-ribose) polymerase inhibitor. *Mol. Pharmacol.* **2003,** *63*, 192-202.
18. Calabrese, C. R.; Batey, M. A.; Thomas, H. D.; Durkacz, B. W.; Wang, L. Z.; Kyle, S.; Skalitzky, D.; Li, J.; Zhang, C.; Boritzki, T.; Maegley, K.; Calvert, A. H.; Hostomsky, Z.; Newell, D. R.; Curtin, N. J. Identification of potent nontoxic poly (ADP-ribose) polymerase-1 inhibitors: Chemopotentiation and pharmacological studies *Clin. Cancer Res.* **2003,** *9*, 2711-2718.
19. Calabrese, C. R.; Almassy, R.; Barton, S.; Batey, M. A.; Calvert, A. H.; Canan-Koch, S.; Durkacz, B. W.; Hostomsky, Z.; Kumpf, R. A.; Kyle, S. Li, J.; Maegley, K.; Newell, D. R.; Notarianni, E.; Stratford, I. J.; Skalitzky, D.; Thomas, H. D.; Wang, L.-Z.; Webber, S. E.; Williams, K. J.; Curtin, N. J. Anticancer chemosensitization and radiosensitization by the novel poly(ADP-ribose) polymerase-1 inhibitor AG14361. *J. Natl. Cancer Inst.* **2004,** *96*, 56-67.
20. Smith, S. The world according to PARP. *Trends Biochem. Sci.* **2001,** *26*, 174-179.
21. Ueda, K.; Hayaishi, O. ADP-ribosylation. *Annu. Rev. Biochem.* **1985,** *54*, 73-100.
22. Chang, P.; Coughlin, M.; Mitchison, T. J. Tankyrase-1 polymerization of poly-(ADP-ribose) is required for spindle structure and function. *Nature Cell Biol.* **2005,** *7*, 1133-1139.

23. Amé, J.-C.; Spenlehauer, C.; de Murcia, G. The PARP superfamily. *Bioessays* **2004,** *26*, 882-893.
24. Kinoshita, T.; Nakanishi, I.; Warizaya, M.; Iwashita, A.; Kido, Y.; Hattori, K.; Fujii, T. Inhibitor-induced structural change of the active site of human poly (ADP-ribose) polymerase. *FEBS Lett.* **2004,** *556*, 43-46.
25. Iwashita, A.; Hattori, K.; Yamamoto, H.; Ishida, J.; Kido, Y.; Kamijo, K.; Murano, K.; Miyake, H.; Kinoshita, T.; Warizaya, M.; Ohkubo, M.; Matsuoka, N.; Mutoh, S. Discovery of quinazoline and quinoxaline derivatives as potent and selective poly(ADP-ribose) polymerase-1/2 inhibitors. *FEBS Lett.* **2005,** *579*, 1389-1393.
26. Iwashita, A.; Yamazaki, S.; Mihara, K.; Hattori, K.; Yamamoto, H.; Ishida, J.; Matsuoka, N.; Mutoh, S. Neuroprotective effects of a novel poly (ADP-ribose) polymerase-1 inhibitor, 2-{3-[4-(4-chlorophenyl)-1-piperazinyl]propyl}-4(3*H*)-quinazolinone (FR255595), in an in vitro model of cell death and in mouse 1-methyl-4-phenyl-1,2,3,6-tetrahydropyridine model of Parkinson's disease. *J. Pharmacol. Exp. Ther.* **2004,** *309*, 1067-1078.
27. D'Amours, D.; Desnoyers, S.; D'Silva, I.; Poirier, G. G. Poly (ADP-ribosyl) ation reactions in the regulation of nuclear functions. *Biochem. J.* **1999,** *342*, 249-268.
28. de Murcia, G.; Ménissier-de Murcia, J. Poly(ADP-ribose) polymerase: a molecular nick-sensor. *Trends Biochem. Sci* **1994,** *19*, 172-176.
29. Amé, J.-C.; Rolli, V.; Schreiber, V.; Niedergang, C.; Apiou, F.; Decker, P.; Muller, S.; Höger, T.; Ménissier-de Murcia, J.; de Murcia, G. PARP-2, A novel mammalian DNA damage-dependent poly (ADP-ribose) polymerase. *J. Biol. Chem.* **1999,** *274*, 17860-17868.
30. Berghammer, H.; Ebner, M.; Marksteiner, R.; Auer, B. pADPRT-2: a novel mammalian polymerizing(ADP-ribosyl)transferase gene related to truncated pADPRT homologues in plants and *Caenorhabditis elegans*. *FEBS Lett.* **1999,** *449*, 259-263.
31. Johansson, M. A human poly (ADP-ribose) polymerase gene family (ADPRTL): cDNA cloning of two novel poly (ADP-ribose) polymerase homologues. *Genomics* **1999,** *57*, 442-445.
32. Augustin, A.; Spenlehauer, C.; Dumond, H.; Ménissier-de Murcia, J.; Piel, M.; Schmit, A.-C.; Apiou, F.; Vonesch, J.-L.; Kock, M.; Bornens, M.; de Murcia, G. PARP-3 localizes preferentially to the daughter centriole and interferes with the G1/S cell cycle progression. *J. Cell Sci.* **2003**, *116*, 1551-1562.

33. Kanai, M.; Tong, W. M., Sugihara, E.; Wang, Z. Q.; Fukasawa K.; Miwa, M. Involvement of poly(ADP-ribose) polymerase 1 and poly(ADP-ribosyl)ation in regulation of centrosome function. *Mol. Cell. Biol*. **2003**, *146*, 917-928.
34. Kickhoefer, V. A.; Siva, A. C.; Kedersha, N. L.; Inman, E. M.; Ruland, C.; Streuli, M.; Rome, L. H. The 193-kD vault protein, VPARP, is a novel poly (ADP-ribose) polymerase. *J. Cell Biol.* **1999,** *146*, 917-928.
35. Ma, Q.; Baldwin, K. T.; Renzelli, A. J.; McDaniel, A.; Dong, L. TCDD-inducible poly(ADP-ribose) polymerase: a novel response to 2,3,7,8-tetrachlorodibenzo-p-dioxin. *Biochem. Biophys. Res. Commun.* **2001**, *289*, 499-506.
36. Yu, M.; Schreek, S.; Cerni, C.; Schamberger, C.; Lesiewicz, K.; Poreba, E.; Vervoorts, J.; Walsemann, G.; Grötzinger, J.; Kremmer, E.; Mehraein, Y.; Mertsching, J.; Kraft, R.; Austen, M.; Lüscher-Fizlaff, J.; Lüscher, B. PARP-10, a novel Myc-interacting protein with poly(ADP-ribose)polymerase activity, inhibits transformation. *Oncogene* **2005**, *24*, 1982-1993.
37. Lehtiö, L.; Collins, R.; van den Berg, S.; Johansson, A.; Dahlgren, L.-G.; Hammarström, M.; Helleday, T.; Holmberg-Schiavone, L.; Karlberg, T.; Weigelt, J. Zinc binding catalytic domain of human tankyrase 1. *J. Mol. Biol.* **2008,** *379*, 136-145.
38. Smith, S.; Giriat, I.; Schmitt, A.; de Lange, T. Tankyrase, a poly(ADP-ribose) polymerase at human telomeres. *Science* **1998,** *282*, 1484-1487.
39. Cook, B. D.; Dynek, J. N.; Chang, W.; Shostak, G.; Smith, S. Role for the related poly(ADP-ribose) polymerases tankyrase 1 and 2 at human telomeres. *Mol. Cell. Biol.* **2002,** *22*, 332-342.
40. Seimiya, H. The telomeric PARP, tankyrases, as target for cancer therapy. *Br. J. Cancer* **2006,** *94*, 341-345.
41. Mosavi, L. K.; Cammett, T. J.; Desrosiers, D. C.; Peng, Z. The ankyrin repeat as molecular architecture for protein recognition. *Protein Sci.* **2004,** *13*, 1435-1448.
42. Breeden, L.; Nasmyth, K. Similarity between cell-cycle genes of budding yeast and fission yeast and the *Notch* gene of *Drosophila*. *Nature* **1987**, *329*, 651-654.
43. Lux, S. E.; John, K. M.; Bennett, V. Analysis of cDNA for human erythrocyte Ankyrin indicates a repeated structure with homology to tissue-differentiation and cell-cycle control proteins. *Nature* **1990**, *344*, 36-42.

44. Seimiya, H.; Smith, S. The telomeric poly(ADP-ribose) polymerase, tankyrase 1, contains multiple binding sites for telomeric repeat binding factor 1 (TRF1) and a novel acceptor, 182-kDa tankyrase-binding protein (TAB182). *J. Biol. Chem.* **2002,** *277*, 14116-14126.
45. Kim, C. A.; Bowie, J. U. SAM domains: uniform structure, diversity of function. *Trends Biochem. Sci.* **2003,** *28*, 625-628.
46. De Rycker, M.; Price, C. M. Tankyrase polymerization is controlled by its sterile alpha motif and poly (ADP-ribose) polymerase domains. *Mol. Cell. Biol.* **2004,** *24*, 9802-9812.
47. De Rycker, M.; Venkatesan, R. N.; Wei, C.; Price, C. M. Vertebrate tankyrase domain structure and sterile alpha motif (SAM)-mediated multimerization. *Biochem. J.* **2003,** *372*, 87-96.
48. Kaminker, P. G.; Kim, S.-H.; Taylor, R. D.; Zebarjadian, Y.; Funk, W. D.; Morin, G. B.; Yaswen, P.; Campisi, J. TANK2, a new TRF1-associated poly (ADP-ribose) polymerase, causes rapid induction of cell death upon overexpression. *J. Biol. Chem.* **2001**, *276*, 35891-35899.
49. Lyons, R. J.; Deane, R.; Lynch, D. K.; Ye, Z.-S. J.; Sanderson, G. M.; Eyre, H. J.; Sutherland, G. R.; Daly, R. J. Identification of a novel human tankyrase through its interaction with the adaptor protein Grb14. *J. Biochem.* **2001**, *276*, 17172-17180.
50. Li, Z.; Yamauchi, Y.; Kamakura, M.; Murayama, T.; Goshima, F.; Kimura, H.; Nishiyama, Y. Herpes simplex virus requires poly(ADP-ribose)polymerase activity for efficient replication and induces extracellular signal-related kinase-dependent phosphorylation and ICP0-dependent nuclear localisation of tankyrase 1. *J. Virol.* **2012**, *86*, 492-503.
51. Guettler, S.; LaRose, J.; Petsalaki, E.; Gish, G.; Scotter, A.; Pawson, T.; Rottapel, R.; Sicheri, F. Structural basis and sequence rules for substrate recognition by tankyrase explain the basis for cherubism disease. *Cell* **2011**, *147*, 1340-1354.
52. Levaot, N.; Voytyuk, O.; Dimitriou, I.; Sircoulomb, F.; Chandrakumar, A.; Deckert, M.; Krzyzanowski, P. M.; Scotter, A.; Gu, S.; Janmohamed, S.; Cong, F.; Simoncic, P.; Ueki, Y.; La Rose, J.; Rottapel, R. Loss of tankyrase-mediated destruction of 3BP2 is the underlying pathogenic mechanism of cherubism. *Cell* **2011**, *147*, 1324-1339.
53. Chi, N.-W.; Lodish, H. F. Tankyrase is a Golgi-associated mitogen-activated protein kinase substrate that interacts with IRAP in GLUT4 vesicles. *J. Biochem.* **2000**, *275*, 38437-38444.

54. Yeh, T.-Y. J.; Sbodio, J. I.; Tsun, Z.-Y.; Luo, B.; Chi, N.-W. Insulin-stimulated exocytosis of GLUT4 is enhanced by IRAP and its partner tankyrase. *Biochem. J.* **2007**, *402*, 279-290.

55. Ozaki, Y.; Matsua, H.; Asou, H.; Nagamachi, A.; Aki, D.; Honda, H.; Yasunaga, S.; Takihara, Y.; Yamamoto, T.; Izumi, S.; Ohsugi, M.; Inaba, T. Poly-ADP ribosylation of Miki by tankyrase-1 promotes centrosome maturation. *Mol. Cell* **2012**, *47*, 694-706.

56. Cho-Park, P. F.; Steller, H. Proteasome regulation by ADP-ribosylation. *Cell* **2013**, *153*, 614-627.

57. Bae, J. Y.; Donigian, J. R.; Hsueh, A. J. W. Tankyrase 1 interacts with Mcl-1 proteins and inhibits their regulation of apoptosis. *J. Biol. Chem.* **2003**, *278*, 5195-5204.

58. Bisht, K. K.; Dudognon, C.; Chang, W. G.; Sokol, E. S.; Ramirez, A.; Smith, S. GDP-Mannose-4,6-dehydratase is a cytosolic partner of tankyrase 1 that inhibits its poly(ADP-ribose) polymerase activity. *Mol. Cell. Biol.* **2012**, *32*, 3044-3053.

59. Deng, Z.; Lezina, L.; Chen, C.-J.; Shtivelband, S.; So, W.; Lieberman, P. L. Telomeric proteins regulate episomal maintenance of Epstein-Barr virus origin of plasmid replication. *Mol. Cell* **2002**, *9*, 493-503.

60. Huang, S.-M. A.; Mishina, Y. M.; Liu, S.; Cheung, A.; Stegmeier, F.; Michaud, G. A.; Charlat, O.; Wiellette, E.; Zhang, Y.; Wiessner, S.; Hild, M.; Shi, X.; Wilson, C. J.; Mickanin, C.; Myer, V.; Fazal, A.; Tomlinson, R.; Serluca, F.; Shao, W.; Cheng, H.; Shultz, M.; Rau, C.; Shirle, M.; Schlegl, J.; Ghidelli, S.; Fawell, S.; Lu, C.; Curtis, D.; Kirschner, M. W.; Lengauer, C.; Finan, P.; Tallarico, J. A.; Bouwmeester, T.; Porter, J. A.; Bauer, A.; Cong, F. Tankyrase inhibition stabilizes axin and antagonizes Wnt signalling. *Nature* **2009,** *461*, 614-620.

61. Hsiao, S. J.; Poitras, M. F.; Cook, B. D.; Liu, Y.; Smith, S. Tankyrase 2 poly(ADP-ribose) polymerase domain-deleted mice exhibit growth defects but have normal telomere length and capping. *Mol. Cell. Biol.* **2006**, *26*, 2044-2054.

62. Seimiya, H.; Muramatsu, Y.; Smith, S.; Tsuruo, T. Functional subdomain in the ankyrin domain of tankyrase 1 required for poly(ADP-ribosyl)ation of TRF1 and telomere elongation. *Mol. Cell. Biol.* **2004**, *24*, 1944-1955.

63. Fuchs, U; Rehkamp, G. F.; Slany, R.; Follo, M.; Borkhardt, A. The formin-binding protein 17, FBP17, binds *via* a TNKS binding motif to tankyrase, a protein involved in telomere maintenance. *FEBS Lett.* **2003**, *554*, 10-16.

64. Pandita, T. K. Telomeres and telomerase. *Encyclopedia of Cancer* **2002,** *4*, 353-361.
65. Martínez, P.; Blasco, M. A. Telomeric and extra-telomeric roles for telomerase and the telomere-binding proteins. *Nature Rev. Cancer* **2011**, *11*, 161-176.
66. Xu, Y. Chemistry in human telomere biology: structure, function and targeting of telomere DNA/RNA. *Chem. Soc. Rev.* **2011,** *40*, 2719-2740.
67. De Lange, T. Shelterin: the protein complex that shapes and safeguards human telomeres. *Genes Dev.* **2005**, *19*, 2100-2110.
68. Palm, W.; de Lange, T. How shelterin protects mammalian telomeres. *Annu. Rev. Genet.* **2008**, *42*, 301-334.
69. Smogorzewska, A.; de Lange, T. Regulation of telomerase by telomeric proteins. *Annu Rev. Biochem.* **2004**, *73*, 177-208.
70. Shay, J. W.; Wright, W. E. Mechanism-based combination telomerase inhibition therapy. *Cancer Cell* **2005,** *7*, 1-2.
71. Hockemeyer, D.; Daniels, J.-P.; Takai, H.; de Lange, T. Recent expansion of the telomeric complex in rodents: Two distinct POT1 proteins protect mouse telomeres. *Cell* **2006**, *126*, 63-77.
72. Wu, L.; Multani, A. S.; He, H.; Cosme-Blanco, W.; Deng, Y.; Deng, J. M.; Bachilo, O.; Pathak, S.; Tahara, H.; Bailey, S. M.; Deng, Y.; Behringer, R. R.; Chang, S. *Pot1* deficiency initiates DNA damage checkpoint activation and aberrant homologous recombination at telomeres. *Cell* **2006**, *126*, 49-62.
73. Sfeir, A.; Kabir, S.; van Overbeek, M.; Celli, G. B.; de Lange, T. Loss of Rap1 induces telomere recombination in the absence of NHEJ or a DNA damage signal. *Science* **2010**, *327*, 1657-1661.
74. Martínez, P.; Thanasoula, M.; Muñoz, P.; Liao, C. Y.; Tejera, A.; McNees, C.; Flores, J. M.; Fernández-Capetillo, O.; Tarsounas, M.; Blasco, M. A. Increased telomere fragility and fusions resulting from TRF1 deficiency lead to degenerative pathologies and increased cancer in mice. *Genes Dev*. **2009**, *23*, 2060-2075.
75. Sfeir, A.; Kosiyatrakul, S. T.; Hockemeyer, D.; MacRae, S. L.; Karlseder, J.; Schildkraut, C. L.; de Lange, T. Mammalian telomeres resemble fragile sites and require TRF1 for efficient replication. *Cell* **2009**, *138*, 90-103.
76. Tejera, A. M.; Stagno d'Alcontres, M.; Thanasoula, M.; Marion, R. M.; Martínez, P.; Liao, C. Y.; Flores, J. M.; Tarsounas, M.; Blasco, M. A. TPP1 is required for TERT recruitment, telomere elongation during nuclear reprogramming and normal skin development in mice. *Dev. Cell* **2010**, *18*, 691-702.

77. Abreu, E.; Aritonovska, E.; Reichenbach, P.; Cristofari, G.; Culp, B.; Terns, R. M.; Lingner, J.; Terns, M. P. TIN2-tethered TPP1 recruits human telomerase to telomeres *in vivo*. *Mol. Cell Biol*. **2010**, *30*, 2971-2982.
78. Chang, W.; Dynek, J. N.; Smith, S. TRF1 is degraded by ubiquitin-mediated proteolysis after release from telomeres. *Genes Dev.* **2003**, *17*, 1328-1333.
79. Lee, T. H.; Perrem, K.; Harper, J. W.; Ping, K. P.; Zhou, X. Z. The F-box protein FBX4 targets PIN2/TRF1 for ubiquitin-mediated degradation and regulates telomere maintenance. *J. Biol. Chem.* **2006**, *281*, 759-768.
80. Chang, W.; Dynek, J.; Smith, S. NuMA is a major acceptor of poly(ADP-ribosyl)-ation by tankyrase 1 in mitosis. *Biochem. J.* **2005,** *391*, 177-184.
81. Hsiao, S. J.; Smith, S. Tankyrase function at telomeres, spindle poles, and beyond. *Biochimie* **2008,** *90*, 83-92.
82. Cleveland, D. W. NuMA: a protein involved in nuclear structure, spindle assembly, and nuclear re-formation. *Trends Cell Biol.* **1995,** *5*, 60-64.
83. Chang, P.; Jacobson, M.; Mitchison, T. Poly(ADP-ribose) is required for spindle assembly and structure. *Nature* **2004**, *432*, 645-649.
84. MacDonald, B. T.; Tamai, K.; He, X. Wnt/β-catenin signaling: components, mechanisms, and diseases. *Dev. Cell* **2009,** *17*, 9-26.
85. Logan, C. Y.; Nusse, R. The Wnt signaling pathway in development and disease. *Annu. Rev. Cell Dev. Biol.* **2004,** *20*, 781-810.
86. Polakis, P. The many ways of Wnt in cancer. *Curr. Opin. Gen. Dev.* **2007**, *17*, 45-51.
87. Camilli, T. C.; Weeraratna, A. T. Striking the target in Wnt-y conditions: Intervening in Wnt signaling during cancer progression. *Biochem. Pharmacol.* **2010,** *80*, 702-711.
88. Lee, E.; Salic, A.; Krüger, R.; Heinrich, R.; Kirschner, M. W. The roles of APC and axin derived from experimental and theoretical analysis of the Wnt pathway. *PLOS Biol.* **2003,** *1*, 116-132.
89. Dodge, M. E.; Lum, L. Drugging the cancer stem cell compartments: lessons learned from the hedgehog and Wnt signal transduction pathways. *Annu. Rev. Pharmacol. Toxicol.* **2011**, *51*, 289-310.
90. Verkaar, F.; Zaman, G. J. R. New avenues to target Wnt/β-catenin signaling. *Drug Discov. Today* **2011,** *16*, 35-41.

91. Morrone, S.; Cheng, Z.; Moon, R. T.; Cong, F.; Xu, W. Crystal structure of a tankyrase-axin complex and its implications for axin turnover and tankyrase substrate recruitment. *Proc. Natl. Acad. Sci. USA* **2012**, *109*, 1500-1505.
92. Ferraris, D. V. Evolution of poly(ADP-ribose) polymerase-1 (PARP-1) inhibitors. From concept to clinic. *J. Med. Chem.* **2010**, *53*, 4561-4584.
93. Miwa, M.; Masutani, M. Poly(ADP-ribosyl)ation and cancer. *Cancer Sci.* **2007**, *98*, 1528-1535.
94. Ljungman, M. Targeting the DNA damage response in cancer. *Chem. Rev.* **2009**, *109*, 2929-2950.
95. Peukert, S.; Schwahn, U. New inhibitors of poly (ADP-ribose) polymerase (PARP). *Expert Opin. Ther. Pat.* **2004,** *14*, 1531-1551.
96. Kaelin, W. G., The concept of synthetic lethality in the context of anticancer therapy. *Nature Rev. Cancer* **2005**, *5*, 689-698.
97. Farmer, H.; McCabe, N.; Lord, C. J.; Tutt, A. N. J.; Johnson, D. A.; Richardson, T. B.; Santarosa, M.; Dillon, K. J.; Hickson, I.; Knights, C.; Martin, N. M. B.; Jackson, S. P.; Smith, G. C. M.; Ashworth, A. Targeting the DNA repair defect in BRCA mutant cells as a therapeutic strategy. *Nature* **2005**, *434*, 917-921.
98. Bryant, H. E.; Schultz, N.; Thomas, H. D.; Parker, K. M.; Flower, D.; Lopez, E.; Kyle, S.; Meuth, M.; Curtin, N. J.; Helleday, T. Specific killing of BRCA2-deficient tumours with inhibitors of poly(ADP-ribose) polymerase. *Nature* **2005**, *434*, 775-777.
99. Ruf, A.; Ménnissier-de Murcia, J.; de Murcia, G. M.; Schulz, G. E. Structure of the catalytic fragment of poly (AD-ribose) polymerase from chicken. *Proc. Natl. Acad. Sci. USA* **1996,** *93*, 7481-7485.
100. Lord, A.-M.; Mahon, M.; Lloyd, M. D.; Threadgill, M. D. Design, synthesis, and evaluation in vitro of quinoline-8-carboxamides, a new class of PARP-1 inhibitor. *J Med. Chem.* **2009,** *52*, 868-877.
101. Menear, K. A.; Adcock, C.; Alonso, F. C.; Blackburn, K.; Copsey, L.; Drzewiecki, J.; Fundo, A.; Le Gall, A.; Gomez, S.; Javaid, H.; Lence, C. F.; Martin, N. M. B.; Mydlowski, C.; Smith, G. C. M. Novel alkoxybenzamide inhibitors of poly(ADP-ribose) polymerase. *Bioorg. Med. Chem. Lett.* **2008**, *18*, 3942-3945.
102. Griffin, R. J.; Pemberton, L. C.; Rhodes, D.; Bleasdale, C.; Bowman, K.; Calvert, A. H.; Curtin, N. J.; Durkacz, B. W.; Newell, D. R.; Porteous, J. K.; Golding B. T. Novel potent inhibitors of the DNA repair enzyme poly(ADP-ribose)polymerase (PARP). *Anti-Cancer Drug Des.* **1995**, *10*, 507-514.

103. Banasik, M.; Ueda, K. Inhibitors and activators of ADP-ribosylation reactions. *Mol. Cell. Biochem.* **1994**, *138*, 185-197.

104. Thomas, H. D.; Calabrese, C. R.; Batey, M. A.; Canan, S.; Hostomsky, Z.; Kyle, S.; Maegley, K. A.; Newell, D. R.; Skalitzky, D.; Wang, L.-Z.; Webber, S. E.; Curtin, N. J. Preclinical selection of a novel poly(ADP-ribose)polymerase inhibitor for clinical trial. *Mol. Cancer Ther.* **2007**, *6*, 945-956.

105. Russo, A. L.; Kwon, H.-C.; Burgan, W. E.; Carter, D.; Beam, K.; Weizheng, X.; Zhang, J.; Slusher, B. S.; Chakravarti, A.; Tofilon, P. J.; Camphausen, K. *In vitro* and *in vivo* radiosensitization of glioblastoma cells by the poly(ADP-ribose)polymerase inhibitor E7016. *Clin. Cancer Res.* **2009**, *15*, 607-612.

106. Penning, T. D.; Zhu, G.-D.; Gandhi, V. B.; Gong, J.; Liu, X.; Shi, Y.; Klinghofer, V.; Johnson, E. F.; Donawho, C. K.; Frost, D. J.; Bontcheva-Diaz, V.; Bouska, J. J.; Osterling, D. J.; Olson, A. M.; Marsh, K. C.; Luo, Y.; Giranda, V. L. Discovery of the poly(ADP-ribose) polymerase (PARP) inhibitor 2-[(*R*)-2-methylpyrrolidin-2-yl]-1*H*-benzimidazole-4-carboxamide (ABT-888) for the treatment of cancer. *J. Med. Chem.* **2009**, *52*, 514-523.

107. Javle, M.; Curtin, N. J. The potential for poly(ADP-ribose) polymerase inhibitors in cancer therapy. *Ther. Adv. Med. Oncol.* **2011**, *3*, 257-267.

108. Tutt, A.; Robson, M.; Garber, J. E.; Domcheck, S. M.; Audeh, M. W.; Weitzel, J. N.; Friedlander, M.; Arun, B.; Loman, N.; Schmutzler, R. K.; Wardley, A.; Mitchell, G.; Earl, H.; Wickens, M.; Carmichael, J. Oral poly(ADP-ribose) polymerase inhibitor olaparib in patients with *BRCA1* or *BRCA2* mutations and advanced breast cancer: a proof-of-concept trial. *Lancet* **2010**, *376*, 235-244.

109. Menear, K. A.; Adcock, C.; Boulter, R.; Cockcroft, X.-L.; Copsey, L.; Cranston, A.; Dillon, K. J.; Drzewiecki, J.; Garman, S.; Gomez, S.; Javaid, H.; Kerrigan, F.; Knights, C.; Lau, A.; Loh, V. M.; Matthews, I. T. W.; Moore, S.; O'Connor, M. J.; Smith, G. C. M.; Martin, N. M. B. 4-[3-(4-Cyclopropanecarbonylpiperazine-1-carbonyl)-4-fluorobenzyl]-2*H*-phthalazin-1-one: a novel bioavailable inhibitor of poly(ADP-ribose) polymerase-1. *J. Med. Chem.* **2008**, *51*, 6581–6591.

110. Sunderland, P. T.; Woon, E. C. Y.; Dhami, A.; Bergin, A. B.; Mahon, M. F.; Wood, P. J.; Jones, L. A.; Tully, S. R.; Lloyd, M. D.; Thompson, A. S.; Javaid, H.; Martin, N. M. B.; Threadgill, M. D. 5-Benzamidoisoquinolin-1-ones and 5-(ω-carboxyalkyl)isoquinolin-1-ones as isoform-selective inhibitors of poly(ADP-ribose)polymerase-2 (PARP-2). *J. Med. Chem.* **2011**, *54*, 2049-2059.

111. Jones, P. Development of poly(ADP-ribose)polymerase (PARP) inhibitors in oncology. *Annu. Rep. Med. Chem.* **2010,** *45*, 229-243.
112. Kelland, L. Targeting the limitless replicative potential of cancer: The telomerase / telomere pathway. *Clin. Cancer Res.* **2007**, *13*, 4960- 4963.
113. Dikmen, Z. G.; Gellert, G. C.; Jackson, S.; Gryaznov, S.; Tressler, R.; Dogan, P.; Wright, W. E.; Shay, J. W. *In vivo* inhibition of lung cancer by GRN163L: A novel human telomerase inhibitor. *Cancer Res.* **2005**, *65*, 7866-7873.
114. Ueno, T.; Takahashi, H.; Oda, M.; Mizunuma, M.; Yokoyama, A.; Goto, Y.; Mizushina, Y.; Sakaguchi, K.; Hayashi, H. Inhibition of human telomerase of rubromycins: Implication of spiroketal system of the compounds as an active moiety. *Biochemistry* **2000**, *39*, 5995−6002.
115. Pascolo, E; Wenz, C.; Lingner, J.; Hauel, N.; Priepke, H.; Kauffman, I.; Garin-Chesa, P.; Rettig, W. J.; Damm, K.; Schnapp, A. Mechanism of human telomerase inhibition by BIBR1532, a synthetic, nonnucleosidedic drug candidate. *J. Biol. Chem.* **2002**, *277*, 15566−15572.
116. Menichincheri, M; Ballinari, D.; Bargiotti, A.; Bonomini, L.; Ceccarelli, W.; D'Alessio, R.; Fretta, A.; Moll, J.; Polucci, P.; Soncini, C.; Tibolla, M.; Trosset, J.-Y.; Vanotti, E. Catecholic flavonoids acting as telomerase inhibitors. *J. Med. Chem.* **2004**, *47*, 6466−6475.
117. Naasani, I.; Seimiya, H.; Tsuruo, T. Telomerase inhibition, telomere shortening, and senescence of cancer cells by tea catechins. *Biochem. Biophys. Res. Commun.* **1998**, *249*, 391−396.
118. Seimiya, H.; Oh-hara, T.; Suzuki, T.; Naasani, I; Shimazaki, T.; Tsuchiya, K.; Tsuruo, T. Telomere shortening and growth inhibition of human cancer cells by novel synthetic telomerase tnhibitors MST-312, MST-295, and MST-199. *Mol. Cancer Ther.* **2002**, *1*, 657−665.
119. Forsyth, N. R.; Wright, W. E.; Shay, J. W. Telomerase and differentiation in multi-cellular organisms: turn it off, turn it on, and turn it off again. *Differentiation* **2002**, *69*, 188-197.
120. Lundblad, V. Telomere maintenance without telomerase. *Oncogene* **2002**, *21*, 522-531.
121. Hackett, J. A.; Greider, C. W. Balancing instability: dual roles for telomerase and telomere dysfunction in tumorigenesis. *Oncogene* **2002**, *21*, 619-626.
122. Bharadwaj, R.; Yu, H. The spindle checkpoint, aneuploidy, and cancer. *Oncogene* **2004,** *23*, 2016–2027.

123. Jordan, M. A.; Wilson, L. Microtubules as a target for anticancer drugs. *Nature Rev. Cancer* **2004**, *4*, 253–265.
124. Barker, N.; Clevers, H. Mining the Wnt pathway for cancer therapeutics. *Nature Rev. Drug Discov.* **2006**, *5*, 997-1014.
125. van de Wetering, M.; Sancho, E.; Verweij, C.; de Lau, W.; Oving, I.; Hurlstone, A.; van der Horn, K.; Batlle, E.; Coudreuse, D.; Haramis, A.-P.; Tjon-Pon-Fong, M.; Moerer, P.; van den Born, M.; Soete, G.; Pals, S.; Eilers, M.; Medema, R.; Clevers, H. The β-catenin/TCF-4 complex imposes a crypt progenitor phenotype on colorectal cancer cells. *Cell* **2002**, *111*, 241-250.
126. DuBois, R. N.; Giardiello, F. M.; Smalley, W. E. Nonsteroidal anti-inflammatory drugs, eicosanoids, and colorectal cancer prevention. *Gastroenterol. Clin. North Am*. **1996**, *25*, 773-791.
127. Giovannucci, E.; Rimm, E. B.; Stampfer, M. J.; Colditz, G. A.; Ascherio, A.; Willett, W. C. Aspirin use and the risk for colorectal cancer and adenoma in male health professionals. *Ann. Intern. Med.* **1994**, *121*, 241-246.
128. Takeda, H.; Sonoshita, M.; Oshima, H.; Sugihara, K.; Chulada, P. C.; Langenbach, R.; Oshima, M.; Taketo, M. M. Cooperation of cyclooxygenase 1 and cyclooxygenase 2 in intestinal polyposis. *Cancer Res.* **2003**, *63*, 4872-4877.
129. Castellone, M. D.; Teramoto, H.; Williams, B. O.; Druey, K.; Gutkind, J. S. Prostaglandin E_2 promotes colon cancer cell growth through a G_s-axin-β-catenin signaling axis. *Science* **2005**, *310*, 1504-1510.
130. Dihlmann, S.; Klein, S.; von Knebel Doeberitz M. Reduction of β-catenin/T-cell transcription factor signalling by aspirin and indomethacin is caused by an increased stabilisation of phosphorylated β-catenin. *Mol. Cancer Ther.* **2003**, *2*, 509-516.
131. Gardner, S. H.; Hawcroft, G.; Hull, M. A. Effect of nonsteroidal anti-inflammatory drugs on β-catenin protein levels and catenin-related transcription in human colorectal cancer cells. *Br. J. Cancer* **2004**, *91*, 153-163.
132. Rigas, B.; Williams, J. L. NO-releasing NSAIDs and colon cancer chemoprevention: a promising novel approach. *Int. J. Oncol.* **2002**, *20*, 885-890.
133. Giovannucci, E.; Platz, E. A. *Epidemiology of cancer risk: Vitamin D and calcium.* In *Vitamin D*, 2nd ed. (D. Feldman, J. W. Pike, and F. Glorieux, eds.) Elsevier Academic Press **2005**, 1617–1634. ISBN: 9780123819796
134. Harris, D. M.; Go, V. L. Vitamin D and colon carcinogenesis. *J. Nutr.* **2004**, *134*, 3463S-3471S.

135. Shah, S.; Islam, M. N.; Dakshanamurthy, S.; Rizvi, I.; Rao, M.; Herrell, R.; Zinser, G.; Valrance, M.; Aranda, A.; Moras, D.; Norman, A.; Welsh, J.; Byers, S. W. The molecular basis of vitamin D receptor and β-catenin crossregulation. *Mol. Cell* **2006**, *21*, 799-809.

136. Rhee, C.-S.; Sen, M.; Lu, D.; Wu, C.; Leoni, L.; Rubin, J.; Corr, M.; Carson, D. A. Wnt and frizzled receptors as potential targets for immunotherapy in head and neck squamous cell carcinomas. *Oncogene* **2002**, *21*, 6598-6605.

137. He, B.; You, L.; Uematsu, K.; Xu, Z.; Lee, A. Y.; Matsangou, M.; McCormick, F.; Jablons, D. M. A monoclonal antibody against Wnt-1 induces apoptosis in human cancer cells. *Neoplasia* **2004**, *6*, 7-14.

138. Graham, T. A.; Weaver, C.; Mao, F.; Kimelman, D.; Xu, W. Crystal structure of a β-catenin / Tcf complex. *Cell* **2000**, *103*, 885-896.

139. Poy, F.; Lepourcelet, M.; Shivdasani, R. A.; Eck, M. J. Structure of a human Tcf4-β-catenin complex. *Nature Struct. Biol.* **2001**, *8*, 1053-1057.

140. Lepourcelet, M.; Chen, Y.-N. P.; France, D. S.; Wang, H.; Crews, P.; Petersen, F.; Bruseo, C.; Wood, A. W.; Shivdasani, R. A. Small-molecule antagonists of the oncogenic Tcf/β-catenin protein complex. *Cancer Cell* **2004**, *5*, 91-102.

141. Trosset, J. Y.; Dalvit, C.; Knapp, S.; Fasolini, M.; Veronesi, M.; Mantegani, S.; Gianellini, L. M.; Catana, C.; Sundström, M.; Stouten, P. F. W.; Moll, J. K. Inhibition of protein-protein interactions: the discovery of druglike β-catenin inhibitors by combining virtual and biophysical screening. *Proteins* **2006**, *64*, 60-67.

142. Emami, K. H.; Nguyen, C.; Ma, H.; Kim, D. H.; Jeong, K. W.; Eguchi, M.; Moon, R. T.; Teo, J.-L.; Oh, S. W.; Kim, H. Y.; Moon, S. H.; Ha, J. R.; Kahn, M. A small molecule inhibitor of β-catenin / CREB-binding protein transcription. *Proc. Natl Acad. Sci. USA* **2004**, *101*, 12682-12687.

143. Shan, J.; Shi, D. L.; Wang, J.; Zheng, J. Identification of a specific inhibitor of the disheveled PDZ domain. *Biochemistry* **2005**, *44*, 15495-15503.

144. Fancy, S. P. J.; Harrington, E. P.; Yuen, T. J.; Silbereis, J. C.; Zhao, C.; Baranzini, S. E.; Bruce, C. C.; Otero, J. J.; Huang, E. J.; Nusse, R.; Franklin, R. J. M.; Rowitch, D. H. Axin2 as regulatory and therapeutic target in newborn brain injury and remyelination. *Nature Neurosci*. **2011**, *14*, 1009-1018.

145. Ulsamer, A.; Wei, Y.; Kim, K. K.; Tan, K.; Wheeler, S.; Xi, Y.; Thies, R. S.; Chapman, H. A. Axin pathway activity regulates in vivo pY654-β-catenin accumulation and pulmonary fibrosis. *J. Biol. Chem*. **2012**, *287*, 5164-5172.

146. Narwal, M.; Venkannagari, H.; Lehtiö, L. Structural basis of selective inhibition of human tankyrases. *J. Med. Chem*. **2012**, *55*, 1360-1367.
147. Chen, B.; Dodge, M. E.; Tang, W.; Lu, J.; Ma, Z.; Fan, C.-W.; Wei, S.; Hao, W.; Kilgore, J.; Williams, N. S.; Roth, M. G.; Amatruda, J. F.; Chen, C.; Lum, L. Small molecule-mediated disruption of Wnt-dependent signaling in tissue regeneration and cancer. *Nature Chem. Biol*. **2009**, *5*, 100-107.
148. Karlberg, T.; Markova, N.; Johansson, I.; Hammarström, M.; Schütz, P.; Weigelt, J.; Schüler, H. Structural basis for the interaction between tankyrase-2 and a potent Wnt-signaling inhibitor. *J. Med. Chem.* **2010,** *53*, 5352-5355.
149. Lu, J.; Ma, Z.; Hsieh, J.-C.; Fan, C.-W.; Chen, B.; Longgood, J. C.; Williams, N. S.; Amatruda, J. F.; Lum, L.; Chen, C. Structure-activity relationship studies of small-molecule inhibitors of Wnt response. *Bioorg. Med. Chem. Lett*. **2009**, *19*, 3825-3827.
150. Riffell, J. L.; Lord, C. L.; Ashworth, A. Tankyrase-targeted therapeutics: expanding opportunities in the PARP family. *Nature Rev. Drug Discov.* **2012**, *11*, 923-936.
151. Gunaydin, H.; Gu, Y.; Huang, X. Novel binding mode of a potent and selective tankyrase inhibitor. *PLoS One* **2012**, *7*, 1-6.
152. Waaler, J.; Machon, O.; Tumova, L.; Dinh, H.; Korinek, V.; Wilson, S. R.; Paulsen, J. E.; Pedersen, N. M.; Eide, T. J.; Machonova, O.; Gradl, D.; Voronkov, A.; von Kries, J. P.; Krauss, S. A novel tankyrase inhibitor decreases canonical Wnt signalling in colon carcinoma cells and reduces tumor growth in conditional APC mutant mice. *Cancer Res.* **2012**, *72*, 2822-2832.
153. Shultz, M. D.; Kirby, C. A.; Stams, T.; Chin, D. N.; Blank, J.; Charlat, O.; Cheng, H.; Cheung, A.; Cong, F.; Feng, Y.; Fortin, P. D.; Hood, T.; Tyagi, V.; Xu, M.; Zhang, B.; Shao, W. [1,2,4]Triazol-3-ylsulfanylmethyl-3-phenyl-[1,2,4]oxadiazoles: antagonists of the *Wnt* pathway that inhibit tankyrases 1 and 2 via novel adenosine pocket binding. *J. Med. Chem.* **2012**, *55*, 1127-1136.
154. Voronkov, A.; Holsworth, D. D.; Waaler, J.; Wilson, S. R.; Ekblad, B.; Perdreau-Dahl, H.; Dinh, H.; Drewes, G.; Hopf, C.; Morth, J. P.; Krauss, S. Structural basis and SAR for G007-LK, a lead stage 1,2,4-triazole based specific tankyrase 1/2 inhibitor. *J. Med. Chem.* **2013**, *56*, 3012-3023.
155. Kirby, C. A.; Cheung, A.; Fazal, A.; Shultz, M. D.; Stams, T. Structure of human tankyrase 1 in complex with small-molecule inhibitors PJ34 and XAV939. *Acta Cryst. F* **2012**, *68*, 115-118.

156. Yashiroda, Y.; Okamoto, R.; Hatsugai, K.; Takemoto, Y.; Goshima, N.; Saito, T.; Hamamoto, M.; Sugimoto, Y.; Osada, H.; Seimiya, H.; Yoshida, M. A novel yeast cell-based screen identifies flavone as a tankyrase inhibitor. *Biochem. Biophys. Res. Commun.* **2012**, *394*, 569-573.

157. Narwal, M.; Fallarero, A.; Vuorela, P.; Lehtiö, L. Homogeneous screening assay for human tankyrase. *J. Biomol. Screening* **2012**, *17*, 593−604.

158. Narwal, M.; Haikarainen, T.; Fallarero, A.; Vuorela, P. M.; Lehtiö, L. Screening and structural analysis of flavones inhibiting tankyrases. *J. Med. Chem.* **2013**, *56*, 3507−3517.

159. Narwal, M.; Koivunen, J.; Haikarainen, T.; Obaji, E.; Legala, O. E.; Venkannagari, H.; Joensuu, P.; Pihlajaniemi, T.; Lehtiö, L. Discovery of tankyrase inhibiting flavones with increased potency and isoenzyme selectivity. *J. Med. Chem.* **2013**, *56*, 7880−7889.

160. Nathubhai, A.; Patterson, R.; Woodman, T. J.; Sharp, H. E. C.; Chui, M. T. Y.; Chung, H. H. K.; Lau, S. W. S.; Zheng, J.; Lloyd, M. D.; Thompson, A. S.; Threadgill, M. D. N^3-Alkylation during formation of quinazolin-4-ones from condensation of anthranilamides and orthoamides. *Org. Biomol. Chem.* **2011**, *9*, 6089-6099.

161. Threadgill, M. D.; Lloyd, M. D.; Thompson, A. S.; Nathubhai, A.; Wood, P. J.; Paine, H. A.; Kumpan, K.; Sunderland, P. T.; Woon, E. C. Y. Tankyrase inhibitors. U.K. Patent Application 1221971.3, **2012**.

162. Sunderland, P. T.; Dhami, A.; Mahon, M. F.; Jones, L. A.; Tully, S. R.; Lloyd, M. D.; Thompson, A. S.; Javaid, H.; Martin, N. M. B.; Threadgill, M. D. Synthesis of 4-alkyl-, 4-aryl- and 4-arylamino-5-aminoisoquinolin-1-ones and identification of a new PARP-2 selective inhibitor. *Org. Biomol. Chem.* **2011**, *9*, 881-891.

163. Cai, L.; Threadgill, M. D.; Wang, Y.; Li, M. Effect of poly (ADP-ribose) polymerase-1 inhibition on the proliferation of murine colon carcinoma CT26 cells. *Pathol. Oncol. Res.* **2009**, *15*, 323-328.

164. Kwong, J. S. W.; Lloyd, M. D.; Threadgill, M. D. Synthesis of cyclic sulfoximine mimics of 2-deoxyribosides as enzyme inhibitors in cancer. *J. Pharm. Pharmacol.* **2006**, *58*, A58-A58.

165. Woon, E. C. Y.; Threadgill, M. D. Poly(ADP-ribose)polymerase inhibition - where now? *Curr. Med. Chem.* **2005**, *12*, 2373-2392.

166. Nathubhai, A.; Wood, P. J.; Lloyd, M. D.; Thompson, A. S.; Threadgill, M. D. Design and discovery of 2-arylquinazolin-4-ones as potent and selective inhibitors of tankyrases. *ACS Med. Chem. Lett.* **2013**, *4*, 1173-1177.

167. Haikarainen, T.; Koivunen, J.; Narwal, M.; Venkannagari, H.; Obaji, E.; Joensuu, P.; Pihlajaniemi, T.; Lehtiö, L. *para*-Substituted 2-phenyl-3,4-dihydroquinazolin-4-ones as potent and selective tankyrase inhibitors. *ChemMedChem* **2013**, *8*, 1978-1985.

168. Lipinski, C. A. Lead- and drug-like compounds: the rule-of-five revolution. *Drug Discov. Today* **2004**, *1*, 337-341.

169. Ghose, A. K.; Viswanadhan, V. N.; Wendoloski, J. J. A knowledge-based approach in designing combinatorial or medicinal chemistry libraries for drug discovery. 1. A qualitative and quantitative characterization of known drug databases. *J. Comb. Chem.*, **1999**, *1*, 55-68.

170. Veber, D. F.; Johnson, S. R.; Cheng, H.-Y.; Smith, B. R.; Ward, K. W.; Kopple, K. D. Molecular properties that influence the oral bioavailability of drug candidates. *J. Med. Chem.* **2002**, *45*, 2615–2623.

171. Nagarajan, A.; Balasubramanian, T. R. Organomercury mediated synthesis of isocoumarins. *Indian J. Chem., Sect. B* **1987**, *26*, 917-919.

172. Larock, R. C.; Harrison, L. W. Mercury in organic chemistry. 26. Synthesis of heterocycles via intramolecular solvomercuration of aryl acetylenes *J. Am. Chem. Soc.* **1984**, *106*, 4218–4227.

173. Woon, E. C. Y.; Dhami, A.; Mahon, M. F.; Threadgill, M. D. 5-Nitroisocoumarins from tandem Castro–Stephens coupling—6-*endo*-dig cyclisation of 2-iodo-3-nitro-benzoic acid and arylethynes and ring-closure of methyl 2-alkynyl-3-nitrobenzoates with electrophiles. *Tetrahedron* **2006**, *62*, 4829-4837.

174. Nishiwaki, N.; Komatsu, M.; Ohshiro, Y. A facile synthesis of 1,6-naphthyridin-5(6*H*)-ones. *Synthesis* **1991**, 41-42.

175. Radziszewski, B. Ueber die Oxydation mittelst Wasserstoffsuperoxyds. *Ber. dtsch. Chem. Ges.* **1884**, *17*, 1289-1290.

176. Watson, C. Y.; Whish, W. J. D.; Threadgill, M. D. Synthesis of 3-substituted benzamides and 5-substituted isoquinolin-1(2*H*)-ones and preliminary evaluation as inhibitors of poly(ADP-ribose)polymerase (PARP). *Bioorg. Med. Chem*. **1998**, *6*, 721-734.

177. Ritter, J. J.; Minieri, P. P. A new reaction of nitriles. I. Amides from alkenes and mononitriles. *J. Am. Chem. Soc.* **1948**, *70*, 4045–4048.

178. Sonogashira, K. Development of Pd–Cu catalyzed cross-coupling of terminal acetylenes with sp^2-carbon halides. *J. Organometall. Chem.* **2002**, *653*, 46-49.
179. Kürti, L.; Czakó, B. *Strategic applications of named reactions in organic synthesis.* Academic Press **2005**. ISBN 978-0124297852.
180. Clayden, J.; Greeves, N.; Warren, S.; Waters, P. *Organic chemistry.* Oxford University Press **2001**. ISBN 978-0198503460.
181. Yin, L.; Liebscher, J. Carbon-carbon coupling reactions catalyzed by heterogeneous palladium catalysts. *Chem. Rev.* **2007**, *107*, 133-173.
182. Novák, Z.; Nemes, P.; Kotschy, A. Tandem Sonogashira coupling: an efficient tool for the synthesis of diarylalkynes. *Org. Lett.* **2004**, *6*, 4917-4920.
183. Glaser, C. A. Beiträge zur Kenntniss des Acetenylbenzols. *Ber. dtsch. Chem. Ges.* **1869**, *2*, 422–424.
184. http://www.chemicalbook.com/ChemicalProductProperty_EN_CB7124406.htm (visited on 18/11/2013).
185. Lavecchia, G.; Berteina-Raboin, S.; Guillaumet, G. Synthesis of 3,5-difunctionalized 1-methyl-1*H*-pyrazolo[3,4-*b*]pyridines involving palladium-mediated coupling reactions. *Tetrahedron Lett.* **2004**, *45*, 6633-6636.
186. Takehiro, F.; Yuji, H.; Takahiro, I.; Toshihiro, S.; Toshiyuki, T.; Akio, K.; Yasuyuki, I.; Akane, I. Novel spiro compounds. U.S. Patent 20020165391, **2002**.
187. Dunn, A. D. A facile synthesis of 3-amino-1(2)*H*-pyrazolo[3,4-*c*]pyridine. *Org. Prep. Proc. Int*. **1997**, *29*, 577-579.
188. Ito, H.; Arimoto, K.; Sensui, H.; Hosomi, A. Direct alkynyl transfer from silicon to copper: New preparation method of alkynylcopper (I) reagents. *Tetrahedron Lett.* **1997**, *38*, 3977-3980.
189. Greene, P. W.; Wuts, P. G. M. *Protective groups in organic synthesis.* Wiley-Interscience. **2006**. ISBN 978-0471697541.
190. Opsteen, J. A.; van Hest, J. C. M. Modular synthesis of block copolymers *via* cycloaddition of terminal azide and alkyne functionalized polymers. *Chem. Commun*., **2005**, 57–59.
191. Cai, C. Z.; Vasella, A. Oligosaccharide analogs of polysaccharides. 3. A new protecting group for alkynes - orthogonally protected dialkynes. *Helv. Chim. Acta*. **1995**, *78*, 732-757.
192. Nielsen, M. B.; Diederich, F. Modules for acetylenic scaffolding. *SynLett* **2002**, 544-552.

193. Eastmond, R.; Walton, D. R. M. Silylation as a protective method in Cadiot-Chodkiewicz couplings - synthesis of aryl-butadiynes and -hexatriynes *Tetrahedron* **1972**, *28*, 4591-4599.
194. Favorsky, A. E. Action de la potasse caustique sur les mélanges des cétones avec le phénylacétylène. *Bull. Soc. Chim. Fr.* **1907**, *2*, 1087–1088.
195. Swindell, C. S.; Fan, W.; Klimko, P. G. Pinacol closure of oxygenated taxane skeleta at C-l-C-2 with stereoinduction by oxygen substituents at C-9 and C-10 *Tetrahedron Lett.* **1994**, *35*, 4959-4962.
196. Elangovan, A.; Wang, Y.-H.; Ho, T.-I. Sonogashira coupling reaction with diminished homocoupling. *Org. Lett.* **2003**, *5*, 1841-1844.
197. Bag, S. S.; Kundu, R.; Das, M. Click-reagent version of Sonogashira coupling protocol to conjugated fluorescent alkynes with no or reduced homocoupling. *J. Org. Chem.* **2011,** *76*, 2332-2337.
198. Riddick, J. A.; Bunger, W. B.; Sakano, T. K. *Techniques of Chemistry.* John Wiley and Sons: New York, **1985**; Vol. 2. Organic solvents.
199. Korte, D. E.; Hegedus, L. S.; Wirth, R. K. Synthesis of isocoumarins, dihydroisocoumarins, and isoquinolones via π-allylnickel halide and π-olefin-palladium complexes. *J. Org. Chem.* **1977**, *42*, 1329-1336.
200. Yao, T.; Larock, R. C. Synthesis of isocoumarins and α-pyrones via electrophilic cyclization. *J. Org. Chem.* **2003**, *68*, 5936-5942.
201. Oliver, M. A.; Gandour, R. D. The identity of 4-bromo-3-phenylisocoumarin. A facile preparation by bromolactonization of alkyl 2-(2-phenylethynyl)benzoates. *J. Org. Chem.* **1984**, *49*, 558-559.
202. Biagetti, M.; Bellina, F.; Carpita, A.; Stabile, P.; Rossi, R. New procedures for the selective synthesis of 2(2*H*)-pyranone derivatives and 3-aryl-4-iodoisocoumarins. *Tetrahedron* **2002**, *58*, 5023-5038.
203. Rossi, R.; Carpita, A.; Bellina, F.; Stabile, P.; Mannina, L. Synthesis of 3-arylisocoumarins, including thunberginols A and B, unsymmetrical 3, 4-disubstituted isocoumarins, and 3-ylidenephthalides *via* iodolactonization of methyl 2-ynylbenzoates or the corresponding carboxylic acids. *Tetrahedron* **2003**, *59*, 2067-2081.
204. Hesse, S.; Kirsch, G. Synthesis of new furocoumarin analogues via cross-coupling reaction of triflate. *Tetrahedron Lett*. **2003**, *44*, 97-99.

205. Rossi, R.; Bellina, F.; Biagetti, M.; Catanese, A.; Mannina, L. Palladium-catalyzed synthesis of stereodefined 3-[(1,1-unsymmetrically disubstituted)methylidene]isobenzofuran-1(3*H*)-ones and stereodefined 5-[(1,1-unsymmetrically disubstituted)methylidene]furan-2(5*H*)-ones. *Tetrahedron Lett*. **2000**, *41*, 5281-5286.
206. Cherry, K.; Parrain, J.-L.; Thibonnet, J.; Duchêne, A.; Abarbri, M. Synthesis of isocoumarins and α-pyrones *via* tandem Stille reaction / heterocyclization. *J. Org. Chem.* **2005**, *70*, 6669-6675.
207. Hiroya, K.; Jouka, R.; Kameda, M.; Yasuhara, A.; Sakamoto, T. Cyclization reactions of 2-alkynylbenzyl alcohol and 2-alkynylbenzylamine derivatives promoted by tetrabutylammonium fluoride. *Tetrahedron* **2001**, *57*, 9697-9710.
208. Uchiyama, M.; Ozawa, H.; Takuma, K.; Matsumoto, Y.; Yonehara, M.; Hiroya, K.; Sakamoto, T. Regiocontrolled intramolecular cyclizations of carboxylic acids to carbon-carbon triple bonds promoted by acid or base catalyst. *Org. Lett.* **2006**, *8*, 5517-5520.
209. Baldwin, J. E. Rules for ring closure. *J. Chem. Soc., Chem. Commun.* **1976**, 734-736.
210. Hellal, M.; Cuny, G. D. Microwave assisted copper-free Sonogashira coupling / 5-*exo*-dig cycloisomerization domino reaction: Access to 3-(phenylmethylene)isoindolin-1-ones and related heterocycles. *Tetrahedron Lett*. **2011**, *52*, 5508-5511.
211. Pearson, R. G.; Williams, F. V. Rates of ionization of *pseudo* acids. V. Steric effects in the base-catalyzed ionization of nitroethane. *J. Am. Chem. Soc.* **1953**, *75*, 3073-3075.
212. Jaffe, H. H.; Doak, G. O. The basicities of substituted pyridines and their 1-oxides *J. Am. Chem. Soc.* **1955**, *77*, 4441-4444.
213. Caron, S.; Do, N. M.; Sieser, J. E. A practical, efficient and rapid method for the oxidation of electron deficient pyridines using trifluoroacetic anhydride and hydrogen peroxide-urea complex. *Tetrahedron Lett.* **2000**, *41*, 2299-2302.
214. Sams, A. G.; Mikkelsen, G. K.; Brodbeck, R. M.; Pu, X.; Ritzen, A. Efficacy switching SAR of mGluR5 allosteric modulators: Highly potent positive and negative modulators from one chemotype. *Bioorg. Med. Chem. Lett.* **2011**, *21*, 3407-3410.
215. Seaton, P. J.; Williamson, R. T.; Mitra, A.; Assarpour, A. Synthesis of quinolines and their characterization by 2-D NMR spectroscopy. *J. Chem. Ed.* **2002**, *79*, 106-110.

216. Wamsler, T.; Nielsen, J. T.; Pedersen, E. J.; Schaumburg, K. NMR studies of pyridine-N-oxide. Determination of spectroscopic constants from [^{15}N]-, [4-^{2}H]-, and the parent species. *J. Magn. Reson.* **1978**, *31*, 177-186.
217. Ding, Y.; Zhao, W.; Song, W.; Zhang, Z.; Ma, B. Mild and recyclable catalytic oxidation of pyridines to N-oxides with H_2O_2 in water mediated by a vanadium-substituted polyoxometalate. *Green Chem.*, **2011**, *13*, 1486-1489.
218. Showalter, H. D. H. Ready access to 7,8-dihydro- and 1,2,3,4-tetrahydro-1,6-naphthyridine-5(6*H*)-ones from simple pyridine precursors. *J. Heterocyclic Chem.* **2006,** *43,* 1311-1317.
219. Jones, K.; Fiumana, A.; Escudero-Hernandez, M. L. Pyridine radicals in synthesis. Part 3: Cyclopentannulation of pyridine *via* the 3-pyridyl radical and a formal synthesis of (±)-oxerine. *Tetrahedron* **2000**, *56*, 397-406.
220. Miknis, G.; Lyssikatos, J. P.; Laird, E.; Tarlton, E.; Buckmelter, A. J.; Ren, L.; Rast, B.; Schlacter, S. T.; Wenglowsky, S. M. New heterocyclic compound useful as Raf (e.g. B-Raf) kinase inhibitor, for treating *e.g.* cancer, rheumatoid arthritis, psoriasis, contact dermatitis, delayed hypersensitivity, stroke, diabetes, hepatomegaly or cardiovascular disease. U.S. Patent US2007/49603 A1, **2007**.
221. Chang, C.-Y.; Liu, H.-M.; Hsu, R.-T. Efficient total synthesis of louisianins C and D. *Tetrahedron* **2009**, *65*, 748-751.
222. Reinecke, M. G. Hetarynes. *Tetrahedron* **1982,** *38,* 427-498.
223. Fang, Y.; Larock, R. C. Nucleophilic addition to 2,3-pyridyne and synthesis of benzonaphthyridinones. *Tetrahedron* **2012**, *68*, 2819-2826.
224. Goetz, A. E.; Garg, N. K. Regioselective reactions of 3,4-pyridynes enabled by the aryne distortion model. *Nature Chem.* **2013**, *5*, 54-60.
225. Lucht, B. L.; Collum, D. B. The preparation of lithio ethyl acetate. A simple procedure for the conversion of aldehydes and ketones to α-hydroxy esters. *J. Am. Chem. Soc.* **1994,** *116*, 6009-6010.
226. Fraser, R. R.; Mansour, T. S. Acidity measurements with lithiated amines: steric reduction and electronic enhancement of acidity. *J. Org. Chem.* **1984**, *49*, 3442–3443.
227. Woon, E. C. Y. PhD thesis, University of Bath, **2004**.
228. Ames, D. E.; Ribeiro, O. Heterocyclic synthesis from *o*-halogeno-acids. 3. Synthesis of 2-methylindole-4-carboxylic acid and related compounds and of some derivatives of 3-phenylisoquinolin-1(2*H*)-one. *J. Chem. Soc., Perkin Trans. 1*, **1976**, 1073-1078.

229. Cai, S.; Wang, F.; Xi, C. Assembly of 3-substituted isocoumarins *via* a CuI-catalyzed domino coupling / addition / deacylation process. *J. Org. Chem.* **2012**, *77*, 2331-2336.

230. Hurtley, W. R. H. Replacement of halogen in *ortho*-bromobenzoic acid. *J. Chem. Soc.* **1929**, 1870-1873.

231. Evano, G.; Blanchard, N. *Copper-mediated cross-coupling reactions*. John Wiley & Sons **2013** ISBN: 978-1-118-06045-2.

232. Setsune, J.; Ueda, T.; Shikata, K.; Matsukawa, K.; Iila, T.; Kitao, T. Synthesis of 2(3*H*)-benzofuranone derivatives by copper(I)-promoted substitution reactions of active methylene carbanions. *Tetrahedron.* **1986**, 2647-2656.

233. Cohen, T.; Wood, J.; Dietz, A. G. Organocopper intermediates in the exchange reaction of aryl halides with salts of copper$^{(I)}$. The possible role of copper$^{(III)}$ *Tetrahedron Lett*. **1974**, *15*, 3555-3558.

234. Beletskaya, I. P.; Cheprakov, A. V. Copper in cross-coupling reactions: The post-Ullmann chemistry. *Coord. Chem. Rev.* **2004**, *248*, 2337-2364.

235. Rovira, M.; Font, M.; Ribas, X. Model C_{sp2}-C_{sp3} Hurtley coupling catalysis that operates through a well-defined Cu^{I} / Cu^{III} Mechanism. *ChemCatChem* **2013**, *5*, 687-691.

236. Andrews, P. C.; Deacon, G. B.; Frank, R.; Fraser, B. H.; Junk, P. C.; MacLellan, J. G.; Massi, M.; Moubaraki, B.; Murray, K. S.; Silberstein, M. Formation of Ho^{III} trinuclear clusters and Gd^{III} monodimensional polymers induced by *ortho* and *para* regioisomers of pyridyl-functionalised β-diketones: Synthesis, structure, and magnetic properties. *Eur. J. Inorg. Chem*. **2009**, 744-751.

237. Popic, V. V.; Korneev, S. M.; Nikolaev, V. A.; Korobitsyna, I. K. An improved synthesis of 2-diazo-1,3-diketones. *Synthesis* **1991**, 195-198.

238. Singh, B.; Lesher, G. Y.; Pluncket, K. C.; Pagani, E. D.; Bode, D. C.; Bentley, R. G.; Connell. M. J.; Hamel, L. T.; Silver, P. J. Novel cAMP PDE III inhibitors: 1,6-Naphthyridin-2(1*H*)-ones. *J. Med. Chem.* **1992**, *35*, 4858-4865.

239. Zhao, J.; Zhao, Y.; Fu, H. Transition-metal-free intramolecular Ullmann-type *O*-arylation: synthesis of chromone derivatives. *Angew. Chem. Int. Ed.* **2011**, *50*, 3769-3733.

240. Liu, L.; Hu, J.; Wang, X-C.; Zhong, M.-J.; Liu, X.-Y.; Yang, S-D.; Liang, Y.-M. *ortho*-Induced transition-metal-free *C*-arylation cyclization reaction for the synthesis of polysubstituted isocoumarins. *Tetrahedron* **2012**, *68*, 5391-5395.

241. Matsui, T.; Sugiura, T.; Nakai, H.; Iguchi, S.; Shigeoka, S.; Takada, H.; Odagaki, Y.; Nagao, Y.; Ushio, Y.; Ohmoto, K.; Iwamura, H.; Yamazaki, S.; Arai, Y.; Kawamura, M. Novel 5-HT_3 antagonists. Isoquinolinones and 3-aryl-2-pyridones. *J. Med. Chem.* **1992**, *35*, 3307-3319.

242. Berry, J. M.; Threadgill, M. D. Labelled compounds of interest as antitumour agents - V. Syntheses of [^{18}O]-5-methylisoquinolinone and 1-(furan-2-yl-[^{18}O]-methoxy)-5-methylisoquinoline: Correction. *J. Labelled Compd. Radiopharm*. **1997**, *39*, 453-453.

243. Berry, J. M.; Watson, C. Y.; Whish, W. J. D.; Threadgill, M. D. 5-Nitrofuran-2-yl-methyl group as a potential bioreductively activated prodrug system. *J. Chem. Soc., Perkin Trans. 1* **1997**, 1147-1156.

244. Deady, L. W.; Finlayson, W. L.; Potts, C. H. Alkylation of salts of pyridinols, quinolinols and isoquinolinols. *Aust. J. Chem.* **1977**, *30*, 1349-1352.

245. Potts, K. T.; Yao, S. 1,3-Diphenyldibenzo[*g*,*i*]thieno[3',4':3,4]pyrrolo[1,2-*a*]-pyridine-*2*-S^{IV}, a new "non-classical" thiophene system. *J. Org. Chem.* **1979**, *44*, 977-979.

246. Kaneko, C.; Katagiri, N.; Uchiyama, K.; Yamada, T. Cyclo-additions in syntheses. 23. Photochemical [2+2] cycloreversion reactions of 1,2,2*a*,8*b*-tetrahydrocyclo-buta[*c*]isoquinolin-4(3*H*)-ones. *Chem. Pharm. Bull.* **1985**, *33*, 4160-4166.

247. Parveen I.; Naughton, D. P.; Whish, W. J. D.; Threadgill, M. D. 2-Nitroimidazol-5-ylmethyl as a potential bioreductively activated prodrug system: reductively triggered release of the PARP inhibitor 5-bromoisoquinolinone. *Bioorg. Med. Chem. Lett.* **1999**, *9*, 2031-2036.

248. Ferrer, S.; Naughton, D. P.; Parveen, I.; Threadgill, M. D. *N*- and *O*-Alkylation of isoquinolin-1-ones in the Mitsunobu reaction: Development of potential drug delivery systems. *J. Chem. Soc., Perkin Trans. 1* **2002**, *3*, 335-340.

249. Griffin, R. J.; Srinivasan, S.; Bowman, K.; Calvert, A. H.; Curtin, N. J.; Newell, D. R.; Pemberton, L. C.; Golding, B. T. Resistance-modifying agents. 5. Synthesis and biological properties of quinazolinone inhibitors of the DNA repair enzyme poly(ADP-ribose) polymerase (PARP). *J. Med. Chem.* **1998**, *41*, 5247-5256.

250. Ismail, A. G.; Wibberley, D. G. The synthesis of pyrido[4,3-*d*]pyrimidin-4(3*H*)-ones from 4-aminonicotinic acid. *J. Chem. Soc.* **1967**, *24*, 2613-2617.

251. Liu, X.; Fu, H.; Jiang, Y.; Zhao, Y. A simple and efficient approach to quinazolin-ones under mild copper-catalyzed conditions. *Angew. Chem. Int. Ed.* **2009**, *48*, 351-351.

252. Rao, H.; Fu, H. Copper-catalyzed coupling reactions. *SynLett* **2011**, *6*, 745-769.
253. Anbazhagan, M.; Boykin, D. W.; Stephens, C. E. Direct conversion of amidoximes to amidines *via* transfer hydrogenation. *Synthesis* **2003**, *16*, 2467-2469.
254. Beltraõ, T. M.; Srivastava, R. M. Preparação e estudo spectral das O-metilbenz-amidoximas. *An. Acad. Brasil. Ciênc.* **1978**, *50*, 159-164.
255. Barros, C. J. P.; de Freitas, J. J. R.; de Oliveira, R. N.; de Freitas Filho, J. R. Synthesis of amidoximes using an efficient and rapid ultrasound method. *J. Chil. Chem. Soc.* **2011**, *56*, 721-722.
256. Koryakova, A. G.; Ivanenkov, Y. A.; Ryzhova, E. A.; Bulanova, E. A.; Karapetian, R. N.; Mikitas, O. V.; Katrukha, E. A.; Kazey, V. I.; Okun, I.; Kravchenko, D. V.; Lavrovsky, Y. V.; Korzinov, O. M.; Ivachtchenko, A. V. Novel aryl and heteroaryl substituted N-[3-(4-phenylpiperazin-1-yl)propyl]-1,2,4-oxadiazole-5-carboxamides as selective GSK-3 inhibitors. *Bioorg. Med. Chem. Let.* **2008**, *18*, 3661-3666.
257. Srivastava, R. M.; Pereira, M. C.; Faustino, W. W. M.; Coutinho, K.; dos Anjos, J. V.; de Melo, S. J. Synthesis, mechanism of formation, and molecular orbital calcul-ations of arylamidoximes. *Monatsh. Chem.* **2009**, *140*, 1319-1324.
258. Yang, X.; Liu, G.; Li, H.; Zhang, Y.; Song, D.; Li, C.; Wang, R.; Liu, B.; Liang, W.; Jing, Y.; Zhao, G. Novel oxadiazole analogues derived from ethacrynic acid: design, synthesis and structure-activity relationships in inhibiting the activity of glutathione S-transferase P1-1 and cancer cell proliferation. *J. Med. Chem.* **2010**, *53*, 1015-1022.
259. Bonnet, M.; Flanagan, J. U.; Chan, D. A.; Lai, E. W.; Nguyen, P.; Giaccia, A. J.; Hay, M. P. SAR studies of 4-pyridyl heterocyclic anilines that selectively induce autophagic cell death in von Hippel-Lindau-deficient renal cell carcinoma cells. *Bioorg. Med. Chem.* **2011**, *19*, 3347-3356.
260. Meiji Seika Kaisha, Ltd. Poly(ADP-ribose) polymerase inhibitors consisting of pyrimidine derivatives. Patent EP1142881 A1, **2001**.
261. Huber, I.; Fülöp, F.; Lázár, J.; Bernáth, G.; Tóth, G. Dehydrogenation of 6-aza-quinazolinone derivatives. Formation of unexpected quinonediimine intermediates. *J. Chem. Soc., Perkin Trans. 1* **1992**, 157-161.
262. Bell, R. P. *The proton in chemistry*, 2nd ed., Cornell University Press, Ithaca, NY, **1973**.
263. Grayson, E. J.; Davis, B. G. A tuneable method for N-debenzylation of benzyl-amino alcohols. *Org. Lett.* **2005,** *7*, 2361-2364.

264. Monković, T.; Wong, H.; Bachand, C. Secondary-amines from the iron(II) ion-catalyzed reaction of amine oxides - a general-method for the dealkylation of tertiary amines. *Synthesis* **1985**, 770-773.
265. Fischer, E.; Speier, A. Darstellung der Ester. *Chem. Ber.* **1895**, *28*, 3252–3258.
266. Bennett, G. M.; Scorah, L. V. D. Studies in the penthian series. Part I. The action of sodium ethoxide on ethyl β-thiodipropionate. *J. Chem. Soc.* **1926**, 194-200.
267. Cross, R. M.; Maignan, J. R.; Mutka, T.; Luong, L.; Sargent, J.; Kyle, D. E.; Manetsch, R. Optimization of 1,2,3,4-tetrahydroacridin-9(10*H*)-ones as anti-malarials utilizing structure-activity and structure-property relationships. *J. Med. Chem.* **2011**, *54*, 4399-4426.
268. Ward, D. E.; Rasheed, M. A.; Gillis, H. M.; Beye, G. E.; Jheengut, V.; Achondun, G. T. Simple and efficient preparation of reagents for thiopyran introduction: methyl tetrahydro-4-oxo-2*H*-thiopyran-3-carboxylate, tetrahydro-4*H*-thiopyran-4-one, and 3,6-dihydro-4-trimethylsilyloxy-2*H*-thiopyran. *Synthesis* **2007**, *10*, 1584-1586.
269. Ghosh, A. K.; Liu, W. Chiral auxiliary mediated conjugate reduction and asymmetric protonation: synthesis of high affinity ligands for HIV protease inhibitors. *J. Org. Chem.* **1995**, *60*, 6198-6201.
270. Berridge, M. V. and Tan, A.S. Characterization of the cellular reduction of 3-(4,5-dimethylthiazol-2-yl)-2,5-diphenyltetrazolium bromide (MTT) - subcellular-localization, substrate dependence, and involvement of mitochondrial electron-transport in MTT reduction. *Arch. Biochem. Biophys.* **1993**, *303*, 474–482.
271. Tyrrell, R.M.; Pidoux, M. Quantitative differences in host cell reactivation of ultraviolet-damaged virus in human skin fibroblasts and epidermal keratinocytes cultured from the same foreskin biopsy. *Cancer Res.* **1986**, *46*, 2665-2669.
272. Zhong, J. L.; Yiakouvaki, A.; Holley, P.; Tyrrell, R. M.; Pourzand, C. Susceptibility of skin cells to uva-induced necrotic cell death reflects the intracellular level of labile iron. *J. Invest. Dermatol.* **2004**, *123*, 771 –780.
273. Wibberley, D. G. Methylnicotinic acids. Part III. Their conversion into pyranopyridines and 1,6-naphthyridines. *J. Chem. Soc.* **1962**, 4528-4531.
274. Bobbitt, J. M.; Doolittle, R. E. Synthesis of isoquinolines. I. Copyrine + isoquinoline systems derived from 3-cyano-4-methylpyridine. *J. Org. Chem.* **1964**, *29*, 2298-2301.

275. Huang, C.; Fu, Y.; Fu, H.; Jiang, Y.; Zhao, Y. Highly efficient copper-catalyzed cascade synthesis of quinazoline and quinazolinone derivatives. *Chem. Commun.* **2008**, 6333-6335.
276. Osselaer, J. P.; Lapiere, C. L. 4-Oxo-3,4-dihydropyrido[2,3-*d*]pyrimidine derivatives with diuretic properties. *Eur. J. Med. Chem.* **1974**, *9*, 305-309.
277. Dejardin, J. V.; Lapiere, C. L. New synthesis of 3-hydroxy-4-pyridinecarboxylic acid and 3-amino-4-pyridinecarboxylic acid. *Bull. Soc. Chim. Fr.* **1976**, 530-532.
278. Fuica, R. A.; Bartulín, F. J.; Fernández, O. Vinilformamidas. I. Condensación de malondinitrilo y cianoacetato de etilo. *Rev. Real Acad. Cienc. Exact. Fís. Natur. Madrid* **1968,** *62*, 249-257.
279. Sakamoto, T.; An-naka, M.; Kondo, Y.; Araki, T.; Yamanaka, H. Condensed heteroaromatic ring systems. XV. Synthesis of pyranopyridinones from halopyridinecarbonitriles. *Chem. Pharm. Bull.* **1988**, *36*, 1890-1894.
280. Begouin, A.; Queiroz, M.-J. R. P. Tandem palladium/charcoal-copper(I) iodide (Pd/C-CuI) catalyzed Sonogashira coupling and intramolecular cyclization from 2-bromonicotinic acid (= 2-bromopyridine-3-carboxylic acid) and ethynylarenes to 4-azaphthalides (= furo[3,4-*b*]pyridin-5(7*H*)-ones) and 5-azaisocoumarins (= 5*H*-pyrano[4,3-*b*]pyridin-5-ones). *Helv. Chim. Acta.* **2011**, *94*, 1792-1801.
281. Suzue, S.; Hirobe, M.; Okamoto, T. Studies on synthetic antimicrobials. 1. Synthesis of pyridine-4-thiocarbonamide derivatives. *Yakugaku Zasshi*, **1973**, *93*, 1331-1340.
282. Taylor, E. C.; Crovetti, A. J. Pyridine-1-oxides. I. Synthesis of some nicotinic acid derivatives. *J. Org. Chem.* **1954**, *19*, 1633-1636.
283. Combret, Y.; Torche, J.-J.; Ple, N.; Duflos, J.; Dupas, G.; Bourguignon, J.; Queguiner, G. Stereoselectivity of hydrogen transfer with chiral NADH models as a function of configuration and conformation. *Tetrahedron* **1991**, *47*, 9369-9382.
284. Nagano, H.; Nawata, Y.; Hamana, M. The mechanism of the reaction of nicotinic acid 1-oxide with acetic anhydide. *Chem. Pharm. Bull.* **1987**, *35*, 4068-4077.
285. Bradlow, H. I.; Vanderwerf, C. A. Studies on the acid hydrolysis of alpha-halogenated pyridine compounds. *J. Org. Chem.* **1949**, *14*, 509-513.
286. Zhou, N.; Wang, L.; Thompson, D. W.; Zhao, Y. OPE/OPV H-mers: synthesis, electronic properties, and spectroscopic responses to binding with transition metal ions. *Tetrahedron* **2011**, *67*, 125-143.

287. Musso, D. L.; Clarke, M. J.; Kelley, J. L.; Boswell, G. E.; Chen, G. Novel 3-phenylprop-2-ynylamines as inhibitors of mammalian squalene epoxidase. *Org. Biomol. Chem.* **2003**, *1*, 498-506.

288. Araki, Y.; Kobayashi, K.; Yonemoto, M.; Kondo, Y. Functionalisation of heteroaromatic *N*-oxides using organic superbase catalyst. *Org. Biomol. Chem.* **2011**, *9*, 78-80.

289. Takahashi, S.; Kuroyama, Y.; Sonogashira, K.; Hagihara, N. A convenient synthesis of ethynylarenes and diethynylarenes. *Synthesis* **1980**, *8*, 627-630.

290. Holmes, B. T.; Pennington, W. T.; Hanks, T. W. Efficient synthesis of a complete donor/acceptor bis(aryl)diyne family. *Synthetic Commun.* **2003**, *33*, 2447-2461.

291. Khabnadideh, S.; Pez, D.; Musso, A.; Brun, R.; Perez, L. M. R.; Gonzalez-Pacanowskac, D.; Gilbert, I. H. Design, synthesis and evaluation of 2,4-diaminoquinazolines as inhibitors of trypanosomal and leishmanial dihydrofolate reductase. *Bioorg. Med. Chem.* **2005,** *13*, 2637-2649.

292. Zhou, N.; Wang, L.; Thompson, D. W.; Zhao, Y. OPE/OPV H-mers: synthesis, electronic properties, and spectroscopic responses to binding with transition metal ions. *Tetrahedron* **2011**, *67*, 125-143.

293. Kodaira, K.; Okuhara, K. Preparation of fluorine-containing phenylacetylenes by the method of introduction of the ethynyl group using 1,1-dichloro-2,2-difluoroethene. *Bull. Chem. Soc. Jpn.* **1988**, *61*, 1625-1631.

294. Kuang, C.; Yang, Q.; Senboku, H.; Tokuda, M. Synthesis of (*Z*)-1-bromo-1-alkenes and terminal alkynes from anti-2,3-dibromoalkanoic acids by microwave-induced reaction. *Tetrahedron* **2005**, *61*, 4043-4052.

295. Leonard, K. A.; Hall, J. P.; Nelen, M. I.; Davies, S. R.; Gollnick, S. O.; Camacho, S.; Oseroff, A. R.; Gibson, S. L.; Hilf, R.; Detty, M. R. A selenopyrylium photosensitizer for photodynamic therapy related in structure to the antitumor agent AA1 with potent in vivo activity and no long-term skin photosensitization. *J. Med. Chem.* **2000**, *43*, 4488-4498.

296. Gonzalo Rodríguez, J.; Martín-Villamil, R.; H. Cano, F.; Fonseca, I. Synthesis of 1,4-di(3-pyridyl)buta-1,3-diyne and formation of charge-transfer complexes. X-Ray structure of 1,4-di(3-pyridyl)buta-1,3-diyne. *J. Chem. Soc. Perkin Trans. 1* **1997**, 709-714.

297. Khabnadideh, S.; Pez, D.; Musso, A.; Brun, R.; Perez, L. M. R.; González-Pacanowskac, D.; Gilbert, I. H. Design, synthesis and evaluation of 2,4-diaminoquinazolines as inhibitors of trypanosomal and leishmanial dihydrofolate reductase. *Bioorg. Med. Chem.* **2005**, *13*, 2637-2649.
298. Botting, N. Synthesis of 13C-labelled estrogen analogues. Patent WO2004/69774 A2, **2004**.
299. Gautam, V.; Chawla, V.; Sonar, P. K.; Saraf, S. K. Syntheses, characterization and antimicrobial evaluation of some 1,3,5-trisubstituted pyrazole derivatives. *E-Journal of Chemistry*, **2010**, *7*, 1190-1195.
300. Han, X.; Widenhoefer, R. A. Palladium-catalyzed oxidative alkoxylation of alpha-alkenyl beta-diketones to form functionalized furans. *J. Org. Chem.* **2004**, *69*, 1738-1740.
301. Lowe, J. U.; Ferguson, L. N. Direction of enolization of benzoylacetones. *J. Org. Chem.* **1965**, *30*, 3000-3002.
302. Choshi, T.; Horimoto, S.; Wang, C. Y.; Nagase, H.; Ichikawa, M.; Sugino, E.; Hibino, S. Synthesis of dibenzoylmethane derivatives and inhibition of mutagenicity in salmonella-typhimurium. *Chem. Pharm. Bull.*, **1992**, *40*, 1047-1049.
303. Circu, V.; Gibbs, T. J. K.; Omnes, L.; Horton, P. N.; Hursthouse, M. B.; Bruce, D. W. Orthometallated palladium(II) imine complexes as candidate materials for the biaxial nematic phase. Crystal and molecular structure of three palladium imine complexes. *J. Mater. Chem.* **2006**, *16*, 4316-4325.
304. Franek, W. New dithio-bis-(diaroylmethanes) and acetyl diaroylchloromethyl disulfides: attractive synthons and precursors for the liberation of highly reactive dithiiranes or thiosulfines. *Monatsh. Chem.* **1996**, *127*, 895-907.
305. Hao, W.; Zhang, Y.; Ying, T.; Lu, P. A facile route to convert acetylacetone into other beta-diketones with acyl chlorides promoted by samarium triiodide. *Synthetic Commun.* **1996**, *26*, 2421-2428.
306. Susanto, W.; Chu, C. Y.; Ang, W. J.; Chou, T.-C.; Lo, L.-C.; Lam, Y. Fluorous oxime palladacycle: a precatalyst for carbon-carbon coupling reactions in aqueous and organic medium. *J. Org. Chem.* **2012**, *77*, 2729-2742.
307. Quan, C.; Kurth, M. Solid-phase synthesis of 5-isoxazol-4-yl-[1,2,4]oxadiazoles. *J. Org. Chem.* **2004**, *69*, 1470-1474.

308. Zhao, Q.; Liu, S.; Li, Y.; Wang, Q. Design, synthesis, and biological activities of novel 2-cyanoacrylates containing oxazole, oxadiazole, or quinoline moieties. *J. Agric. Food Chem.* **2009**, *57*, 2849-2855.
309. Quan, C.; Kurth, M. Solid-phase synthesis of 5-isoxazol-4-yl-[1,2,4]oxadiazoles. *J. Org. Chem.* **2004**, *69*, 1470-1474.
310. Ogurtsov, V. A.; Rakitin, O. A.; Strelenko, Yu. A.; Obruchnikova, N. V.; Khmel'nitskii, L. I. Syntheses based on nitrile oxides. 3. Interaction of aromatic nitrile oxides with bis-trimethylsilylthiodiimide. *Russ. Chem. Bull.* **1993**, *42*, 706-708.
311. Boehringer Ingelheim Pharma GmbH and Co. KG. Process for the preparation of 4-(benzimidazolylmethylamino)-benzamidines. Patent EP1609784 A1, **2005**.
312. Bernasek, E. Pyridineamidoximes. *J. Org. Chem.* **1957**, *22*, 1263-1263.
313. Exner, O.; Jehlicka, V.; Reiser, A. Uber die Konfiguration und Konformation der o-Alkylhydroxamsauren. *Collect. Czech. Chem. C.* **1959**, *24*, 3207-3222.
314. Kuzmenko, I.; Kindermann, M.; Kjaer, K.; Howes, P. B.; Als-Nielsen, J.; Granek, R.; von Kiedrowski, G.; Leiserowitz, L.; Lahav, L. Crystalline films of interdigitated structures formed via amidinium-carboxylate interactions at the air-water interface. *J. Am. Chem. Soc.* **2001**, *123*, 3771-3783.
315. Kelly, S.; Fuenfschilling, J. Synthesis, transition temperatures and some physical properties of some low-melting smectic C materials. *Mol. Cryst. Liq. Crys. A*, **1995**, *260*, 139-156.
316. Abbott Lab. Substituted 5-nitro-2-furylamidoximes. U.S. Patent US3660390, **1972**.
317. Singh, B.; Lesher, G. Y. Convenient and novel syntheses of 4-amino-2-arylpyrimidines. *J. Heterocyclic Chem*. **1977**, *14*, 1413-1414.
318. Gozlan; H.; Rips, R. New methyl-derivatives of 4-methylbenzamide oxime. *Cr. Acad. Sci. II C*, **1974**, *278*, 629-632.
319. Gershbein, L. L.; Hurd, C. D. The reaction of hydrogen sulfide with acrylonitrile, acrylic ester and crotonaldehyde. *J. Am. Chem. Soc.* **1947**, *69*, 242-243.
320. Parham, W. E.; Wilbur, J. M. The mechanism of action of bisalkylating agents in cancer chemotherapy. II. The reaction of myleran with mercaptans. *J. Org. Chem.* **1961**, *26*, 1569-1572.
321. Lindgren, A. E. G.; Karlberg, T.; Thorsell, A. G.; Hesse, M.; Spjut, S.; Ekblad, T.; Andersson, C. D.; Pinto, A. F.; Weigelt, J.; Hottiger, M. O.; Linusson, A.; Elofsson, M.; Schuler, H. PARP inhibitor with selectivity toward ADP-ribosyltransferase ARTD3/PARP3. *ACS Chem. Biol.* **2013**, *8*, 1698-1703.